

Memorizing without overfitting: Bias, variance, and interpolation in over-parameterized models

Jason W. Rocks¹ and Pankaj Mehta^{1,2}

¹*Department of Physics, Boston University, Boston, Massachusetts 02215, USA*

²*Faculty of Computing and Data Sciences, Boston University, Boston, Massachusetts 02215, USA*

The bias-variance trade-off is a central concept in supervised learning. In classical statistics, increasing the complexity of a model (e.g., number of parameters) reduces bias but also increases variance. Until recently, it was commonly believed that optimal performance is achieved at intermediate model complexities which strike a balance between bias and variance. Modern Deep Learning methods flout this dogma, achieving state-of-the-art performance using “over-parameterized models” where the number of fit parameters is large enough to perfectly fit the training data. As a result, understanding bias and variance in over-parameterized models has emerged as a fundamental problem in machine learning. Here, we use methods from statistical physics to derive analytic expressions for bias and variance in three minimal models for over-parameterization (linear regression and two-layer neural networks with linear and nonlinear activation functions), allowing us to disentangle properties stemming from the model architecture and random sampling of data. All three models exhibit a phase transition to an interpolation regime where the training error is zero. At the interpolation transition for each model, the test error diverges due to diverging variance (while bias remains finite). In contrast with classical intuition, we also show that over-parameterized models can overfit even in the absence of noise and exhibit bias even if the student and teacher models match. We synthesize these results to construct a holistic understanding of generalization error and the bias-variance trade-off in over-parameterized models and relate our results to random matrix theory.

I. INTRODUCTION

Machine Learning (ML) is one of the most exciting and fastest-growing areas of modern research and application. Over the last decade, we have witnessed incredible progress in our ability to learn statistical relationships from large data sets and make accurate predictions. Modern ML techniques have now made it possible to automate tasks such as speech recognition, language translation, and visual object recognition, with wide-ranging implications for fields such as genomics, physics, and even mathematics. These techniques – in particular the Deep Learning methods that underlie many of the most prominent recent advancements – are especially successful at tasks that can be recast as supervised learning problems [1]. In supervised learning, the goal is to learn statistical relationships from labeled data (e.g., a collection of pictures labeled as containing a cat or not containing a cat). Common examples of supervised learning tasks include classification and regression.

A fundamental concept in supervised learning is the bias-variance trade-off. In general, the out-of-sample, generalization, or test error, of a statistical model can be decomposed into three sources: bias (errors resulting from erroneous assumptions which can hamper a statistical model’s ability to fully express the patterns hidden in the data), variance (errors arising from over-sensitivity to the particular choice of training set), and noise. This bias-variance decomposition provides a natural intuition for understanding how complex a model must be in order to make accurate predictions on unseen data. As model complexity (e.g., the number of fit parameters) increases, bias decreases as a result of the model becoming

more expressive and better able to capture complicated statistical relationships in the underlying data distribution. However, a more complex model may also exhibit higher variance as it begins to overfit, becoming less constrained and therefore more sensitive to the quirks of the training set (e.g., noise) that do not generalize to other data sets. This trade-off is reflected in the generalization error in the form of a classical “U-shaped” curve: the test error first decreases with model complexity until it reaches a minimum before increasing dramatically as the model overfits the training data. For this reason, it was commonly believed until recently that optimal performance is achieved at intermediate model complexities which strike a balance between bias (underfitting) and variance (overfitting).

Modern Deep Learning methods defy this understanding, achieving state-of-the-art performance using “over-parameterized models” where the number of fit parameters is so large – often orders of magnitude larger than the number of data points [2] – that one would expect a model’s accuracy to be overwhelmed by overfitting. In fact, empirical experiments show that convolutional networks commonly used in image classification are so overly expressive that they can easily fit training data with randomized labels, or even images generated from random noise, with almost perfect accuracy [3]. Despite the apparent risks of overfitting, these models seem to perform at least as well as, if not better than, traditional statistical models. As a result, modern best practices in Deep Learning recommend using highly over-parameterized models that are expressive enough to achieve zero error on the training data [4].

Clearly, the classical picture provided by the bias-

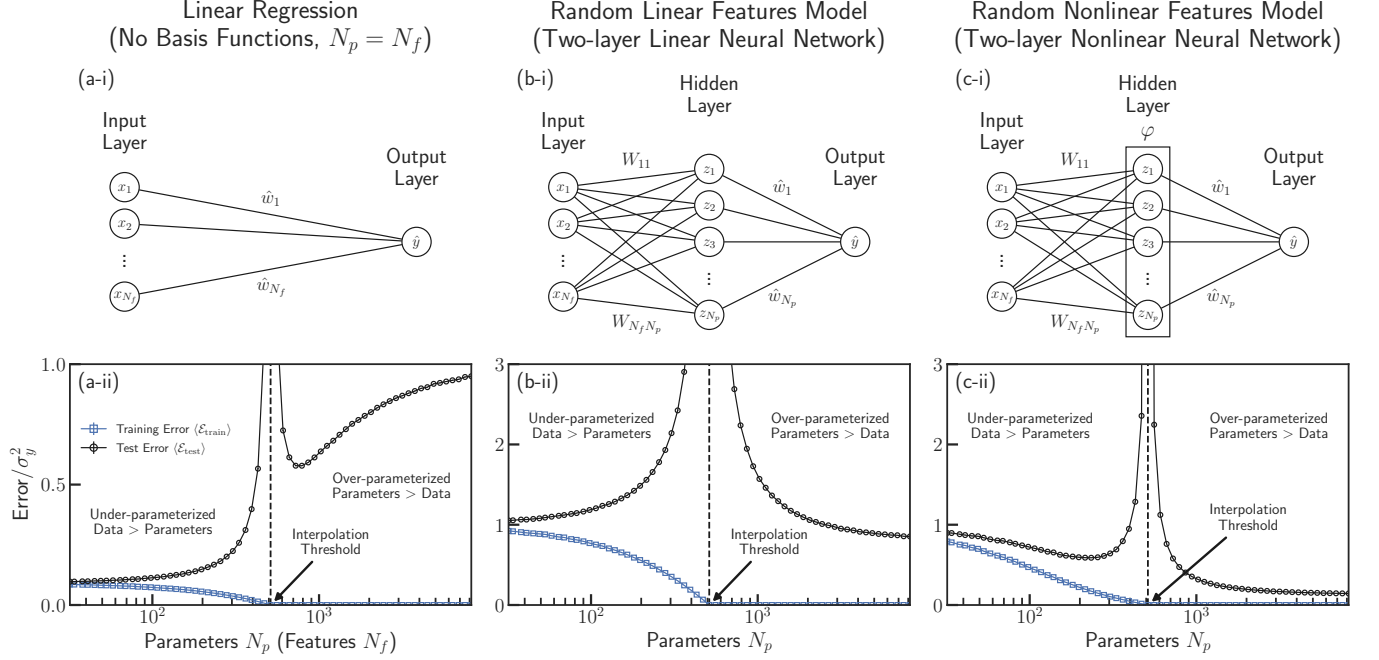


FIG. 1. **Double-descent phenomenon for three different model architectures.** (Top Row) Schematics of the three model architectures considered and (Bottom Row) examples of the average training error (blue squares) and test error (black circles) for each model calculated via numerical simulations. In each model, the test error diverges when the training error reaches zero at the interpolation threshold, located where the number of parameters N_p matches the number of points in the training data set M (indicated by a black dashed vertical line). (a) In linear regression without basis functions, the number of features in the data N_f matches the number of fit parameters N_p . (b) The random linear features model (two-layer linear neural network where the parameters of the middle layer are random but fixed) decouples the number of features N_f and the number of fit parameters N_p by incorporating an additional “hidden layer”. (c) The random nonlinear features model (two-layer nonlinear neural network where the parameters of the middle layer are random but fixed) transforms the data using a nonlinear activation function (e.g., ReLU), resulting in the canonical double-descent behavior. In (b) there are more features than data points, $N_f = 4M$, while in (c) there are less features than data points $N_f = M/4$. Results are shown for a linear teacher model $y(\vec{x}) = \vec{x} \cdot \vec{\beta} + \varepsilon$, a signal-to-noise ratio of $\sigma_\beta^2 \sigma_X^2 / \sigma_\varepsilon^2 = 10$, and a small regularization parameter of $\lambda = 10^{-6}$. The y -axes have been scaled by the variance of the training set labels $\sigma_y^2 = \sigma_\beta^2 \sigma_X^2 + \sigma_\varepsilon^2$. Each point is averaged over at least 1000 independent simulations trained on $M = 512$ data points with small error bars indicating the error on the mean. See Sec. II for precise definitions and Sec. S6 of Supplemental Material [5] for additional simulation details.

variance trade-off is incomplete. Classical statistics largely focuses on under-parameterized models which are simple enough that they have a nonzero training error. In contrast, Modern Deep Learning methods push model complexity past the *interpolation threshold*, the point at which the training error reaches zero [6–10]. In the classical picture, approaching the interpolation threshold coincides with a large increase, or even divergence, in the test error via the variance. However, numerical experiments suggest that the predictive performance of over-parameterized models are better described by “double-descent” curves which extend the classic U-shape past the interpolation threshold to account for over-parameterized models with zero training error [6, 11, 12]. Surprisingly, if model complexity is increased past the interpolation threshold, the test error once again decreases, often resulting in over-parameterized models with even better out-of-sample performance than their under-parameterized counter-

parts [see Fig. 1(c-ii)].

This double-descent behavior stands in stark contrast with the classical statistical intuition based on the bias-variance trade-off as both bias and variance appear to decrease past the interpolation threshold. Therefore, understanding this phenomena requires generalizing the bias-variance decomposition to over-parameterized models. More broadly, explaining the unexpected success of over-parameterized models represents a fundamental problem in ML and modern statistics.

Relation to Previous Work

In recent years, many attempts have been made to understand the origins of this double-descent behavior via numerical and/or analytical approaches. While much of this work has relied on well constructed numerical experiments on complex Deep Learning models [3, 13], many

theoretical studies have focused on a much simpler setting: the so-called “lazy training” regime. Previously, it was observed that in the limit of an infinitely wide network, the learning process appears to mimic that of an approximate kernel method in which the kernel used by the model to express the data – the Neural Tangent Kernel (NTK) – remains fixed [14, 15]. This stands in contrast to the so-called “feature training” regime in which the kernel evolves over time as the model learns the most informative way to express the relationships in the data [16].

Making use of the observation that the kernel remains approximately fixed in the lazy regime, many analytical studies have considered neural networks where the top layer is trained, but the middle layer(s) remained fixed, effectively reducing these models to linear regression with various types of nontrivial basis functions [17–43]. Despite this simplification, the closed-form solutions for the training and test error obtained for these models exhibit the double-descent phenomenon, demonstrating that many of the key features of more complex Deep Learning architectures can arise in much simpler settings.

A smaller subset of these studies have also attempted to extend these calculations to compute the bias-variance decomposition [17, 19, 25–27, 29, 30, 33, 37, 39, 41, 43]. However, this literature is rife with qualitative and quantitative disagreements, and as a result, a consensus has not formed regarding many of the basic properties of bias and variance in over-parameterized models (e.g., whether bias remains finite at the interpolation threshold).

Underlying these disagreements is the ubiquitous use of non-standard and varying definitions of bias and variance, leading to unintended side effects (see Sec. III for an in-depth discussion). For example, some studies consider a fixed design matrix for the training data set in the definitions of bias and variance, but not for the test set, resulting in an effective mismatch in their data distributions [17, 19, 27, 29, 30, 33, 39]. Meanwhile, other studies do not distinguish between sources of randomness stemming from the model architecture (e.g., due to initialization) and sampling of the training data set, leading to models that inadvertently add additional sources of noise to the data distribution [17, 25, 26, 30, 37, 43].

In fact, of these studies, closed-form expressions using the standard definitions of bias and variance have only been obtained for the simple case of linear regression without basis functions [41]. While this setting captures some qualitative aspects of the double-descent phenomenon [see Fig. 1(a-ii)], it requires a one-to-one correspondence between features in the data and fit parameters, making it difficult to understand, if and how these results generalize to more complicated statistical models.

In line with previous studies, in this work, we also focus on the lazy regime by considering three different linear models that emulate many properties of more complicated neural network architectures (see next section). However, our approach differs in that we utilize the traditional definitions of bias and variance, allowing us to

clear up much of the confusion surrounding the bias-variance decomposition in over-parameterized models. In this way, we connect Modern Deep Learning to the statistical literature of the last century and in doing so, gain proper intuition for the origins of the double-descent phenomenon.

Overview of Approach

In this work, we use methods from statistical physics to derive analytic results for bias and variance in the over-parameterized regime for three minimal model architectures. These models, depicted in Fig. 1, are (i) *linear regression* (ridge regression without basis functions and in the limit where the regularization parameter goes to zero – often called “ridge-less regression” in the statistics and ML literature), (ii) the *random linear features model* (a two-layer linear neural network where the top layer is trained and parameters for the intermediate layer are chosen to be random but fixed), and (iii) the *random non-linear features model* (a two-layer neural network with an arbitrary nonlinear activation function where the top layer is trained and parameters for the intermediate layer are chosen to be random but fixed). We generate the data used to train all three models using a non-linear “teacher model” where the labels are related to the features through a non-linear function (usually with additive noise). Using similar terminology, we often refer to the details of a model’s architecture as the “student model.” Crucially, the differences between the three models we consider allow us to disentangle the effects of model architecture on bias and variance versus effects arising from randomly sampling the underlying data distribution.

Linear regression is one of the simplest models in which the test error diverges at the interpolation threshold but then decreases in the over-parameterized regime [Fig. 1(a)]. Because this model uses the features in the data directly without modification (i.e., it lacks a hidden layer), it provides evidence that the process of randomly sampling the data itself plays an integral part in the double-descent phenomena. The two random features models [Figs. 1(b) and (c)] provide insight into the effects of filtering the features through an additional transformation, in effect, changing the way the model views the data. This disconnect between features and their representations in the model is crucial for understanding bias and variance in more complex over-parameterized models.

To treat these models analytically, we make use of the “zero-temperature cavity method” which has a long history in the physics of disordered systems and statistical learning theory [44–46]. In particular, our calculations follow the style of Ref. 47 and assume that the solutions can be described using a Replica-Symmetric Ansatz, which we confirm numerically. Our analytic results are exact in the thermodynamic limit where the number of data points M , the number of features in the

data N_f , and the number of fit parameters (hidden features) N_p all tend towards infinity. Crucially, when taking this limit, the ratios between these three quantities are assumed to be fixed and finite, allowing us to ask how varying these ratios and other model properties (such as linear versus nonlinear activation functions) affect generalization. We confirm that all our analytic expressions agree extremely well with numerical results, even for relatively small system sizes ($N_f, N_p, M \sim 10 - 1000$).

Summary of Major Results

Before proceeding further, we briefly summarize our major results:

- We derive analytic expressions for the test (generalization) error, training error, bias, and variance for all three models using the zero-temperature cavity method.
- We show that all three models exhibit a phase transition at an interpolation threshold to an interpolation regime where the training error is zero, with the random linear features model (linear neural network) possessing an additional phase transition between a zero and nonzero bias regime for a linear teacher model.
- We show that the variance (but not the bias) diverges at the interpolation threshold, leading to extremely large generalization error. This is in contrast to earlier calculations using non-standard definitions of bias and variance that suggested that both bias and variance can diverge.
- We show that bias in over-parameterized models has two sources: error resulting from mismatches between the student and teacher models (i.e., the model is incapable of fully capturing the full data distribution) and incomplete sampling of the data’s feature space. We show that as a result of the latter case, one can have nonzero bias even if the student and teacher models are identical.
- We show that biased models can overfit even in the absence of noise. In other words, biased models can interpret signal as noise.
- We show that bias and variance decrease with model complexity in the interpolation regime (i.e., where the training error is zero), but only if the number of features in the data remains fixed.
- We show that the zero-temperature susceptibilities that appear in our cavity calculations measure the sensitivity of a fitted model to small perturbations. We discuss how these susceptibilities can be used to identify phase transitions and are each related to different aspects of the double-descent phenomena.

- We combine these observations to provide a comprehensive intuitive explanation of the double-descent curves for test error observed in over-parameterized models, making connections to random matrix theory.

Organization of Paper

In Sec. II, we start by providing the theoretical setup for the three models and briefly summarize the methods we use to derive analytic expressions. In Sec. III, we provide precise definitions of bias and variance, taking great care to distinguish between different sources of randomness. We also provide additional decompositions of the training labels and hidden features, allowing us to easily interpret the sources of error that contribute to our analytic expressions of the test error, training error, bias, and variance. In Sec. IV, we report our analytic results and compare them to numerical simulations. In Sec. V, we use these analytic expressions to understand how bias and variance generalize to over-parameterized models and also discuss the roles of the susceptibilities that arise as part of our cavity calculations. Finally, in Sec. VI, we conclude and discuss the implications of our results for modern ML methods.

II. THEORETICAL SETUP

A. Supervised Learning Task

In this work, we consider data points (y, \vec{x}) , each consisting of a continuous label y paired with a set of N_f continuous features \vec{x} . To distinguish the features in the data from those in the model, we often refer to \vec{x} as the “input features.” We frame the supervised learning task as follows: using the relationships learned from a training data set, construct a model to accurately predict the labels y of new data points based on their input features \vec{x} .

B. Data Distribution (Teacher Model)

We assume that the relationship between the input features and labels (the data distribution or teacher model) can be expressed as

$$y(\vec{x}) = y^*(\vec{x}; \vec{\beta}) + \varepsilon \quad (1)$$

where ε is the label noise and $y^*(\vec{x}; \vec{\beta})$ is an unknown function representing the “true” labels. This function takes the features as arguments and combines them with a set of N_f “ground truth” parameters $\vec{\beta}$ which characterize the correlations between the features and labels (see Sec. III A).

We draw the input features for each data point independently and identically from a normal distribution with zero mean and variance σ_X^2/N_f . Normalizing the variance by N_f ensures that the magnitude of each feature vector is independent of the number of features and that a proper thermodynamic limit exists. Note that in this work, we consider features that do not contain noise. We also choose each element of the ground truth parameters $\vec{\beta}$ and the label noise ε to be independent of the input features and mutually independent from one another, drawn from normal distributions with zero mean and variances σ_β^2 and σ_ε^2 , respectively.

In this work, we restrict ourselves to a teacher model of the form

$$y^*(\vec{x}; \vec{\beta}) = \frac{\sigma_\beta \sigma_X}{\langle f' \rangle} f\left(\frac{\vec{x} \cdot \vec{\beta}}{\sigma_X \sigma_\beta}\right) \quad (2)$$

where the function f is an arbitrary nonlinear function and $\langle f' \rangle = \frac{1}{\sqrt{2\pi}} \int_{-\infty}^{\infty} dh e^{-\frac{h^2}{2}} f'(h)$ is a normalization constant chosen for convenience (see Sec. III A). We place a factor of $1/(\sigma_X \sigma_\beta)$ inside the function f so that its argument has unit variance, while the pre-factor $\sigma_\beta \sigma_X$ ensures that y^* reduces to a linear teacher model $y^*(\vec{x}) = \vec{x} \cdot \vec{\beta}$ when $f(h) = h$. Furthermore, we assume both the labels and input features are centered so that f has zero mean with respect to its argument. While the results we report hold for a general f of this form, all figures show numerical simulations for a linear teacher model unless otherwise specified.

C. Model Architectures (Student Models)

We consider three different student models that we discuss in detail below: i) linear regression, ii) the random linear features model, and iii) the random nonlinear features model. Schematics of the network architectures for the three models are depicted in Fig. 1. All three student models take the general form

$$\hat{y}(\vec{x}) = \vec{z}(\vec{x}) \cdot \hat{\mathbf{w}}. \quad (3)$$

where $\hat{\mathbf{w}}$ is a vector of fit parameters and $\vec{z}(\vec{x})$ is a vector of “hidden” features which each may depend on a combination of the input features \vec{x} . The hidden features \vec{z} are effectively the representations of the data points from the perspective of the model.

Since we only fit the top layer of the network in all three models, the number of fit parameters N_p equals the number of hidden features, and Eq. (3) is equivalent to a linear model with basis functions. Despite its simplicity, we will show that this model reproduces much of the interesting behaviors observed in more complicated neural networks.

1. Linear Regression

For linear regression without basis functions [Fig. 1(a)], the representations of the features from the perspective of the model are simply the input features themselves so that $\vec{z}(\vec{x}) = \vec{x}$. In other words, the hidden and input features are identical, leading to exactly one fit parameter for each feature, $N_p = N_f$.

2. Random Linear Features Model

In the random linear features model [Fig. 1(b)], the hidden features for each data point are related to the input features via a random transformation matrix W of size $N_f \times N_p$,

$$\vec{z}(\vec{x}) = W^T \vec{x}. \quad (4)$$

We take each element of W to be independent and identically distributed, drawn from a normal distribution with zero mean and variance σ_W^2/N_p . The normalization by N_p is chosen so that the magnitude of each hidden feature vector only depends on the ratio of the number of input features to parameters which we always take to be finite. We also assume W is independent of all other random variables, including \vec{x} , $\vec{\beta}$, and ε .

3. Random Nonlinear Features Model

The random nonlinear features model [Fig. 1(c)] is a generalization of the previous model where the hidden features are related to the input features via a nonlinear activation function φ ,

$$\vec{z}(\vec{x}) = \frac{1}{\langle \varphi' \rangle} \frac{\sigma_W \sigma_X}{\sqrt{N_p}} \varphi\left(\frac{\sqrt{N_p}}{\sigma_W \sigma_X} W^T \vec{x}\right), \quad (5)$$

where φ acts separately on each element of its input and $\langle \varphi' \rangle = \frac{1}{\sqrt{2\pi}} \int_{-\infty}^{\infty} dh e^{-\frac{h^2}{2}} \varphi'(h)$ is a normalization constant chosen for convenience (see Sec. III B). We place a factor of $\sqrt{N_p}/(\sigma_W \sigma_X)$ inside the activation function so that its argument has approximately unit variance. The corresponding pre-factor of $\sigma_W \sigma_X / \sqrt{N_p}$ in front of φ ensures that \vec{z} reduces to Eq. (4) when the activation function is linear [i.e., $\varphi(h) = h$]. We note that while the random nonlinear features model is technically a linear model with a specific choice of basis functions, it is equivalent to a two-layer neural network where the weights of the middle layer are chosen to be random and only the top layer is trained. Although our analytic results hold for an arbitrary nonlinear activation function φ , all figures show results for ReLU activation where $\varphi(h) = \max(0, h)$.

D. Fitting Procedure

We train each model on a training data set consisting of M data points, $\mathcal{D} = \{(y_a, \vec{x}_a)\}_{a=1}^M$. For convenience, we organize the vectors of input features in the training set into an observation matrix X of size $M \times N_f$ and define the length- M vectors of training labels \vec{y} , training label noise $\vec{\epsilon}$, and label predictions for the training set \hat{y} . We also organize the vectors of hidden features evaluated on the input features of the training set, $\{\vec{z}(\vec{x}_a)\}_{a=1}^M$, into the rows of a hidden feature matrix Z of size $M \times N_p$.

Given a set of training data \mathcal{D} , we solve for the optimal values of the fit parameters $\hat{\mathbf{w}}$ by minimizing the standard loss function used for ridge regression,

$$L(\hat{\mathbf{w}}; \mathcal{D}) = \frac{1}{M} \|\Delta \vec{y}\|^2 + \frac{\lambda}{N_p} \|\hat{\mathbf{w}}\|^2, \quad (6)$$

where the notation $\|\cdot\|$ indicates an L_2 norm and $\Delta \vec{y} = \vec{y} - \hat{y}$ is the vector of residual label errors for the training set. The first term is simply the mean squared error between the true labels and their predicted values, while the second term imposes standard L_2 regularization with regularization parameter λ . We will often work in the “ridge-less limit” where we take the limit $\lambda \rightarrow 0$.

E. Model Evaluation

To evaluate each model’s prediction accuracy, we measure the training and test (generalization) errors. We define the training error as the mean squared residual label error of the training data,

$$\mathcal{E}_{\text{train}} = \frac{1}{M} \|\Delta \vec{y}\|^2. \quad (7)$$

We define the interpolation threshold as the model complexity at which the training error becomes exactly zero (in the thermodynamic and ridge-less limits). Analogously, we define the test error as the mean squared error evaluated on a test data set, $\mathcal{D}' = \{(y'_a, \vec{x}'_a)\}_{a=1}^{M'}$, composed of M' new data points drawn independently from the same data distribution as the training data,

$$\mathcal{E}_{\text{test}} = \frac{1}{M'} \|\Delta \vec{y}'\|^2, \quad (8)$$

where $\Delta \vec{y}' = \vec{y}' - \hat{y}'$ is a length- M' vector of residual label errors between the vector of true labels \vec{y}' and their predicted values \hat{y}' for the test set.

F. Exact Solutions

To solve for unique optimal solution, we set the gradient with respect to the fit parameters to zero, giving us a set of N_p equations with N_p unknowns,

$$0 = \frac{\partial L(\hat{\mathbf{w}})}{\partial \hat{\mathbf{w}}} = -Z^T \Delta \vec{y} + \lambda \hat{\mathbf{w}}, \quad (9)$$

where we have multiplied by $M/2$ and redefined our regularization parameter as $(M/2N_p)\lambda \rightarrow \lambda$ for convenience. Solving this set of equations results in a unique solution for the fit parameters,

$$\hat{\mathbf{w}} = [\lambda I_{N_p} + Z^T Z]^{-1} Z^T \vec{y}. \quad (10)$$

For simplicity, we also take the ridge-less limit where λ is infinitesimally small ($\lambda \rightarrow 0$). While our calculations do provide exact solutions for finite λ , the solutions in the limits of small λ are much more insightful. In this limit, Eq. (10) and Eq. (3) are approximated to lowest order in λ as

$$\hat{\mathbf{w}} \approx Z^+ \vec{y}, \quad \hat{y}(\vec{x}) \approx \vec{z}(\vec{x}) \cdot Z^+ \vec{y} \quad (11)$$

where $^+$ denotes a Moore-Penrose inverse, or pseudoinverse.

G. Kernel Matrix

We note that the solution for the fit parameters in Eq. (10) depends on the matrix $Z^T Z$, known as the kernel, or Gram matrix [48]. This matrix measures the similarity between different data points in the training set from the perspective of the model and $Z^T Z/M$ can be interpreted as an empirical covariance matrix of the hidden features sampled by the training set when the hidden features are centered. The authors of Ref. [49] showed that for ridge regression the divergence of the test error at the interpolation threshold can be naturally understood in terms of the spectrum of the kernel matrix. Inspired by this observation, we also explore the relationship between the eigenvalues of the kernel and the double-descent phenomenon in our more general setting. To do so, we reproduce the known eigenvalue distribution for the kernel matrix for each of the three models. We note that in linear regression (no basis functions), the kernel is simply a Wishart matrix whose eigenvalues follow the Marchenko-Pastur distribution [50], while the kernel of the random linear features model is described by a Wishart product matrix whose spectrum was calculated in Ref. 51. Finally, the eigenvalue spectrum for the kernel for the random nonlinear features model was explored in Ref. 52. For each of these models, we provide an alternative derivation of these spectra using the zero-temperature cavity method, allowing us to directly relate the eigenvalues of the kernel matrix to the double-descent phenomenon.

H. Derivation of Closed-Form Solutions

While the expressions in the previous section are quite general, they hide much of the complexity of the problem and are difficult to analyze carefully. For this reason, we make use of the zero-temperature cavity method to find closed-form solutions for all quantities of interest. The

zero-temperature cavity method has a long history in the physics of disordered systems and statistical learning theory and has been used to analyze the Hopfield model [53] and more recently, compressed sensing [20, 54]. The cavity method is an alternative to the more commonly used Replica Method or analyses based on Random Matrix Theory.

Like the Replica Method, finding closed-form solutions requires some additional assumptions. In particular, we assume that the solutions satisfy a Replica-Symmetric Ansatz (an assumption we confirm numerically by showing remarkable agreement between our analytic results and simulations). Furthermore, we work in the thermodynamic limit, where $N_f, M, N_p \rightarrow \infty$ and keep terms to leading order in these quantities. Our results are exact under these assumptions.

To apply the zero-temperature cavity method, we start by defining the ratio of the number of input features to training data points $\alpha_f = N_f/M$ and the ratio of fit parameters to training data points $\alpha_p = N_p/M$. Next, we take the thermodynamic limit $N_f, M, N_p \rightarrow \infty$, while keeping the ratios α_f and α_p finite. The essence of the cavity method is to expand the solutions of Eq. (9) with $M+1$ data points, N_f+1 features and N_p+1 parameters about the solutions where one quantity of each type has been removed: $(M+1, N_f+1, N_p+1) \rightarrow (M, N_f, N_p)$. These two solutions are then related using generalized self-consistency equations that can be solved for the distributions of the removed quantities. The central limit theorem then allows us to approximate any quantity defined as a sum over a large number of random variables (e.g., the training and test errors) using just distributions for the removed quantities. Furthermore, using the procedure described in Ref. [55], we use the susceptibilities resulting from the cavity method to reproduce the known closed-form solutions for the eigenvalues spectra of the kernel matrices for all three models. We refer the reader to the Supplemental Material [5] for further details on these calculations.

III. THE BIAS-VARIANCE DECOMPOSITION AND ITS GENERALIZATIONS

The bias-variance decomposition separates test error into components stemming from three distinct sources: bias, variance, and noise. Informally, bias captures a model's tendency to underfit, reflecting the erroneous assumptions made by a model that limit its ability to fully express the relationships underlying the data. On the other hand, variance captures a model's tendency to overfit, capturing characteristics of the training set that are not a reflection of the data's true relationships, but rather a by-product of random sampling (e.g., noise). As a result, a model with high variance may not generalize well to other data sets drawn from the same data distribution. Noise simply refers to an irreducible error

inherent in generating a set of test data (i.e., the label noise in the test set).

Formally, bias represents the extent to which the label predictions $\hat{y}(\vec{x})$ differs from the true function underlying the data distribution $y^*(\vec{x})$ when evaluated on an arbitrary test data point \vec{x} and averaged over all possible training sets \mathcal{D} [48],

$$\text{Bias}[\hat{y}(\vec{x})] = \mathbb{E}_{\mathcal{D}}[\hat{y}(\vec{x})] - y^*(\vec{x}). \quad (12)$$

Likewise, variance formally measures the extent to which solutions of $\hat{y}(\vec{x})$ for individual training sets \mathcal{D} vary around the average [48],

$$\text{Var}[\hat{y}(\vec{x})] = \mathbb{E}_{\mathcal{D}}[\hat{y}^2(\vec{x})] - \mathbb{E}_{\mathcal{D}}[\hat{y}(\vec{x})]^2. \quad (13)$$

Finally, the noise is simply the mean squared label noise associated with an arbitrary test data point \vec{x} ,

$$\text{Noise} = \mathbb{E}[\varepsilon^2] = \sigma_\varepsilon^2. \quad (14)$$

The standard bias-variance decomposition relates these three quantities to the test error (averaged over all possible training sets \mathcal{D}). In addition, we must take into account the fact that the test error is evaluated on M' test data points, while the bias and variance only consider a single test point. Since each test point is drawn from the same distribution, averaging the test error over all possible test sets \mathcal{D}' is equivalent to averaging the bias and variance over the point \vec{x} . This gives us the canonical bias-variance decomposition [48],

$$\mathbb{E}_{\mathcal{D}', \mathcal{D}}[\mathcal{E}_{\text{test}}] = \mathbb{E}_{\vec{x}}[\text{Bias}^2[\hat{y}(\vec{x})]] + \mathbb{E}_{\vec{x}}[\text{Var}[\hat{y}(\vec{x})]] + \sigma_\varepsilon^2. \quad (15)$$

In this work, we also consider other sources of randomness (e.g., $\vec{\beta}$ and W). To incorporate these random variables, we define the more general ensemble-averaged squared bias and variance, respectively, as

$$\begin{aligned} \langle \text{Bias}^2[\hat{y}] \rangle &= \mathbb{E}_{\vec{\beta}, W, \vec{x}}[\text{Bias}[\hat{y}(\vec{x})]^2] \\ &= \mathbb{E}_{\vec{\beta}, W, \vec{x}}[(\mathbb{E}_{X, \vec{\varepsilon}}[\hat{y}(\vec{x})] - y^*(\vec{x}))^2] \end{aligned} \quad (16)$$

$$\begin{aligned} \langle \text{Var}[\hat{y}] \rangle &= \mathbb{E}_{\vec{\beta}, W, \vec{x}}[\text{Var}[\hat{y}(\vec{x})]] \\ &= \mathbb{E}_{\vec{\beta}, W, \vec{x}}[\mathbb{E}_{X, \vec{\varepsilon}}[\hat{y}^2(\vec{x})] - \mathbb{E}_{X, \vec{\varepsilon}}[\hat{y}(\vec{x})]^2] \end{aligned} \quad (17)$$

where we have explicitly included all random variables considered in this work. All analytic expressions we report are ensemble-averaged (denoted by angle brackets $\langle \cdot \rangle$) and utilize the ensemble-averaged bias-variance decomposition of the test error,

$$\langle \mathcal{E}_{\text{test}} \rangle = \langle \text{Bias}^2[\hat{y}] \rangle + \langle \text{Var}[\hat{y}] \rangle + \sigma_\varepsilon^2. \quad (18)$$

By fixing any parameters that do not pertain to the random sampling process of the test or training data (in this case, $\vec{\beta}$ and W), this formula properly reduces to the canonical bias-variance decomposition in Eq. (15).

Much of the confusion in recent literature can be attributed to two sources. The first is the precise definition of what we call the *sampling average* in the above equations for bias and variance, denoted by subscript \mathcal{D} . The sampling average considers sources of variation from sampling the training data given a particular data distribution (i.e., keeping the set of ground truth parameters $\vec{\beta}$ fixed). This average includes both the noise associated with the labels of the training data $\vec{\epsilon}$ and the set of input features under consideration X . Non-standard definitions that disregard the latter – such as the so-called fixed-design setting [17, 19, 27, 29, 30, 33, 39] – can result in bizarre behavior such as bias that diverges at the interpolation threshold [19, 39]. This counter-intuitive result arises because fixing the design matrix for the training set in the sampling average, but not elsewhere, can cause a mismatch between the data distributions for the training and test sets, introducing an artificial source of bias.

The second source of confusion arises from the desire to incorporate additional sources of randomness into the definitions of bias and variance. These additional “ensemble” variables can include parameters that determine the data distribution itself (e.g., the ground truth parameters $\vec{\beta}$), random parameters associated with the model (e.g., the random weights W), fluctuations associated with optimization (such as in stochastic gradient descent), etc. In general, all sources of randomness contribute to the ensemble of learning problems under consideration. However, only the noise and input features of the training set contribute to the sampling average. Therefore, any averages over quantities that do not contribute to the randomness of the sampling process must be performed *after* any sampling averages are evaluated. In particular, many recent studies include the random initialization of the hidden layer via W as part of the sampling average [17, 25, 26, 30, 37, 43]. Whether intentional or not, this choice can be interpreted as fixing the model architecture, while including an additional source of noise in the data distribution characterized by a random transformation of the input features by W . This makes it unclear which properties of the bias and variance stem from the model architecture or initialization (W) as opposed to the random sampling of the data ($\vec{\epsilon}$ and X).

A. Label Decomposition

Here, we introduce a decomposition of the labels in Eq. (1), which applies to any teacher model with true labels of the form given by Eq. (2),

$$y(\vec{x}) = \vec{x} \cdot \vec{\beta} + \delta y_{\text{NL}}^*(\vec{x}) + \epsilon \quad (19)$$

where we have explicitly defined $\vec{\beta}$ as

$$\vec{\beta} \equiv \Sigma_{\vec{x}}^{-1} \text{Cov}_{\vec{x}}[\vec{x}, y^*(\vec{x})]. \quad (20)$$

The notation $\text{Cov}_{\vec{x}}[\cdot, \cdot]$ represents the covariance evaluated with respect to the distribution of input features and we define $\Sigma_{\vec{x}} \equiv \text{Cov}_{\vec{x}}[\vec{x}, \vec{x}^T]$ as the covariance matrix of the input features (assumed to be invertible).

The first term of $y(\vec{x})$ captures the linear correlations between the input features \vec{x} and the true labels y^* , as characterized by the parameters $\vec{\beta}$. As a result of normalizing y^* according to Eq. (2), the parameters $\vec{\beta}$ as defined in Eq. (20) are identical to the ground truth parameters in the thermodynamic limit (see Sec. S1C of Supplemental Material [5]). The second term $\delta y_{\text{NL}}^*(\vec{x})$ captures the remaining nonlinear component of y^* [defined as $\delta y_{\text{NL}}^*(\vec{x}) \equiv y^*(\vec{x}) - \vec{x} \cdot \vec{\beta}$] and is statistically independent of the linear term with respect to the distribution of input features (see Sec. S1C of Supplemental Material [5]). Furthermore, $\delta y_{\text{NL}}^*(\vec{x})$ has zero mean (since the labels are centered with zero mean) and we define its variance as $\sigma_{\delta y^*}^2$. Previously it was observed that $\delta y_{\text{NL}}^*(\vec{x})$ can be approximated as a Gaussian process with the previously stated statistical properties [39]. Here, we note that it is not necessary to make this assumption, as the properties of $\delta y_{\text{NL}}^*(\vec{x})$ follow naturally from defining $\vec{\beta}$ as in Eq. (20).

Since all three terms in the label decomposition are statistically independent with zero mean, the average training error, test error, bias, and variance all decompose according to these three terms. The contribution of each term to these quantities is proportional to its respective variance, which allows us to simply read off the sources of each type of error from our analytic results. In particular, the contributions of the linear components of the labels are proportional to $\sigma_{\vec{\beta}}^2$, the contributions of the nonlinear components of the labels are proportional to $\sigma_{\delta y^*}^2$, and the contributions of the label noise are proportional to σ_{ϵ}^2 .

B. Hidden Feature Decomposition

We also decompose the hidden features in Eq. (5) in a manner similar to that of the labels

$$\vec{z}(\vec{x}) = \frac{\mu_z}{\sqrt{N_p}} \vec{1} + W^T \vec{x} + \delta \vec{z}_{\text{NL}}(\vec{x}) \quad (21)$$

where we have explicitly defined W as

$$W \equiv \Sigma_{\vec{x}}^{-1} \text{Cov}_{\vec{x}}[\vec{x}, \vec{z}(\vec{x})^T]. \quad (22)$$

The first term of $\vec{z}(\vec{x})$ is defined as the mean of each hidden feature with respect to the distribution of input features, where $\vec{1}$ is a length- N_p vector of ones. Analogously to the label decomposition, the second term of Eq. (21) captures the linear correlations between the input features \vec{x} and the hidden features $\vec{z}(\vec{x})$ via the matrix of parameters W . Again, normalizing $\vec{z}(\vec{x})$ according to Eq. (5) allows us to identify W as the same matrix used in the definitions of the two random features models in the thermodynamic limit with $W = I_{N_f}$

in the case of linear regression (see Sec. S1C of Supplemental Material [5]). The third term $\delta\vec{z}_{\text{NL}}(\vec{x})$ captures the remaining nonlinear component of $\vec{z}(\vec{x})$ [defined as $\delta\vec{z}_{\text{NL}}(\vec{x}) \equiv \vec{z}(\vec{x}) - \mu_z \vec{1}/\sqrt{N_p} - W^T \vec{x}$] and is statistically independent of the linear term with respect to the distribution of input features (see Sec. S1C of Supplemental Material [5]). Furthermore, $\delta\vec{z}_{\text{NL}}(\vec{x})$ has zero mean and we define its variance as $\sigma_{\delta z}^2$. Like the nonlinear teacher model, it was previously observed that the nonlinear component of the hidden features behaves like a Gaussian process with the previously stated statistical properties [39], and this approximation has since been used as a common trick to attain closed-form solutions for nonlinear models. Here, we find that this approximation naturally follows as a result of defining W as in Eq. (22).

This decomposition allows us to read off the contributions of the linear and nonlinear components of the hidden features to the training error, test error, bias, and variance. Since our labels are centered and we do not include a y -intercept in our model, the mean of $\vec{z}(\vec{x})$ represented by the first term does not appear in our analytic solutions. The contributions of the linear hidden feature component are proportional to σ_W^2 , while the contributions of the nonlinear hidden feature component are

proportional to $\sigma_{\delta z}^2$.

IV. RESULTS

In this section, we provide analytic expressions for the training error, test error, bias, and variance, along with partial comparisons to numerical results. We limit ourselves to simply discussing major features of our analytic expressions, deferring a discussion of the implications of these results to the next section. Analytic derivations and complete comparisons to numerical results are left to Secs. S1 and S7, respectively, of the Supplemental Material [5].

A. Linear Regression

We start by presenting results for linear regression (no basis functions). Generally, our solutions are most naturally expressed in terms of $\alpha_f = N_f/M$, the ratio of input features to training data points, and $\alpha_p = N_p/M$, the ratio of fit parameters to training data points. However, in this case, the input and hidden features coincide ($N_f = N_p$), so all expressions depend only on α_f . The ensemble-averaged training error, test error, bias, and variance for linear regression are:

$$\langle \mathcal{E}_{\text{train}} \rangle = \begin{cases} (\sigma_\varepsilon^2 + \sigma_{\delta y^*}^2)(1 - \alpha_f) & \text{if } N_f < M \\ 0 & \text{if } N_f > M \end{cases} \quad (23)$$

$$\langle \mathcal{E}_{\text{test}} \rangle = \begin{cases} (\sigma_\varepsilon^2 + \sigma_{\delta y^*}^2) \frac{1}{(1 - \alpha_f)} & \text{if } N_f < M \\ \sigma_\beta^2 \sigma_X^2 \frac{(\alpha_f - 1)}{\alpha_f} + (\sigma_\varepsilon^2 + \sigma_{\delta y^*}^2) \frac{\alpha_f}{(\alpha_f - 1)} & \text{if } N_f > M \end{cases} \quad (24)$$

$$\langle \text{Bias}^2[\hat{y}] \rangle = \begin{cases} \sigma_{\delta y^*}^2 & \text{if } N_f < M \\ \sigma_\beta^2 \sigma_X^2 \frac{(\alpha_f - 1)^2}{\alpha_f^2} + \sigma_{\delta y^*}^2 & \text{if } N_f > M \end{cases} \quad (25)$$

$$\langle \text{Var}[\hat{y}] \rangle = \begin{cases} (\sigma_\varepsilon^2 + \sigma_{\delta y^*}^2) \frac{\alpha_f}{(1 - \alpha_f)} & \text{if } N_f < M \\ \sigma_\beta^2 \sigma_X^2 \frac{(\alpha_f - 1)}{\alpha_f^2} + (\sigma_\varepsilon^2 + \sigma_{\delta y^*}^2) \frac{1}{(\alpha_f - 1)} & \text{if } N_f > M, \end{cases} \quad (26)$$

where the variance of the nonlinear components of the labels $\sigma_{\delta y^*}^2$ (defined in Sec. III A) is found to depend on integrals of the true label function f in Eq. (2),

$$\sigma_{\delta y^*}^2 = \sigma_\beta^2 \sigma_X^2 \Delta f, \quad \Delta f = \frac{\langle f^2 \rangle - \langle f' \rangle^2}{\langle f' \rangle^2} \quad (27)$$

$$\langle f^2 \rangle = \frac{1}{\sqrt{2\pi}} \int_{-\infty}^{\infty} dh e^{-\frac{1}{2}h^2} f(h)^2 \quad (28)$$

$$\langle f' \rangle = \frac{1}{\sqrt{2\pi}} \int_{-\infty}^{\infty} dh e^{-\frac{1}{2}h^2} f'(h). \quad (29)$$

In writing these expressions, we have taken the ridgeless limit, $\lambda \rightarrow 0$ (when a quantity is reported as zero, leading terms of order λ^2 are reported in Sec. S1E of the Supplemental Material [5]).

In Figs. 2(a), we plot the expressions in Eqs. (23) and (24) with comparisons to numerical results for a linear teacher model $y^*(\vec{x}) = \vec{x} \cdot \vec{\beta}$ ($\sigma_{\delta y^*}^2 = 0$). We find that the model's behavior falls into two broad regimes, depending on whether $\alpha_f > 1$ or $\alpha_f < 1$ (or equivalently, $\alpha_p > 1$ or $\alpha_p < 1$, since the number of input features equals the number of fit parameters). In Fig. 2(a), we observe that below $\alpha_f = 1$, the training error is finite, decreasing monotonically as α_f increases until reaching zero at

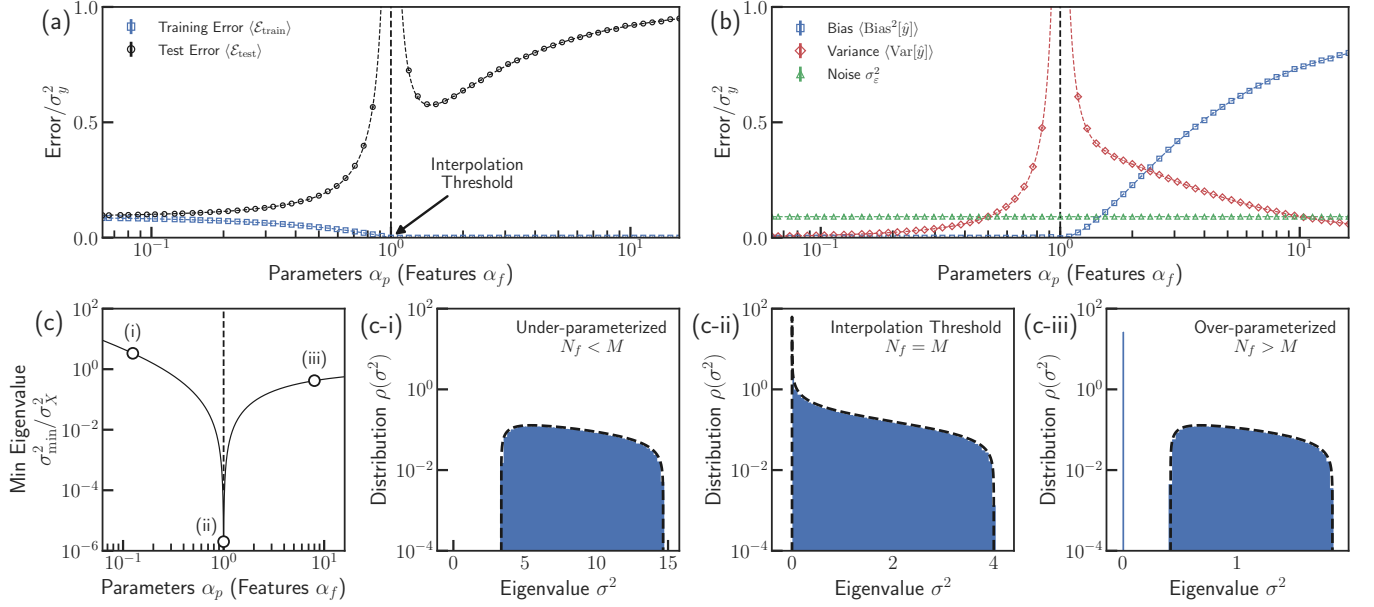


FIG. 2. Linear Regression (No Basis Functions). The ensemble-averaged (a) training error (blue squares), test error (black circles), and (b) bias-variance decomposition of test error with contributions from the squared bias (blue squares), variance (red squares), and test set label noise (green triangles), each plotted as a function of $\alpha_p = N_p/M$ (or equivalently, $\alpha_f = N_f/M$ for this model). Analytic solutions are indicated as dashed lines with numerical results shown as points with small error bars indicating the error on the mean. In each panel, a black dashed vertical line marks the interpolation threshold $\alpha_p = 1$. Results are shown for a linear teacher model $y(\vec{x}) = \vec{x} \cdot \vec{\beta} + \varepsilon$, a signal-to-noise ratio of $\sigma_\beta^2 \sigma_X^2 / \sigma_\varepsilon^2 = 10$, and have been scaled by the variance of the training set labels $\sigma_y^2 = \sigma_\beta^2 \sigma_X^2 + \sigma_\varepsilon^2$. (c) Analytic solution for the minimum eigenvalue σ_{\min}^2 of the kernel matrix $Z^T Z$. Examples of the eigenvalue distributions are shown (c-i) in the under-parameterized regime with $\alpha_p = 1/8$, (c-ii) at the interpolation threshold, $\alpha_p = 1$, and (c-iii) in the over-parameterized regime with $\alpha_p = 8$. Analytic solutions for the distributions are depicted as black dashed curves with numerical results shown as blue histograms. See Sec. S6 of Supplemental Material [5] for additional simulation details.

$\alpha_f = 1$. Beyond this threshold, the addition of extra features/parameters has no effect as the training error remains pinned at zero. Thus, $\alpha_f = 1$ corresponds to the interpolation threshold, separating the regions where the model has zero and nonzero training error, i.e., the under- and over-parameterized regimes. At the interpolation threshold, the test error diverges [Fig. 2(a)], indicative of a phase transition based on the divergence of the corresponding susceptibilities in the cavity equations (see Sec. S1E of Supplemental Material [5]).

The bias and variance, reported in Eqs. (25) and (26), are plotted in Fig. 2(b) for a linear teacher model. When $\alpha_f \leq 1$, the bias is zero. This can be understood by noting that the teacher and student models match and there are more data points than parameters (i.e., we are working in a regime where intuitions for classical statistics apply). In this regime, the variance increases monotonically as α_f is increased, diverging at the interpolation threshold as the model succumbs to overfitting. However, when $\alpha_f > 1$, the variance exhibits the opposite behavior, decreasing monotonically as α_f is increased. The bias, on the other hand, *increases* monotonically towards the limit $\sigma_\beta^2 \sigma_X^2 + \sigma_{\delta y^*}^2$ as α_f goes to infinity. Consequently, the test error in the over-parameterized regime is characterized by a surprising “inverted bias-variance

trade-off” where the bias increases with model complexity while the variance decreases.

For a nonlinear teacher model, we observe that the contribution of the nonlinear label components $\sigma_{\delta y^*}^2$ is characterized by the quantity Δf , which can be interpreted as the ratio of the average sizes of the nonlinear and linear components of the labels $\Delta f = \sigma_{\delta y^*}^2 / \sigma_\beta^2 \sigma_X^2$. In the linear limit, $f(h) = h$, the integrals evaluate to $\langle f^2 \rangle = 1$ and $\langle f' \rangle = 1$, resulting in $\Delta f = 0$ and $\sigma_{\delta y^*}^2 = 0$ as expected. In the solutions for the training error, test error, and variance, we observe that the nonlinear label component $\sigma_{\delta y^*}^2$ always appears as an additive component to the label noise σ_ε^2 . However, unlike the label noise, the nonlinear label component also appears in the bias as an additional irreducible term that arises as a result of attempting to fit a nonlinear data distribution with a model that is linear in the fit parameters.

Finally, in Fig. 2(c), we report the minimum nonzero eigenvalue σ_{\min}^2 of the kernel matrix $Z^T Z$, with examples of the full eigenvalue spectrum shown in Figs. 2(c-i)-(c-iii). Since $Z^T Z = X^T X$ for our model of linear regression, the eigenvalue spectrum is simply the Marchenko-Pastur distribution. Importantly, we find the interpolation threshold $\alpha_f = 1$ coincides with the point at which

σ_{\min}^2 goes to zero. In the under-parameterized regime, there is a finite gap in the eigenvalue spectrum, with no small eigenvalues. In the over-parameterized, there is also a finite gap, but instead between the bulk of the spectrum and a buildup of eigenvalues at exactly zero. We discuss the implications of these findings later in Sec. VB.

B. Random Linear Features Model

The closed-form solutions for the linear random features model are characterized by three distinct regimes, each defined by which of the following three quantities is the smallest: the size of the training set M , the number of input features N_f , or the number of fit parameters (hidden features) N_p . In terms of $\alpha_f = N_f/M$ and $\alpha_p = N_p/M$, the expressions for the training error, test error, bias, and variance are

$$\langle \mathcal{E}_{\text{train}} \rangle = \begin{cases} (\sigma_\varepsilon^2 + \sigma_{\delta y^*}^2)(1 - \alpha_f) & \text{if } N_f < N_p, M \\ \sigma_\beta^2 \sigma_X^2 \frac{(1 - \alpha_p)(\alpha_f - \alpha_p)}{\alpha_f} + (\sigma_\varepsilon^2 + \sigma_{\delta y^*}^2)(1 - \alpha_p) & \text{if } N_p < N_f, M \\ 0 & \text{if } M < N_f, N_p \end{cases} \quad (30)$$

$$\langle \mathcal{E}_{\text{test}} \rangle = \begin{cases} (\sigma_\varepsilon^2 + \sigma_{\delta y^*}^2) \frac{1}{(1 - \alpha_f)} & \text{if } N_f < N_p, M \\ \sigma_\beta^2 \sigma_X^2 \frac{(\alpha_f - \alpha_p)}{\alpha_f(1 - \alpha_p)} + (\sigma_\varepsilon^2 + \sigma_{\delta y^*}^2) \frac{1}{(1 - \alpha_p)} & \text{if } N_p < N_f, M \\ \sigma_\beta^2 \sigma_X^2 \frac{\alpha_p(\alpha_f - 1)}{\alpha_f(\alpha_p - 1)} + (\sigma_\varepsilon^2 + \sigma_{\delta y^*}^2) \frac{(\alpha_f \alpha_p - 1)}{(\alpha_f - 1)(\alpha_p - 1)} & \text{if } M < N_f, N_p \end{cases} \quad (31)$$

$$\langle \text{Bias}^2[\hat{y}] \rangle = \begin{cases} \sigma_{\delta y^*}^2 & \text{if } N_f < N_p, M \\ \sigma_\beta^2 \sigma_X^2 \frac{(\alpha_f - \alpha_p)}{\alpha_f} + \sigma_{\delta y^*}^2 & \text{if } N_p < N_f, M \\ \sigma_\beta^2 \sigma_X^2 \frac{\alpha_p(\alpha_f - 1)^2}{\alpha_f(\alpha_f \alpha_p - 1)} + \sigma_{\delta y^*}^2 & \text{if } M < N_f, N_p \end{cases} \quad (32)$$

$$\langle \text{Var}[\hat{y}] \rangle = \begin{cases} (\sigma_\varepsilon^2 + \sigma_{\delta y^*}^2) \frac{\alpha_f}{(1 - \alpha_f)} & \text{if } N_f < N_p, M \\ \sigma_\beta^2 \sigma_X^2 \frac{\alpha_p(\alpha_f - \alpha_p)}{\alpha_f(1 - \alpha_p)} + (\sigma_\varepsilon^2 + \sigma_{\delta y^*}^2) \frac{\alpha_p}{(1 - \alpha_p)} & \text{if } N_p < N_f, M \\ \sigma_\beta^2 \sigma_X^2 \frac{\alpha_p(\alpha_f - 1)(\alpha_f - 1 + \alpha_p - 1)}{\alpha_f(\alpha_p - 1)(\alpha_f \alpha_p - 1)} + (\sigma_\varepsilon^2 + \sigma_{\delta y^*}^2) \frac{(\alpha_f - 1 + \alpha_p - 1)}{(\alpha_f - 1)(\alpha_p - 1)} & \text{if } M < N_f, N_p, \end{cases} \quad (33)$$

where we have once again taken the limit $\lambda \rightarrow 0$ (with leading order terms of order λ^2 reported in Sec. S1F of the Supplemental Material [5] for quantities reported here as zero). The variance of the nonlinear components of the labels $\sigma_{\delta y^*}^2$ is the same as for linear regression, given by Eqs. (27)-(29).

In Figs. 3(a) and (b), we plot the bias-variance decomposition of the test error as a function of α_p for fixed α_f for the two cases $\alpha_f < 1$ and $\alpha_f > 1$, respectively. To gain a better grasp of the full set of solutions, we also plot all quantities in Eqs. (30)-(33) as a function of both α_p and α_f in Figs. 3(c)-(f). All solutions are once again shown for a linear teacher model $y^*(\vec{x}) = \vec{x} \cdot \vec{\beta}$ ($\sigma_{\delta y^*}^2 = 0$). Examining the training error in Fig. 3(c), we find that it goes to zero when both $\alpha_p \geq 1$ and $\alpha_f \geq 1$ (i.e., when the number of data points is less than both the number of input features and fit parameters), giving rise to an interpolation boundary, rather than a single threshold. As a result of this piece-wise boundary, a model can never achieve zero error on the training data set – even with an infinite number of fit parameters – as long as $\alpha_f < 1$. In other words, a model is only over-parameterized when there are both more input features *and* fit parameter than data points.

Once again, the boundaries between the three dif-

ferent solutions correspond to phase transitions marked by diverging susceptibilities in the cavity equations (see Sec. S1F of Supplemental Material [5]). Furthermore, the test error [Fig. 3(d)] diverges along the entire interpolation boundary. Examining Figs. 3(a) and (b), we find that the test error exhibits very different behavior as a function of α_p , depending on whether $\alpha_f < 1$ (more data points than input features $M > N_f$) or $\alpha_f > 1$ (less data points than input features $N_f > M$). When $\alpha_f > 1$, the test error diverges at $\alpha_p = 1$ and decreases monotonically in the over-parameterized regime. In contrast, when $\alpha_f < 1$, the test error monotonically decreases to a small, constant value when α_p is large. Although this model does not display the full canonical double-descent behavior in either case, the test error in the over-parameterized regime is always at least as small as – if not smaller than – that of the under-parameterized regime. The fact that this is not true for linear regression without basis functions indicates that the mismatch between the input and hidden features ($N_f \neq N_p$) plays a crucial role in the success of over-parameterized models.

Consistent with linear regression, we find that the divergence in the test error is solely due to a divergence in the variance [Fig. 3(f)], while the bias always remains finite [Fig. 3(e)]. In addition, examining the bias in this

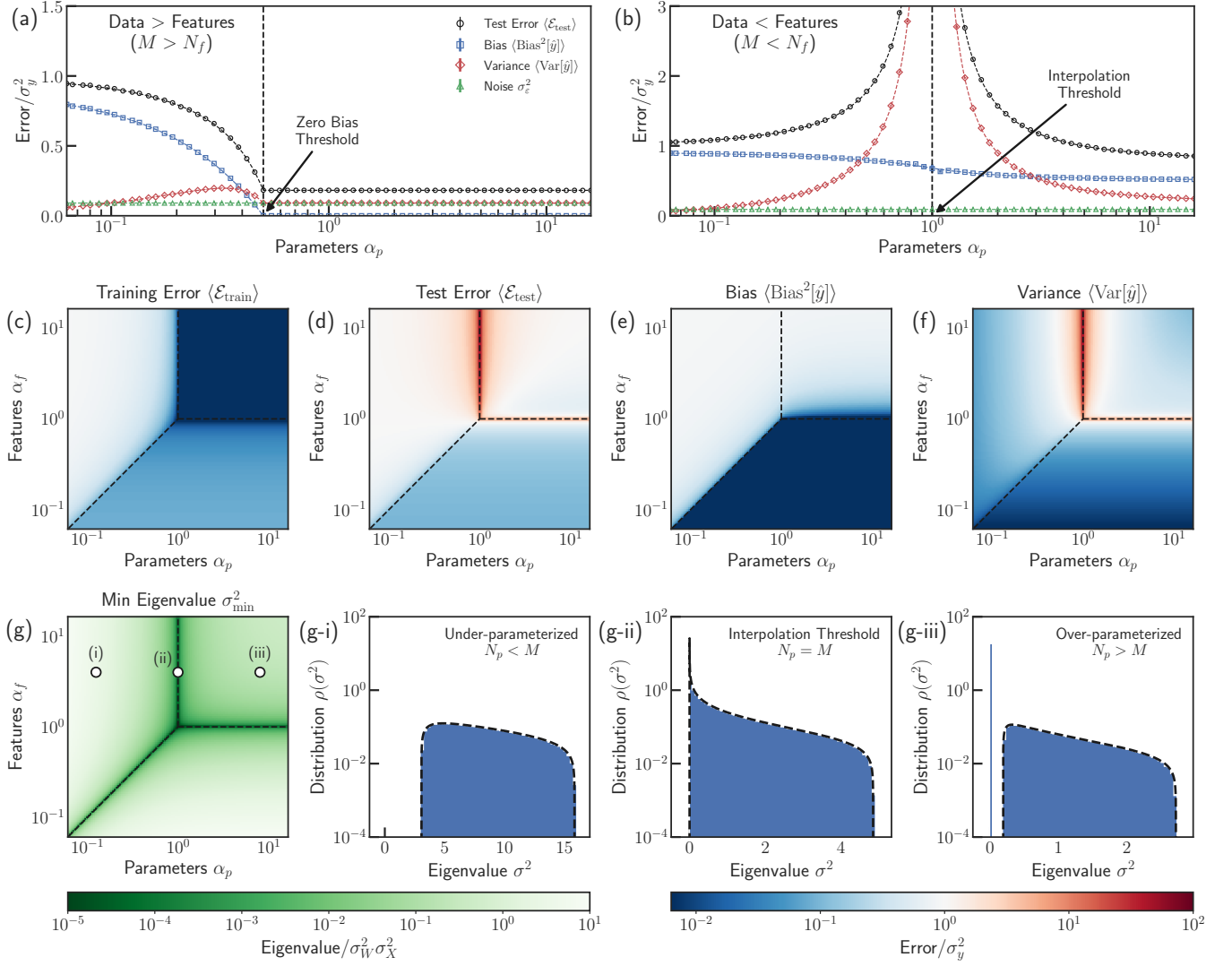


FIG. 3. Random Linear Features Model (Two-layer Linear Neural Network). Solutions for the bias-variance decomposition of the test error plotted as a function of $\alpha_p = N_p/M$ with fixed (a) $\alpha_f = 1/2$ and (b) $\alpha_f = 4$. Shown are the ensemble-averaged test error (black circles), squared bias (blue squares), variance (red diamonds), and test set label noise (green triangles). Analytic solutions are indicated as dashed lines with numerical results shown as points. In (a), a black dashed vertical line marks the boundary between the biased and unbiased regimes (for a linear teacher model) at $\alpha_p = \alpha_f$, while in (b), a similar line marks the boundary between the under- and over-parameterized regimes at $\alpha_p = 1$. Analytic solutions as a function of $\alpha_p = N_p/M$ and $\alpha_f = N_f/M$ are also shown for the ensemble-averaged (c) training error, (d) test error, (e) squared bias, and (f) variance. Results are shown for a linear teacher model $y(\vec{x}) = \vec{x} \cdot \vec{\beta} + \epsilon$, a signal-to-noise ratio of $\sigma_\beta^2 \sigma_X^2 / \sigma_\epsilon^2 = 10$, and have been scaled by the variance of the training set labels $\sigma_y^2 = \sigma_\beta^2 \sigma_X^2 + \epsilon^2$. In each panel, black dashed lines indicate boundaries between different regimes of the solutions depending on which is the smallest of the quantities M , N_f , or N_p . The vertical and horizontal lines bound the interpolation, or over-parameterized, regime, located at $\alpha_p \geq 1$ and $\alpha_f \geq 1$, while the diagonal line marks the boundary between the biased and unbiased regimes for a linear teacher model. (g) Analytic solution for the minimum eigenvalue σ_{\min}^2 of the kernel matrix $Z^T Z$. Examples of the eigenvalue distributions are shown (g-i) in the under-parameterized regime with $\alpha_p = 1/8$, (g-ii) at the interpolation threshold, $\alpha_p = 1$, and (g-iii) in the over-parameterized regime with $\alpha_p = 8$, all for $\alpha_f = 4$. Analytic solutions for the distributions are shown as black dashed lines with numerical results shown as blue histograms. See Sec. S6 of Supplemental Material [5] for additional simulation details.

model reveals that there is an additional phase transition located at the boundary $\alpha_f = \alpha_p$ for $\alpha_p \leq 1$ and $\alpha_f \leq 1$ (i.e., when the number of input features N_f equals the number of hidden features N_p , with both N_f and N_p less

than the number of data points). For a linear teacher model, this transition divides the non-interpolation solutions into two pieces: a biased regime where $\alpha_p < \alpha_f$ (N_p is smaller than both N_f and M) and an unbiased regime

where $\alpha_p > \alpha_f$ (N_f is smaller than both N_p and M). For a nonlinear teacher model, both regimes also contain an additional constant bias $\sigma_{\delta y^*}^2$ due to the nonlinear components of the labels. Just as in linear regression, this nonlinearity also contributes to the training error, test error, and variance as an additive component to the label noise.

In Fig. 3(g), we also report the minimum nonzero eigenvalue σ_{\min}^2 of the kernel matrix $Z^T Z$ as a function of both α_p and α_f . We find that σ_{\min}^2 approaches zero at each of the three boundaries marking the phase transitions between different regimes. In Figs. 3(g-i)-(g-iii), we show examples of the full eigenvalue spectrum for $\alpha_f > 1$ for the under- and over-parameterized regimes, along with the interpolation threshold. We find that the spectra in these three cases are qualitatively similar to those in Figs. 2(c-i)-(c-iii) for the Marchenko-Pastur distribution.

C. Random Nonlinear Features Model

To represent the closed-form solutions for the random nonlinear features model, we first derive general forms for the training error, test error, bias, and variance that apply to all three models. To start, we decompose the expression for a predicted label for an arbitrary data point \vec{x} in Eq. (11). Using Eq. (21), we decompose the hidden features $\vec{z}(\vec{x})$ used to construct the label prediction, giving us

$$\hat{y}(\vec{x}) = \vec{x} \cdot \hat{\beta} + \frac{\mu_Z}{\sqrt{N_p}} \sum_J \hat{w}_J + \delta \vec{z}_{\text{NL}}(\vec{x}) \cdot \hat{\mathbf{w}}. \quad (34)$$

Here, we have defined the vector $\hat{\beta} \equiv W \hat{\mathbf{w}}$, which can be interpreted as the set of N_f ground truth parameters estimated by the model. To see this, we note that $\hat{\beta}$ can be defined analogously to $\vec{\beta}$ in Eq. (20) as capturing the correlations between the input features and the label predictions (see Sec. S2 of Supplemental Material [5] for proof),

$$\hat{\beta} \equiv \Sigma_{\vec{x}}^{-1} \text{Cov}_{\vec{x}}[\vec{x}, \hat{y}(\vec{x})]. \quad (35)$$

We also define the residual parameter error $\Delta \vec{\beta} \equiv \vec{\beta} - \hat{\beta}$. In analogy to the test error, it is possible to define the average parameter error $\mathcal{E}_{\text{param}} = \|\Delta \vec{\beta}\|^2 / N_f$ to characterize the accuracy of $\hat{\beta}$ in estimating $\vec{\beta}$. In Sec. S2 of the Supplemental Material [5], we discuss how this parameter error can be decomposed into a parameter bias and parameter variance which are intimately related to the test error, bias, and variance for the label error discussed here.

Using the above decomposition of the label predictions, along with the decompositions of the labels in Eq. (19) and the hidden features in Eq. (21), we express the training error, test error, bias, and variance in terms of a set

of five key ensemble-averaged quantities, $\langle \Delta y^2 \rangle$, $\langle \Delta \beta^2 \rangle$, $\langle \hat{w} \rangle^2$, $\langle \Delta \beta_1 \Delta \beta_2 \rangle$, and $\langle \hat{w}_1 \hat{w}_2 \rangle$,

$$\langle \mathcal{E}_{\text{train}} \rangle = \langle \Delta y^2 \rangle \quad (36)$$

$$\langle \mathcal{E}_{\text{test}} \rangle = \sigma_X^2 \langle \Delta \beta^2 \rangle + \sigma_{\delta z}^2 \langle \hat{w} \rangle^2 + \sigma_{\delta y^*}^2 + \sigma_\epsilon^2 \quad (37)$$

$$\langle \text{Bias}^2[\hat{y}] \rangle = \sigma_X^2 \langle \Delta \beta_1 \Delta \beta_2 \rangle + \sigma_{\delta z}^2 \langle \hat{w}_1 \hat{w}_2 \rangle + \sigma_{\delta y^*}^2 \quad (38)$$

$$\langle \text{Var}[\hat{y}] \rangle = \sigma_X^2 [\langle \Delta \beta^2 \rangle - \langle \Delta \beta_1 \Delta \beta_2 \rangle] + \sigma_{\delta z}^2 [\langle \hat{w}^2 \rangle - \langle \hat{w}_1 \hat{w}_2 \rangle], \quad (39)$$

where the variance of the nonlinear components of the hidden features $\sigma_{\delta z}^2$ (defined in Sec. IIIB) is found to depend on integrals of the activation function φ ,

$$\sigma_{\delta z}^2 = \sigma_W^2 \sigma_X^2 \Delta \varphi, \quad \Delta \varphi = \frac{\langle \varphi^2 \rangle - \langle \varphi \rangle^2 - \langle \varphi' \rangle^2}{\langle \varphi' \rangle^2} \quad (40)$$

$$\langle \varphi^2 \rangle = \frac{1}{\sqrt{2\pi}} \int_{-\infty}^{\infty} dh e^{-\frac{1}{2}h^2} \varphi(h)^2 \quad (41)$$

$$\langle \varphi \rangle = \frac{1}{\sqrt{2\pi}} \int_{-\infty}^{\infty} dh e^{-\frac{1}{2}h^2} \varphi(h) \quad (42)$$

$$\langle \varphi' \rangle = \frac{1}{\sqrt{2\pi}} \int_{-\infty}^{\infty} dh e^{-\frac{1}{2}h^2} \varphi'(h), \quad (43)$$

and the variance of the nonlinear components of the labels $\sigma_{\delta y^*}^2$ is again the same as for linear regression [Eqs. (27)-(29)].

The quantities $\langle \Delta y^2 \rangle$ and $\langle \Delta \beta^2 \rangle$ are the mean squared residual error of the predicted training labels and the estimated parameters, respectively, while $\langle \hat{w}^2 \rangle$ is the mean squared fit parameter size. The quantities $\langle \Delta \beta_1 \Delta \beta_2 \rangle$ and $\langle \hat{w}_1 \hat{w}_2 \rangle$ measure the covariances of the residual parameter errors and fit parameters, respectively, between identical models trained on different training sets drawn independently from the same data distribution (see Sec. S1G of Supplemental Material [5]). In addition, we have dropped terms proportional to μ_Z since we find the mean value of the fit parameters $\sum_J \hat{w}_J / N_p$ to be zero in the thermodynamic limit for centered labels with zero mean.

In the same way that the nonlinear components of the labels $\sigma_{\delta y^*}^2$ are characterized by the quantity Δf , we find that the nonlinear nature of the activation function φ represented by $\sigma_{\delta z}^2$ is characterized by the quantity $\Delta \varphi$, the ratio of the average sizes of the nonlinear and linear components of the hidden features $\Delta \varphi = \sigma_{\delta z}^2 / \sigma_W^2 \sigma_X^2$. For ReLU activation via the form $\varphi(h) = \max(h, 0)$, we find that the integrals of φ evaluate to $\langle \varphi^2 \rangle = 1/2$, $\langle \varphi \rangle = 1/\sqrt{2\pi}$, and $\langle \varphi' \rangle = 1/2$, resulting in $\Delta \varphi = 1 - 2/\pi$. Eqs. (36)-(39) also describe the behavior of the random linear features model for the special case of a linear activation function, $\varphi(h) = h$, where as expected, the integrals evaluate to $\langle \varphi^2 \rangle = 1$, $\langle \varphi \rangle = 0$, and $\langle \varphi' \rangle = 1$, resulting in $\Delta \varphi = 0$ and $\sigma_{\delta z}^2 = 0$. Furthermore, this

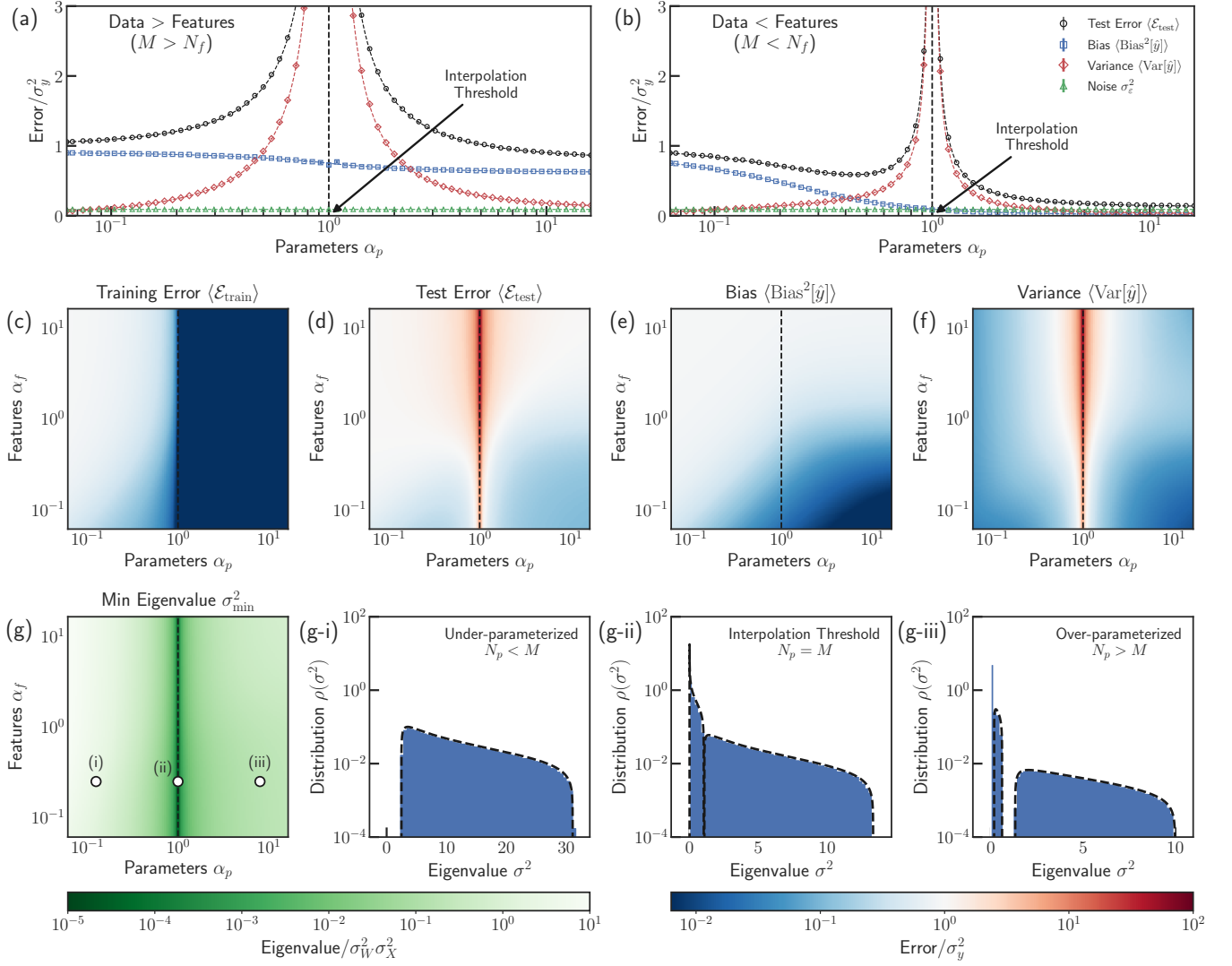


FIG. 4. **Random Nonlinear Features Model (Two-layer Nonlinear Neural Network).** Analytic solutions for the bias-variance decomposition of the test error plotted as a function of $\alpha_p = N_p/M$ with fixed (a) $\alpha_f = 1/4$ and (b) $\alpha_f = 4$. Shown are the ensemble-averaged test error (black circles), squared bias (blue squares), variance (red diamonds), and test set label noise (green triangles). Analytic solutions are indicated as dashed lines with numerical results shown as points. Analytic solutions as a function of $\alpha_p = N_p/M$ and $\alpha_f = N_f/M$ are also shown for the ensemble-averaged (c) training error, (d) test error, (e) squared bias, and (f) variance. Results are shown for a linear teacher model $y(\vec{x}) = \vec{x} \cdot \vec{\beta} + \varepsilon$, a signal-to-noise ratio of $\sigma_{\beta}^2 \sigma_X^2 / \sigma_{\varepsilon}^2 = 10$, and have been scaled by the variance of the training set labels $\sigma_y^2 = \sigma_{\beta}^2 \sigma_X^2 + \varepsilon^2$. In all panels, a black dashed line marks the boundary between the under- and over-parameterized regimes at $\alpha_p = 1$. (g) Analytic solution for the minimum eigenvalue σ_{\min}^2 of the kernel matrix $Z^T Z$. Examples of the eigenvalue distributions are shown (g-i) in the under-parameterized regime with $\alpha_p = 1/8$, (g-ii) at the interpolation threshold, $\alpha_p = 1$, and (g-iii) in the over-parameterized regime with $\alpha_p = 8$, all for $\alpha_p = 1/4$. Analytic solutions for the distributions are shown as black dashed lines with numerical results shown as blue histograms. See Sec. S6 of Supplemental Material [5] for additional simulation details.

linear limit also applies to linear regression if we identify the estimated ground truth parameters with the fit parameter themselves, $\hat{\beta} = \hat{\mathbf{w}}$.

The solutions for the five averages used to express the solutions in Eqs. (36)-(39) are in turn related to a set of five scalar susceptibilities that are a natural result of

the cavity method, ν , χ , κ , ω , and ϕ . Each of these susceptibilities is defined as the ensemble average of the trace of a different susceptibility matrix which measures the responses of quantities such as the residual label error, residual parameter error, fit parameter values, etc., to small perturbations (see Sec. V E). Collectively, the ensemble-averaged quantities satisfy the equations

$$\begin{pmatrix} \langle \hat{w}^2 \rangle \\ \langle \hat{u}^2 \rangle \\ \langle \Delta y^2 \rangle \\ \langle \Delta \beta^2 \rangle \end{pmatrix} = \begin{pmatrix} 1 & -\sigma_W^2 \frac{\alpha_f}{\alpha_p} \nu^2 & -\sigma_{\delta z}^2 \alpha_p^{-1} \nu^2 & 0 \\ -\sigma_W^2 \omega^2 & 1 & -\sigma_X^2 \alpha_f^{-1} \kappa^2 & 0 \\ -\sigma_{\delta z}^2 \chi^2 & 0 & 1 & -\sigma_X^2 \chi^2 \\ -\sigma_W^2 \kappa^2 & 0 & -\sigma_X^2 \alpha_f^{-1} \phi^2 & 1 \end{pmatrix}^{-1} \begin{pmatrix} 0 \\ \sigma_\beta^2 \omega^2 \\ (\sigma_\varepsilon^2 + \sigma_{\delta y^*}^2) \chi^2 \\ \sigma_\beta^2 \kappa^2 \end{pmatrix} \quad (44)$$

$$\langle \hat{w}_1 \hat{w}_2 \rangle = \frac{\sigma_\beta^2}{\sigma_W^2} \frac{\sigma_W^4 \frac{\alpha_f}{\alpha_p} \omega^2 \nu^2}{\left(1 - \sigma_W^4 \frac{\alpha_f}{\alpha_p} \omega^2 \nu^2\right)}, \quad \langle \Delta \beta_1 \Delta \beta_2 \rangle = \sigma_\beta^2 \frac{\kappa^2}{\left(1 - \sigma_W^4 \frac{\alpha_f}{\alpha_p} \omega^2 \nu^2\right)}. \quad (45)$$

The quantity $\langle \hat{u}^2 \rangle$ is the mean squared average of the length- N_f vector quantity $\hat{\mathbf{u}} = \mathbf{X}^T \Delta \vec{\mathbf{y}}$ obtained as a byproduct of the cavity derivation. These equations also reduce to those for the linear random features model for a linear activation function. The solutions for linear regression can be formulated similarly in terms of a pair of scalar susceptibilities that are related to χ and ν (see

Sec. S1E of Supplemental Material [5]).

In each model, a subset of the scalar susceptibilities diverges wherever two different sets of solutions meet, indicating the existence of a second-order phase transition. For the random nonlinear features model, these susceptibilities are (to leading order in small λ)

$$\chi = \begin{cases} \frac{\lambda}{2\sigma_{\delta z}^2} \frac{\alpha_p}{(\alpha_p - 1)} \left[1 - (1 + \Delta\varphi)\alpha_f + \sqrt{[1 - (1 + \Delta\varphi)\alpha_f]^2 + 4\Delta\varphi\alpha_f} \right] & \text{if } N_p < M \\ \frac{\lambda}{2\sigma_{\delta z}^2} \frac{\alpha_p}{(1 - \alpha_p)} \left[\alpha_p - (1 + \Delta\varphi)\alpha_f + \sqrt{[\alpha_p - (1 + \Delta\varphi)\alpha_f]^2 + 4\Delta\varphi\alpha_f\alpha_p} \right] & \text{if } N_p > M \end{cases} \quad (46)$$

$$\nu = \begin{cases} \frac{1}{2\sigma_{\delta z}^2} \frac{1}{(1 - \alpha_p)} \left[\alpha_p - (1 + \Delta\varphi)\alpha_f + \sqrt{[\alpha_p - (1 + \Delta\varphi)\alpha_f]^2 + 4\Delta\varphi\alpha_f\alpha_p} \right] & \text{if } N_p < M \\ \frac{1}{\lambda} \frac{(\alpha_p - 1)}{\alpha_p} & \text{if } N_p > M \end{cases} \quad (47)$$

$$\kappa = \frac{1}{1 + \sigma_X^2 \sigma_W^2 \alpha_f^{-1} \chi \nu}, \quad \omega = \sigma_X^2 \alpha_f^{-1} \chi \kappa, \quad \phi = -\sigma_W^2 \nu \kappa. \quad (48)$$

We provide the full forms of the corresponding matrix susceptibilities for all three models in Sec. S3 of the Supplemental Material [5], along with solutions for the scalar susceptibilities for the two linear models in Sec. S1. We note that the strength of the nonlinear nature of the activation function $\Delta\varphi$ in Eqs. 46 and 47 appears in a manner analogous to the regularization parameter λ in linear regression with finite regularization (see Sec. S1G of Supplemental Material [5]). This suggests that the nonlinear activation function plays a role as a form of implicit regularization.

In Figs. 4(a) and (b), we plot the bias-variance decomposition of the test error as a function of $\alpha_p = N_p/M$ for $\alpha_f < 1$ (more data points M than input features N_f) and $\alpha_f > 1$ (less data points M than input features N_f), respectively, while in Figs. 4(c)-(f), we plot all quantities in Eqs. (36)-(39) as a function of both α_p and α_f . In all plots, we depict the special case of a linear teacher model and ReLU activation. In contrast to the linear random features model, the nonlinear model has two distinct regimes separated by the line $\alpha_p = 1$. In Fig. 4(c), we find that the training error is finite when $\alpha_p < 1$ and

goes to zero when $\alpha_p \geq 1$, marking the boundary $\alpha_p = 1$ as the interpolation threshold.

In Eqs. (46) and (47), we explicitly find that one of the susceptibilities diverges on approach from each side of the interpolation threshold, indicating a phase transition (see Sec. VE for further discussion). Fig. 4(d) shows that the test error diverges at each point along this boundary and no longer diverges when $\alpha_f = 1$ as in the linear case [Fig. 3(d)]. In addition, the test error only displays a small qualitative difference between the regimes where $\alpha_f < 1$ and $\alpha_f > 1$. As shown in Figs. 4(a) and (b), the test error appears very similar to that of the linear model when $\alpha_f > 1$, but shows a canonical double-descent behavior when $\alpha_f < 1$. As in the two linear models, the variance [Fig. 4(f)], accounts for the divergence of the test error at the phase boundaries, while the bias [Fig. 4(e)] remains finite. However, unlike the two linear models, the bias of the nonlinear model never reaches zero, even for a linear teacher model. Furthermore, the closed-form solutions show that the nonlinear components of the labels $\sigma_{\delta y^*}^2$ contribute in the same way as in the two linear models, adding a small constant irreducible bias, along

with an additive component to the label noise.

Finally, in Fig. 4(g), we report the minimum nonzero eigenvalue σ_{\min}^2 of the kernel matrix $Z^T Z$ as a function of both α_p and α_f . We find that σ_{\min}^2 approaches zero along the entire interpolation boundary $\alpha_p = 1$. In Figs. 4(g-i)-(g-iii), we show examples of the full eigenvalue spectrum for $\alpha_f < 1$ for the under- and over-parameterized regimes, along with the interpolation threshold. We find that the spectrum in the under-parameterized regime displays a finite gap that goes to zero near the interpolation threshold. In the over-parameterized regime, we find that although the gap between the buildup of eigenvalues at zero and the nonzero eigenvalues is much smaller, it is still finite. Interestingly, we also find that additional gaps can appear in the eigenvalue distribution between sets of finite-valued eigenvalues, which likely reflects the fact that ReLU activation functions result in a large fraction of zero-valued entries in Z .

V. UNDERSTANDING BIAS AND VARIANCE IN OVER-PARAMETERIZED MODELS

Having presented our analytic results, we now discuss the implications of our calculations for understanding bias and variance in a more general setting. Our discussion emphasizes the qualitatively new phenomena that are present in over-parameterized models.

A. Two sources of bias: Imperfect models and incomplete exploration of features

Traditionally, bias is viewed as a symptom of a model making incorrect assumptions about the data distribution (a mismatch between the teacher and student models). However, our calculations show that this description of the origin of bias is incomplete. A striking feature of our results is that over-parameterized models can be biased even if our statistical models are expressive enough to fully capture all relationships underlying the data. In fact, linear regression shows us that one can have a nonzero bias even if the student and teacher models are identical [e.g., $\varphi(h) = h$ with $f(h) = h$]. Even when the student and teacher model are the same, the bias is nonzero if there are more input features N_f than data points M [see $\alpha_f > 1$ region of Fig. 2(b)].

To better understand this phenomenon, it is helpful to think of the input features as spanning an N_f -dimensional space. The training data can be embedded in this N_f -dimensional input feature space by considering the eigenvectors, or principal components, of the empirical covariance matrix of input features $X^T X/M$, with X defined as the $M \times N_f$ design matrix whose rows correspond to training data points and columns to input features (see Sec. II). When there are more data points than input features ($M > N_f$), the training data will typically span the entire N_f -dimensional input feature space (i.e.,

the principal components of $X^T X$ generically span all of input feature space). In contrast, when there are fewer training data points than input features ($M < N_f$), the training data will typically span only a fraction of the entire input feature space (i.e., the principal components will span a subspace of the full N_f -dimensional input feature space). For this reason, when $M < N_f$ the model is “blind” to data that varies along these unsampled directions. Consequently, any predictions the model makes about these directions will reflect assumptions implicitly or explicitly built into the model rather than relationships learned from the training data set. This can result in a nonzero bias even when the teacher and student models are identical.

We observe similar behavior in the random linear features model [Fig. 3(e)]. When there are fewer hidden features than input features ($N_p < N_f$), the model exhibits nonzero bias even for a linear teacher model as it is not expressive enough to capture all the variation in the data distribution. Somewhat surprisingly, even if the number of hidden features is increased to exceed the number of input features ($N_p > N_f$), the random linear features model can still exhibit a nonzero bias. In particular, if the number of input features is greater than the number of data points ($N_f > M$), the model is biased even though *in principle* it is expressive enough to represent the data since $N_p > N_f$. In contrast, when there are both more data points and more hidden features than input features ($N_p, M > N_f$), the model is unbiased. The reason for this behavior is essentially the same as for linear regression since the hidden and input features are related by a linear transformation.

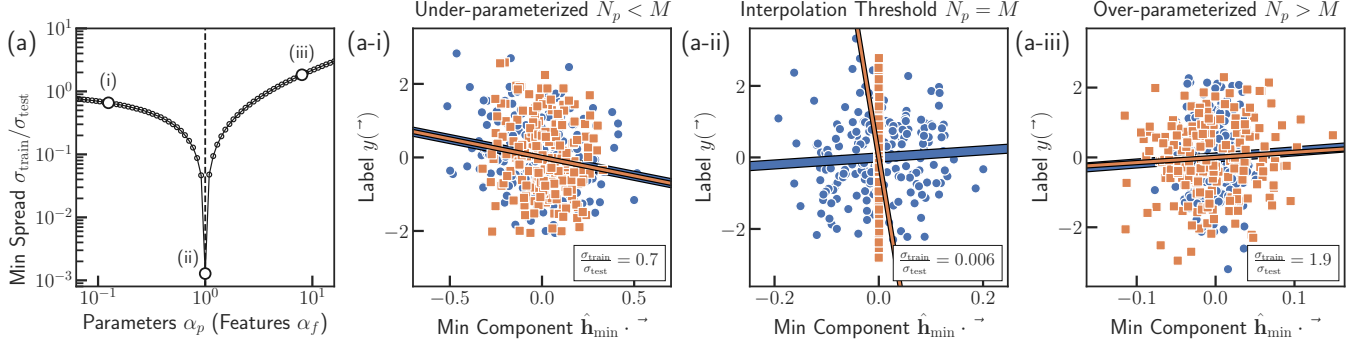
In the random nonlinear features model, the nonlinear activation function makes it impossible to perfectly represent the input features via the hidden features, even for a linear teacher model. While increasing the number of hidden features does reduce bias, the nonlinear model is never able to perfectly capture the linear nature of the data distribution and is always biased. Similarly, none of the three models are able to express the nonlinear components of the labels for a nonlinear teacher model, resulting in a constant, irreducible bias in all cases.

Finally, we wish to point out that unlike some previous studies [19, 39], we find that the bias never diverges, including at the interpolation transition. The use of non-standard definitions of bias and variance in earlier studies led to this confusion, highlighting the importance of using the standard definition from classical statistics.

B. Variance: Overfitting stems from poorly sampled direction in space of feature

Variance measures the tendency of a model to overfit, or attribute too much significance to, aspects of the training data that do not generalize to other data sets. Even when all data is drawn from the same distribution, the predictions of a trained model can vary depending on the

Linear Regression (Without Basis Functions, $N_p = N_f$)



Random Nonlinear Features Model (Two-layer Nonlinear Neural Network)

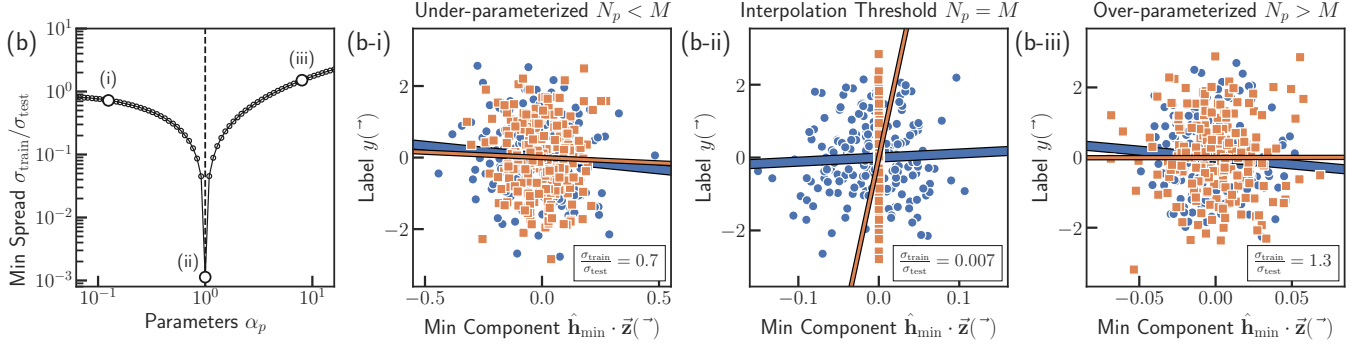


FIG. 5. **Poorly sampled directions in space of features lead to overfitting.** Demonstrations of this phenomenon are shown for (a) linear regression and (b) the random nonlinear features model. Columns (i), (ii), and (iii) correspond to models which are under-parameterized, exactly at the interpolation threshold, or over-parameterized, respectively. In each example, the relationship between the labels and the projection of their associated input or hidden features onto the minimum principal component $\hat{\mathbf{h}}_{\min}$ of $\mathbf{Z}^T \mathbf{Z}$ is depicted for a set of training data (orange squares) and a test set (blue circles). Orange lines indicate the relationship learned by a model from the training set, while the expected relationship for an average test set is shown as a blue line. In the left-most column, the spread (standard deviation) of an average training set along the x -axis, $\sigma_{\text{train}}^2 = \sigma_{\min}^2/M$, is plotted relative to the spread that would be expected for an average test set, σ_{test}^2 , for simulated data as a function of α_p . Smaller values are associated with lower prediction accuracy on out-of-sample data, coinciding with small eigenvalues in $\mathbf{Z}^T \mathbf{Z}$. See Supplemental Material [5] for analytic derivations of learned and expected relationships and spreads along minimum principal components (Sec. S5), along with additional details of numerical simulations (Sec. S6).

details of each particular training set. More specifically, a model may exhibit high variance when a direction in feature space is present in the training data, but not sampled well enough to reflect its true nature in the underlying data distribution. When presented with new data that has a significant contribution along this under-sampled direction, the model is forced to extrapolate (often incorrectly) based on the little information it can glean from the training set.

In linear regression, the empirical variance along each principal direction is explicitly measured by its associated eigenvalue in the empirical covariance matrix $\mathbf{X}^T \mathbf{X}/M$. Generally, a model's variance will be dominated by the most poorly sampled principal direction, or minimum component $\hat{\mathbf{h}}_{\min}$, corresponding to the smallest nonzero eigenvalue σ_{\min}^2 of $\mathbf{X}^T \mathbf{X}$. The projection of an arbitrary data point $\vec{\mathbf{x}}$ onto $\hat{\mathbf{h}}_{\min}$ can be found by taking a dot product, $\hat{\mathbf{h}}_{\min} \cdot \vec{\mathbf{x}}$. The observed variance of $\hat{\mathbf{h}}_{\min} \cdot \vec{\mathbf{x}}$ for

a given training set is $\sigma_{\text{train}}^2 = \sigma_{\min}^2/M$. For comparison, we define the true, or expected, variance of $\hat{\mathbf{h}}_{\min} \cdot \vec{\mathbf{x}}$ for an average test set as σ_{test}^2 , representing data points drawn from the full data distribution (see Sec. S5 of Supplemental Material [5]).

The first row of Fig. 5 shows how observing a small variance along a particular direction sampled by the training data can lead to overfitting in linear regression. In Fig. 5(a), we plot the average ratio $\sigma_{\text{train}}/\sigma_{\text{test}}$ as a function of α_p for simulated data. In Figs. 5(a-i)-(a-iii), we then plot the labels y versus $\hat{\mathbf{h}}_{\min} \cdot \vec{\mathbf{x}}$ for the training set (orange points) and an equally-sized test data set (blue points), representative of the full data distribution. In each panel, the relationship between the labels and $\hat{\mathbf{h}}_{\min} \cdot \vec{\mathbf{x}}$ as predicted by the model based on the training set is depicted as an orange line. For comparison, we also show the expected relationship for an average test set as a blue line, representing the true relationship underlying

the data (see Sec. S5 of Supplemental Material [5] for explicit formulas).

In Fig. 5(a-i), we see that when the model is under-parameterized ($N_f < M$), the spread of the training set along the minimum component is comparable to that of the test set ($\sigma_{\text{train}}/\sigma_{\text{test}} = 0.7$). Because there are more data points than input features, many of the data points are likely to contain significant contributions from each direction, including the minimum component, corresponding to a finite gap in the corresponding eigenvalue distribution depicted in Fig. 2(c-i). As a result, the training set will provide the model with an accurate representation of the data distribution along this direction in feature space. In this case, we see that the model is able to closely approximate the true relationship in the data even in the presence of noise.

However, at the interpolation threshold when the number of input features equals the number of data points ($N_f = M$), Fig. 5(a-ii) shows that the spread of the training data points along the minimum component is very narrow compared to the test data ($\sigma_{\text{train}}/\sigma_{\text{test}} \approx 0.006$), while in Fig. 2(c-ii), we observe that the gap in the eigenvalue distribution disappears. In this case, the training set contains a very small, but insufficient, amount of information about the data distribution along this direction. This poor sampling causes the model to overfit the noise of the training set, resulting in a slope that is much larger than that of the true relationship. When presented with a new data point with a significant contribution along $\hat{\mathbf{h}}_{\text{min}}$, the model will be forced to extrapolate beyond the narrow range of $\hat{\mathbf{h}}_{\text{min}} \cdot \bar{\mathbf{x}}$ observed in the training set. This extrapolation will hamper the model's ability to generalize, leading to inaccurate predictions that are highly dependent on the precise details of the noise sampled by the training set.

Surprisingly, we find in Fig. 5(a-iii) that further increasing the number of features so that the model becomes over-parameterized ($N_f > M$) actually *increases* the spread in the training data along the minimum component ($\sigma_{\text{train}}/\sigma_{\text{test}} \approx 1.9$), *reducing* the effects of overfitting. When there are more features than data points, each data point is likely to explore a never-before-seen combination of features. Naively, one would expect this to leave many of the directions poorly sampled. However, because the norm of each data point is approximately the same in the thermodynamic limit, the fact that each data point is different means that all are likely to make independent contributions of different sizes to the sampled directions, including $\hat{\mathbf{h}}_{\text{min}}$. Even if this means only a single data point contributes to the minimum component, this contribution must be of significant size for the data point to be independent of the rest. So while some directions are not represented in the training set at all, the ones that are present are typically well-sampled by at least one – if not many – data points, providing a sufficient amount of spread to reveal relationships in the underlying distribution. Consequently, the model is able to learn the true relationship between the labels and features, just as in the

under-parameterized case. We observe this phenomenon directly in the eigenvalue distribution in Fig. 2(c-iii), with a buildup of eigenvalues at exactly zero corresponding to unsampled directions accompanied by a finite gap separating these eigenvalues from the rest of the distribution. This is the underlying reason that the variance decreases with model complexity beyond the interpolation threshold. A similar observation was made in Ref. 18 in the context of ridge regression using methods from Random Matrix Theory.

In the second row of Fig. 5, we demonstrate that the same patterns also lead to overfitting in the random nonlinear features model, indicating that the intuition gained from linear regression translates directly to more complex settings. In this case, the model can be interpreted as indirectly sampling the data distribution via the empirical covariance matrix of hidden features $Z^T Z/M$. We calculate the minimum component $\hat{\mathbf{h}}_{\text{min}}$ as the principal component of $Z^T Z$ with the smallest eigenvalue. In Figs. 5(b-i)-(b-iii), we plot the labels y versus the projection of each data point's hidden features $\bar{\mathbf{z}}$ onto this minimum component $\hat{\mathbf{h}}_{\text{min}} \cdot \bar{\mathbf{z}}$, with the ratio $\sigma_{\text{train}}/\sigma_{\text{test}}$ shown in Fig. 5(b). In contrast to linear regression, we see that overfitting results from poorly sampling – or observing very limited spread along – a direction in the space of hidden features rather than input features. In the random nonlinear features model, overfitting is most pronounced when the number of hidden features matches the number of data points at the interpolation threshold ($N_p = M$), where the gap in the eigenvalue distribution at zero disappears [Fig. 4(g-ii)].

The random linear features model shows the same behavior as the nonlinear model when $N_p < N_f$ (i.e., when the model is biased due to an insufficient number of fit parameters). However, it behaves similarly to linear regression when $N_p \geq N_f$ because the linear nature of the transformation is able to preserve linear relationships in the input features. As a result, the test error does not diverge along the $N_p = N_f$ phase boundary, even though the gap in the eigenvalue spectrum disappears [Fig. 4(g)].

C. Biased models can interpret signal as noise

Typically, variance is attributed to overfitting inconsistencies in the labels due to noise in the training set. Indeed, we observe that the contribution to the variance due to noise is nonzero in each model. Surprisingly, we also find that overfitting can occur in the absence of noise when a model is biased. In each model, we observe a direct correspondence between each source of bias and a source of variance. In other words, in the absence of noise, the variance is zero only when the bias is zero.

To illustrate this, in Figs. 6(a) and (b), we plot the contributions to the bias and variance, respectively, for our model of linear regression with a nonlinear teacher model of the form $f(h) = \tanh(h)$ [see Eq. (2)]. In this case, note that our model can never fully represent the

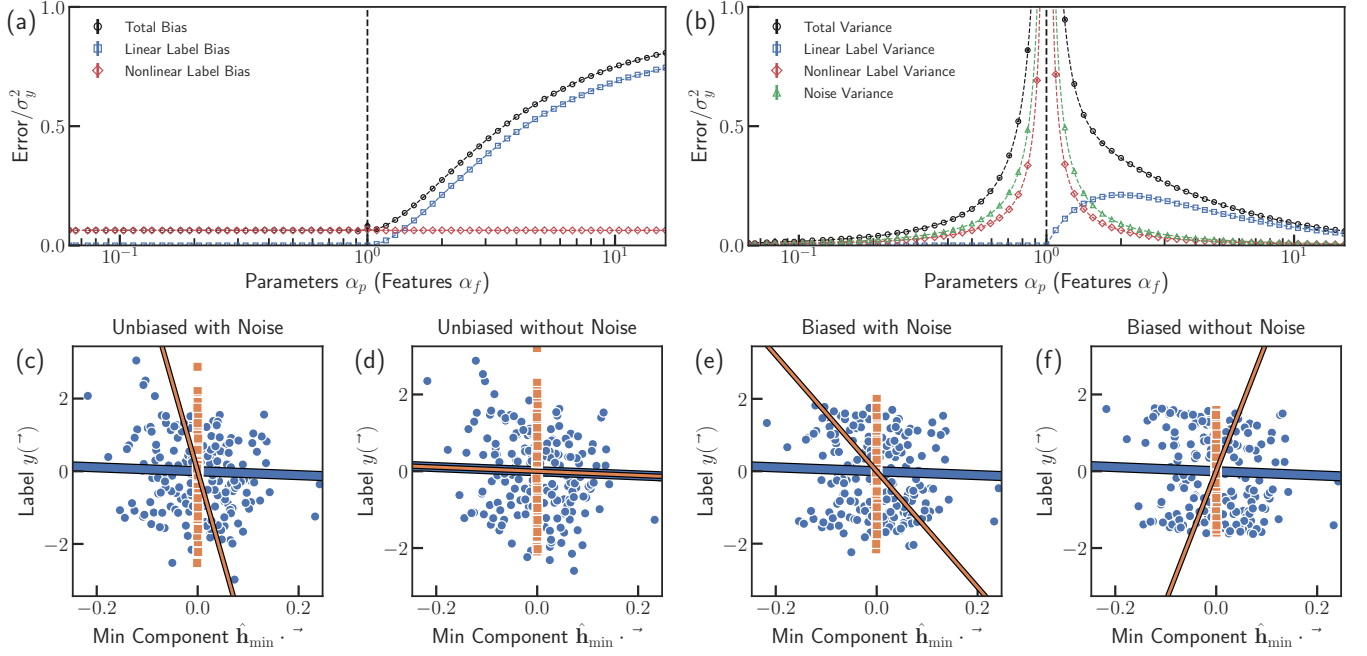


FIG. 6. **Biased models can interpret signal as noise.** (a) The total bias (black circles) with contributions from the linear label components (blue squares) and nonlinear label components (red diamonds), and the (b) the total variance (black circles) with contributions from the linear label components (blue squares), nonlinear label components (red diamonds), and the label noise (green triangles) are shown for linear regression with a nonlinear teacher model $f(h) = \tanh(h)$ [see Eq. (2)]. Analytic solutions are indicated as dashed lines with numerical results shown as points. Each source of bias acts as effective noise, giving rise to a corresponding source of variance. The effects of this phenomenon on the relationships learned by a linear regression model are depicted at the interpolation threshold for an unbiased model with linear data, $f(h) = h$, (c) with noise and (d) without noise, and for a biased model with nonlinear data, $f(h) = \tanh(h)$, (e) with noise and (f) without noise. In each example, the relationship between the labels and the projection of their associated input features onto the minimum principal component $\hat{\mathbf{h}}_{\min}$ of $X^T X$ is depicted for a set of training data (orange squares) and a test set (blue circles). Orange lines indicate the relationship learned by a model from the training set, while the expected relationship for an average test set is shown as a blue line. See Supplemental Material [5] for analytic derivations of learned and expected relationships (Sec. S5), along with additional details of numerical simulations (Sec. S6).

true data distribution and hence will always be biased. We see that both contributions to the bias from the linear (blue) and nonlinear (red) components of the training labels, proportional to σ_β^2 and $\sigma_{\delta y^*}^2$, respectively, in Eq. 25 (see Sec. III A), have a corresponding contribution to the variance for all values of α_f in Eq. 26. This suggests the following interpretation: a model with nonzero bias gives rise to variance by interpreting part of the training set's signal y^* as noise. In other words, a model which cannot fully express the relationships underlying the data distribution may inadvertently treat this unexpressed signal as noise.

We demonstrate this phenomena in Figs. 6(c)-(f) using our model of linear regression trained at the interpolation threshold ($N_p = M$), where the only contribution to the bias stems from the nonlinear components of the training labels. In each panel, we plot the labels as a function of the projection of each data point's input features onto the minimum principal component $\hat{\mathbf{h}}_{\min} \cdot \bar{\mathbf{x}}$ for a set of training data (orange) and a set of test data (blue). We then compare the resulting model (orange line) to the

expected relationship for an average test set (blue line), representing the underlying relationship in the data distribution.

To confirm that bias is necessary for this phenomena, Figs. 6(c) and (d) show additional simulations, now with a linear teacher model $f(h) = h$ with and without label noise. In this case, the student and teacher models match and the model is unbiased. As expected, we find that with label noise, the model overfits the training data and the resulting slope does not accurately reflect the true relationship underlying the data, while without label noise, the model is able to avoid overfitting and provides a good approximation of the true relationship

In Figs. 6(e) and (f), we performed the same simulations for a non-linear teacher model $f(h) = \tanh(h)$ with and without label noise. In this case, the student and teacher models do not match and the model is always biased. With label noise, the model again overfits the training data. However, even in the absence of label noise, the model *still* overfits the training data. Collectively, our simulations indicate that even if the label noise

is zero, any finite amount of bias can result in overfitting, especially if the training set severely undersamples the data along a particular direction in feature space.

We find that this observation holds for all three models for every observed source of bias, including contributions stemming from the linear and nonlinear components of the labels (proportional to σ_β^2 and $\sigma_{\delta y^*}^2$, respectively) and the linear and nonlinear components of the hidden features (proportional to σ_W^2 and $\sigma_{\delta z}^2$, respectively). As a result, in the absence of label noise, the test error can only diverge at an interpolation threshold when a model is biased. Finally, we note that this behavior also manifests in contributions to the training error in the under-parameterized regime for each model, with each source of bias corresponding to an additional source of training error.

D. Interpolating is not the same as overfitting

Our results make clear that interpolation (zero training error) occurs independently from overfitting (poor generalization) in over-parameterized models. Interpolation occurs when the number of independent directions in the space of hidden features (or equivalently, input features in linear regression) sampled by the training set is sufficient to account for the variations in the labels. In all three models, the interpolation threshold is located where the number of principal components (measured via the rank of $Z^T Z$) matches the number of data points. On the other hand, the test error diverges as a result of the variance diverging at the interpolation threshold. These large variances result from poor sampling along directions in $Z^T Z$ (small eigenvalues), resulting in very little spread of data along these directions in the training set relative to the full distribution.

In under-parameterized models, interpolation and overfitting coincide. Increasing the number of fit parameters results in a greater number of sampled directions in the space of features, but makes it more likely to poorly sample any particular direction, resulting in large variance. The result is that the interpolation threshold always coincides with a divergence in the test error. In contrast, interpolation and overfitting occur independently in over-parameterized models. Once the interpolation threshold is reached, further increasing the number of fit parameters cannot improve the training error since it is already at a minimum. However, increasing the model complexity can reduce the effects of overfitting and decrease the variance by allowing for better sampling along the directions captured by the training set (Fig. 5). For this reason, increasing model complexity past the interpolation threshold can actually result in an *increase* in model performance without succumbing to overfitting.

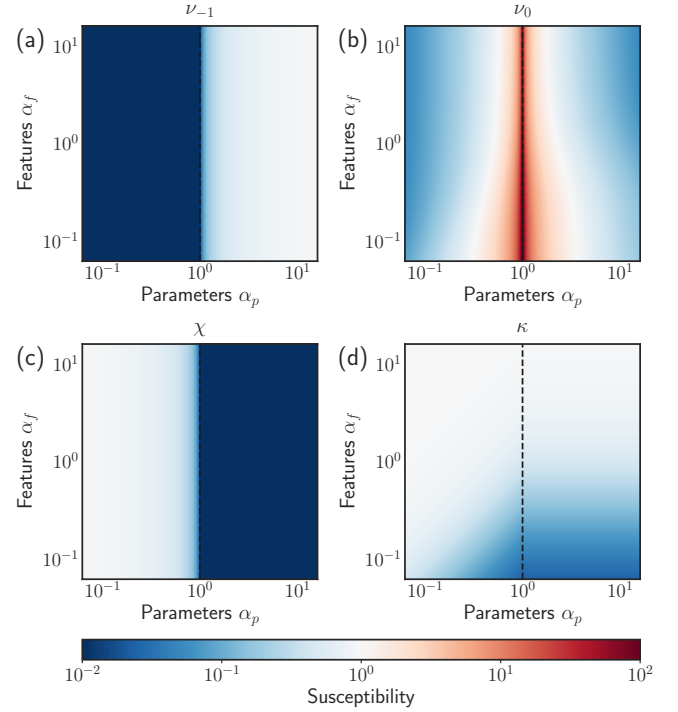


FIG. 7. Susceptibilities for Random Nonlinear Features Model. Analytic solutions for three key susceptibilities as a function of $\alpha_p = N_p/M$ and $\alpha_f = N_f/M$. **(a)-(b)** The susceptibility ν measures the sensitivity of the fit parameters with respect to small perturbations in the gradient. In the small λ limit, we make the approximation $\nu \approx \lambda^{-1}\nu_{-1} + \nu_0$. **(a)** The coefficient ν_{-1} characterizes over-parameterization, equal to the fraction of fit parameters in excess of that needed to achieve zero training error. **(b)** The coefficient ν_0 characterizes over-fitting, diverging at the interpolation threshold when $Z^T Z$ has a small eigenvalue. **(c)** The susceptibility χ measures the sensitivity of the residual label errors of the training set to small perturbations in the label noise. As a result, χ characterizes interpolation, equal to the fraction of data points that would need to be removed from the training set to achieve zero training error. **(d)** The susceptibility κ measures the sensitivity of the residual parameter errors to small perturbations in the ground truth parameters. We observe that κ decreases as a model becomes less biased, indicating that the model is better able to express the relationships underlying the data. In each panel, a black dashed line marks the boundary between the under- and over-parameterized regimes at $\alpha_p = 1$.

E. Susceptibilities measure sensitivity to perturbations

Here, we discuss the roles of the susceptibilities that naturally arise as part of our cavity calculations [e.g., ν , χ , and κ in Eqs. (46)-(48)]. In many physical systems, susceptibilities are quantities of interest that measure the effects on a system due to small perturbations. In particular, ν , χ and κ in our models each characterize a different type of perturbation and in doing so, a differ-

ent aspect of the double-descent phenomenon. Each of these susceptibilities can be expressed as the trace of a corresponding susceptibility matrix. Setting the gradient equation in Eq. (9) equal to a small nonzero field $\vec{\eta}$, such that $\partial L / \partial \hat{\mathbf{w}} = \vec{\eta}$, the susceptibilities ν , χ and κ can be written

$$\begin{aligned} \nu &= \frac{1}{N_p} \text{Tr} \frac{\partial \hat{\mathbf{w}}}{\partial \vec{\eta}}, & \chi &= \frac{1}{M} \text{Tr} \frac{\partial \Delta \vec{\mathbf{y}}}{\partial \vec{\epsilon}} \\ \kappa &= \frac{1}{N_f} \text{Tr} \frac{\partial \Delta \vec{\beta}}{\partial \vec{\beta}}. \end{aligned} \quad (49)$$

We provide exact matrix forms for each susceptibility matrix in Sec. S3 of the Supplemental Material [5].

In Fig. 7, we plot each of these quantities as a function of α_p and α_f for the random nonlinear features model. The susceptibility ν measures perturbations to the fit parameters $\hat{\mathbf{w}}$ due to small changes in the gradient $\vec{\eta}$. In the small λ limit, we make the approximation $\nu \approx \lambda^{-1} \nu_{-1} + \nu_0$ and find that the coefficient of each term has a different interpretation. The first coefficient ν_{-1} , shown in Fig. 7(a), characterizes over-parameterization, counting the fraction of fit parameters in excess of that needed to achieve zero training error. Since these degrees of freedom are effectively unconstrained in the small λ limit, this term diverges as λ approaches zero. The second coefficient ν_0 , shown in Fig. 7(b), characterizes overfitting and diverges at the interpolation threshold in concert with the variance when $Z^T Z$ has a small eigenvalue. We note that ν is actually the trace of the inverse Hessian of the loss function in Eq. (6), or is equivalently the Green’s function, and can be used to extract the eigenvalue spectrum of the kernel matrix [55].

The second susceptibility χ , shown in Fig. 7(c), measures the sensitivity of the residual label errors of the training set $\Delta \vec{\mathbf{y}}$ to small changes in the label noise $\vec{\epsilon}$. We observe that χ goes to zero at the interpolation threshold and remains zero in the interpolation regime. Accordingly, χ acts to characterize interpolation by measuring the fractions of data points that would need to be removed from the training set to achieve zero training error.

Finally, κ , shown in Fig. 7(d), measures the sensitivity of the residual parameter errors $\Delta \vec{\beta}$ to small changes in the underlying ground truth parameters $\vec{\beta}$. We observe that κ decreases as the model becomes less biased, indicating that the model is better able to express the relationships underlying the data (the relationship of κ to the bias is explored in more detail Ref. [56]).

VI. CONCLUSIONS

Understanding how the bias-variance trade-off manifests in over-parameterized models where the number of fit parameters far exceeds the number of data points is a fundamental problem in modern statistics and machine learning. Here, we have used the zero-temperature

cavity method, a technique from statistical physics, to derive exact analytic expressions for the training error, test error, bias, and variance in the thermodynamic limit for three minimal model architectures: linear regression (no basis functions), the random linear features model (a two-layer neural network with linear activation functions where only the top layer is trained), and the random nonlinear features model (a two-layer neural network with nonlinear activation functions where only the top layer is trained). These analytic expressions, when combined with numerical simulations, help explain one of the most puzzling features of modern ML methods: the ability to generalize well while simultaneously achieving zero error on the training data.

We observe this phenomenon of “memorizing without overfitting” in all three of our models. Importantly, our results show that this ability to generalize is not unique to modern ML methods such as those employed in Deep Learning; all three models we consider here are convex. We also note that we do not employ commonly used methods such as stochastic gradient descent to train our model. Instead, we use a straightforward regularization procedure based on an L_2 penalty and even work in the limit where the strength of the regularization is sent to zero. This shows that the ability to generalize while achieving zero training error, sometimes referred to as interpolation, seems to be a generic property of even the simplest over-parameterized models and does not require any special training or regularization methods.

Our results show that in stark contrast with the kinds of models considered in classical statistics, the variance of over-parameterized models actually decreases with model complexity beyond the interpolation threshold (the model complexity at which one can achieve zero error on the training data set). However, over-parameterized models also introduce new sources of bias and variance. Bias in over-parameterized models can result not only from a mismatch between the model and the underlying data distribution, but also from training data sets that span only a subset of the data’s feature space. Over-parameterized models with bias can also mistake signal for noise, resulting in a nonzero variance even in the absence of noise. This shows that understanding bias and variance in over-parameterized models arises through a subtle interplay between model architecture and random sampling of the data distribution via the training data set.

Finally, we note that our models are limited to the “lazy regime” and do not consider the “feature regime.” Recent work suggests that in the latter, more complex setting, generalization error may be improved by looking for wider, more representative minima in the landscape [57–59]. Understanding bias, variance, and generalization in the context of non-convex fitting functions and the relationship of these quantities to the width and local entropy of minima represents an important future area of investigation. One possible direction for exploring these ideas may be to exploit the relationship between

wide neural nets and Gaussian processes [14, 15, 60] and explore how the spectrum changes with the properties of various minima.

ACKNOWLEDGMENTS

We would like to thank Robert Marsland III for extremely useful discussions. This work was supported by

NIH NIGMS grant 1R35GM119461 and a Simons Investigator in the Mathematical Modeling of Living Systems (MMLS) award to PM. The authors also acknowledge support from the Shared Computing Cluster administered by Boston University Research Computing Services.

-
- [1] Yann Lecun, Yoshua Bengio, and Geoffrey Hinton, “Deep learning,” *Nature* **521**, 436–444 (2015).
 - [2] Alfredo Canziani, Adam Paszke, and Eugenio Culurciello, “An Analysis of Deep Neural Network Models for Practical Applications,” (2017), [arXiv:1605.07678](https://arxiv.org/abs/1605.07678).
 - [3] Chiyuan Zhang, Samy Bengio, Moritz Hardt, Benjamin Recht, and Oriol Vinyals, “Understanding Deep Learning Requires Re-thinking Generalization,” *International Conference on Learning Representations (ICLR)* (2017).
 - [4] Pankaj Mehta, Marin Bukov, Ching Hao Wang, Alexandre G.R. Day, Clint Richardson, Charles K. Fisher, and David J. Schwab, “A high-bias, low-variance introduction to Machine Learning for physicists,” *Physics Reports* **810**, 1–124 (2019).
 - [5] “See Supplemental Material at [URL] for complete analytic derivations and additional numerical results.”
 - [6] Mikhail Belkin, Daniel Hsu, Siyuan Ma, and Soumik Mandal, “Reconciling modern machine-learning practice and the classical bias–variance trade-off,” *Proceedings of the National Academy of Sciences* **116**, 15849–15854 (2019).
 - [7] Mario Geiger, Stefano Spigler, Stéphane D’Ascoli, Levent Sagun, Marco Baity-Jesi, Giulio Biroli, and Matthieu Wyart, “Jamming transition as a paradigm to understand the loss landscape of deep neural networks,” *Physical Review E* **100**, 012115 (2019).
 - [8] S. Spigler, M. Geiger, S D’Ascoli, L. Sagun, G. Biroli, and M. Wyart, “A jamming transition from under- to over-parametrization affects generalization in deep learning,” *Journal of Physics A: Mathematical and Theoretical* **52**, 474001 (2019).
 - [9] M Mailman and B Chakraborty, “A signature of a thermodynamic phase transition in jammed granular packings: growing correlations in force space,” *Journal of Statistical Mechanics: Theory and Experiment* **2011**, L07002 (2011).
 - [10] Yasaman Bahri, Jonathan Kadmon, Jeffrey Pennington, Sam S. Schoenholz, Jascha Sohl-Dickstein, and Surya Ganguli, “Statistical Mechanics of Deep Learning,” *Annual Review of Condensed Matter Physics* **11**, 501–528 (2020).
 - [11] Dmitry Kobak [@hippopedoid], “Twitter Thread: twitter.com/hippopedoid/status/1243229021921579010,” (2020).
 - [12] Marco Loog, Tom Viering, Alexander Mey, Jesse H. Krijthe, and David M. J. Tax, “A brief prehistory of double descent,” *Proceedings of the National Academy of Sciences* **117**, 10625–10626 (2020).
 - [13] Preetum Nakkiran, Gal Kaplun, Yamini Bansal, Tristan Yang, Boaz Barak, and Ilya Sutskever, “Deep Double Descent: Where Bigger Models and More Data Hurt,” *International Conference on Learning Representations (ICLR)* (2020).
 - [14] Arthur Jacot, Franck Gabriel, and Clément Hongler, “Neural tangent kernel: Convergence and generalization in neural networks,” *Advances in Neural Information Processing Systems (NeurIPS)* **31** (2018).
 - [15] Jaehoon Lee, Lechao Xiao, Samuel S. Schoenholz, Yasaman Bahri Roman Novak, Jascha Sohl-Dickstein, and Jeffrey Pennington, “Wide neural networks of any depth evolve as linear models under gradient descent,” *Advances in Neural Information Processing Systems (NeurIPS)* **32** (2019).
 - [16] Mario Geiger, Stefano Spigler, Arthur Jacot, and Matthieu Wyart, “Disentangling feature and lazy training in deep neural networks,” *Journal of Statistical Mechanics: Theory and Experiment* **2020**, 113301 (2020).
 - [17] Ben Adlam and Jeffrey Pennington, “Understanding double descent requires a fine-grained bias-variance decomposition,” *Advances in Neural Information Processing Systems (NeurIPS)* **33**, 11022–11032 (2020).
 - [18] Madhu S. Advani, Andrew M. Saxe, and Haim Sompolinsky, “High-dimensional dynamics of generalization error in neural networks,” *Neural Networks* **132**, 428–446 (2020).
 - [19] Jimmy Ba, Murat Erdogdu, Taiji Suzuki, Denny Wu, and Tianzong Zhang, “Generalization of Two-layer Neural Networks: An Asymptotic Viewpoint,” *International Conference on Learning Representations (ICLR)* (2020).
 - [20] Jean Barbier, Florent Krzakala, Nicolas Macris, Léo Miolane, and Lenka Zdeborová, “Optimal errors and phase transitions in high-dimensional generalized linear models,” *Proceedings of the National Academy of Sciences* **116**, 5451–5460 (2019).
 - [21] Peter L. Bartlett, Philip M. Long, Gábor Lugosi, and Alexander Tsigler, “Benign overfitting in linear regression,” *Proceedings of the National Academy of Sciences* **117**, 30063–30070 (2020).
 - [22] Mikhail Belkin, Daniel Hsu, and Ji Xu, “Two Models of Double Descent for Weak Features,” *SIAM Journal on Mathematics of Data Science* **2**, 1167–1180 (2020).
 - [23] Koby Bibas, Yaniv Fogel, and Meir Feder, “A New Look at an Old Problem: A Universal Learning Approach to Linear Regression,” *IEEE International Symposium on Information Theory (ISIT)*, 2304–2308 (2019).
 - [24] Zeyu Deng, Abba Kammoun, and Christos Thrampoulidis, “A Model of Double Descent for High-

- Dimensional Logistic Regression,” *IEEE International Conference on Acoustics, Speech and Signal Processing (ICASSP)*, 4267–4271 (2020).
- [25] Stéphane D’Ascoli, Levent Sagun, and Giulio Biroli, “Triple descent and the two kinds of overfitting: Where & why do they appear?” (2020), [arXiv:2006.03509](#).
- [26] Stéphane D’Ascoli, Maria Refinetti, Giulio Biroli, and Florent Krzakala, “Double Trouble in Double Descent: Bias and Variance(s) in the Lazy Regime,” *Proceedings of the 37th International Conference on Machine Learning (ICML) PMLR*, **119**, 2280–2290 (2020).
- [27] Michał Dereziński, Feynman Liang, and Michael W. Mahoney, “Exact expressions for double descent and implicit regularization via surrogate random design,” *Advances in Neural Information Processing Systems (NeurIPS)* **33**, 5152–5164 (2020).
- [28] Federica Gerace, Bruno Loureiro, Florent Krzakala, Marc Mézard, and Lenka Zdeborová, “Generalisation error in learning with random features and the hidden manifold model,” *Proceedings of the 37th International Conference on Machine Learning (ICML) PMLR*, **119**, 3452–3462 (2020).
- [29] Trevor Hastie, Andrea Montanari, Saharon Rosset, and Ryan J. Tibshirani, “Surprises in High-Dimensional Ridgeless Least Squares Interpolation,” (2019), [arXiv:1903.08560](#).
- [30] Arthur Jacot, Berfin Şimşek, Francesco Spadaro, Clément Hongler, and Franck Gabriel, “Implicit regularization of random feature models,” *Proceedings of the 37th International Conference on Machine Learning (ICML) PMLR*, **119**, 4631–4640 (2020).
- [31] Ganesh Ramachandra Kini and Christos Thrampoulidis, “Analytic Study of Double Descent in Binary Classification: The Impact of Loss,” *IEEE International Symposium on Information Theory (ISIT)*, 2527–2532 (2020).
- [32] Andrew K. Lampinen and Surya Ganguli, “An analytic theory of generalization dynamics and transfer learning in deep linear networks,” *International Conference on Learning Representations (ICLR)* (2019).
- [33] Zhu Li, Weijie J. Su, and Dino Sejdinovic, “Benign overfitting and noisy features,” (2020), [arXiv:2008.02901](#).
- [34] Tengyuan Liang and Alexander Rakhlin, “Just interpolate: Kernel “Ridgeless” regression can generalize,” *Annals of Statistics* **48**, 1329–1347 (2020).
- [35] Tengyuan Liang, Alexander Rakhlin, and Xiyu Zhai, “On the Multiple Descent of Minimum-Norm Interpolants and Restricted Lower Isometry of Kernels,” *Proceedings of Thirty Third Conference on Learning Theory PMLR*, **125**, 2683–2711 (2020).
- [36] Zhenyu Liao, Romain Couillet, and Michael W Mahoney, “A random matrix analysis of random Fourier features: beyond the Gaussian kernel, a precise phase transition, and the corresponding double descent,” *Advances in Neural Information Processing Systems (NeurIPS)* **33** (2020).
- [37] Licong Lin and Edgar Dobriban, “What causes the test error? Going beyond bias-variance via ANOVA,” (2020), [arXiv:2010.05170](#).
- [38] Partha P Mitra, “Understanding overfitting peaks in generalization error: Analytical risk curves for l_2 and l_1 penalized interpolation,” (2019), [arXiv:1906.03667](#).
- [39] Song Mei and Andrea Montanari, “The generalization error of random features regression: Precise asymptotics and double descent curve,” (2019), [arXiv:1908.05355](#).
- [40] Vidya Muthukumar, Kailas Vodrahalli, and Anant Sahai, “Harmless interpolation of noisy data in regression,” *IEEE International Symposium on Information Theory (ISIT)*, 2299–2303 (2019).
- [41] Preetum Nakkiran, “More Data Can Hurt for Linear Regression: Sample-wise Double Descent,” (2019), [arXiv:1912.07242](#).
- [42] Ji Xu and Daniel Hsu, “On the number of variables to use in principal component regression,” *Advances in Neural Information Processing Systems (NeurIPS)* **32** (2019).
- [43] Zitong Yang, Yaodong Yu, Chong You, Jacob Steinhardt, and Yi Ma, “Rethinking Bias-Variance Trade-off for Generalization of Neural Networks,” *Proceedings of the 37th International Conference on Machine Learning (ICML) PMLR*, **119**, 10767–10777 (2020).
- [44] A Engel, C den Broeck, and C Broeck, *Statistical Mechanics of Learning*, Statistical Mechanics of Learning (Cambridge University Press, 2001).
- [45] Marc Mézard and Giorgio Parisi, “The Cavity Method at Zero Temperature,” *Journal of Statistical Physics* **111**, 1–34 (2003).
- [46] Mohammad Ramezanali, Partha P. Mitra, and Anirvan M. Sengupta, “The cavity method for analysis of large-scale penalized regression,” (2015), [arXiv:1501.03194](#).
- [47] Pankaj Mehta, Wenping Cui, Ching Hao Wang, and Robert Marsland, “Constrained optimization as ecological dynamics with applications to random quadratic programming in high dimensions,” *Physical Review E* **99**, 52111 (2019).
- [48] Christopher M. Bishop, *Pattern Recognition and Machine Learning* (Springer, 2006).
- [49] Madhu Advani, Guy Bunin, and Pankaj Mehta, “Statistical physics of community ecology: a cavity solution to MacArthur’s consumer resource model,” *Journal of Statistical Mechanics: Theory and Experiment* **2018**, 033406 (2018).
- [50] Vladimir Alexandrovich Marčenko and Leonid Andreevich Pastur, “Distribution of eigenvalues for some sets of random matrices,” *Mathematics of the USSR-Sbornik* **1**, 457–483 (1967).
- [51] Thomas Dupic and Isaac Pérez Castillo, “Spectral density of products of Wishart dilute random matrices. Part I: the dense case,” (2014), [arXiv:1401.7802](#).
- [52] Jeffrey Pennington and Pratik Worah, “Nonlinear random matrix theory for deep learning,” *Journal of Statistical Mechanics: Theory and Experiment* **2019**, 124005 (2019).
- [53] Marc Mézard, “Mean-field message-passing equations in the Hopfield model and its generalizations,” *Physical Review E* **95**, 022117 (2017).
- [54] Mohammad Ramezanali, Partha P. Mitra, and Anirvan M. Sengupta, “Critical Behavior and Universality Classes for an Algorithmic Phase Transition in Sparse Reconstruction,” *Journal of Statistical Physics* **175**, 764–788 (2019).
- [55] Wenping Cui, Jason W. Rocks, and Pankaj Mehta, “The perturbative resolvent method: Spectral densities of random matrix ensembles via perturbation theory,” (2020), [arXiv:2012.00663](#).
- [56] Jason W. Rocks and Pankaj Mehta, “The Geometry of Over-parameterized Regression and Adversarial Perturbations,” (2021), [arXiv:2103.14108](#).

- [57] Pratik Chaudhari, Anna Choromanska, Stefano Soatto, Yann LeCun, Carlo Baldassi, Christian Borgs, Jennifer Chayes, Levent Sagun, and Riccardo Zecchina, “Entropy-SGD: biasing gradient descent into wide valleys,” [Journal of Statistical Mechanics: Theory and Experiment](#) **2019**, 124018 (2019).
- [58] Carlo Baldassi, Enrico M. Malatesta, Matteo Negri, and Riccardo Zecchina, “Wide flat minima and optimal generalization in classifying high-dimensional Gaussian mixtures,” [Journal of Statistical Mechanics: Theory and Experiment](#) **2020**, 124012 (2020).
- [59] Fabrizio Pittorino, Carlo Lucibello, Christoph Feinauer, Enrico M. Malatesta, Gabriele Perugini, Carlo Baldassi, Matteo Negri, Elizaveta Demyanenko, and Riccardo Zecchina, “Entropic gradient descent algorithms and wide flat minima,” (2020), [arXiv:2006.07897](#).
- [60] Sho Yaida, “Non-Gaussian processes and neural networks at finite widths,” [Proceedings of The First Mathematical and Scientific Machine Learning Conference PMLR](#), **107**, 165–192 (2020).

Supplemental Material: Memorizing without overfitting: Bias, variance, and interpolation in over-parameterized models

Jason W. Rocks¹ and Pankaj Mehta^{1,2}

¹*Department of Physics, Boston University, Boston, Massachusetts 02215, USA*

²*Faculty of Computing and Data Sciences, Boston University, Boston, Massachusetts 02215, USA*

CONTENTS

S1. Cavity Derivations	2
A. Notation Conventions	2
B. Theoretical Setup	2
C. Nonlinear Function Statistics	3
1. Integrals	3
2. Label Decomposition	6
3. Hidden Feature Decomposition	7
D. General System of Equations	9
E. Linear Regression (No Basis Functions)	9
1. Cavity Expansion	10
2. Approximations of Large Sums: Unperturbed Quantities	11
3. Approximations of Large Sums: Square Susceptibilities	11
4. Approximations of Large Sums: Rectangular Susceptibilities	12
5. Self-consistency Equations	13
6. Solutions with Finite Regularization ($\lambda \sim \mathcal{O}(1)$)	14
7. Solutions in Ridge-less Limit ($\lambda \rightarrow 0$)	14
8. Test Error	16
9. Bias-Variance Decomposition	17
F. Random Linear Features Model (Two-layer Linear Neural Network)	18
1. Cavity Expansion	19
2. Approximations of Large Sums: Unperturbed Quantities	20
3. Approximations of Large Sums: Square Susceptibilities	20
4. Approximations of Large Sums: Rectangular Susceptibilities	21
5. Self-consistency Equations	21
6. Solution with Finite Regularization ($\lambda \sim 1$)	22
7. Solutions in Ridge-less Limit ($\lambda \rightarrow 0$)	23
8. Test Error	26
9. Bias-Variance Decomposition	27
G. Random Nonlinear Features Model (Two-layer Nonlinear Neural Network)	30
1. Cavity Expansion	31
2. Approximations of Large Sums: Unperturbed Quantities	32
3. Approximations of Large Sums: Square Susceptibilities	32
4. Approximations of Large Sums: Rectangular Susceptibilities	33
5. Self-consistency Equations	33
6. Solution with Finite Regularization ($\lambda \sim \mathcal{O}(1)$)	34
7. Solutions in Ridge-less Limit ($\lambda \rightarrow 0$)	35
8. Test Error	36
9. Bias-Variance Decomposition	37
S2. Parameter Error and Parameter Bias-Variance Decomposition	39
S3. Matrix Forms of Susceptibilities	40
A. Linear Regression	40
B. Random Linear Features Model	41
C. Random Nonlinear Features Model	42

S4. Spectral Densities of Kernel Matrices	43
A. Linear Regression	44
B. Random Linear Features Model	45
C. Random Nonlinear Features Model	46
S5. Accuracy of Minimum Principal Component	47
A. Linear Regression	49
B. Random Linear Features Model	49
C. Random Nonlinear Features Model	50
S6. Numerical Simulation Details	50
A. General Details	50
B. Bias-Variance Decompositions	51
C. Eigenvalue Decompositions of Kernel Matrices	51
D. Spread Along Mimimum Principal Components	51
S7. Complete Numerical Results	52

S1. CAVITY DERIVATIONS

In this section, we provide detailed derivations of all closed-form solutions for each model. We begin by introducing the general procedure behind the zero-temperature cavity method. We then derive solutions for linear regression, the simplest of the three models. Using this derivation as a template, we then repeat the procedure for the two random features models, explaining any additional steps or approximations as necessary. These calculations follow the general procedure laid out in Ref. 47.

A. Notation Conventions

- We define M as the number of points in the training data set, N_f as the number of input features, and N_p as the number of fit parameters/hidden features. We define the ratios $\alpha_f = N_f/M$ and $\alpha_p = N_p/M$.
- Unless otherwise specified, the type of symbol used for an index label (e.g., Δy_a) or as a summation index (e.g., \sum_a) implies its range. The symbols a , b , or c imply ranges over the training data points from 1 to M , the symbols j , k , or l imply ranges over the input features from 1 to N_f , and the symbols J , K , or L imply ranges over the fit parameters/hidden features from 1 to N_p .
- The notation $E_x[\cdot]$, $\text{Var}_x[\cdot]$ and $\text{Cov}_x[\cdot, \cdot]$ represent the mean, variance, and covariance, respectively, with respect to one or more random variables x . A lack of subscript implies averages taken with respect to the total ensemble distribution, i.e., taken over all possible sources of randomness. A subscript 0 implies averages taken with respect to random variables containing one or more 0-valued indices (e.g., X_{a0} , X_{0j} , W_{0J} , or W_{j0}).
- We use the notation $\mathcal{O}(\cdot)$ to represent standard “Big-O” notation, indicating an upper bound on the limiting scaling behavior of a quantity with respect to the argument.

B. Theoretical Setup

For completeness, we begin by reproducing some of our theoretical setup from the main text. We consider data points (y, \vec{x}) , each consisting of a label y and a vector \vec{x} of N_f input features. The labels are related to the input features via the teacher model

$$y(\vec{x}) = y^*(\vec{x}; \vec{\beta}) + \varepsilon \quad (\text{S1})$$

where $\vec{\beta}$ is the vector the set of “ground truth” parameters and ε is the label noise. We consider features and label noise that are independently and identically distributed, drawn from a normal distributions with zero mean and

variances σ_X^2/N_f and σ_ε^2 , respectively, so that

$$\mathbb{E}[x_{a,j}] = 0, \quad \text{Cov}[x_{a,j}, x_{b,k}] = \frac{\sigma_X^2}{N_f} \delta_{ab} \delta_{jk} \quad (\text{S2})$$

$$\mathbb{E}[\varepsilon_a] = 0, \quad \text{Cov}[\varepsilon_a, \varepsilon_b] = \sigma_\varepsilon^2 \delta_{ab} \quad (\text{S3})$$

for two data points $\vec{\mathbf{x}}_a$ and $\vec{\mathbf{x}}_b$ with label noise ε_a and ε_b . Similarly, we assume the ground truth parameters are independent of all other random parameters and are also normally distributed with zero mean and variance σ_β^2 ,

$$\mathbb{E}[\beta_k] = 0, \quad \text{Cov}[\beta_j, \beta_k] = \sigma_\beta^2 \delta_{jk}. \quad (\text{S4})$$

We consider a training set of M data points, $\mathcal{D} = \{(y_b, \vec{\mathbf{x}}_b)\}_{b=1}^M$. We organize each input feature vector into the rows of an observation matrix X of size $M \times N_f$.

We consider a linear student model,

$$\hat{y}(\vec{\mathbf{x}}) = \vec{\mathbf{z}}(\vec{\mathbf{x}}) \cdot \hat{\mathbf{w}}, \quad (\text{S5})$$

where $\hat{\mathbf{w}}$ is a vector of N_p fit parameters. The values of the fit parameters are determined by minimizing the loss function

$$L(\hat{w}) = \frac{1}{2} \sum_b \Delta y_b^2 + \frac{\lambda}{2} \sum_k \hat{w}_k^2 \quad (\text{S6})$$

where we have defined the residual label error as $\Delta y_a = y_a - \hat{y}_a$. This loss function is equivalent to that in Eq. (6), but we have multiplied by a factor of $M/2$ and absorbed the extra factor of M/N_f into the definition λ . Taking the gradient of the loss with respect to the fit parameters and setting it to zero results in a system of N_p equations for the N_p fit parameter,

$$0 = \frac{\partial L(\hat{w})}{\partial \hat{w}_J} = - \sum_b \Delta y_b Z_{bJ} + \lambda \hat{w}_J. \quad (\text{S7})$$

Note that the regularization term ensures that this system of equations always has a unique solution.

C. Nonlinear Function Statistics

Here, we show how the labels and hidden features can each be decomposed into linear and nonlinear components that are statistically independent of one another. We also derive the statistical properties of the resulting nonlinear components.

1. Integrals

First, we derive closed forms for a few useful integrals. While throughout this work we consider input features that are independently distributed, in this section, we consider a more general case in which the input features are correlated, but still collectively follow a multivariate normal distribution with mean zero and covariance matrix $\Sigma_{\vec{\mathbf{x}}}$,

$$\mathbb{E}[\vec{\mathbf{x}}] = 0, \quad \text{Cov}[\vec{\mathbf{x}}, \vec{\mathbf{x}}^T] = \Sigma_{\vec{\mathbf{x}}}, \quad (\text{S8})$$

where the covariance is normalized so that $\text{Tr} \Sigma_{\vec{\mathbf{x}}} = \sigma_X^2$. When the input features are independent the covariance matrix is implied to be $\Sigma_{\vec{\mathbf{x}}} = \frac{\sigma_X^2}{N_f} I_{N_f}$.

We then define the differential over all elements of a vector of input features $\vec{\mathbf{x}}$ as,

$$\mathcal{D}\vec{\mathbf{x}} = \frac{d\vec{\mathbf{x}}}{\sqrt{(2\pi)^{N_f} \det \Sigma_{\vec{\mathbf{x}}}}} e^{-\frac{1}{2} \vec{\mathbf{x}}^T \Sigma_{\vec{\mathbf{x}}}^{-1} \vec{\mathbf{x}}}. \quad (\text{S9})$$

We also define a random vector $\vec{\mathbf{a}}$ of length N_f whose elements are independent of $\vec{\mathbf{x}}$ with zero mean and variance σ_a^2 ,

$$\mathbb{E}[a_j] = 0, \quad \text{Cov}[a_j, a_k] = \sigma_a^2 \delta_{jk}. \quad (\text{S10})$$

The first integral we consider is the average over an arbitrary function $g\left(\frac{\vec{x} \cdot \vec{a}}{\sigma_X \sigma_a}\right)$ with respect to \vec{x} ,

$$\begin{aligned}
\mathbb{E}_{\vec{x}} \left[g\left(\frac{\vec{x} \cdot \vec{a}}{\sigma_X \sigma_a}\right) \right] &= \int \mathcal{D}\vec{x} g\left(\frac{\vec{x} \cdot \vec{a}}{\sigma_X \sigma_a}\right) \\
&= \int \mathcal{D}\vec{x} dh g(h) \delta\left(h - \frac{\vec{x} \cdot \vec{a}}{\sigma_X \sigma_a}\right) \\
&= \int \mathcal{D}\vec{x} dh \frac{d\tilde{h}}{2\pi} g(h) e^{i\tilde{h}\left(h - \frac{\vec{x} \cdot \vec{a}}{\sigma_X \sigma_a}\right)} \\
&= \int dh \frac{d\tilde{h}}{2\pi} g(h) e^{i\tilde{h}h} \int \frac{d\vec{x}}{\sqrt{(2\pi)^{N_f} \det \Sigma_{\vec{x}}}} e^{-\frac{1}{2} \vec{x}^T \Sigma_{\vec{x}}^{-1} \vec{x} - i\tilde{h} \frac{\vec{x} \cdot \vec{a}}{\sigma_X \sigma_a}} \\
&= \int dh \frac{d\tilde{h}}{2\pi} g(h) e^{i\tilde{h}h - \frac{\tilde{h}^2}{2} \frac{\vec{a}^T \Sigma_{\vec{x}} \vec{a}}{\sigma_X^2 \sigma_a^2}}.
\end{aligned} \tag{S11}$$

At this point, we approximate the sum in the exponential using the central limit theorem. Alternatively, one could perform a saddle-point approximation. Since the sum is over a thermodynamically large number of independent terms, we approximate it with its mean and variance with respect to \vec{a} . The mean of this sum is

$$\mathbb{E}_{\vec{a}} [\vec{a}^T \Sigma_{\vec{x}} \vec{a}] = \sigma_a^2 \text{tr} \Sigma_{\vec{x}} = \sigma_a^2 \sigma_X^2. \tag{S12}$$

To calculate its variance, we use Wick's theorem to calculate the fourth moment of the elements of \vec{a} ,

$$\mathbb{E}[a_j a_k a_l a_m] = \sigma_a^4 (\delta_{jk} \delta_{lm} + \delta_{jl} \delta_{km} + \delta_{jm} \delta_{kl}). \tag{S13}$$

Using this, we find the variance to be

$$\begin{aligned}
\text{Var}_{\vec{a}} [\vec{a}^T \Sigma_{\vec{x}} \vec{a}] &= \sum_{jklm} \Sigma_{\vec{x},jk} \Sigma_{\vec{x},lm} \text{Cov}_{\vec{a}}[a_j a_k, a_l a_m] \\
&= \sum_{jklm} \Sigma_{\vec{x},jk} \Sigma_{\vec{x},lm} (\mathbb{E}_{\vec{a}}[a_j a_k a_l a_m] - \mathbb{E}_{\vec{a}}[a_j a_k] \mathbb{E}_{\vec{a}}[a_l a_m]) \\
&= 2\sigma_a^4 \text{Tr} \Sigma_{\vec{x}}^2.
\end{aligned} \tag{S14}$$

Since the trace of $\Sigma_{\vec{x}}$ is $\mathcal{O}(1)$, its eigenvalues must each be $\mathcal{O}(1/N_f)$ on average. Therefore, the trace of $\Sigma_{\vec{x}}^2$, which is just the sum of the squared eigenvalues, must be $\mathcal{O}(1/N_f)$. As a result, the variance will also be small and can be neglected. Using this approximation, we find

$$\begin{aligned}
\mathbb{E}_{\vec{x}} \left[g\left(\frac{\vec{x} \cdot \vec{a}}{\sigma_X \sigma_a}\right) \right] &\approx \int dh \frac{d\tilde{h}}{2\pi} g(h) e^{i\tilde{h}h - \frac{\tilde{h}^2}{2}} \\
&= \frac{1}{\sqrt{2\pi}} \int dh e^{-\frac{h^2}{2}} g(h) \\
&= \langle g \rangle,
\end{aligned} \tag{S15}$$

where we have defined the quantity $\langle g \rangle$ according to the second-to-last line.

Next, we consider the average of the product of $g\left(\frac{\vec{x} \cdot \vec{a}}{\sigma_X \sigma_a}\right)$ and the vector \vec{x} . Using the same approximation above

for large N_f , we find

$$\begin{aligned}
\mathbb{E}_{\vec{x}} \left[\vec{x} g \left(\frac{\vec{x} \cdot \vec{a}}{\sigma_X \sigma_a} \right) \right] &= \int \mathcal{D}\vec{x} \vec{x} g \left(\frac{\vec{x} \cdot \vec{a}}{\sigma_X \sigma_a} \right) \\
&= \int \mathcal{D}\vec{x} dh \vec{x} g(h) \delta \left(h - \frac{\vec{x} \cdot \vec{a}}{\sigma_X \sigma_a} \right) \\
&= \int \mathcal{D}\vec{x} dh \frac{d\tilde{h}}{2\pi} \vec{x} g(h) e^{i\tilde{h} \left(h - \frac{\vec{x} \cdot \vec{a}}{\sigma_X \sigma_a} \right)} \\
&= \sigma_X \sigma_a \int \mathcal{D}\vec{x} dh \frac{d\tilde{h}}{2\pi} g(h) \left(\frac{i}{\tilde{h}} \nabla_{\vec{a}} \right) e^{i\tilde{h} \left(h - \frac{\vec{x} \cdot \vec{a}}{\sigma_X \sigma_a} \right)} \\
&= \sigma_X \sigma_a \int dh \frac{d\tilde{h}}{2\pi} g(h) \left(\frac{i}{\tilde{h}} \nabla_{\vec{a}} \right) e^{i\tilde{h}h} \int \frac{d\vec{x}}{\sqrt{(2\pi)^{N_f} \det \Sigma_{\vec{x}}}} e^{-\frac{1}{2} \vec{x}^T \Sigma_{\vec{x}}^{-1} \vec{x} - i\tilde{h} \frac{\vec{x} \cdot \vec{a}}{\sigma_X \sigma_a}} \\
&= \sigma_X \sigma_a \int dh \frac{d\tilde{h}}{2\pi} g(h) \left(\frac{i}{\tilde{h}} \nabla_{\vec{a}} \right) e^{i\tilde{h}h - \frac{\tilde{h}^2}{2} \frac{\vec{a}^T \Sigma_{\vec{x}} \vec{a}}{\sigma_X^2 \sigma_a^2}} \\
&= -i \frac{\Sigma_{\vec{x}} \vec{a}}{\sigma_X \sigma_a} \int dh \frac{d\tilde{h}}{2\pi} g(h) \tilde{h} e^{i\tilde{h}h - \frac{\tilde{h}^2}{2} \frac{\vec{a}^T \Sigma_{\vec{x}} \vec{a}}{\sigma_X^2 \sigma_a^2}} \\
&= -\frac{\Sigma_{\vec{x}} \vec{a}}{\sigma_X \sigma_a} \int dh \frac{d\tilde{h}}{2\pi} g(h) \frac{\partial}{\partial h} e^{i\tilde{h}h - \frac{\tilde{h}^2}{2} \frac{\vec{a}^T \Sigma_{\vec{x}} \vec{a}}{\sigma_X^2 \sigma_a^2}} \\
&\approx -\frac{\Sigma_{\vec{x}} \vec{a}}{\sigma_X \sigma_a} \int dh \frac{d\tilde{h}}{2\pi} g(h) \frac{\partial}{\partial h} e^{i\tilde{h}h - \frac{\tilde{h}^2}{2}} \\
&= -\frac{\Sigma_{\vec{x}} \vec{a}}{\sigma_X \sigma_a} \frac{1}{\sqrt{2\pi}} \int dh g(h) \frac{\partial}{\partial h} e^{-\frac{h^2}{2}} \\
&= \frac{\Sigma_{\vec{x}} \vec{a}}{\sigma_X \sigma_a} \frac{1}{\sqrt{2\pi}} \int dh e^{-\frac{h^2}{2}} g'(h) \\
&= \frac{\Sigma_{\vec{x}} \vec{a}}{\sigma_X \sigma_a} \langle g' \rangle,
\end{aligned} \tag{S16}$$

where the definition of $\langle g' \rangle$ is implied by the second-to-last line.

The last integral we consider is the average of the product $g \left(\frac{\vec{x} \cdot \vec{a}}{\sigma_X \sigma_a} \right) g \left(\frac{\vec{x} \cdot \vec{b}}{\sigma_X \sigma_b} \right)$ where \vec{b} is a second random vector with similar properties to \vec{a} , but with variance σ_b^2 ,

$$\begin{aligned}
\mathbb{E}_{\vec{x}} \left[g \left(\frac{\vec{x} \cdot \vec{a}}{\sigma_X \sigma_a} \right) g \left(\frac{\vec{x} \cdot \vec{b}}{\sigma_X \sigma_b} \right) \right] &= \int \mathcal{D}\vec{x} g \left(\frac{\vec{x} \cdot \vec{a}}{\sigma_X \sigma_a} \right) g \left(\frac{\vec{x} \cdot \vec{b}}{\sigma_X \sigma_b} \right) \\
&= \int \mathcal{D}\vec{x} dh dh' g(h) g(h') \delta \left(h - \frac{\vec{x} \cdot \vec{a}}{\sigma_X \sigma_a} \right) \delta \left(h' - \frac{\vec{x} \cdot \vec{b}}{\sigma_X \sigma_b} \right) \\
&= \int \mathcal{D}\vec{x} dh \frac{d\tilde{h}}{2\pi} dh' \frac{d\tilde{h}'}{2\pi} g(h) g(h') e^{i\tilde{h} \left(h - \frac{\vec{x} \cdot \vec{a}}{\sigma_X \sigma_a} \right) + i\tilde{h}' \left(h' - \frac{\vec{x} \cdot \vec{b}}{\sigma_X \sigma_b} \right)} \\
&= \int dh \frac{d\tilde{h}}{2\pi} dh' \frac{d\tilde{h}'}{2\pi} g(h) g(h') e^{i\tilde{h}h + i\tilde{h}'h'} \int \frac{d\vec{x}}{\sqrt{(2\pi)^{N_f} \det \Sigma_{\vec{x}}}} e^{-\frac{1}{2} \vec{x}^T \Sigma_{\vec{x}}^{-1} \vec{x} - i\tilde{h} \frac{\vec{x} \cdot \vec{a}}{\sigma_X \sigma_a} - i\tilde{h}' \frac{\vec{x} \cdot \vec{b}}{\sigma_X \sigma_b}} \\
&= \int dh \frac{d\tilde{h}}{2\pi} dh' \frac{d\tilde{h}'}{2\pi} g(h) g(h') e^{i\tilde{h}h + i\tilde{h}'h' - \frac{\tilde{h}^2}{2} \frac{\vec{a}^T \Sigma_{\vec{x}} \vec{a}}{\sigma_X^2 \sigma_a^2} - \frac{(\tilde{h}')^2}{2} \frac{\vec{b}^T \Sigma_{\vec{x}} \vec{b}}{\sigma_X^2 \sigma_b^2} - \tilde{h} \tilde{h}' \frac{\vec{a}^T \Sigma_{\vec{x}} \vec{b}}{\sigma_X^2 \sigma_a \sigma_b}}.
\end{aligned} \tag{S17}$$

We know that we can approximate the first two sums in the exponential as just their means as before. However, for the third sum, we must again calculate the mean and variance. The mean of this sum is clearly zero since \vec{a} and \vec{b}

are uncorrelated. The variance is then

$$\begin{aligned}
\text{Var}_{\vec{\mathbf{a}}, \vec{\mathbf{b}}} \left[\vec{\mathbf{a}}^T \Sigma_{\vec{\mathbf{x}}} \vec{\mathbf{b}} \right] &= \sum_{jklm} \Sigma_{\vec{\mathbf{x}},jk} \Sigma_{\vec{\mathbf{x}},lm} \text{Cov}_{\vec{\mathbf{a}}} [a_j b_k, a_l b_m] \\
&= \sum_{jklm} \Sigma_{\vec{\mathbf{x}},jk} \Sigma_{\vec{\mathbf{x}},lm} (\mathbb{E}_{\vec{\mathbf{a}}} [a_j a_l] \mathbb{E}_{\vec{\mathbf{b}}} [b_k b_m] - \mathbb{E}_{\vec{\mathbf{a}}} [a_j] \mathbb{E}_{\vec{\mathbf{b}}} [b_k] \mathbb{E}_{\vec{\mathbf{a}}} [a_l] \mathbb{E}_{\vec{\mathbf{b}}} [b_m]) \\
&= \sigma_a^2 \sigma_b^2 \text{Tr} \Sigma_{\vec{\mathbf{x}}}^2.
\end{aligned} \tag{S18}$$

As before, the trace of $\Sigma_{\vec{\mathbf{x}}}^2$ is $\mathcal{O}(1/N_f)$, and therefore the variance can be neglected. This gives us

$$\begin{aligned}
\mathbb{E}_{\vec{\mathbf{x}}} \left[g \left(\frac{\vec{\mathbf{x}} \cdot \vec{\mathbf{a}}}{\sigma_X \sigma_a} \right) g \left(\frac{\vec{\mathbf{x}} \cdot \vec{\mathbf{b}}}{\sigma_X \sigma_b} \right) \right] &\approx \int d\tilde{h} \frac{d\tilde{h}'}{2\pi} g(\tilde{h}) g(\tilde{h}') e^{i\tilde{h}h + i\tilde{h}'h' - \frac{\tilde{h}^2}{2} - \frac{(\tilde{h}')^2}{2}} \\
&= \left[\frac{1}{\sqrt{2\pi}} \int d\tilde{h} e^{-\frac{\tilde{h}^2}{2}} g(\tilde{h}) \right]^2 \\
&= \langle g \rangle^2 \\
&\approx \mathbb{E}_{\vec{\mathbf{x}}} \left[g \left(\frac{\vec{\mathbf{x}} \cdot \vec{\mathbf{a}}}{\sigma_X \sigma_a} \right) \right] \mathbb{E}_{\vec{\mathbf{x}}} \left[g \left(\frac{\vec{\mathbf{x}} \cdot \vec{\mathbf{b}}}{\sigma_X \sigma_b} \right) \right].
\end{aligned} \tag{S19}$$

From this result, we observe that the two functions $g\left(\frac{\vec{\mathbf{x}} \cdot \vec{\mathbf{a}}}{\sigma_X \sigma_a}\right)$ and $g\left(\frac{\vec{\mathbf{x}} \cdot \vec{\mathbf{b}}}{\sigma_X \sigma_b}\right)$ are statistically independent from one another in the thermodynamic limit.

2. Label Decomposition

By defining the ground truth parameters as shown below, we are able to decompose the labels into linear and nonlinear components,

$$y(\vec{\mathbf{x}}) = \vec{\mathbf{x}} \cdot \vec{\beta} + \delta y_{\text{NL}}^*(\vec{\mathbf{x}}) + \varepsilon, \quad \vec{\beta} \equiv \Sigma_{\vec{\mathbf{x}}}^{-1} \text{Cov}_{\vec{\mathbf{x}}}[\vec{\mathbf{x}}, y^*(\vec{\mathbf{x}})], \tag{S20}$$

where $\delta y_{\text{NL}}^*(\vec{\mathbf{x}}) \equiv y^*(\vec{\mathbf{x}}) - \vec{\mathbf{x}} \cdot \vec{\beta}$ and the covariance matrix of the input features $\Sigma_{\vec{\mathbf{x}}} = \text{Cov}_{\vec{\mathbf{x}}}[\vec{\mathbf{x}}, \vec{\mathbf{x}}^T]$ is assumed to be invertible.

We prove that the linear and nonlinear terms are statistically independent with respect the input features $\vec{\mathbf{x}}$ as follows:

$$\begin{aligned}
\text{Cov}_{\vec{\mathbf{x}}}[\vec{\mathbf{x}} \cdot \vec{\beta}, \delta y_{\text{NL}}^*(\vec{\mathbf{x}})] &= \text{Cov}_{\vec{\mathbf{x}}}[\vec{\mathbf{x}} \cdot \vec{\beta}, y(\vec{\mathbf{x}}) - \vec{\mathbf{x}} \cdot \vec{\beta}] \\
&= \vec{\beta} \cdot \text{Cov}_{\vec{\mathbf{x}}}[\vec{\mathbf{x}}, y(\vec{\mathbf{x}})] - \vec{\beta} \cdot \text{Cov}_{\vec{\mathbf{x}}}[\vec{\mathbf{x}}, \vec{\mathbf{x}}^T] \vec{\beta} \\
&= \vec{\beta} \cdot \Sigma_{\vec{\mathbf{x}}} \vec{\beta} - \vec{\beta} \cdot \Sigma_{\vec{\mathbf{x}}} \vec{\beta} \\
&= 0.
\end{aligned} \tag{S21}$$

Furthermore, we can show that the ground truth parameters as defined in Eq. S20 coincide with those of the teacher model,

$$y^*(\vec{\mathbf{x}}) = \frac{\sigma_\beta \sigma_X}{\langle f' \rangle} f \left(\frac{\vec{\mathbf{x}} \cdot \vec{\beta}}{\sigma_X \sigma_\beta} \right). \tag{S22}$$

To do this, we evaluate the covariance in the definition of $\vec{\beta}$ and use the second integral in Sec. S1C1 to find

$$\begin{aligned}
\vec{\beta} &= \Sigma_{\vec{\mathbf{x}}}^{-1} \text{Cov}_{\vec{\mathbf{x}}}[\vec{\mathbf{x}}, y^*(\vec{\mathbf{x}})] \\
&= \Sigma_{\vec{\mathbf{x}}}^{-1} \frac{\sigma_\beta \sigma_X}{\langle f' \rangle} \mathbb{E}_{\vec{\mathbf{x}}} \left[\vec{\mathbf{x}} f \left(\frac{\vec{\mathbf{x}} \cdot \vec{\beta}}{\sigma_X \sigma_\beta} \right) \right] \\
&\approx \Sigma_{\vec{\mathbf{x}}}^{-1} \frac{\sigma_\beta \sigma_X}{\langle f' \rangle} \frac{\Sigma_{\vec{\mathbf{x}}} \vec{\beta}}{\sigma_X \sigma_\beta} \langle f' \rangle \\
&= \vec{\beta}.
\end{aligned} \tag{S23}$$

So we see that the definitions are consistent with one another.

Next, we calculate the variance of the nonlinear components of the labels $\delta y_{\text{NL}}^*(\vec{x})$. To do this, we first calculate the mean of the squared true label using the first integral from Sec. [S1 C 1](#),

$$\mathbb{E}_{\vec{x}}[(y^*(\vec{x}))^2] = \frac{\sigma_\beta^2 \sigma_X^2}{\langle f' \rangle^2} \mathbb{E}_{\vec{x}} \left[f \left(\frac{\vec{x} \cdot \vec{\beta}}{\sigma_X \sigma_\beta} \right)^2 \right] \approx \sigma_\beta^2 \sigma_X^2 \frac{\langle f^2 \rangle}{\langle f' \rangle^2} \quad (\text{S24})$$

Using this, the variance of the nonlinear components in the thermodynamic limit is then

$$\begin{aligned} \text{Var}_{\vec{x}}[\delta y_{\text{NL}}^*(\vec{x})] &= \mathbb{E}_{\vec{x}} \left[\left(y^*(\vec{x}) - \vec{x} \cdot \vec{\beta} \right)^2 \right] \\ &= \mathbb{E}_{\vec{x}} \left[(y^*(\vec{x}))^2 \right] + \mathbb{E}_{\vec{x}} \left[(\vec{x} \cdot \vec{\beta})^2 \right] - 2 \mathbb{E}_{\vec{x}} [y^*(\vec{x}) \vec{x} \cdot \vec{\beta}] \\ &= \mathbb{E}_{\vec{x}} \left[(y^*(\vec{x}))^2 \right] - \sigma_\beta^2 \sigma_X^2 \\ &= \sigma_\beta^2 \sigma_X^2 \frac{\langle f^2 \rangle - \langle f' \rangle^2}{\langle f' \rangle^2}. \end{aligned} \quad (\text{S25})$$

Since there are no other random variables present in the variance, we summarize the statistical properties of the nonlinear components of the labels for data points \vec{x}_a and \vec{x}_b with full ensemble averages, giving us

$$\mathbb{E}[\delta y_{\text{NL}}^*(\vec{x}_a)] = 0, \quad \text{Cov}[\delta y_{\text{NL}}^*(\vec{x}_a), \delta y_{\text{NL}}^*(\vec{x}_b)] = \sigma_{\delta y^*}^2 \delta_{ab} \quad (\text{S26})$$

where we have defined the quantities

$$\sigma_{\delta y^*}^2 = \sigma_\beta^2 \sigma_X^2 \Delta f, \quad \Delta f = \frac{\langle f^2 \rangle - \langle f' \rangle^2}{\langle f' \rangle^2} \quad (\text{S27})$$

with the integrals

$$\langle f^2 \rangle = \frac{1}{\sqrt{2\pi}} \int_{-\infty}^{\infty} dh e^{-\frac{h^2}{2}} f^2(h), \quad \langle f' \rangle = \frac{1}{\sqrt{2\pi}} \int_{-\infty}^{\infty} dh e^{-\frac{h^2}{2}} f'(h). \quad (\text{S28})$$

3. Hidden Feature Decomposition

Similar to the decomposition of the labels, we decompose the hidden features into linear and nonlinear components that are statistically independent with respect to the input features by defining W as follows:

$$\vec{z}(\vec{x}) = \frac{\mu_z}{\sqrt{N_p}} \vec{\mathbf{1}} + W^T \vec{x} + \delta \vec{z}_{\text{NL}}(\vec{x}), \quad W \equiv \Sigma_{\vec{x}}^{-1} \text{Cov}_{\vec{x}}[\vec{x}, \vec{z}^T(\vec{x})], \quad (\text{S29})$$

where we have defined the nonlinear component as $\delta \vec{z}_{\text{NL}}(\vec{x}) \equiv \vec{z}(\vec{x}) - \frac{\mu_z}{\sqrt{N_p}} \vec{\mathbf{1}} - W^T \vec{x}$ and the mean as $\mu_z / \sqrt{N_p}$. We also use $\vec{\mathbf{1}}$ to indicate a length- N_p vector of ones.

We prove that the linear and nonlinear terms are statistically independent with respect to the input features \vec{x} as follows:

$$\begin{aligned} \text{Cov}_{\vec{x}}[W^T \vec{x}, \delta \vec{z}_{\text{NL}}(\vec{x})^T] &= \text{Cov}_{\vec{x}}[W^T \vec{x}, \vec{z}^T(\vec{x}) - \frac{\mu_z}{\sqrt{N_p}} \vec{\mathbf{1}}^T - \vec{x}^T W] \\ &= W^T \text{Cov}_{\vec{x}}[\vec{x}, \vec{z}^T(\vec{x})] - \frac{\mu_z}{\sqrt{N_p}} W^T \text{Cov}_{\vec{x}}[\vec{x}, \vec{\mathbf{1}}^T] - W^T \text{Cov}_{\vec{x}}[\vec{x}, \vec{x}^T] W \\ &= W^T \Sigma_{\vec{x}} W - W^T \Sigma_{\vec{x}} W \\ &= 0. \end{aligned} \quad (\text{S30})$$

We also show that W as defined in Eq. [S29](#) coincides with that in the definition of the hidden features,

$$\vec{z}(\vec{x}) = \frac{1}{\langle \varphi' \rangle} \frac{\sigma_W \sigma_X}{\sqrt{N_p}} \varphi \left(\frac{\sqrt{N_p}}{\sigma_W \sigma_X} W^T \vec{x} \right). \quad (\text{S31})$$

As in the previous section, we evaluate the covariance in the definition of W and use the second integral from Sec. S1C1 to find

$$\begin{aligned}
W &= \Sigma_{\vec{x}}^{-1} \text{Cov}_{\vec{x}}[\vec{x}, \vec{z}^T(\vec{x})] \\
&= \Sigma_{\vec{x}}^{-1} \frac{1}{\langle \varphi' \rangle} \frac{\sigma_W \sigma_X}{\sqrt{N_p}} \mathbb{E}_{\vec{x}} \left[\vec{x} \varphi \left(\frac{\sqrt{N_p}}{\sigma_W \sigma_X} \vec{x}^T W \right) \right] \\
&\approx \Sigma_{\vec{x}}^{-1} \frac{1}{\langle \varphi' \rangle} \frac{\sigma_W \sigma_X}{\sqrt{N_p}} \frac{\sqrt{N_p}}{\sigma_W \sigma_X} \Sigma_{\vec{x}} W \langle \varphi' \rangle \\
&= W.
\end{aligned} \tag{S32}$$

So we see that the definitions are consistent with one another.

Next, we calculate the covariance of the nonlinear component of the hidden features $\delta \vec{z}_{\text{NL}}(\vec{x})$ with respect to the full ensemble distribution. To do this, we first calculate the mean of each hidden feature using the first integral from Sec. S1C1,

$$\mathbb{E}_{\vec{x}}[z_J(\vec{x})] = \frac{1}{\langle \varphi' \rangle} \frac{\sigma_W \sigma_X}{\sqrt{N_p}} \mathbb{E}_{\vec{x}} \left[\varphi \left(\frac{\sqrt{N_p}}{\sigma_W \sigma_X} \sum_k W_{kJ} x_k \right) \right] \approx \frac{\sigma_W \sigma_X}{\sqrt{N_p}} \frac{\langle \varphi \rangle}{\langle \varphi' \rangle}, \tag{S33}$$

from which we see that

$$\mu_z = \sigma_W \sigma_X \frac{\langle \varphi \rangle}{\langle \varphi' \rangle}. \tag{S34}$$

We also calculate the mean of the square of each hidden feature,

$$\mathbb{E}_{\vec{x}}[z_J^2(\vec{x})] = \frac{1}{\langle \varphi' \rangle^2} \frac{\sigma_W^2 \sigma_X^2}{N_p} \mathbb{E}_{\vec{x}} \left[\varphi^2 \left(\frac{\sqrt{N_p}}{\sigma_W \sigma_X} \sum_k W_{kJ} x_k \right) \right] \approx \frac{\sigma_W^2 \sigma_X^2}{N_p} \frac{\langle \varphi^2 \rangle}{\langle \varphi' \rangle^2}. \tag{S35}$$

Using these two results, we calculate the variance of each hidden feature

$$\begin{aligned}
\text{Var}_{\vec{x}}[\delta z_{\text{NL},J}(\vec{x})] &= \mathbb{E}_{\vec{x}} \left[\left(z_J(\vec{x}) - \frac{\mu_Z}{\sqrt{N_p}} - \sum_k W_{kJ} x_k \right)^2 \right] \\
&= \mathbb{E}_{\vec{x}}[z_J^2(\vec{x})] + \frac{\mu_Z^2}{N_p} + \mathbb{E}_{\vec{x}} \left[\left(\sum_k W_{kJ} x_k \right)^2 \right] \\
&\quad - 2\mathbb{E}_{\vec{x}} \left[z_J(\vec{x}) \sum_k W_{kJ} x_k \right] - 2\mathbb{E}_{\vec{x}} \left[z_J(\vec{x}) \frac{\mu_Z}{\sqrt{N_p}} \right] + 2\mathbb{E}_{\vec{x}} \left[\frac{\mu_Z}{\sqrt{N_p}} \sum_k W_{kJ} x_k \right] \\
&= \mathbb{E}_{\vec{x}}[z_J^2(\vec{x})] - \frac{\mu_Z^2}{N_p} - \frac{\sigma_W^2 \sigma_X^2}{N_p} \\
&= \frac{\sigma_W^2 \sigma_X^2}{N_p} \frac{\langle \varphi^2 \rangle - \langle \varphi \rangle^2 - \langle \varphi' \rangle^2}{\langle \varphi' \rangle^2}.
\end{aligned} \tag{S36}$$

Finally, we calculate the mean of the product of two different hidden features $J \neq K$ for the same input features using the third integral in Sec. S1C1,

$$\begin{aligned}
\mathbb{E}_{\vec{x}}[z_J(\vec{x}) z_K(\vec{x})] &= \frac{1}{\langle \varphi' \rangle^2} \frac{\sigma_W^2 \sigma_X^2}{N_p} \mathbb{E}_{\vec{x}} \left[\varphi \left(\frac{\sqrt{N_p}}{\sigma_W \sigma_X} \sum_k W_{kJ} x_k \right) \varphi \left(\frac{\sqrt{N_p}}{\sigma_W \sigma_X} \sum_k W_{kK} x_k \right) \right] \\
&\approx \frac{1}{\langle \varphi' \rangle^2} \frac{\sigma_W^2 \sigma_X^2}{N_p} \mathbb{E}_{\vec{x}} \left[\varphi \left(\frac{\sqrt{N_p}}{\sigma_W \sigma_X} \sum_k W_{kJ} x_k \right) \right] \mathbb{E}_{\vec{x}} \left[\varphi \left(\frac{\sqrt{N_p}}{\sigma_W \sigma_X} \sum_k W_{kK} x_k \right) \right] \\
&= \mathbb{E}_{\vec{x}}[z_J(\vec{x})] \mathbb{E}_{\vec{x}}[z_K(\vec{x})].
\end{aligned} \tag{S37}$$

We find that different hidden features are independent in the thermodynamic limit. Since there are no other random variables present in any of the formulas, we summarize the statistical properties of the nonlinear components of the hidden features for data points $\vec{\mathbf{x}}_a$ and $\vec{\mathbf{x}}_b$ with full ensemble averages, giving us

$$\mathbb{E}[\delta z_{\text{NL},J}(\vec{\mathbf{x}}_a)] = 0, \quad \text{Cov}[\delta z_{\text{NL},J}(\vec{\mathbf{x}}_a), \delta z_{\text{NL},K}(\vec{\mathbf{x}}_b)] = \frac{\sigma_{\delta z}^2}{N_P} \delta_{ab} \delta_{JK} \quad (\text{S38})$$

where we have defined the quantities

$$\sigma_{\delta z}^2 = \sigma_W^2 \sigma_X^2 \Delta\varphi, \quad \Delta\varphi = \frac{\langle \varphi^2 \rangle - \langle \varphi \rangle^2 - \langle \varphi' \rangle^2}{\langle \varphi' \rangle^2} \quad (\text{S39})$$

with the integrals

$$\langle \varphi \rangle = \frac{1}{\sqrt{2\pi}} \int_{-\infty}^{\infty} dh e^{-\frac{h^2}{2}} \varphi(h), \quad \langle \varphi^2 \rangle = \frac{1}{\sqrt{2\pi}} \int_{-\infty}^{\infty} dh e^{-\frac{h^2}{2}} \varphi^2(h), \quad \langle \varphi' \rangle = \frac{1}{\sqrt{2\pi}} \int_{-\infty}^{\infty} dh e^{-\frac{h^2}{2}} \varphi'(h). \quad (\text{S40})$$

D. General System of Equations

Here, we establish the general system of equations that we will solve using the cavity method. The first set of N_p equations is given by the gradient in Eq. (S7), while the second is a set of M equations are those for the residual label errors for the training data points. Applying the decompositions of the labels in Eq. (S20) and the hidden features in Eq. (S29) gives us the following system of equations that we solve for each model:

$$\begin{aligned} \lambda \hat{w}_J &= \sum_{bk} \Delta y_b X_{bk} W_{kJ} + \sum_b \Delta y_b \delta z_J(\vec{\mathbf{x}}_b) \\ \Delta y_a &= \sum_k \beta_k X_{ak} + \delta y_{\text{NL}}^*(\vec{\mathbf{x}}_a) + \varepsilon_a - \sum_{Kk} \hat{w}_K W_{kK} X_{ak} - \sum_K \hat{w}_K \delta z_K(\vec{\mathbf{x}}_a). \end{aligned} \quad (\text{S41})$$

We will further refine these equations for each model, depending on the definition of the hidden features.

E. Linear Regression (No Basis Functions)

In linear regression without basis functions, the hidden features are the same as the input features,

$$\vec{z}(\vec{\mathbf{x}}) = \vec{\mathbf{x}}. \quad (\text{S42})$$

We substitute this set of hidden features into the system of equations in Eq. (S41) and then decompose the equations further, giving us three equations

$$\begin{aligned} \lambda \hat{w}_j &= \sum_b \Delta y_b X_{bj} + \eta_j \\ \Delta y_a &= \sum_k \Delta \beta_k X_{ak} + \delta y_{\text{NL}}^*(\vec{\mathbf{x}}_a) + \varepsilon_a + \xi_a \\ \Delta \beta_j &= \beta_j - \hat{w}_j. \end{aligned} \quad (\text{S43})$$

We define an additional set of unknowns, the residual parameter errors $\Delta \beta_j$, which measure the difference between the j th ground truth parameter estimated by the model – in this case, simply the fit parameter \hat{w}_j – and the actual ground truth parameter β_j (see Sec. S2). We also add small auxiliary fields η_j and ξ_a to the two equations containing sums. We will use these extra fields to define perturbations about the solutions to these equations with the intent of setting the fields to zero by the end of the derivation.

1. Cavity Expansion

Next, we add an additional variable of each type, resulting in a total of $M + 1$ data points and $N_f + 1$ features. We specify each new variable using an index value of 0, giving us the new unknown quantities \hat{w}_0 , Δy_0 , and $\Delta\beta_0$. These new variables result in the addition of an extra term in each sum, giving us the equations

$$\begin{aligned}\lambda\hat{w}_j &= \sum_b \Delta y_b X_{bj} + \eta_j + \Delta y_0 X_{0j} \\ \Delta y_a &= \sum_k \Delta\beta_k X_{ak} + \delta y_{\text{NL}}^*(\vec{x}_a) + \varepsilon_a + \xi_a + \Delta\beta_0 X_{a0}.\end{aligned}\tag{S44}$$

Each new variable is also described by a new equation,

$$\begin{aligned}\lambda\hat{w}_0 &= \sum_b \Delta y_b X_{b0} + \eta_0 + \Delta y_0 X_{00} \\ \Delta y_0 &= \sum_k \Delta\beta_k X_{0k} + \delta y_{\text{NL}}^*(\vec{x}_0) + \varepsilon_0 + \xi_0 + \Delta\beta_0 X_{00} \\ \Delta\beta_0 &= \beta_0 - \hat{w}_0.\end{aligned}\tag{S45}$$

As a reminder, sums always start at an index value of 1. Therefore, we explicitly specify any terms with an index value of 0.

Now we take the thermodynamic limit in which M and N_f tend towards infinity, but their ratio α_f remains fixed. In this limit, we can interpret the extra terms in Eq. (S44) as small perturbations to the auxiliary fields since they each contain an element of X which has mean zero and an infinitesimal variance of $\mathcal{O}(1/N_f)$,

$$\delta\eta_j = \Delta y_0 X_{0j}, \quad \delta\xi_a = \Delta\beta_0 X_{a0}.\tag{S46}$$

This allows us to expand each variable about its solution in the absence of the 0-indexed quantities, corresponding to the solution for M data points and N_f features,

$$\begin{aligned}\hat{w}_j &\approx \hat{w}_{j\setminus 0} + \sum_k \nu_{jk}^{\hat{w}} \delta\eta_k + \sum_b \chi_{jb}^{\hat{w}} \delta\xi_b \\ \Delta y_a &\approx \Delta y_{a\setminus 0} + \sum_k \nu_{ak}^{\Delta y} \delta\eta_k + \sum_b \chi_{ab}^{\Delta y} \delta\xi_b \\ \Delta\beta_j &\approx \Delta\beta_{j\setminus 0} + \sum_k \nu_{jk}^{\Delta\beta} \delta\eta_k + \sum_b \chi_{jb}^{\Delta\beta} \delta\xi_b.\end{aligned}\tag{S47}$$

We use subscripts with $\setminus 0$ to refer to the unperturbed solutions for each unknown quantity; that is, the solutions in the absence of the 0-indexed variables. We also define the susceptibility matrices as the following derivatives with respect to the auxiliary fields:

$$\begin{aligned}\nu_{jk}^{\hat{w}} &= \frac{\partial \hat{w}_j}{\partial \eta_k}, & \chi_{jb}^{\hat{w}} &= \frac{\partial \hat{w}_j}{\partial \xi_b}, \\ \nu_{ak}^{\Delta y} &= \frac{\partial \Delta y_a}{\partial \eta_k}, & \chi_{ab}^{\Delta y} &= \frac{\partial \Delta y_a}{\partial \xi_b}, \\ \nu_{jk}^{\Delta\beta} &= \frac{\partial \Delta\beta_j}{\partial \eta_k}, & \chi_{jb}^{\Delta\beta} &= \frac{\partial \Delta\beta_j}{\partial \xi_b}.\end{aligned}\tag{S48}$$

It is useful to note that the susceptibilities for the residual parameter errors are related to those for the fit parameters via a negative sign,

$$\nu_{jk}^{\Delta\beta} = -\nu_{jk}^{\hat{w}}, \quad \chi_{jb}^{\Delta\beta} = -\chi_{jb}^{\hat{w}}.\tag{S49}$$

Substituting the expansions in Eq. (S47) into the equations for the 0-indexed variables, Eq. (S45), we arrive at the following equations:

$$\begin{aligned}\lambda\hat{w}_0 &= \sum_a \left(\Delta y_{a\setminus 0} + \sum_k \nu_{ak}^{\Delta y} \delta\eta_k + \sum_b \chi_{ab}^{\Delta y} \delta\xi_b \right) X_{a0} + \eta_0 + X_{00} \Delta y_0 \\ \Delta y_0 &= \sum_j \left(\Delta\beta_{j\setminus 0} - \sum_k \nu_{jk}^{\hat{w}} \delta\eta_k - \sum_b \chi_{jb}^{\hat{w}} \delta\xi_b \right) X_{0j} + \delta y_{\text{NL}}^*(\vec{x}_0) + \varepsilon_0 + \xi_0 + \Delta\beta_0 X_{00}.\end{aligned}\tag{S50}$$

Our next step is to simplify these equations by approximating the sums over large numbers of random variables.

2. Approximations of Large Sums: Unperturbed Quantities

Each of the sums in Eq. (S50) contains a thermodynamically large – $\mathcal{O}(N_f)$ – number of statistically uncorrelated terms. This means that each sum satisfies the conditions necessary to apply the central limit theorem, allowing us to express each in terms of a single normally-distributed random variable described by just its mean and its variance.

First, we approximate the two sums that contain one of the unperturbed unknown quantities, $\Delta y_{a \setminus 0}$ or $\Delta \beta_{j \setminus 0}$. In both sums, the unperturbed quantities are statistically independent of any elements of X with a 0-index such as X_{a0} or X_{0j} . Using this independence, we find that the average of the sum in Eq. (S50) containing $\Delta y_{b \setminus 0}$ evaluates to zero when taken with respect to the elements of X with a 0-index,

$$\mathbb{E}_0 \left[\sum_b \Delta y_{b \setminus 0} X_{b0} \right] = \sum_b \Delta y_{b \setminus 0} \mathbb{E}_0[X_{b0}] = 0, \quad (\text{S51})$$

while its variance evaluates to

$$\begin{aligned} \text{Var}_0 \left[\sum_b \Delta y_{b \setminus 0} X_{b0} \right] &= \sum_b \Delta y_{b \setminus 0}^2 \text{Var}_0[X_{b0}] \\ &= \frac{\sigma_X^2}{N_f} \sum_b \Delta y_{b \setminus 0}^2. \end{aligned} \quad (\text{S52})$$

Using these results, we express the sum in terms of a single random variable $z_{\hat{w}}$ with zero mean and unit variance (labeled with subscript \hat{w} since this term occurs in the equation for \hat{w}_0),

$$\sum_b \Delta y_{b \setminus 0} X_{b0} \approx \sigma_{\hat{w}} z_{\hat{w}}, \quad \sigma_{\hat{w}}^2 = \sigma_X^2 \alpha_f^{-1} \langle \Delta y^2 \rangle, \quad \langle \Delta y^2 \rangle = \frac{1}{M} \sum_b \Delta y_{b \setminus 0}^2, \quad (\text{S53})$$

where $\sigma_{\hat{w}}^2$ is the total variance of the sum and $\langle \Delta y^2 \rangle$ is the mean squared residual label error. Performing an analogous procedure for the sum containing $\Delta \beta_{k \setminus 0}$ in Eq. (S50), we find that it approximates to

$$\sum_k \Delta \beta_{k \setminus 0} X_{0k} \approx \sigma_{\Delta y} z_{\Delta y}, \quad \sigma_{\Delta y}^2 = \sigma_X^2 \langle \Delta \beta^2 \rangle, \quad \langle \Delta \beta^2 \rangle = \frac{1}{N_f} \sum_k \Delta \beta_{k \setminus 0}^2 \quad (\text{S54})$$

where $z_{\Delta y}$ is again a random variable with zero mean and unit variance, $\sigma_{\Delta y}^2$ is the total variance of the sum, and $\langle \Delta \beta^2 \rangle$ is the mean squared residual parameter error.

The random variables $z_{\hat{w}}$ and $z_{\Delta y}$ are statistically independent since the two sums are independent,

$$\text{Cov}_0 \left[\sum_b \Delta y_{b \setminus 0} X_{b0}, \sum_k \Delta \beta_{k \setminus 0} X_{0k} \right] = \sum_{bk} \Delta y_{b \setminus 0} \Delta \beta_{k \setminus 0} \text{Cov}_0[X_{b0}, X_{0k}] = 0. \quad (\text{S55})$$

3. Approximations of Large Sums: Square Susceptibilities

Next, we approximate the sums that include either of the square susceptibility matrices, $\chi_{ab}^{\Delta y}$ or $\nu_{jk}^{\hat{w}}$. Similar to the unperturbed unknown quantities, we use the property that the susceptibilities are statistically independent of the elements of X with 0-valued indices. The mean of the sum containing $\chi_{ab}^{\Delta y}$ in Eq. (S50) evaluates to

$$\begin{aligned} \mathbb{E}_0 \left[\sum_{ab} \chi_{ab}^{\Delta y} X_{a0} X_{b0} \right] &= \sum_{ab} \chi_{ab}^{\Delta y} \mathbb{E}_0[X_{a0} X_{b0}] \\ &= \frac{\sigma_X^2}{N_f} \sum_b \chi_{bb}^{\Delta y}. \end{aligned} \quad (\text{S56})$$

To calculate the variance, we need to know the fourth moment of the distribution of elements of X . Because the elements of X are independent and normally-distributed, we use Wick's theorem to represent the fourth moment as

$$\mathbb{E}[X_{aj}X_{bk}X_{cl}X_{dm}] = \frac{\sigma_X^4}{N_f^2}(\delta_{ab}\delta_{cd}\delta_{jk}\delta_{lm} + \delta_{ac}\delta_{bd}\delta_{jl}\delta_{km} + \delta_{ad}\delta_{bc}\delta_{jm}\delta_{kl}). \quad (\text{S57})$$

Using this formula, we evaluate the variance to be

$$\begin{aligned} \text{Var}_0 \left[\sum_{ab} \chi_{ab}^{\Delta y} X_{a0} X_{b0} \right] &= \sum_{abcd} \chi_{ab}^{\Delta y} \chi_{cd}^{\Delta y} \text{Cov}_0[X_{a0} X_{b0}, X_{c0} X_{d0}] \\ &= \sum_{abcd} \chi_{ab}^{\Delta y} \chi_{cd}^{\Delta y} (\mathbb{E}_0[X_{a0} X_{b0} X_{c0} X_{d0}] - \mathbb{E}_0[X_{a0} X_{b0}] \mathbb{E}_0[X_{c0} X_{d0}]) \\ &= \frac{\sigma_X^4}{N_f^2} \sum_{ab} (\chi_{ab}^{\Delta y} \chi_{ab}^{\Delta y} + \chi_{ab}^{\Delta y} \chi_{ba}^{\Delta y}). \end{aligned} \quad (\text{S58})$$

If we consider decomposing $\chi_{ab}^{\Delta y}$ in term of its eigenvalue decomposition with eigenvalues σ_i , the variance becomes

$$\text{Var}_0 \left[\sum_{ab} \chi_{ab}^{\Delta y} X_{a0} X_{b0} \right] = 2 \frac{\sigma_X^4}{N_f^2} \sum_i \sigma_i^2. \quad (\text{S59})$$

If each eigenvalue is $\mathcal{O}(1)$, then the variance is $\mathcal{O}(1/N_f)$ and can therefore be neglected. As a result, we approximate the overall sum using just its mean,

$$\sum_{ab} \chi_{ab}^{\Delta y} X_{a0} X_{b0} \approx \sigma_X^2 \alpha_f^{-1} \chi, \quad \chi = \frac{1}{M} \sum_b \chi_{bb}^{\Delta y}, \quad (\text{S60})$$

where χ can be interpreted as a scalar susceptibility.

Analogously, the sum containing $\nu_{jk}^{\hat{w}}$ in Eq. (S50) becomes

$$\sum_{jk} \nu_{jk}^{\hat{w}} X_{0j} X_{0k} \approx \sigma_X^2 \nu, \quad \nu = \frac{1}{N_f} \sum_k \nu_{kk}^{\hat{w}} \quad (\text{S61})$$

where ν is an additional scalar susceptibility.

4. Approximations of Large Sums: Rectangular Susceptibilities

The final pair of sums we approximate are those containing one of the rectangular susceptibility matrices, $\nu_{ak}^{\Delta y}$ or $\chi_{jb}^{\hat{w}}$. Performing the same procedure as the previous section, we find that the mean of the sum containing $\chi_{jb}^{\hat{w}}$ is zero,

$$\mathbb{E}_0 \left[\sum_{jb} \chi_{jb}^{\hat{w}} X_{0j} X_{b0} \right] = \sum_{jb} \chi_{jb}^{\hat{w}} \mathbb{E}_0[X_{0j} X_{b0}] = 0, \quad (\text{S62})$$

while its variance is small in the thermodynamic limit,

$$\begin{aligned} \text{Var}_0 \left[\sum_{jb} \chi_{jb}^{\hat{w}} X_{0j} X_{b0} \right] &= \sum_{jkab} \chi_{jb}^{\hat{w}} \chi_{ka}^{\hat{w}} \text{Cov}_0[X_{0j} X_{b0}, X_{0k} X_{a0}] \\ &= \sum_{jkab} \chi_{jb}^{\hat{w}} \chi_{ka}^{\hat{w}} (\mathbb{E}_0[X_{0j} X_{0k}] \mathbb{E}_0[X_{a0} X_{b0}] - \mathbb{E}_0[X_{0j}] \mathbb{E}_0[X_{b0}] \mathbb{E}_0[X_{0k}] \mathbb{E}_0[X_{a0}]) \\ &= \frac{\sigma_X^4}{N_f^2} \sum_{jb} (\chi_{jb}^{\hat{w}})^2 \\ &= \frac{\sigma_X^4}{N_f^2} \sum_i \sigma_i^2 \\ &\approx \mathcal{O}\left(\frac{1}{N_f}\right), \end{aligned} \quad (\text{S63})$$

where in the second-to-last step, we have decomposed $\chi_{jb}^{\hat{w}}$ into its singular value decomposition with singular values σ_i , assumed to each be $\mathcal{O}(1)$.

This allows us to approximate the sum as zero,

$$\sum_{jb} \chi_{jb}^{\hat{w}} X_{0j} X_{b0} \approx 0. \quad (\text{S64})$$

We find the same result for the sum containing $\nu_{ak}^{\Delta y}$,

$$\sum_{ak} \nu_{ak}^{\Delta y} X_{a0} X_{0k} \approx 0. \quad (\text{S65})$$

These two results allow us to neglect these two sums in the thermodynamic limit.

5. Self-consistency Equations

Applying the approximations of the large sums from the previous sections to Eq. (S50), we obtain the following set of self-consistency equations for the 0-indexed variables, \hat{w}_0 , Δy_0 , and $\Delta\beta_0$:

$$\begin{aligned} \lambda \hat{w}_0 &\approx \sigma_{\hat{w}} z_{\hat{w}} + \Delta\beta_0 \sigma_X^2 \alpha_f^{-1} \chi + \eta_0 \\ \Delta y_0 &\approx \sigma_{\Delta y} z_{\Delta y} - \Delta y_0 \sigma_X^2 \nu + \delta y_{\text{NL}}^*(\vec{x}_0) + \varepsilon_0 + \xi_0 \\ \Delta\beta_0 &\approx \beta_0 - \hat{w}_0. \end{aligned} \quad (\text{S66})$$

In these equations, we have also dropped terms proportional to X_{00} since this quantity has zero mean and a variance which goes to zero in the thermodynamic limit. Next, we solve these three equations for the 0-indexed variables, giving us

$$\begin{aligned} \hat{w}_0 &= \frac{\beta_0 \sigma_X^2 \alpha_f^{-1} \chi + \sigma_{\hat{w}} z_{\hat{w}} + \eta_0}{\lambda + \sigma_X^2 \alpha_f^{-1} \chi} \\ \Delta y_0 &= \frac{\sigma_{\Delta y} z_{\Delta y} + \delta y_{\text{NL}}^*(\vec{x}_0) + \varepsilon_0 + \xi_0}{1 + \sigma_X^2 \nu} \\ \Delta\beta_0 &= \frac{\beta_0 \lambda - \sigma_{\hat{w}} z_{\hat{w}} - \eta_0}{\lambda + \sigma_X^2 \alpha_f^{-1} \chi}. \end{aligned} \quad (\text{S67})$$

Note that all random variables within each of the above equations are statistically independent from one another.

Next, we make the approximation that in the thermodynamic limit, each of the unknown quantities is “self-averaging.” In other words, we assume that an average over a set of non-0-indexed variables is equivalent to taking an ensemble average of the single corresponding 0-indexed variable.

This allows us to use Eq. (S67) to find a set of self-consistent equations for the scalar susceptibilities by evaluating the appropriate derivatives with respect to the 0-indexed auxiliary fields and performing ensemble averages,

$$\begin{aligned} \chi &= \frac{1}{M} \sum_b \chi_{bb}^{\Delta y} \approx \text{E}[\chi_{00}^{\Delta y}] = \text{E}\left[\frac{\partial \Delta y_0}{\partial \xi_0}\right] = \frac{1}{1 + \sigma_X^2 \nu} \\ \nu &= \frac{1}{N_f} \sum_k \nu_{kk}^{\hat{w}} \approx \text{E}[\nu_{00}^{\hat{w}}] = \text{E}\left[\frac{\partial \hat{w}_0}{\partial \eta_0}\right] = \frac{1}{\lambda + \sigma_X^2 \alpha_f^{-1} \chi}. \end{aligned} \quad (\text{S68})$$

Furthermore, we find the following self-consistent equations for quantities, $\langle \Delta y^2 \rangle$ and $\langle \Delta\beta^2 \rangle$, by taking the appropriate expectation values of the 0-indexed quantities, plugging in the forms of the scalar susceptibilities, and setting the auxiliaries fields to zero:

$$\begin{aligned} \langle \hat{w}^2 \rangle &= \frac{1}{N_f} \sum_k \hat{w}_{k0}^2 \approx \text{E}[\hat{w}_0^2] = \nu^2 \left(\sigma_{\beta}^2 \sigma_X^4 \alpha_f^{-2} \chi^2 + \sigma_X^2 \alpha_f^{-1} \langle \Delta y^2 \rangle \right) \\ \langle \Delta y^2 \rangle &= \frac{1}{M} \sum_b \Delta y_{b0}^2 \approx \text{E}[\Delta y_0^2] = \chi^2 (\sigma_X^2 \langle \Delta\beta^2 \rangle + \sigma_{\delta y}^2 + \sigma_{\varepsilon}^2) \\ \langle \Delta\beta^2 \rangle &= \frac{1}{N_f} \sum_k \Delta\beta_{k0}^2 \approx \text{E}[\Delta\beta_0^2] = \nu^2 \left(\sigma_{\beta}^2 \lambda^2 + \sigma_X^2 \alpha_f^{-1} \langle \Delta y^2 \rangle \right). \end{aligned} \quad (\text{S69})$$

Note that we have also defined the mean squared fit parameter size $\langle \hat{w}^2 \rangle$. In addition, each of the three mean squared quantities can be interpreted as a full ensemble average. These self-consistent equations, along with those for the scalar susceptibilities, capture almost all behavior of our model of linear regression in the thermodynamic limit.

6. Solutions with Finite Regularization ($\lambda \sim \mathcal{O}(1)$)

Next, we derive the solutions when the regularization parameter λ is finite. By combining the two scalar susceptibilities in Eq. (S68), we find a quadratic equation for χ ,

$$\chi^2 + [(\alpha_f - 1) + \bar{\lambda}\alpha_f]\chi - \bar{\lambda}\alpha_f = 0, \quad (\text{S70})$$

where we have defined the dimensionless regularization parameter

$$\bar{\lambda} = \frac{\lambda}{\sigma_X^2}. \quad (\text{S71})$$

Solving Eq. (S70), we find two solutions:

$$\chi = \frac{1}{2} \left[1 - \alpha_f(1 + \bar{\lambda}) \pm \sqrt{[1 - \alpha_f(1 + \bar{\lambda})]^2 + 4\alpha_f\bar{\lambda}} \right]. \quad (\text{S72})$$

Using these solutions we can also find similar solutions for ν . Next, we solve Eq. (S69) to find closed-form solutions for $\langle \hat{w}^2 \rangle$, $\langle \Delta y^2 \rangle$, and $\langle \Delta \beta^2 \rangle$:

$$\begin{pmatrix} \langle \hat{w}^2 \rangle \\ \langle \Delta y^2 \rangle \\ \langle \Delta \beta^2 \rangle \end{pmatrix} = \begin{pmatrix} 1 & -\sigma_X^2 \alpha_f^{-1} \nu^2 & 0 \\ 0 & 1 & -\sigma_X^2 \chi^2 \\ 0 & -\sigma_X^2 \alpha_f^{-1} \nu^2 & 1 \end{pmatrix}^{-1} \begin{pmatrix} \sigma_\beta^2 \sigma_X^4 \alpha_f^{-2} \chi^2 \nu^2 \\ (\sigma_\varepsilon^2 + \sigma_{\delta y^*}^2) \chi^2 \\ \bar{\lambda}^2 \sigma_\beta^2 \sigma_X^2 \nu^2 \end{pmatrix}. \quad (\text{S73})$$

In combination with the solutions for χ and ν , these solutions are exact in the thermodynamic limit.

7. Solutions in Ridge-less Limit ($\lambda \rightarrow 0$)

In order to make the solutions in the previous section easier to interpret, we take the ridge-less limit where $\lambda \rightarrow 0$. Based on the form of Eq. (S70), we make the ansatz that the lowest order contribution to χ is $\mathcal{O}(1)$ in small $\bar{\lambda}$. Accordingly, we expand χ in small $\bar{\lambda}$ up to $\mathcal{O}(\bar{\lambda})$ as

$$\chi \approx \chi_0 + \bar{\lambda}\chi_1. \quad (\text{S74})$$

Substituting this approximation into the formula for χ in Eq. (S70), we find the following equation at $\mathcal{O}(1)$:

$$\begin{aligned} 0 &= \chi_0^2 + (\alpha_f - 1)\chi_0 \\ &= (\chi_0 + \alpha_f - 1)\chi_0. \end{aligned} \quad (\text{S75})$$

Solving this equation, we find two solutions for χ_0 ,

$$\chi_0^{(1)} = 1 - \alpha_f, \quad \chi_0^{(2)} = 0. \quad (\text{S76})$$

We label each set of solutions for all quantities with a superscript (1) or (2). These two solutions correspond to the two solutions in the exact formula for χ in Eq. (S72). Next, we collect terms in Eq. (S70) at $\mathcal{O}(\bar{\lambda})$,

$$0 = 2\chi_0\chi_1 + (\alpha_f - 1)\chi_1 + \alpha_f(\chi_0 - 1). \quad (\text{S77})$$

Solving, we obtain an equation for χ_1 in terms of χ_0 ,

$$\chi_1 = \frac{\alpha_f(1 - \chi_0)}{2\chi_0 + \alpha_f - 1}. \quad (\text{S78})$$

Combining this equation with the solutions for χ_0 , we obtain the two corresponding solutions for χ_1 ,

$$\chi_1^{(1)} = \frac{\alpha_f^2}{1 - \alpha_f}, \quad \chi_1^{(2)} = \frac{\alpha_f}{\alpha_f - 1}. \quad (\text{S79})$$

Next, we solve for the two solutions for ν . By inspecting the equation for ν in terms of χ in Eq. (S68), we make the ansatz that the lowest contribution of ν is $\mathcal{O}(1/\bar{\lambda})$,

$$\nu \approx \frac{1}{\bar{\lambda}} \nu_{-1} + \nu_0. \quad (\text{S80})$$

Substituting the solutions for χ_0 and χ_1 into the equation for ν , we find that the solutions for ν_{-1} are

$$\nu_{-1}^{(1)} = 0, \quad \nu_{-1}^{(2)} = \frac{1}{\sigma_X^2 + \frac{\sigma_X^2}{\alpha_f} \chi_1} = \frac{1}{\sigma_X^2} \frac{\alpha_f - 1}{\alpha_f}. \quad (\text{S81})$$

Since $\nu_{-1}^{(1)}$ is zero, we also solve for the next order term for solution (1),

$$\nu_0^{(1)} = \frac{1}{\sigma_X^2} \frac{\alpha_f}{(1 - \alpha_f)}. \quad (\text{S82})$$

We also expand each of the ensemble-averaged quantities $\langle \hat{w}^2 \rangle$, $\langle \Delta y^2 \rangle$, and $\langle \Delta \beta^2 \rangle$ in small $\bar{\lambda}$. We make the ansatz that each of these quantities is $\mathcal{O}(1)$ to lowest order with the next terms in the expansion at $\mathcal{O}(\bar{\lambda}^2)$:

$$\begin{aligned} \langle \hat{w}^2 \rangle &\approx \langle \hat{w}^2 \rangle_0 + \bar{\lambda}^2 \langle \hat{w}^2 \rangle_2 \\ \langle \Delta y^2 \rangle &\approx \langle \Delta y^2 \rangle_0 + \bar{\lambda}^2 \langle \Delta y^2 \rangle_2 \\ \langle \Delta \beta^2 \rangle &\approx \langle \Delta \beta^2 \rangle_0 + \bar{\lambda}^2 \langle \Delta \beta^2 \rangle_2. \end{aligned} \quad (\text{S83})$$

Solution (1): For the first set of solutions, the self-consistent equations, Eq. (S69), to lowest order, are

$$\begin{aligned} \langle \hat{w}^2 \rangle_0^{(1)} &= (\nu_0^{(1)})^2 \left[\sigma_\beta^2 \sigma_X^4 \alpha_f^{-2} (\chi_0^{(1)})^2 + \sigma_X^2 \alpha_f^{-1} \langle \Delta y^2 \rangle_0^{(1)} \right] \\ \langle \Delta y^2 \rangle_0^{(1)} &= (\chi_0^{(1)})^2 \left[\sigma_X^2 \langle \Delta \beta^2 \rangle_0^{(1)} + \sigma_{\delta y^*}^2 + \sigma_\varepsilon^2 \right] \\ \langle \Delta \beta^2 \rangle_0^{(1)} &= (\nu_0^{(1)})^2 \sigma_X^2 \alpha_f^{-1} \langle \Delta y^2 \rangle_0^{(1)}. \end{aligned} \quad (\text{S84})$$

Substituting the solutions for the susceptibilities into these equations and solving, we find

$$\begin{aligned} \langle \hat{w}^2 \rangle_0^{(1)} &= \sigma_\beta^2 + \frac{1}{\sigma_X^2} (\sigma_\varepsilon^2 + \sigma_{\delta y^*}^2) \frac{\alpha_f}{(1 - \alpha_f)} \\ \langle \Delta y^2 \rangle_0^{(1)} &= (\sigma_\varepsilon^2 + \sigma_{\delta y^*}^2) (1 - \alpha_f) \\ \langle \Delta \beta^2 \rangle_0^{(1)} &= \frac{1}{\sigma_X^2} (\sigma_\varepsilon^2 + \sigma_{\delta y^*}^2) \frac{\alpha_f}{(1 - \alpha_f)}. \end{aligned} \quad (\text{S85})$$

Solution (2): For the second set of solutions, the self-consistent equations to lowest order, are

$$\begin{aligned} \langle \hat{w}^2 \rangle_0^{(2)} &= (\nu_{-1}^{(2)})^2 \left[\sigma_\beta^2 \sigma_X^4 \alpha_f^{-2} (\chi_1^{(2)})^2 + \sigma_X^2 \alpha_f^{-1} \langle \Delta y^2 \rangle_2^{(2)} \right] \\ \langle \Delta y^2 \rangle_0^{(2)} &= 0 \\ \langle \Delta \beta^2 \rangle_0^{(2)} &= (\nu_{-1}^{(2)})^2 \left[\sigma_\beta^2 \sigma_X^4 + \sigma_X^2 \alpha_f^{-1} \langle \Delta y^2 \rangle_2^{(2)} \right]. \end{aligned} \quad (\text{S86})$$

We see that we also need the solution for $\langle \Delta y^2 \rangle$ to next lowest order,

$$\langle \Delta y^2 \rangle_2^{(2)} = (\chi_1^{(2)})^2 \left[\sigma_X^2 \langle \Delta \beta^2 \rangle_0^{(2)} + \sigma_{\delta y^*}^2 + \sigma_\varepsilon^2 \right]. \quad (\text{S87})$$

Substituting the solutions for the susceptibilities into these equations and solving, we find

$$\begin{aligned} \langle \hat{w}^2 \rangle_0^{(2)} &= \sigma_\beta^2 \frac{1}{\alpha_f} + \frac{1}{\sigma_X^2} (\sigma_\varepsilon^2 + \sigma_{\delta y^*}^2) \frac{1}{(\alpha_f - 1)} \\ \langle \Delta y^2 \rangle_2^{(2)} &= \sigma_\beta^2 \sigma_X^2 \frac{\alpha_f}{(\alpha_f - 1)} + (\sigma_\varepsilon^2 + \sigma_{\delta y^*}^2) \frac{\alpha_f^3}{(\alpha_f - 1)^3} \\ \langle \Delta \beta^2 \rangle_0^{(2)} &= \sigma_\beta^2 \frac{(\alpha_f - 1)}{\alpha_f} + \frac{1}{\sigma_X^2} (\sigma_\varepsilon^2 + \sigma_{\delta y^*}^2) \frac{1}{(\alpha_f - 1)}. \end{aligned} \quad (\text{S88})$$

Combined solutions: To determine when each of the two solutions applies, we use the fact that each of the ensemble-averaged quantities $\langle \hat{w}^2 \rangle$, $\langle \Delta y^2 \rangle$, and $\langle \Delta \beta^2 \rangle$ must always be positive by definition. Imposing this constraint, we find that solution (1) only applies when $\alpha_f < 1$, while solution (2) only applies when $\alpha_f > 1$. Combining these solutions, we arrive at the final forms for the three ensemble-averaged quantities in the $\lambda \rightarrow 0$ limit,

$$\begin{aligned} \langle \hat{w}^2 \rangle &= \begin{cases} \sigma_\beta^2 + \frac{(\sigma_\varepsilon^2 + \sigma_{\delta y^*}^2)}{\sigma_X^2} \frac{\alpha_f}{(1-\alpha_f)} & \text{if } N_f < M \\ \sigma_\beta^2 \frac{1}{\alpha_f} + \frac{(\sigma_\varepsilon^2 + \sigma_{\delta y^*}^2)}{\sigma_X^2} \frac{1}{(\alpha_f-1)} & \text{if } N_f > M \end{cases} \\ \langle \Delta y^2 \rangle &= \begin{cases} (\sigma_\varepsilon^2 + \sigma_{\delta y^*}^2)(1 - \alpha_f) & \text{if } N_f < M \\ \frac{\lambda^2}{\sigma_X^4} \left[\sigma_\beta^2 \sigma_X^2 \frac{\alpha_f}{(\alpha_f-1)} + (\sigma_\varepsilon^2 + \sigma_{\delta y^*}^2) \frac{\alpha_f^3}{(\alpha_f-1)^3} \right] & \text{if } N_f > M \end{cases} \\ \langle \Delta \beta^2 \rangle &= \begin{cases} \frac{(\sigma_\varepsilon^2 + \sigma_{\delta y^*}^2)}{\sigma_X^2} \frac{\alpha_f}{(1-\alpha_f)} & \text{if } N_f < M \\ \sigma_\beta^2 \frac{(\alpha_f-1)}{\alpha_f} + \frac{(\sigma_\varepsilon^2 + \sigma_{\delta y^*}^2)}{\sigma_X^2} \frac{1}{(\alpha_f-1)} & \text{if } N_f > M. \end{cases} \end{aligned} \quad (\text{S89})$$

For completeness, we also report solutions for the two scalar susceptibilities,

$$\chi = \begin{cases} 1 - \alpha_f & \text{if } N_f < M \\ \frac{\lambda}{\sigma_X^2} \frac{\alpha_f}{(\alpha_f-1)} & \text{if } N_f > M \end{cases}, \quad \nu = \begin{cases} \frac{1}{\sigma_X^2} \frac{\alpha_f}{(1-\alpha_f)} & \text{if } N_f < M \\ \frac{1}{\lambda} \frac{1}{\alpha_f} & \text{if } N_f > M. \end{cases} \quad (\text{S90})$$

Recall that the training error is defined as

$$\mathcal{E}_{\text{train}} = \frac{1}{M} \sum_b \Delta y_b^2. \quad (\text{S91})$$

We find that the ensemble-average of this quantity can be explicitly expressed as

$$\langle \mathcal{E}_{\text{train}} \rangle = \langle \Delta y^2 \rangle. \quad (\text{S92})$$

8. Test Error

We evaluate the test error on a data set, $\mathcal{D}' = \{(y'_b, \vec{x}'_b)\}_{b=1}^{M'}$, sampled independently from the same distribution as the training set. Recall that the test error is defined as

$$\mathcal{E}_{\text{test}} = \frac{1}{M'} \sum_b (\Delta y'_b)^2 \quad (\text{S93})$$

where the sum ranges from 1 to M' . We note that the residual label error of each test data point is described by the same distribution in the ensemble. Therefore, once we have taken the ensemble average, the test error can be expressed as an average over a single arbitrary test data point, (y, \vec{x}) , giving us

$$\begin{aligned} \langle \mathcal{E}_{\text{test}} \rangle &= \text{E} \left[\frac{1}{M'} \sum_b (\Delta y'_b)^2 \right] \\ &= \text{E} [\Delta y^2] \\ &= \text{E} \left[\left(\vec{x} \cdot \Delta \vec{\beta} + \delta y_{\text{NL}}^*(\vec{x}) + \varepsilon \right)^2 \right] \\ &= \text{E} \left[\left(\vec{x} \cdot \Delta \vec{\beta} \right)^2 \right] + \text{E} [(\delta y_{\text{NL}}^*(\vec{x}))^2] + \text{E} [(\varepsilon)^2] \\ &= \sigma_X^2 \text{E} \left[\frac{1}{N_f} \sum_k \Delta \beta_k^2 \right] + \sigma_{\delta y^*}^2 + \sigma_\varepsilon^2 \\ &\approx \sigma_X^2 \langle \Delta \beta^2 \rangle + \sigma_{\delta y^*}^2 + \sigma_\varepsilon^2, \end{aligned} \quad (\text{S94})$$

where we have used the self-averaging approximation to arrive at the final line.

Using this formula, the solutions for the test error in the limit $\lambda \rightarrow 0$ are

$$\langle \mathcal{E}_{\text{test}} \rangle = \begin{cases} (\sigma_\varepsilon^2 + \sigma_{\delta y^*}^2) \frac{1}{(1-\alpha_f)} & \text{if } N_f < M \\ \sigma_\beta^2 \sigma_X^2 \frac{(\alpha_f-1)}{\alpha_f} + (\sigma_\varepsilon^2 + \sigma_{\delta y^*}^2) \frac{\alpha_f}{(\alpha_f-1)} & \text{if } N_f > M. \end{cases} \quad (\text{S95})$$

9. Bias-Variance Decomposition

The bias-variance decomposition of the ensemble-averaged test error is

$$\langle \mathcal{E}_{\text{test}} \rangle = \langle \text{Bias}^2[\hat{y}(\vec{x})] \rangle + \langle \text{Var}[\hat{y}(\vec{x})]^2 \rangle + \text{Noise} \quad (\text{S96})$$

where the noise term is simply the mean squared average of the label noise associated with an arbitrary test data point (y, \vec{x}) ,

$$\text{Noise} = \text{E}[(\varepsilon)^2] = \sigma_\varepsilon^2. \quad (\text{S97})$$

The primary difficulty in computing the ensemble average of the squared bias is correctly calculating the square of the sampling average over possible training sets \mathcal{D} contained within its definition,

$$\langle \text{Bias}^2[\hat{y}(\vec{x})] \rangle = \text{E}_{\vec{\beta}, \vec{x}} \left[(\text{E}_{\mathcal{D}}[\hat{y}(\vec{x})] - y^*(\vec{x}))^2 \right]. \quad (\text{S98})$$

Note that averaging over \mathcal{D} implies averaging over only the features X and noise $\vec{\varepsilon}$ of the training set. In order to compute this average correctly, we make use of the following trick: we reinterpret the squared average over \mathcal{D} as two separate averages over uncorrelated training data sets \mathcal{D}_1 and \mathcal{D}_2 , drawn from the same distribution with the same ground truth parameters $\vec{\beta}$. Now, instead of a single regression problem trained on a single data set \mathcal{D} , we consider two separate regression problems each trained independently on a different training set, \mathcal{D}_1 and \mathcal{D}_2 , but which share all other random variables including $\vec{\beta}$, the test data point \vec{x} , etc. This allows us to express the ensemble-averaged squared bias as

$$\langle \text{Bias}^2[\hat{y}(\vec{x})] \rangle = \text{E}_{\vec{\beta}, \vec{x}, \mathcal{D}_1, \mathcal{D}_2} [(\hat{y}(\vec{x}; \hat{\mathbf{w}}_1) - y^*(\vec{x}))(\hat{y}(\vec{x}; \hat{\mathbf{w}}_2) - y^*(\vec{x}))] \quad (\text{S99})$$

where we use subscripts 1 and 2 to denote quantities that result from training on data sets \mathcal{D}_1 and \mathcal{D}_2 , respectively.

Using the definition of the residual parameter error and performing the appropriate averages, we find a simple expression for the ensemble-averaged squared bias for linear regression,

$$\begin{aligned} \langle \text{Bias}^2[\hat{y}(\vec{x})] \rangle &= \text{E} \left[\left(\vec{x} \cdot \Delta \vec{\beta}_1 - \delta y_{\text{NL}}^*(\vec{x}) \right) \left(\vec{x} \cdot \Delta \vec{\beta}_2 - \delta y_{\text{NL}}^*(\vec{x}) \right) \right] \\ &= \text{E} \left[\left(\vec{x} \cdot \Delta \vec{\beta}_1 \right) \left(\vec{x} \cdot \Delta \vec{\beta}_2 \right) \right] + \text{E} \left[(\delta y_{\text{NL}}^*(\vec{x}))^2 \right] \\ &= \sigma_X^2 \text{E} \left[\frac{1}{N_f} \sum_k \Delta \beta_{1,k} \Delta \beta_{2,k} \right] + \sigma_{\delta y^*}^2 \\ &\approx \sigma_X^2 \langle \Delta \beta_1 \Delta \beta_2 \rangle + \sigma_{\delta y^*}^2 \end{aligned} \quad (\text{S100})$$

where we have used the fact that all residual parameter errors are described by the same distribution, allowing us to define

$$\langle \Delta \beta_1 \Delta \beta_2 \rangle = \frac{1}{N_f} \sum_k \Delta \beta_{1,k} \Delta \beta_{2,k}. \quad (\text{S101})$$

Here, we find an alternative interpretation for the bias as the average covariance between the residual parameter errors from training on two independent training sets [it is clear from Eq. (S67) that $\text{E}[\Delta \beta_j] = 0$]. From here, we derive an expression for the variance,

$$\begin{aligned} \langle \text{Var}[\hat{y}(\vec{x})] \rangle &= \langle \mathcal{E}_{\text{test}} \rangle - \langle \text{Bias}^2[\hat{y}(\vec{x})] \rangle - \text{Noise} \\ &= \sigma_X^2 (\langle \Delta \beta^2 \rangle - \langle \Delta \beta_1 \Delta \beta_2 \rangle). \end{aligned} \quad (\text{S102})$$

To find $\langle \Delta \beta_1 \Delta \beta_2 \rangle$, we use the formula for $\Delta \beta_0$ in Eq. (S67) to characterize its behavior when trained separately on each of the two training sets,

$$\begin{aligned} \Delta \beta_{1,0} &= \nu(\beta_0 \lambda - \sigma_{\hat{w}} z_{\hat{w}_1}) \\ \Delta \beta_{2,0} &= \nu(\beta_0 \lambda - \sigma_{\hat{w}} z_{\hat{w}_2}). \end{aligned} \quad (\text{S103})$$

Note that while the random variables $z_{\hat{w}_1}$ and $z_{\hat{w}_2}$ are defined separately for the two regression problems, both equations share the same β_0 . Multiplying these two equations together and using the self-averaging approximation, we find an expression for $\langle \Delta\beta_1 \Delta\beta_2 \rangle$,

$$\langle \Delta\beta_1 \Delta\beta_2 \rangle = \frac{1}{N_f} \sum_k \Delta\beta_{1,k} \Delta\beta_{2,k} \approx \mathbb{E}[\Delta\beta_{1,0} \Delta\beta_{2,0}] = \nu^2 (\sigma_\beta^2 \lambda^2 + \mathbb{E}[\sigma_{\hat{w}}^2 z_{\hat{w}_1} z_{\hat{w}_2}]). \quad (\text{S104})$$

Next, we calculate the expectation value of the product $z_{\hat{w}_1} z_{\hat{w}_2}$ and find that it evaluates to zero as a result of the statistical independence of the two design matrices, X_1 and X_2 ,

$$\begin{aligned} \mathbb{E}[\sigma_{\hat{w}}^2 z_{\hat{w}_1} z_{\hat{w}_2}] &\approx \mathbb{E}\left[\sum_{ab} \Delta y_{1,a \setminus 0} \Delta y_{2,b \setminus 0} X_{1,a0} X_{2,b0}\right] \\ &= \sum_{ab} \mathbb{E}[\Delta y_{1,a \setminus 0} \Delta y_{2,b \setminus 0}] \mathbb{E}[X_{1,a0} X_{2,b0}] \\ &= 0. \end{aligned} \quad (\text{S105})$$

Substituting this solution into Eq. (S104), we find an expression for $\langle \Delta\beta_1 \Delta\beta_2 \rangle$,

$$\langle \Delta\beta_1 \Delta\beta_2 \rangle = \sigma_\beta^2 \lambda^2 \nu^2. \quad (\text{S106})$$

Inserting the solutions for ν , we find in the $\lambda \rightarrow 0$ limit that

$$\langle \Delta\beta_1 \Delta\beta_2 \rangle = \begin{cases} \frac{\lambda^2}{\sigma_X^2} \sigma_\beta^2 \frac{\alpha_f^2}{(1-\alpha_f)^2} & \text{if } N_f < M \\ \sigma_\beta^2 \frac{(\alpha_f-1)^2}{\alpha_f^2} & \text{if } N_f > M. \end{cases} \quad (\text{S107})$$

From this, we arrive at the final expressions for the model bias and variance in the $\lambda \rightarrow 0$ limit,

$$\begin{aligned} \langle \text{Bias}^2[\hat{y}(\vec{x})] \rangle &= \begin{cases} \sigma_{\delta y^*}^2 & \text{if } N_f < M \\ \sigma_\beta^2 \sigma_X^2 \frac{(\alpha_f-1)^2}{\alpha_f^2} + \sigma_{\delta y^*}^2 & \text{if } N_f > M \end{cases} \\ \langle \text{Var}[\hat{y}(\vec{x})] \rangle &= \begin{cases} (\sigma_\varepsilon^2 + \sigma_{\delta y^*}^2) \frac{\alpha_f}{(1-\alpha_f)} & \text{if } N_f < M \\ \sigma_\beta^2 \sigma_X^2 \frac{(\alpha_f-1)}{\alpha_f^2} + (\sigma_\varepsilon^2 + \sigma_{\delta y^*}^2) \frac{1}{(\alpha_f-1)} & \text{if } N_f > M. \end{cases} \end{aligned} \quad (\text{S108})$$

F. Random Linear Features Model (Two-layer Linear Neural Network)

This cavity derivation for the random linear features model follows closely with the previous derivation for linear regression. Therefore, we omit most of the justification for each step and refer the reader to the analogous steps laid out in the previous section.

In the random linear features model, the student model takes the form

$$\vec{z}(\vec{x}) = W^T \vec{x} \quad (\text{S109})$$

where the elements of the random transformation matrix W are identically and independently distributed, drawn from a normal distribution with zero mean and variance σ_W^2/N_p ,

$$\mathbb{E}[W_{jJ}] = 0, \quad \text{Cov}[W_{jJ}, W_{kK}] = \frac{\sigma_W^2}{N_p} \delta_{jk} \delta_{JK}. \quad (\text{S110})$$

We also assume that the elements of W are statistically independent of the ground truth parameters $\vec{\beta}$, the label noise $\vec{\varepsilon}$, the features X , etc.

For this model, we decompose the system of equations in Eq. (S41) such that they are linear in the random matrices

W and X , resulting in four different sets of equations,

$$\begin{aligned}
\lambda \hat{w}_J &= \sum_k \hat{u}_k W_{kJ} + \eta_J \\
\hat{u}_j &= \sum_b \Delta y_b X_{bj} + \psi_j \\
\Delta y_a &= \sum_k \Delta \beta_k X_{ak} + \delta y_{\text{NL}}^*(\vec{x}_a) + \varepsilon_a + \xi_a \\
\Delta \beta_j &= \beta_j - \sum_K \hat{w}_K W_{jK} + \zeta_j,
\end{aligned} \tag{S111}$$

where we have added a different auxiliary field to each equation. Similar to the procedure for linear regression, we will eventually evaluate each field at zero by the end of the calculation. The quantities $\Delta \beta_j$ are the residual parameter error (see Sec. S2), while the quantities \hat{u}_j can be interpreted as representations of the fit parameters in the space of input features.

1. Cavity Expansion

Next, we add an additional variable of each type, resulting in a total of $M + 1$ data points, $N_f + 1$ input features and $N_p + 1$ fit parameters. Each additional variable is represented using an index value of 0, written as \hat{w}_0 , \hat{u}_0 , Δy_0 , and $\Delta \beta_0$. After including these new unknown quantities, the four equations become

$$\begin{aligned}
\lambda \hat{w}_J &= \sum_k \hat{u}_k W_{kJ} + \eta_J + \hat{u}_0 W_{0J} \\
\hat{u}_j &= \sum_b \Delta y_b X_{bj} + \psi_j + \Delta y_0 X_{0j} \\
\Delta y_a &= \sum_k \Delta \beta_k X_{ak} + \delta y_{\text{NL}}^*(\vec{x}_a) + \varepsilon_a + \xi_a + X_{a0} \Delta \beta_0 \\
\Delta \beta_j &= \beta_j - \sum_K \hat{w}_K W_{jK} + \zeta_j - \hat{w}_0 W_{j0}
\end{aligned} \tag{S112}$$

with each new variable described by a new equation,

$$\begin{aligned}
\lambda \hat{w}_0 &= \sum_k \hat{u}_k W_{k0} + \eta_0 + \hat{u}_0 W_{00} \\
\hat{u}_0 &= \sum_b \Delta y_b X_{b0} + \psi_0 + \Delta y_0 X_{00} \\
\Delta y_0 &= \sum_k \Delta \beta_k X_{0k} + \delta y_{\text{NL}}^*(\vec{x}_0) + \varepsilon_0 + \xi_0 + \Delta \beta_0 X_{00} \\
\Delta \beta_0 &= \beta_0 - \sum_K \hat{w}_K W_{0K} + \zeta_0 - \hat{w}_0 W_{00}.
\end{aligned} \tag{S113}$$

Now we take the thermodynamic limit in which M , N_f , and N_p tend towards infinity, but their ratios, $\alpha_f = N_f/M$ and $\alpha_p = N_p/M$, remain fixed. We interpret the extra terms in Eq. (S112) as small perturbations to the auxiliary fields,

$$\delta \eta_J = \hat{u}_0 W_{0J}, \quad \delta \psi_j = \Delta y_0 X_{0j}, \quad \delta \xi_a = \Delta \beta_0 X_{a0}, \quad \delta \zeta_j = -\hat{w}_0 W_{j0}, \tag{S114}$$

allowing us to expand each unknown quantity about its solution in the absence of the 0-indexed variables which

correspond to the solutions for M data points, N_f input features, and N_p fit parameters,

$$\begin{aligned}
\hat{w}_J &\approx \hat{w}_{J\setminus 0} + \sum_K \nu_{JK}^{\hat{w}} \delta\eta_K + \sum_k \phi_{Jk}^{\hat{w}} \delta\psi_k + \sum_b \chi_{Jb}^{\hat{w}} \delta\xi_b + \sum_k \omega_{Jk}^{\hat{w}} \delta\zeta_k \\
\hat{u}_j &\approx \hat{u}_{j\setminus 0} + \sum_K \nu_{jK}^{\hat{u}} \delta\eta_K + \sum_k \phi_{jk}^{\hat{u}} \delta\psi_k + \sum_b \chi_{jb}^{\hat{u}} \delta\xi_b + \sum_k \omega_{jk}^{\hat{u}} \delta\zeta_k \\
\Delta y_a &\approx \Delta y_{a\setminus 0} + \sum_K \nu_{aK}^{\Delta y} \delta\eta_K + \sum_k \phi_{ak}^{\Delta y} \delta\psi_k + \sum_b \chi_{ab}^{\Delta y} \delta\xi_b + \sum_k \omega_{ak}^{\Delta y} \delta\zeta_k \\
\Delta\beta_j &\approx \Delta\beta_{j\setminus 0} + \sum_K \nu_{jK}^{\Delta\beta} \delta\eta_K + \sum_k \phi_{jk}^{\Delta\beta} \delta\psi_k + \sum_b \chi_{jb}^{\Delta\beta} \delta\xi_b + \sum_k \omega_{jk}^{\Delta\beta} \delta\zeta_k.
\end{aligned} \tag{S115}$$

We define each of the susceptibility matrices as a derivative of a variable with respect to an auxiliary field,

$$\begin{aligned}
\nu_{JK}^{\hat{w}} &= \frac{\partial \hat{w}_J}{\partial \eta_K}, & \phi_{Jk}^{\hat{w}} &= \frac{\partial \hat{w}_J}{\partial \psi_k}, & \chi_{Jb}^{\hat{w}} &= \frac{\partial \hat{w}_J}{\partial \xi_b}, & \omega_{Jk}^{\hat{w}} &= \frac{\partial \hat{w}_J}{\partial \zeta_k}, \\
\nu_{jK}^{\hat{u}} &= \frac{\partial \hat{u}_j}{\partial \eta_K}, & \phi_{jk}^{\hat{u}} &= \frac{\partial \hat{u}_j}{\partial \psi_k}, & \chi_{jb}^{\hat{u}} &= \frac{\partial \hat{u}_j}{\partial \xi_b}, & \omega_{jk}^{\hat{u}} &= \frac{\partial \hat{u}_j}{\partial \zeta_k}, \\
\nu_{aK}^{\Delta y} &= \frac{\partial \Delta y_a}{\partial \eta_K}, & \phi_{ak}^{\Delta y} &= \frac{\partial \Delta y_a}{\partial \psi_k}, & \chi_{ab}^{\Delta y} &= \frac{\partial \Delta y_a}{\partial \xi_b}, & \omega_{ak}^{\Delta y} &= \frac{\partial \Delta y_a}{\partial \zeta_k}, \\
\nu_{jK}^{\Delta\beta} &= \frac{\partial \Delta\beta_j}{\partial \eta_K}, & \phi_{jk}^{\Delta\beta} &= \frac{\partial \Delta\beta_j}{\partial \psi_k}, & \chi_{jb}^{\Delta\beta} &= \frac{\partial \Delta\beta_j}{\partial \xi_b}, & \omega_{jk}^{\Delta\beta} &= \frac{\partial \Delta\beta_j}{\partial \zeta_k}.
\end{aligned} \tag{S116}$$

Substituting the expansions of Eqs. (S115) into the 0-indexed equations in Eq. (S113), we arrive at equations analogous to those of Eq. (S50). Next, we aim to approximate each of the resulting sums in these expanded equations.

2. Approximations of Large Sums: Unperturbed Quantities

We approximate each of the sums containing one of the unperturbed quantities, $\hat{w}_{J\setminus 0}$, $\hat{u}_{j\setminus 0}$, $\Delta y_{a\setminus 0}$, or $\Delta\beta_{j\setminus 0}$, using the central limit theorem in the same manner described in Sec. S1E2. The unperturbed quantities in each of these sums are statistically independent of all elements of both X and W with a 0-valued index. Using this fact, we find

$$\begin{aligned}
\sum_k \hat{u}_{k\setminus 0} W_{k0} &\approx \sigma_{\hat{w}} z_{\hat{w}}, & \sigma_{\hat{w}}^2 &= \sigma_W^2 \frac{\alpha_f}{\alpha_p} \langle \hat{u}^2 \rangle, & \langle \hat{u}^2 \rangle &= \frac{1}{N_f} \sum_k \hat{u}_{k\setminus 0}^2 \\
\sum_b \Delta y_{b\setminus 0} X_{b0} &\approx \sigma_{\hat{u}} z_{\hat{u}}, & \sigma_{\hat{u}}^2 &= \sigma_X^2 \alpha_f^{-1} \langle \Delta y^2 \rangle, & \langle \Delta y^2 \rangle &= \frac{1}{M} \sum_b \Delta y_{b\setminus 0}^2 \\
\sum_k \Delta\beta_{k\setminus 0} X_{0k} &\approx \sigma_{\Delta y} z_{\Delta y}, & \sigma_{\Delta y}^2 &= \sigma_X^2 \langle \Delta\beta^2 \rangle, & \langle \Delta\beta^2 \rangle &= \frac{1}{N_f} \sum_k \Delta\beta_{k\setminus 0}^2 \\
\sum_K \hat{w}_{K\setminus 0} W_{0K} &\approx \sigma_{\Delta\beta} z_{\Delta\beta}, & \sigma_{\Delta\beta}^2 &= \sigma_W^2 \langle \hat{w}^2 \rangle, & \langle \hat{w}^2 \rangle &= \frac{1}{N_p} \sum_K \hat{w}_{K\setminus 0}^2
\end{aligned} \tag{S117}$$

where $z_{\hat{w}}$, $z_{\hat{u}}$, $z_{\Delta y}$, and $z_{\Delta\beta}$ are all random variables with zero mean and unit variance and can easily be shown to be statistically independent from one another.

3. Approximations of Large Sums: Square Susceptibilities

Next, we approximate each of the sums containing a square susceptibility matrix. Using the fact that all of the susceptibility matrices are statistically independent of all elements of both X and W with a 0-valued index, we follow

the procedure in Sec. S1E3 to find

$$\begin{aligned}
\sum_{jk} \omega_{jk}^{\hat{u}} W_{j0} W_{k0} &\approx \sigma_W^2 \frac{\alpha_f}{\alpha_p} \omega, & \omega &= \frac{1}{N_f} \sum_k \omega_{kk}^{\hat{u}} \\
\sum_{ab} \chi_{ab}^{\Delta y} X_{a0} X_{b0} &\approx \sigma_X^2 \alpha_f^{-1} \chi, & \chi &= \frac{1}{M} \sum_b \chi_{bb}^{\Delta y} \\
\sum_{jk} \phi_{jk}^{\Delta \beta} X_{0j} X_{0k} &\approx \sigma_X^2 \phi, & \phi &= \frac{1}{N_f} \sum_k \phi_{kk}^{\Delta \beta} \\
\sum_{JK} \nu_{JK}^{\hat{w}} W_{0J} W_{0K} &\approx \sigma_W^2 \nu, & \nu &= \frac{1}{N_p} \sum_K \nu_{KK}^{\hat{w}}.
\end{aligned} \tag{S118}$$

4. Approximations of Large Sums: Rectangular Susceptibilities

Analogously to those in Sec. S1E4, it is straightforward to show that each of the sums containing a rectangular susceptibility matrix approximates to zero in the thermodynamic limit.

5. Self-consistency Equations

Next, we substitute the expansions in Eq. (S115) into Eqs. (S113) and apply the large sum approximations from the previous sections, resulting in a set of self-consistent equations for \hat{w}_0 , \hat{u}_0 , Δy_0 , and $\Delta \beta_0$,

$$\begin{aligned}
\lambda \hat{w}_0 &\approx \sigma_{\hat{w}} z_{\hat{w}} - \hat{w}_0 \sigma_W^2 \frac{\alpha_f}{\alpha_p} \omega + \eta_0 \\
\hat{u}_0 &\approx \sigma_{\hat{u}} z_{\hat{u}} + \Delta \beta_0 \sigma_X^2 \alpha_f^{-1} \chi + \psi_0 \\
\Delta y_0 &\approx \sigma_{\Delta y} z_{\Delta y} + \Delta y_0 \sigma_X^2 \phi + \delta y_{\text{NL}}^*(\vec{\mathbf{x}}_0) + \varepsilon_0 + \xi_0 \\
\Delta \beta_0 &\approx \beta_0 - \sigma_{\Delta \beta} z_{\Delta \beta} - \hat{u}_0 \sigma_W^2 \nu + \zeta_0.
\end{aligned} \tag{S119}$$

We have also made use of the fact that the terms including X_{00} or W_{00} are infinitesimally small in the thermodynamic limit with zero mean and variances of $\mathcal{O}(1/N_f)$ and $\mathcal{O}(1/N_p)$, respectively. Solving these equations for the 0-indexed variables, we find

$$\begin{aligned}
\hat{w}_0 &= \frac{\sigma_{\hat{w}} z_{\hat{w}} + \eta_0}{\lambda + \sigma_W^2 \frac{\alpha_f}{\alpha_p} \omega} \\
\hat{u}_0 &= \frac{\sigma_{\hat{u}} z_{\hat{u}} + \psi_0 + \sigma_X^2 \alpha_f^{-1} \chi (\beta_0 - \sigma_{\Delta \beta} z_{\Delta \beta} + \zeta_0)}{1 + \sigma_W^2 \sigma_X^2 \alpha_f^{-1} \chi \nu} \\
\Delta y_0 &= \frac{\sigma_{\Delta y} z_{\Delta y} + \delta y_{\text{NL}}^*(\vec{\mathbf{x}}_0) + \varepsilon_0 + \xi_0}{1 - \sigma_X^2 \phi} \\
\Delta \beta_0 &= \frac{\beta_0 - \sigma_{\Delta \beta} z_{\Delta \beta} + \zeta_0 - \sigma_W^2 \nu^2 (\sigma_{\hat{u}} z_{\hat{u}} + \psi_0)}{1 + \sigma_W^2 \sigma_X^2 \alpha_f^{-1} \chi \nu}.
\end{aligned} \tag{S120}$$

We derive a set of self-consistent equations for the scalar susceptibilities by taking appropriate derivatives of these variables with respect to the auxiliary fields,

$$\begin{aligned}
\nu &= \frac{1}{N_p} \sum_K \nu_{KK}^{\hat{w}} \approx \text{E}[\nu_{00}^{\hat{w}}] = \text{E}\left[\frac{\partial \hat{w}_0}{\partial \eta_0}\right] = \frac{1}{\lambda + \sigma_W^2 \frac{\alpha_f}{\alpha_p} \omega} \\
\omega &= \frac{1}{N_f} \sum_k \omega_{kk}^{\hat{u}} \approx \text{E}[\omega_{00}^{\hat{u}}] = \text{E}\left[\frac{\partial \hat{u}_0}{\partial \zeta_0}\right] = \frac{\sigma_X^2 \alpha_f^{-1} \chi}{1 + \sigma_W^2 \sigma_X^2 \alpha_f^{-1} \chi \nu} \\
\chi &= \frac{1}{M} \sum_b \chi_{bb}^{\Delta y} \approx \text{E}[\chi_{00}^{\Delta y}] = \text{E}\left[\frac{\partial \Delta y_0}{\partial \xi_0}\right] = \frac{1}{1 - \sigma_X^2 \phi} \\
\phi &= \frac{1}{N_f} \sum_k \phi_{kk}^{\Delta \beta} \approx \text{E}[\phi_{00}^{\Delta \beta}] = \text{E}\left[\frac{\partial \Delta \beta_0}{\partial \psi_0}\right] = -\frac{\sigma_W^2 \nu}{1 + \sigma_W^2 \sigma_X^2 \alpha_f^{-1} \chi \nu}.
\end{aligned} \tag{S121}$$

Furthermore, we note that there are two additional derivatives that have not yet appeared in the calculation up to this point, $\partial\hat{u}_j/\partial\psi_j$ and $\partial\Delta\beta_j/\partial\zeta_j$. It is clear to see from the equations for \hat{u}_0 and $\Delta\beta_0$ that these two additional derivatives are equivalent. Using these derivatives, we define a fifth scalar susceptibility,

$$\kappa = \frac{1}{N_f} \sum_k \phi_{kk}^{\hat{u}} = \frac{1}{N_f} \sum_k \omega_{kk}^{\Delta\beta} \approx \mathbb{E} \left[\frac{\partial\hat{u}_0}{\partial\psi_0} \right] = \mathbb{E} \left[\frac{\partial\Delta\beta_0}{\partial\zeta_0} \right] = \frac{1}{1 + \sigma_W^2 \sigma_X^2 \alpha_f^{-1} \chi \nu}. \quad (\text{S122})$$

Using this formula for κ , we re-express the four other susceptibilities as

$$\omega = \sigma_X^2 \alpha_f^{-1} \chi \kappa, \quad \phi = -\sigma_W^2 \nu \kappa, \quad \chi = \frac{1}{1 + \sigma_W^2 \sigma_X^2 \nu \kappa}, \quad \nu = \frac{1}{\lambda + \sigma_W^2 \sigma_X^2 \alpha_p^{-1} \chi \kappa}. \quad (\text{S123})$$

From here, we observe that χ and ν are closely related to those for linear regression and that κ plays an important role in capturing the effects of the additional linear transformation matrix W . Finally, we square and average each of Eq. (S120) to find self-consistent equations for the four mean squared averages (setting the auxiliary fields to zero),

$$\begin{aligned} \langle \hat{w}^2 \rangle &= \frac{1}{N_p} \sum_K \hat{w}_{K\setminus 0}^2 \approx \mathbb{E}[\hat{w}_0^2] = \nu^2 \sigma_W^2 \frac{\alpha_f}{\alpha_p} \langle \hat{u}^2 \rangle \\ \langle \hat{u}^2 \rangle &= \frac{1}{N_f} \sum_k \hat{u}_{k\setminus 0}^2 \approx \mathbb{E}[\hat{u}_0^2] = \kappa^2 \sigma_X^2 \alpha_f^{-1} \langle \Delta y^2 \rangle + \omega^2 (\sigma_\beta^2 + \sigma_W^2 \langle \hat{w}^2 \rangle) \\ \langle \Delta y^2 \rangle &= \frac{1}{M} \sum_b \Delta y_{b\setminus 0}^2 \approx \mathbb{E}[\Delta y_0^2] = \chi^2 (\sigma_X^2 \langle \Delta \beta^2 \rangle + \sigma_{\delta y^*}^2 + \sigma_\varepsilon^2) \\ \langle \Delta \beta^2 \rangle &= \frac{1}{N_f} \sum_k \Delta \beta_{k\setminus 0}^2 \approx \mathbb{E}[\Delta \beta_0^2] = \kappa^2 (\sigma_\beta^2 + \sigma_W^2 \langle \hat{w}^2 \rangle) + \phi^2 \sigma_X^2 \alpha_f^{-1} \langle \Delta y^2 \rangle. \end{aligned} \quad (\text{S124})$$

6. Solution with Finite Regularization ($\lambda \sim 1$)

To derive the solutions with finite regularization ($\lambda \sim 1$), we start by solving both equations for χ and ν in Eq. (S123) for κ and then setting them equal,

$$\kappa = \frac{1 - \chi}{\sigma_W^2 \sigma_X^2 \chi \nu} = \frac{\alpha_p (1 - \lambda \nu)}{\sigma_W^2 \sigma_X^2 \chi \nu}. \quad (\text{S125})$$

From here, we find the following relation between ν and χ :

$$\nu = \frac{\chi + \alpha_p - 1}{\lambda \alpha_p}. \quad (\text{S126})$$

We then substitute κ into original equation for χ and plug in the equation for ν we just found. After multiplying so as to eliminate any denominators, we find a cubic equation for χ ,

$$\chi^3 + (\alpha_f + \alpha_p - 2)\chi^2 + [(\alpha_f - 1)(\alpha_p - 1) + \alpha_f \alpha_p \bar{\lambda}] \chi - \alpha_f \alpha_p \bar{\lambda} = 0, \quad (\text{S127})$$

where we have defined the dimensionless regularization parameter

$$\bar{\lambda} = \frac{\lambda}{\sigma_W^2 \sigma_X^2}. \quad (\text{S128})$$

This cubic equation indicates that we should expect three different solutions for χ . Using these solutions, we can derive the associated solutions for the rest of the susceptibilities. Furthermore, we solve Eq. (S124) to find

$$\begin{pmatrix} \langle \hat{w}^2 \rangle \\ \langle \hat{u}^2 \rangle \\ \langle \Delta y^2 \rangle \\ \langle \Delta \beta^2 \rangle \end{pmatrix} = \begin{pmatrix} 1 & -\sigma_W^2 \frac{\alpha_f}{\alpha_p} \nu^2 & 0 & 0 \\ -\sigma_W^2 \omega^2 & 1 & -\sigma_X^2 \alpha_f^{-1} \kappa^2 & 0 \\ 0 & 0 & 1 & -\sigma_X^2 \chi^2 \\ -\sigma_W^2 \kappa^2 & 0 & -\sigma_X^2 \alpha_f^{-1} \phi^2 & 1 \end{pmatrix}^{-1} \begin{pmatrix} 0 \\ \sigma_\beta^2 \omega^2 \\ (\sigma_\varepsilon^2 + \sigma_{\delta y^*}^2) \chi^2 \\ \sigma_\beta^2 \kappa^2 \end{pmatrix}. \quad (\text{S129})$$

In combination with the solutions for the five scalar susceptibilities, these solutions are exact in the thermodynamic limit.

7. Solutions in Ridge-less Limit ($\lambda \rightarrow 0$)

Next, we take the ridge-less limit in which $\lambda \rightarrow 0$. Based on the cubic equation for χ , Eq. (S127), we make the ansatz that the lowest order contribution to χ is $\mathcal{O}(1)$ in small $\bar{\lambda}$,

$$\chi \approx \chi_0 + \bar{\lambda}\chi_1. \quad (\text{S130})$$

Substituting this approximation into Eq. (S127), we find the following equation at $\mathcal{O}(1)$:

$$\begin{aligned} 0 &= \chi_0^3 + (\alpha_f + \alpha_p - 2)\chi_0^2 + (\alpha_f - 1)(\alpha_p - 1)\chi_0 \\ &= (\chi_0 + \alpha_f - 1)(\chi_0 + \alpha_p - 1)\chi_0. \end{aligned} \quad (\text{S131})$$

Solving this, we find three solutions for χ_0 ,

$$\chi_0^{(1)} = 1 - \alpha_f, \quad \chi_0^{(2)} = 1 - \alpha_p, \quad \chi_0^{(3)} = 0, \quad (\text{S132})$$

where we have labeled the three solutions with superscript (1), (2) or (3). At $\mathcal{O}(\bar{\lambda})$, we find the equation

$$0 = 3\chi_0^2\chi_1 + 2(\alpha_f + \alpha_p - 2)\chi_0\chi_1 + (\alpha_f - 1)(\alpha_p - 1)\chi_1 + \alpha_f\alpha_p\chi_0 - \alpha_f\alpha_p. \quad (\text{S133})$$

Solving for χ_1 , we find

$$\chi_1 = \frac{\alpha_f\alpha_p(1 - \chi_0)}{3\chi_0^2 + 2(\alpha_f + \alpha_p - 2)\chi_0 + (1 - \alpha_f)(1 - \alpha_p)}. \quad (\text{S134})$$

Inserting the solutions for χ_0 , we obtain the three corresponding solutions for χ_1 ,

$$\chi_1^{(1)} = \frac{\alpha_f^2\alpha_p}{(1 - \alpha_f)(\alpha_p - \alpha_f)}, \quad \chi_1^{(2)} = \frac{\alpha_f\alpha_p^2}{(1 - \alpha_p)(\alpha_f - \alpha_p)}, \quad \chi_1^{(3)} = \frac{\alpha_f\alpha_p}{(\alpha_f - 1)(\alpha_p - 1)}. \quad (\text{S135})$$

Next, we solve for the four remaining scalar susceptibilities. Based on inspecting Eq. (S123), we make the following ansatz for the dependence of these susceptibilities on small $\bar{\lambda}$:

$$\begin{aligned} \nu &\approx \frac{1}{\bar{\lambda}}\nu_{-1} + \nu_0 \\ \kappa &\approx \kappa_0 + \bar{\lambda}\kappa_1 \\ \phi &\approx \frac{1}{\bar{\lambda}}\phi_{-1} + \phi_0 \\ \omega &\approx \omega_0 + \bar{\lambda}\omega_1. \end{aligned} \quad (\text{S136})$$

Substituting the solutions for χ into Eq. (S126) and expanding in small $\bar{\lambda}$, we find the lowest order solutions for ν ,

$$\nu_{-1}^{(1)} = \frac{1}{\sigma_W^2\sigma_X^2} \frac{(\alpha_p - \alpha_f)}{\alpha_p}, \quad \nu_{-1}^{(2)} = 0, \quad \nu_{-1}^{(3)} = \frac{1}{\sigma_W^2\sigma_X^2} \frac{(\alpha_p - 1)}{\alpha_p}. \quad (\text{S137})$$

Since $\nu_{-1}^{(2)}$ is zero, we also solve for the next order term for solution (2),

$$\nu_0^{(2)} = \frac{1}{\sigma_W^2\sigma_X^2} \frac{\alpha_f\alpha_p}{(1 - \alpha_p)(\alpha_f - \alpha_p)}. \quad (\text{S138})$$

Next, we substitute the solutions for χ and ν into Eq. (S122) to find the lowest order solutions for κ ,

$$\kappa_0^{(1)} = 0, \quad \kappa_0^{(2)} = \frac{(\alpha_f - \alpha_p)}{\alpha_f}, \quad \kappa_0^{(3)} = \frac{(\alpha_f - 1)}{\alpha_f}. \quad (\text{S139})$$

Again, since $\kappa_0^{(1)}$ is zero, we also solve for the $\mathcal{O}(\bar{\lambda})$ term for solution (1),

$$\kappa_1^{(1)} = \frac{\alpha_f\alpha_p}{(1 - \alpha_f)(\alpha_p - \alpha_f)}. \quad (\text{S140})$$

Substituting the solutions for ν and κ into the equation for ϕ in Eq. (S123), the lowest order terms for ϕ are

$$\phi_{-1}^{(1)} = 0, \quad \phi_{-1}^{(2)} = 0, \quad \phi_{-1}^{(3)} = -\frac{1}{\sigma_X^2} \frac{(\alpha_f - 1)(\alpha_p - 1)}{\alpha_f \alpha_p} \quad (\text{S141})$$

while the next order terms for solutions (1) and (2) are

$$\phi_0^{(1)} = -\frac{1}{\sigma_X^2} \frac{\alpha_f}{(1 - \alpha_f)}, \quad \phi_0^{(2)} = -\frac{1}{\sigma_X^2} \frac{\alpha_p}{(1 - \alpha_p)}. \quad (\text{S142})$$

Finally, substituting the solutions for χ and κ into the equation for ω in Eq. (S123), the lowest order terms for ω are

$$\omega_0^{(1)} = 0, \quad \omega_0^{(2)} = \sigma_X^2 \frac{(1 - \alpha_p)(\alpha_f - \alpha_p)}{\alpha_f^2}, \quad \omega_0^{(3)} = 0 \quad (\text{S143})$$

with the $\mathcal{O}(\bar{\lambda})$ terms for solutions (1) and (3),

$$\omega_1^{(1)} = \sigma_X^2 \frac{\alpha_p}{(\alpha_p - \alpha_f)}, \quad \omega_1^{(3)} = \sigma_X^2 \frac{\alpha_p}{\alpha_f(\alpha_p - 1)}. \quad (\text{S144})$$

Analogously to the derivation for linear regression, we make the ansatz that the lowest order terms of each of ensemble-averaged squared quantities is $\mathcal{O}(1)$ in small $\bar{\lambda}$ with the next terms at $\mathcal{O}(\bar{\lambda}^2)$,

$$\begin{aligned} \langle \hat{w}^2 \rangle &\approx \langle \hat{w}^2 \rangle_0 + \bar{\lambda}^2 \langle \hat{w}^2 \rangle_2 \\ \langle \hat{u}^2 \rangle &\approx \langle \hat{u}^2 \rangle_0 + \bar{\lambda}^2 \langle \hat{u}^2 \rangle_2 \\ \langle \Delta y^2 \rangle &\approx \langle \Delta y^2 \rangle_0 + \bar{\lambda}^2 \langle \Delta y^2 \rangle_2 \\ \langle \Delta \beta^2 \rangle &\approx \langle \Delta \beta^2 \rangle_0 + \bar{\lambda}^2 \langle \Delta \beta^2 \rangle_2 \end{aligned} \quad (\text{S145})$$

Solution (1): Expressing the susceptibilities in terms of their leading order terms in $\bar{\lambda}$ for the first set of solutions, the self-consistent equations, Eq. (S124), to lowest order in small $\bar{\lambda}$, are

$$\begin{aligned} \langle \hat{w}^2 \rangle_0^{(1)} &= (\nu_{-1}^{(1)})^2 \sigma_W^2 \frac{\alpha_f}{\alpha_p} \langle \hat{u}^2 \rangle_2^{(1)} \\ \langle \hat{u}^2 \rangle_0^{(1)} &= 0 \\ \langle \Delta y^2 \rangle_0^{(1)} &= (\chi_0^{(1)})^2 \left(\sigma_X^2 \langle \Delta \beta^2 \rangle_0^{(1)} + \sigma_{\delta y^*}^2 + \sigma_\varepsilon^2 \right) \\ \langle \Delta \beta^2 \rangle_0^{(1)} &= (\phi_0^{(1)})^2 \sigma_X^2 \alpha_f^{-1} \langle \Delta y^2 \rangle_0^{(1)}. \end{aligned} \quad (\text{S146})$$

We find that we also need the solution for $\langle \hat{u}^2 \rangle$ to next lowest order in $\bar{\lambda}$,

$$\langle \hat{u}^2 \rangle_2^{(1)} = (\kappa_1^{(1)})^2 \sigma_X^2 \alpha_f^{-1} \langle \Delta y^2 \rangle_0^{(1)} + (\omega_1^{(1)})^2 \left(\sigma_\beta^2 + \sigma_W^2 \langle \hat{w}^2 \rangle_0^{(1)} \right). \quad (\text{S147})$$

Combining with the solutions for the susceptibilities and solving, we find

$$\begin{aligned} \langle \hat{w}^2 \rangle_0^{(1)} &= \frac{\sigma_\beta^2}{\sigma_W^2} \frac{\alpha_f}{(\alpha_p - \alpha_f)} + \frac{1}{\sigma_W^2 \sigma_X^2} (\sigma_\varepsilon^2 + \sigma_{\delta y^*}^2) \frac{\alpha_f^2}{(1 - \alpha_f)(\alpha_p - \alpha_f)} \\ \langle \hat{u}^2 \rangle_2^{(1)} &= \sigma_\beta^2 \sigma_X^4 \frac{\alpha_p^3}{(\alpha_p - \alpha_f)^3} + \sigma_X^2 (\sigma_\varepsilon^2 + \sigma_{\delta y^*}^2) \frac{\alpha_f \alpha_p^3}{(1 - \alpha_f)(\alpha_p - \alpha_f)^3} \\ \langle \Delta y^2 \rangle_0^{(1)} &= (\sigma_\varepsilon^2 + \sigma_{\delta y^*}^2)(1 - \alpha_f) \\ \langle \Delta \beta^2 \rangle_0^{(1)} &= \frac{1}{\sigma_X^2} (\sigma_\varepsilon^2 + \sigma_{\delta y^*}^2) \frac{\alpha_f}{(1 - \alpha_f)}. \end{aligned} \quad (\text{S148})$$

Solution (2): The lowest order forms of the self-consistent equations for the second set of solutions are

$$\begin{aligned} \langle \hat{w}^2 \rangle_0^{(2)} &= (\nu_0^{(2)})^2 \sigma_W^2 \frac{\alpha_f}{\alpha_p} \langle \hat{u}^2 \rangle_0^{(2)} \\ \langle \hat{u}^2 \rangle_0^{(2)} &= (\kappa_0^{(2)})^2 \sigma_X^2 \alpha_f^{-1} \langle \Delta y^2 \rangle_0^{(2)} + (\omega_0^{(2)})^2 \left(\sigma_\beta^2 + \sigma_W^2 \langle \hat{w}^2 \rangle_0^{(2)} \right) \\ \langle \Delta y^2 \rangle_0^{(2)} &= (\chi_0^{(2)})^2 \left(\sigma_X^2 \langle \Delta \beta^2 \rangle_0^{(2)} + \sigma_{\delta y^*}^2 + \sigma_\varepsilon^2 \right) \\ \langle \Delta \beta^2 \rangle_0^{(2)} &= (\kappa_0^{(2)})^2 \left(\sigma_\beta^2 + \sigma_W^2 \langle \hat{w}^2 \rangle_0^{(2)} \right) + (\phi_0^{(2)})^2 \sigma_X^2 \alpha_f^{-1} \langle \Delta y^2 \rangle_0^{(2)}. \end{aligned} \quad (\text{S149})$$

Again inserting the solutions for the susceptibilities and solving, we find

$$\begin{aligned}
\langle \hat{w}^2 \rangle_0^{(2)} &= \frac{\sigma_\beta^2}{\sigma_W^2} \frac{(1 - \alpha_p + \alpha_f - \alpha_p)}{(1 - \alpha_p)(\alpha_f - \alpha_p)} + \frac{1}{\sigma_W^2 \sigma_X^2} (\sigma_\varepsilon^2 + \sigma_{\delta y^*}^2) \frac{\alpha_f \alpha_p}{(1 - \alpha_p)(\alpha_f - \alpha_p)} \\
\langle \hat{u}^2 \rangle_0^{(2)} &= \sigma_\beta^2 \sigma_X^4 \frac{(1 - \alpha_p)(\alpha_f - \alpha_p)(1 - \alpha_p + \alpha_f - \alpha_p)}{\alpha_f^3} + \sigma_X^2 (\sigma_\varepsilon^2 + \sigma_{\delta y^*}^2) \frac{(1 - \alpha_p)(\alpha_f - \alpha_p)}{\alpha_f^2} \\
\langle \Delta y^2 \rangle_0^{(2)} &= \sigma_\beta^2 \sigma_X^2 \frac{(1 - \alpha_p)(\alpha_f - \alpha_p)}{\alpha_f} + (\sigma_\varepsilon^2 + \sigma_{\delta y^*}^2)(1 - \alpha_p) \\
\langle \Delta \beta^2 \rangle_0^{(2)} &= \sigma_\beta^2 \frac{(\alpha_f - \alpha_p)}{\alpha_f(1 - \alpha_p)} + \frac{1}{\sigma_X^2} (\sigma_\varepsilon^2 + \sigma_{\delta y^*}^2) \frac{\alpha_p}{(1 - \alpha_p)}.
\end{aligned} \tag{S150}$$

Solution (3): For the third set of solutions, the self-consistent equations take the form

$$\begin{aligned}
\langle \hat{w}^2 \rangle_0^{(3)} &= (\nu_{-1}^{(3)})^2 \sigma_W^2 \frac{\alpha_f}{\alpha_p} \langle \hat{u}^2 \rangle_2^{(3)} \\
\langle \hat{u}^2 \rangle_0^{(3)} &= 0 \\
\langle \Delta y^2 \rangle_0^{(3)} &= 0 \\
\langle \Delta \beta^2 \rangle_0^{(3)} &= (\kappa_0^{(3)})^2 \left(\sigma_\beta^2 + \sigma_W^2 \langle \hat{w}^2 \rangle_0^{(3)} \right) + (\phi_{-1}^{(3)})^2 \sigma_X^2 \alpha_f^{-1} \langle \Delta y^2 \rangle_2^{(3)}.
\end{aligned} \tag{S151}$$

Here we see that we need the $\mathcal{O}(\bar{\lambda}^2)$ terms for both $\langle \hat{u}^2 \rangle$ and $\langle \Delta y^2 \rangle_2^{(3)}$,

$$\begin{aligned}
\langle \hat{u}^2 \rangle_2^{(3)} &= (\kappa_0^{(3)})^2 \sigma_X^2 \alpha_f^{-1} \langle \Delta y^2 \rangle_2^{(3)} + (\omega_1^{(3)})^2 \left(\sigma_\beta^2 + \sigma_W^2 \langle \hat{w}^2 \rangle_0^{(3)} \right) \\
\langle \Delta y^2 \rangle_2^{(3)} &= (\chi_1^{(3)})^2 \left(\sigma_X^2 \langle \Delta \beta^2 \rangle_0^{(3)} + \sigma_{\delta y^*}^2 + \sigma_\varepsilon^2 \right).
\end{aligned} \tag{S152}$$

Combining with the susceptibilities and solving, we arrive at

$$\begin{aligned}
\langle \hat{w}^2 \rangle_0^{(3)} &= \frac{\sigma_\beta^2}{\sigma_W^2} \frac{1}{(\alpha_p - 1)} + \frac{1}{\sigma_W^2 \sigma_X^2} (\sigma_\varepsilon^2 + \sigma_{\delta y^*}^2) \frac{\alpha_f}{(\alpha_f - 1)(\alpha_p - 1)} \\
\langle \hat{u}^2 \rangle_2^{(3)} &= \sigma_\beta^2 \sigma_X^4 \frac{\alpha_p^3}{\alpha_f(\alpha_p - 1)^3} + \sigma_X^2 (\sigma_\varepsilon^2 + \sigma_{\delta y^*}^2) \frac{\alpha_p^3}{(\alpha_f - 1)(\alpha_p - 1)^3} \\
\langle \Delta y^2 \rangle_2^{(3)} &= \sigma_\beta^2 \sigma_X^2 \frac{\alpha_f \alpha_p^3}{(\alpha_f - 1)(\alpha_p - 1)^3} + (\sigma_\varepsilon^2 + \sigma_{\delta y^*}^2) \frac{\alpha_f^2 \alpha_p^2 (\alpha_f - 1 + \alpha_p - 1)}{(\alpha_f - 1)^3 (\alpha_p - 1)^3} \\
\langle \Delta \beta^2 \rangle_0^{(3)} &= \sigma_\beta^2 \frac{\alpha_p(\alpha_f - 1)}{\alpha_f(\alpha_p - 1)} + \frac{1}{\sigma_X^2} (\sigma_\varepsilon^2 + \sigma_{\delta y^*}^2) \frac{(\alpha_f - 1 + \alpha_p - 1)}{(\alpha_f - 1)(\alpha_p - 1)}.
\end{aligned} \tag{S153}$$

Combined solutions: Similar to linear regression, we use the fact that each of the ensemble-averaged quantities $\langle \hat{w}^2 \rangle$, $\langle \hat{u}^2 \rangle$, $\langle \Delta y^2 \rangle$, and $\langle \Delta \beta^2 \rangle$ must be positive in order to determine when each of the three solutions applies. We find that solution (1) applies when $\alpha_f < 1$ and $\alpha_f < \alpha_p$, solution (2) applies when $\alpha_p < 1$ and $\alpha_p < \alpha_f$, and solution (3) applies when $\alpha_f > 1$ and $\alpha_p > 1$. All together, the solutions for the ensemble-averaged squared quantities in the

$\lambda \rightarrow 0$ limit are

$$\begin{aligned}
\langle \dot{w}^2 \rangle &= \begin{cases} \frac{\sigma_\beta^2}{\sigma_W^2} \frac{\alpha_f}{(\alpha_p - \alpha_f)} + \frac{(\sigma_\varepsilon^2 + \sigma_{\delta y^*}^2)}{\sigma_W^2 \sigma_X^2} \frac{\alpha_f^2}{(1 - \alpha_f)(\alpha_p - \alpha_f)} & \text{if } N_f < N_p, M \\ \frac{\sigma_\beta^2}{\sigma_W^2} \frac{(1 - \alpha_p + \alpha_f - \alpha_p)}{(1 - \alpha_p)(\alpha_f - \alpha_p)} + \frac{(\sigma_\varepsilon^2 + \sigma_{\delta y^*}^2)}{\sigma_W^2 \sigma_X^2} \frac{\alpha_f \alpha_p}{(1 - \alpha_p)(\alpha_f - \alpha_p)} & \text{if } N_p < N_f, M \\ \frac{\sigma_\beta^2}{\sigma_W^2} \frac{1}{(\alpha_p - 1)} + \frac{(\sigma_\varepsilon^2 + \sigma_{\delta y^*}^2)}{\sigma_W^2 \sigma_X^2} \frac{\alpha_f}{(\alpha_f - 1)(\alpha_p - 1)} & \text{if } M < N_f, N_p \end{cases} \\
\langle \dot{u}^2 \rangle &= \begin{cases} \frac{\lambda^2}{\sigma_X^4 \sigma_W^4} \left[\sigma_\beta^2 \sigma_X^4 \frac{\alpha_p^3}{(\alpha_p - \alpha_f)^3} + \sigma_X^2 (\sigma_\varepsilon^2 + \sigma_{\delta y^*}^2) \frac{\alpha_f \alpha_p^3}{(1 - \alpha_f)(\alpha_p - \alpha_f)^3} \right] & \text{if } N_f < N_p, M \\ \sigma_\beta^2 \sigma_X^4 \frac{(1 - \alpha_p)(\alpha_f - \alpha_p)}{\alpha_f^3} + \sigma_X^2 (\sigma_\varepsilon^2 + \sigma_{\delta y^*}^2) \frac{(1 - \alpha_p)(\alpha_f - \alpha_p)}{\alpha_f^2} & \text{if } N_p < N_f, M \\ \frac{\lambda^2}{\sigma_X^4 \sigma_W^4} \left[\sigma_\beta^2 \sigma_X^4 \frac{\alpha_p^3}{\alpha_f (\alpha_p - 1)^3} + \sigma_X^2 (\sigma_\varepsilon^2 + \sigma_{\delta y^*}^2) \frac{\alpha_p^3}{(\alpha_f - 1)(\alpha_p - 1)^3} \right] & \text{if } M < N_f, N_p \end{cases} \\
\langle \Delta y^2 \rangle &= \begin{cases} \frac{(\sigma_\varepsilon^2 + \sigma_{\delta y^*}^2)(1 - \alpha_f)}{\sigma_\beta^2 \sigma_X^2} & \text{if } N_f < N_p, M \\ \frac{\sigma_\beta^2 \sigma_X^2 \frac{(1 - \alpha_p)(\alpha_f - \alpha_p)}{\alpha_f} + (\sigma_\varepsilon^2 + \sigma_{\delta y^*}^2)(1 - \alpha_p)}{\sigma_X^4 \sigma_W^4} & \text{if } N_p < N_f, M \\ \frac{\lambda^2}{\sigma_X^4 \sigma_W^4} \left[\sigma_\beta^2 \sigma_X^2 \frac{\alpha_f \alpha_p^3}{(\alpha_f - 1)(\alpha_p - 1)^3} + (\sigma_\varepsilon^2 + \sigma_{\delta y^*}^2) \frac{\alpha_f^2 \alpha_p^2 (\alpha_f - 1 + \alpha_p - 1)}{(\alpha_f - 1)^3 (\alpha_p - 1)^3} \right] & \text{if } M < N_f, N_p \end{cases} \\
\langle \Delta \beta^2 \rangle &= \begin{cases} \frac{(\sigma_\varepsilon^2 + \sigma_{\delta y^*}^2)}{\sigma_X^2} \frac{\alpha_f}{(1 - \alpha_f)} & \text{if } N_f < N_p, M \\ \sigma_\beta^2 \frac{(\alpha_f - \alpha_p)}{\alpha_f (1 - \alpha_p)} + \frac{(\sigma_\varepsilon^2 + \sigma_{\delta y^*}^2)}{\sigma_X^2} \frac{\alpha_p}{(1 - \alpha_p)} & \text{if } N_p < N_f, M \\ \sigma_\beta^2 \frac{\alpha_p (\alpha_f - 1)}{\alpha_f (\alpha_p - 1)} + \frac{(\sigma_\varepsilon^2 + \sigma_{\delta y^*}^2)}{\sigma_X^2} \frac{(\alpha_f - 1 + \alpha_p - 1)}{(\alpha_f - 1)(\alpha_p - 1)} & \text{if } M < N_f, N_p. \end{cases}
\end{aligned} \tag{S154}$$

In addition, to lowest order in small λ , the five scalar susceptibilities are

$$\begin{aligned}
\chi &= \begin{cases} 1 - \alpha_f & \text{if } N_f < N_p, M \\ 1 - \alpha_p & \text{if } N_p < N_f, M \\ \frac{\lambda}{\sigma_W^2 \sigma_X^2} \frac{\alpha_f \alpha_p}{(1 - \alpha_f)(1 - \alpha_p)} & \text{if } M < N_f, N_p \end{cases} \\
\nu &= \begin{cases} \frac{1}{\lambda} \frac{(\alpha_p - \alpha_f)}{\alpha_p} & \text{if } N_f < N_p, M \\ \frac{1}{\sigma_W^2 \sigma_X^2} \frac{\alpha_f \alpha_p}{(1 - \alpha_p)(\alpha_f - \alpha_p)} & \text{if } N_p < N_f, M \\ \frac{1}{\lambda} \frac{(\alpha_p - 1)}{\alpha_p} & \text{if } M < N_f, N_p \end{cases} \\
\kappa &= \begin{cases} \frac{\lambda}{\sigma_W^2 \sigma_X^2} \frac{\alpha_f \alpha_p}{(1 - \alpha_f)(\alpha_p - \alpha_f)} & \text{if } N_f < N_p, M \\ \frac{\alpha_f}{(\alpha_f - \alpha_p)} & \text{if } N_p < N_f, M \\ \frac{(\alpha_f - 1)}{\alpha_f} & \text{if } M < N_f, N_p \end{cases} \\
\omega &= \begin{cases} \frac{\lambda}{\sigma_W^2} \frac{\alpha_p}{(\alpha_p - \alpha_f)} & \text{if } N_f < N_p, M \\ \sigma_X^2 \frac{(1 - \alpha_p)(\alpha_f - \alpha_p)}{\alpha_f^2} & \text{if } N_p < N_f, M \\ \frac{\lambda}{\sigma_W^2} \frac{\alpha_p}{\alpha_f (\alpha_p - 1)} & \text{if } M < N_f, N_p \end{cases} \\
\phi &= \begin{cases} -\frac{1}{\sigma_X^2} \frac{\alpha_f}{(1 - \alpha_f)} & \text{if } N_f < N_p, M \\ -\frac{1}{\sigma_X^2} \frac{\alpha_p}{(1 - \alpha_p)} & \text{if } N_p < N_f, M \\ -\frac{\sigma_W^2}{\lambda} \frac{(\alpha_f - 1)(\alpha_p - 1)}{\alpha_f \alpha_p} & \text{if } M < N_f, N_p. \end{cases}
\end{aligned} \tag{S155}$$

The training error is then simply

$$\langle \mathcal{E}_{\text{train}} \rangle = \langle \Delta y^2 \rangle. \tag{S156}$$

8. Test Error

For the linear random features model, it is straightforward to see that the derivation for the test error follows the exact same set of steps as for linear regression in Eq. (S94), resulting in the same expression relating the test error and the parameter error,

$$\langle \mathcal{E}_{\text{test}} \rangle = \sigma_X^2 \langle \Delta \beta^2 \rangle + \sigma_{\delta y^*}^2 + \sigma_\varepsilon^2. \tag{S157}$$

Substituting the solution for $\langle \Delta\beta^2 \rangle$ into this expression, we find that the test error in the $\lambda \rightarrow 0$ limit is

$$\langle \mathcal{E}_{\text{test}} \rangle = \begin{cases} (\sigma_\varepsilon^2 + \sigma_{\delta y^*}^2) \frac{1}{(1-\alpha_f)} & \text{if } N_f < N_p, M \\ \sigma_\beta^2 \sigma_X^2 \frac{(\alpha_f - \alpha_p)}{\alpha_f(1-\alpha_p)} + (\sigma_\varepsilon^2 + \sigma_{\delta y^*}^2) \frac{1}{(1-\alpha_p)} & \text{if } N_p < N_f, M \\ \sigma_\beta^2 \sigma_X^2 \frac{\alpha_p(\alpha_f - 1)}{\alpha_f(\alpha_p - 1)} + (\sigma_\varepsilon^2 + \sigma_{\delta y^*}^2) \frac{(\alpha_f \alpha_p - 1)}{(\alpha_f - 1)(\alpha_p - 1)} & \text{if } M < N_f, N_p. \end{cases} \quad (\text{S158})$$

9. Bias-Variance Decomposition

Following the derivation in the context of linear regression in Sec. [S1E9](#), we find that the bias and variance for the random linear features model are described by the same expressions,

$$\langle \text{Bias}^2[\hat{y}(\vec{x})] \rangle = \sigma_X^2 \langle \Delta\beta_1 \Delta\beta_2 \rangle + \sigma_{\delta y^*}^2, \quad \langle \text{Var}[\hat{y}(\vec{x})] \rangle = \sigma_X^2 (\langle \Delta\beta^2 \rangle - \langle \Delta\beta_1 \Delta\beta_2 \rangle), \quad (\text{S159})$$

where $\langle \Delta\beta_1 \Delta\beta_2 \rangle$ is the covariance of the residual parameter errors from training two models with the same W on two training sets drawn independently from the same data distribution (same $\vec{\beta}$ and form of y^*). We specify which quantities depend on each of the training sets using a subscript 1 or 2 for data sets \mathcal{D}_1 and \mathcal{D}_2 , respectively. To calculate $\langle \Delta\beta_1 \Delta\beta_2 \rangle$, we apply the self-consistent equations, Eq. [\(S120\)](#), to each of the two models trained separately on one of the two training sets. For training set \mathcal{D}_1 , these equations are

$$\begin{aligned} \hat{w}_{1,0} &= \nu \sigma_{\hat{w}} z_{\hat{w}_1} \\ \hat{u}_{1,0} &= \kappa \sigma_{\hat{u}} z_{\hat{u}_1} + \omega(\beta_0 - \sigma_{\Delta\beta} z_{\Delta\beta_1}) \\ \Delta y_{1,0} &= \chi(\sigma_{\Delta y} z_{\Delta y_1} + \delta y_{\text{NL}}^*(\vec{x}_{1,0}) + \varepsilon_{1,0}) \\ \Delta\beta_{1,0} &= \kappa(\beta_0 - \sigma_{\Delta\beta} z_{\Delta\beta_1}) + \phi \sigma_{\hat{u}} z_{\hat{u}_1}, \end{aligned} \quad (\text{S160})$$

while for training set \mathcal{D}_2 , they are

$$\begin{aligned} \hat{w}_{2,0} &= \nu \sigma_{\hat{w}} z_{\hat{w}_2} \\ \hat{u}_{2,0} &= \kappa \sigma_{\hat{u}} z_{\hat{u}_2} + \omega(\beta_0 - \sigma_{\Delta\beta} z_{\Delta\beta_2}) \\ \Delta y_{2,0} &= \chi(\sigma_{\Delta y} z_{\Delta y_2} + \delta y_{\text{NL}}^*(\vec{x}_{2,0}) + \varepsilon_{2,0}) \\ \Delta\beta_{2,0} &= \kappa(\beta_0 - \sigma_{\Delta\beta} z_{\Delta\beta_2}) + \phi \sigma_{\hat{u}} z_{\hat{u}_2}. \end{aligned} \quad (\text{S161})$$

Multiplying these equations and making the self-averaging approximation, we find equations for the covariance of each of the unknown variables,

$$\begin{aligned} \langle \hat{w}_1 \hat{w}_2 \rangle &= \frac{1}{N_p} \sum_K \hat{w}_{1,K} \hat{w}_{2,K} \approx \text{E}[\hat{w}_{1,0} \hat{w}_{2,0}] = \nu^2 \text{E}[\sigma_{\hat{w}}^2 z_{\hat{w}_1} z_{\hat{w}_2}] \\ \langle \hat{u}_1 \hat{u}_2 \rangle &= \frac{1}{N_f} \sum_k \hat{u}_{1,k} \hat{u}_{2,k} \approx \text{E}[\hat{u}_{1,0} \hat{u}_{2,0}] = \kappa^2 \text{E}[\sigma_{\hat{u}}^2 z_{\hat{u}_1} z_{\hat{u}_2}] + \omega^2 (\sigma_\beta^2 + \text{E}[\sigma_{\Delta\beta}^2 z_{\Delta\beta_1} z_{\Delta\beta_2}]) \\ \langle \Delta y_1 \Delta y_2 \rangle &= \frac{1}{M} \sum_b \Delta y_{1,b} \Delta y_{2,b} \approx \text{E}[\Delta y_{1,0} \Delta y_{2,0}] = \chi^2 \text{E}[\sigma_{\Delta y}^2 z_{\Delta y_1} z_{\Delta y_2}] \\ \langle \Delta\beta_1 \Delta\beta_2 \rangle &= \frac{1}{N_f} \sum_k \Delta\beta_{1,k} \Delta\beta_{2,k} \approx \text{E}[\Delta\beta_{1,0} \Delta\beta_{2,0}] = \kappa^2 (\sigma_\beta^2 + \text{E}[\sigma_{\Delta\beta}^2 z_{\Delta\beta_1} z_{\Delta\beta_2}]) + \phi^2 \text{E}[\sigma_{\hat{u}}^2 z_{\hat{u}_1} z_{\hat{u}_2}]. \end{aligned} \quad (\text{S162})$$

Next, we calculate each of the four resulting expectation values of products of random variables. The average of the product $z_{\hat{w}_1} z_{\hat{w}_2}$ is

$$\begin{aligned} \text{E}[\sigma_{\hat{w}}^2 z_{\hat{w}_1} z_{\hat{w}_2}] &= \text{E} \left[\sum_{jk} \hat{u}_{1,j \setminus 0} \hat{u}_{2,k \setminus 0} W_{j0} W_{k0} \right] \\ &= \sum_{jk} \text{E}[\hat{u}_{1,j \setminus 0} \hat{u}_{2,k \setminus 0}] \text{E}[W_{j0} W_{k0}] \\ &= \frac{\sigma_W^2}{N_p} \sum_k \text{E}[\hat{u}_{1,j \setminus 0} \hat{u}_{2,j \setminus 0}] \\ &\approx \sigma_W^2 \frac{\alpha_f}{\alpha_p} \langle \hat{u}_1 \hat{u}_2 \rangle, \end{aligned} \quad (\text{S163})$$

while the average of the product $z_{\Delta\beta_1} z_{\Delta\beta_2}$ results in

$$\begin{aligned}
\mathbb{E}[\sigma_{\Delta\beta}^2 z_{\Delta\beta_1} z_{\Delta\beta_2}] &= \mathbb{E}\left[\sum_{JK} \hat{w}_{1,J\setminus 0} \hat{w}_{2,K\setminus 0} W_{0J} W_{0K}\right] \\
&= \sum_{JK} \mathbb{E}[\hat{w}_{1,J\setminus 0} \hat{w}_{2,K\setminus 0}] \mathbb{E}[W_{0J} W_{0K}] \\
&= \frac{\sigma_W^2}{N_p} \sum_K \mathbb{E}[\hat{w}_{1,K\setminus 0} \hat{w}_{2,K\setminus 0}] \\
&\approx \sigma_W^2 \langle \hat{w}_1 \hat{w}_2 \rangle.
\end{aligned} \tag{S164}$$

We find that the other two products average to zero due to the independence of X_1 and X_2 , giving us

$$\begin{aligned}
\mathbb{E}[\sigma_{\hat{u}}^2 z_{\hat{u}_1} z_{\hat{u}_2}] &= \mathbb{E}\left[\sum_{ab} \Delta y_{1,a\setminus 0} \Delta y_{2,b\setminus 0} X_{1,a0} X_{2,b0}\right] \\
&= \sum_{ab} \mathbb{E}[\Delta y_{1,a\setminus 0} \Delta y_{2,b\setminus 0}] \mathbb{E}[X_{1,a0}] \mathbb{E}[X_{2,b0}] \\
&= 0
\end{aligned} \tag{S165}$$

and

$$\begin{aligned}
\mathbb{E}[\sigma_{\Delta y}^2 z_{\Delta y_1} z_{\Delta y_2}] &= \mathbb{E}\left[\sum_{jk} \Delta\beta_{1,j\setminus 0} \Delta\beta_{2,k\setminus 0} X_{1,0j} X_{2,0k}\right] \\
&= \sum_{jk} \mathbb{E}[\Delta\beta_{1,j\setminus 0} \Delta\beta_{2,k\setminus 0}] \mathbb{E}[X_{1,0j}] \mathbb{E}[X_{2,0k}] \\
&= 0.
\end{aligned} \tag{S166}$$

Substituting these results into Eq. (S162), we find the self-consistent equations

$$\begin{aligned}
\langle \hat{w}_1 \hat{w}_2 \rangle &= \nu^2 \sigma_W^2 \frac{\alpha_f}{\alpha_p} \langle \hat{u}_1 \hat{u}_2 \rangle \\
\langle \hat{u}_1 \hat{u}_2 \rangle &= \omega^2 (\sigma_\beta^2 + \sigma_W^2 \langle \hat{w}_1 \hat{w}_2 \rangle) \\
\langle \Delta y_1 \Delta y_2 \rangle &= 0 \\
\langle \Delta\beta_1 \Delta\beta_2 \rangle &= \kappa^2 (\sigma_\beta^2 + \sigma_W^2 \langle \hat{w}_1 \hat{w}_2 \rangle).
\end{aligned} \tag{S167}$$

Next, we make the ansatz that the ensemble-averaged covariances are $\mathcal{O}(1)$ in small $\bar{\lambda}$ with the next order terms at $\mathcal{O}(\bar{\lambda}^2)$,

$$\begin{aligned}
\langle \hat{w}_1 \hat{w}_2 \rangle &\approx \langle \hat{w}_1 \hat{w}_2 \rangle_0 + \bar{\lambda}^2 \langle \hat{w}_1 \hat{w}_2 \rangle_2 \\
\langle \hat{u}_1 \hat{u}_2 \rangle &\approx \langle \hat{u}_1 \hat{u}_2 \rangle_0 + \bar{\lambda}^2 \langle \hat{u}_1 \hat{u}_2 \rangle_2 \\
\langle \Delta\beta_1 \Delta\beta_2 \rangle &\approx \langle \Delta\beta_1 \Delta\beta_2 \rangle_0 + \bar{\lambda}^2 \langle \Delta\beta_1 \Delta\beta_2 \rangle_2.
\end{aligned} \tag{S168}$$

Solution (1): Combining the leading order terms of the susceptibilities for the first set of solutions with the self-consistent equations for the covariances, we find

$$\begin{aligned}
\langle \hat{w}_1 \hat{w}_2 \rangle_0^{(1)} &= (\nu_{-1}^{(1)})^2 \sigma_W^2 \frac{\alpha_f}{\alpha_p} \langle \hat{u}_1 \hat{u}_2 \rangle_2^{(1)} \\
\langle \hat{u}_1 \hat{u}_2 \rangle_0^{(1)} &= 0 \\
\langle \Delta\beta_1 \Delta\beta_2 \rangle_0^{(1)} &= 0.
\end{aligned} \tag{S169}$$

We also require the next lowest order terms for $\langle \hat{u}_1 \hat{u}_2 \rangle$ and $\langle \hat{w}_1 \hat{w}_2 \rangle$,

$$\begin{aligned}
\langle \hat{u}_1 \hat{u}_2 \rangle_2^{(1)} &= (\omega_1^{(1)})^2 (\sigma_\beta^2 + \sigma_W^2 \langle \hat{w}_1 \hat{w}_2 \rangle_0^{(1)}) \\
\langle \Delta\beta_1 \Delta\beta_2 \rangle_2^{(1)} &= (\kappa_1^{(1)})^2 (\sigma_\beta^2 + \sigma_W^2 \langle \hat{w}_1 \hat{w}_2 \rangle_0^{(1)}).
\end{aligned} \tag{S170}$$

Substituting the solutions for the susceptibilities into these equations and solving, we find

$$\begin{aligned}
\langle \hat{w}_1 \hat{w}_2 \rangle_0^{(1)} &= \frac{\sigma_\beta^2}{\sigma_W^2} \frac{\alpha_f}{(\alpha_p - \alpha_f)} \\
\langle \hat{u}_1 \hat{u}_2 \rangle_2^{(1)} &= \sigma_\beta^2 \sigma_X^4 \frac{\alpha_p^3}{(\alpha_p - \alpha_f)^3} \\
\langle \Delta \beta_1 \Delta \beta_2 \rangle_2^{(1)} &= \sigma_\beta^2 \frac{\alpha_f^2 \alpha_p^3}{(1 - \alpha_f)^2 (\alpha_p - \alpha_f)^3}.
\end{aligned} \tag{S171}$$

Solution (2): Similarly, the lowest order forms of the self-consistent equations for the covariances for the second set of solutions are

$$\begin{aligned}
\langle \hat{w}_1 \hat{w}_2 \rangle_0^{(2)} &= (\nu_0^{(2)})^2 \sigma_W^2 \frac{\alpha_f}{\alpha_p} \langle \hat{u}_1 \hat{u}_2 \rangle_0^{(2)} \\
\langle \hat{u}_1 \hat{u}_2 \rangle_0^{(2)} &= (\omega_0^{(2)})^2 \left(\sigma_\beta^2 + \sigma_W^2 \langle \hat{w}_1 \hat{w}_2 \rangle_0^{(2)} \right) \\
\langle \Delta \beta_1 \Delta \beta_2 \rangle_0^{(2)} &= (\kappa_0^{(2)})^2 \left(\sigma_\beta^2 + \sigma_W^2 \langle \hat{w}_1 \hat{w}_2 \rangle_0^{(2)} \right).
\end{aligned} \tag{S172}$$

Substituting the solutions for the susceptibilities into these equations and solving, we find

$$\begin{aligned}
\langle \hat{w}_1 \hat{w}_2 \rangle_0^{(2)} &= \frac{\sigma_\beta^2}{\sigma_W^2} \frac{\alpha_p}{(\alpha_f - \alpha_p)} \\
\langle \hat{u}_1 \hat{u}_2 \rangle_0^{(2)} &= \sigma_\beta^2 \sigma_X^4 \frac{(1 - \alpha_p)^2 (\alpha_f - \alpha_p)}{\alpha_f^3} \\
\langle \Delta \beta_1 \Delta \beta_2 \rangle_0^{(2)} &= \sigma_\beta^2 \frac{(\alpha_f - \alpha_p)}{\alpha_f}.
\end{aligned} \tag{S173}$$

Solution (3): For the third set of solutions, the self-consistent equations become

$$\begin{aligned}
\langle \hat{w}_1 \hat{w}_2 \rangle_0^{(3)} &= (\nu_{-1}^{(3)})^2 \sigma_W^2 \frac{\alpha_f}{\alpha_p} \langle \hat{u}_1 \hat{u}_2 \rangle_2^{(3)} \\
\langle \hat{u}_1 \hat{u}_2 \rangle_0^{(3)} &= 0 \\
\langle \Delta \beta_1 \Delta \beta_2 \rangle_0^{(3)} &= (\kappa_0^{(3)})^2 \left(\sigma_\beta^2 + \sigma_W^2 \langle \hat{w}_1 \hat{w}_2 \rangle_0^{(3)} \right)
\end{aligned} \tag{S174}$$

with the next order term in $\langle \hat{u}_1 \hat{u}_2 \rangle$ described by

$$\langle \hat{u}_1 \hat{u}_2 \rangle_2^{(3)} = (\omega_1^{(3)})^2 \left(\sigma_\beta^2 + \sigma_W^2 \langle \hat{w}_1 \hat{w}_2 \rangle_0^{(3)} \right). \tag{S175}$$

Substituting the solutions for the susceptibilities into these equations and solving, we find

$$\begin{aligned}
\langle \hat{w}_1 \hat{w}_2 \rangle_0^{(2)} &= \frac{\sigma_\beta^2}{\sigma_W^2} \frac{1}{(\alpha_f \alpha_p - 1)} \\
\langle \hat{u}_1 \hat{u}_2 \rangle_2^{(2)} &= \sigma_\beta^2 \sigma_X^4 \frac{\alpha_p^3}{\alpha_f (\alpha_p - 1)^2 (\alpha_f \alpha_p - 1)} \\
\langle \Delta \beta_1 \Delta \beta_2 \rangle_0^{(2)} &= \sigma_\beta^2 \frac{\alpha_p (\alpha_f - 1)^2}{\alpha_f (\alpha_f \alpha_p - 1)}.
\end{aligned} \tag{S176}$$

Combined solutions: All together, the covariances in the limit $\lambda \rightarrow 0$ are

$$\begin{aligned}
\langle \hat{w}_1 \hat{w}_2 \rangle &= \begin{cases} \frac{\sigma_\beta^2}{\sigma_W^2} \frac{\alpha_f}{(\alpha_p - \alpha_f)} & \text{if } N_f < N_p, M \\ \frac{\sigma_\beta^2}{\sigma_W^2} \frac{\alpha_p}{(\alpha_f - \alpha_p)} & \text{if } N_p < N_f, M \\ \frac{\sigma_\beta^2}{\sigma_W^2} \frac{1}{(\alpha_f \alpha_p - 1)} & \text{if } M < N_f, N_p \end{cases} \\
\langle \hat{u}_1 \hat{u}_2 \rangle &= \begin{cases} \frac{\lambda^2}{\sigma_X^4 \sigma_W^4} \sigma_\beta^2 \sigma_X^4 \frac{\alpha_p^3}{(\alpha_p - \alpha_f)^3} & \text{if } N_f < N_p, M \\ \sigma_\beta^2 \sigma_X^4 \frac{(1 - \alpha_p)^2 (\alpha_f - \alpha_p)}{\alpha_f^3} & \text{if } N_p < N_f, M \\ \frac{\lambda^2}{\sigma_X^4 \sigma_W^4} \sigma_\beta^2 \sigma_X^4 \frac{\alpha_p^3}{\alpha_f (\alpha_p - 1)^2 (\alpha_f \alpha_p - 1)} & \text{if } M < N_f, N_p \end{cases} \\
\langle \Delta y_1 \Delta y_2 \rangle &= 0 \\
\langle \Delta \beta_1 \Delta \beta_2 \rangle &= \begin{cases} \frac{\lambda^2}{\sigma_X^4 \sigma_W^4} \sigma_\beta^2 \frac{\alpha_f^2 \alpha_p^3}{(1 - \alpha_f)^2 (\alpha_p - \alpha_f)^3} & \text{if } N_f < N_p, M \\ \sigma_\beta^2 \frac{(\alpha_f - \alpha_p)}{\alpha_f} & \text{if } N_p < N_f, M \\ \sigma_\beta^2 \frac{\alpha_p (\alpha_f - 1)^2}{\alpha_f (\alpha_f \alpha_p - 1)} & \text{if } M < N_f, N_p \end{cases}
\end{aligned} \tag{S177}$$

and the resulting expressions for the bias and variance are

$$\begin{aligned}
\langle \text{Bias}^2[\hat{f}] \rangle &= \begin{cases} \sigma_{\delta y^*}^2 & \text{if } N_f < N_p, M \\ \sigma_\beta^2 \sigma_X^2 \frac{(\alpha_f - \alpha_p)}{\alpha_f} + \sigma_{\delta y^*}^2 & \text{if } N_p < N_f, M \\ \sigma_\beta^2 \sigma_X^2 \frac{\alpha_p (\alpha_f - 1)^2}{\alpha_f (\alpha_f \alpha_p - 1)} + \sigma_{\delta y^*}^2 & \text{if } M < N_f, N_p \end{cases} \\
\langle \text{Var}[\hat{f}] \rangle &= \begin{cases} (\sigma_\varepsilon^2 + \sigma_{\delta y^*}^2) \frac{\alpha_f}{(1 - \alpha_f)} & \text{if } N_f < N_p, M \\ \sigma_\beta^2 \sigma_X^2 \frac{\alpha_p (\alpha_f - \alpha_p)}{\alpha_f (1 - \alpha_p)} + (\sigma_\varepsilon^2 + \sigma_{\delta y^*}^2) \frac{\alpha_p}{(1 - \alpha_p)} & \text{if } N_p < N_f, M \\ \sigma_\beta^2 \sigma_X^2 \frac{\alpha_p (\alpha_f - 1) (\alpha_f - 1 + \alpha_p - 1)}{\alpha_f (\alpha_p - 1) (\alpha_f \alpha_p - 1)} + (\sigma_\varepsilon^2 + \sigma_{\delta y^*}^2) \frac{(\alpha_f - 1 + \alpha_p - 1)}{(\alpha_f - 1) (\alpha_p - 1)} & \text{if } M < N_f, N_p. \end{cases}
\end{aligned} \tag{S178}$$

G. Random Nonlinear Features Model (Two-layer Nonlinear Neural Network)

This cavity derivation for the random nonlinear features model again follows closely with the two previous derivations. Therefore, we again omit most of the justification for each step and refer the reader to the analogous steps laid out in the previous sections.

In the random nonlinear features model, the student model takes the form

$$\vec{z}(\vec{x}) = \frac{1}{\langle \varphi' \rangle} \frac{\sigma_W \sigma_X}{\sqrt{N_p}} \varphi \left(\frac{\sqrt{N_p}}{\sigma_W \sigma_X} W^T \vec{x} \right) \tag{S179}$$

where W is again a random matrix whose elements are independent with zero mean and variance σ_W^2/N_p .

For this model, we again decompose the system of equations in Eq. (S41) such that they are linear in the random matrices W and X , resulting in four different sets of equations,

$$\begin{aligned}
\lambda \hat{w}_J &= \sqrt{M} \alpha_p^{-\frac{1}{2}} \mu_z \langle \Delta y \rangle + \sum_k \hat{u}_k W_{kJ} + \sum_b \Delta y_b \delta z_{\text{NL},J}(\vec{x}_b) + \eta_J \\
\hat{u}_j &= \sum_b \Delta y_b X_{bj} + \psi_j \\
\Delta y_a &= -\sqrt{N_p} \mu_z \langle \hat{w} \rangle + \sum_k \Delta \beta_k X_{ak} - \sum_K \hat{w}_K \delta z_{\text{NL},K}(\vec{x}_a) + \delta y_{\text{NL}}^*(\vec{x}_a) + \varepsilon_a + \xi_a \\
\Delta \beta_j &= \beta_j - \sum_K \hat{w}_K W_{jK} + \zeta_j,
\end{aligned} \tag{S180}$$

where we have added a different auxiliary field to each equation and have defined the mean residual label error and fit parameter as

$$\langle \Delta y \rangle = \frac{1}{M} \sum_b \Delta y_b, \quad \langle \hat{w} \rangle = \frac{1}{N_p} \sum_K \hat{w}_K. \tag{S181}$$

We note that these four sets of equations reduce to those of the random linear features model when the hidden features are linear $\delta \vec{z}_{\text{NL}}(\vec{x}) = 0$ and zero mean $\mu_z = 0$.

1. Cavity Expansion

Next, we add an additional variable of each type, resulting in a total of $M + 1$ data points, $N_f + 1$ input features and $N_p + 1$ fit parameters. Each additional variable is represented using an index value of 0, written as \hat{w}_0 , \hat{u}_0 , Δy_0 , and $\Delta \beta_0$. After including these new unknown quantities, the four equations become

$$\begin{aligned} \lambda \hat{w}_J &= \sqrt{M} \alpha_p^{-\frac{1}{2}} \langle \Delta y \rangle + \sum_k \hat{u}_k W_{kJ} + \sum_b \Delta y_b \delta z_{\text{NL},J}(\vec{x}_b) + \eta_J + \hat{u}_0 W_{0J} + \Delta y_0 \delta z_{\text{NL},J}(\vec{x}_0) \\ \hat{u}_j &= \sum_b \Delta y_b X_{bj} + \psi_j + \Delta y_0 X_{0j} \\ \Delta y_a &= -\sqrt{N_p} \mu_z \langle \hat{w} \rangle + \sum_k \Delta \beta_k X_{ak} - \sum_K \hat{w}_K \delta z_{\text{NL},K}(\vec{x}_a) + \delta y_{\text{NL}}^*(\vec{x}_a) + \varepsilon_a + \xi_a + \Delta \beta_0 X_{a0} - \hat{w}_0 \delta z_{\text{NL},0}(\vec{x}_a) \\ \Delta \beta_j &= \beta_j - \sum_K \hat{w}_K W_{jK} + \zeta_j - \hat{w}_0 W_{j0} \end{aligned} \tag{S182}$$

with each new variable described by a new equation,

$$\begin{aligned} \lambda \hat{w}_0 &= \sqrt{M} \alpha_p^{-\frac{1}{2}} \langle \Delta y \rangle + \sum_k \hat{u}_k W_{k0} + \sum_b \Delta y_b \delta z_{\text{NL},0}(\vec{x}_b) + \eta_J + \hat{u}_0 W_{00} + \Delta y_0 \delta z_{\text{NL},0}(\vec{x}_0) \\ \hat{u}_0 &= \sum_b \Delta y_b X_{b0} + \psi_0 + \Delta y_0 X_{00} \\ \Delta y_0 &= -\sqrt{N_p} \mu_z \langle \hat{w} \rangle + \sum_k \Delta \beta_k X_{0k} - \sum_K \hat{w}_K \delta z_{\text{NL},K}(\vec{x}_0) + \delta y_{\text{NL}}^*(\vec{x}_0) + \varepsilon_0 + \xi_0 + \Delta \beta_0 X_{00} - \hat{w}_0 \delta z_{\text{NL},0}(\vec{x}_0) \\ \Delta \beta_0 &= \beta_0 - \sum_K \hat{w}_K W_{0K} + \zeta_0 - \hat{w}_0 W_{00}. \end{aligned} \tag{S183}$$

Now we take the thermodynamic limit in which M , N_f , and N_p tend towards infinity, but their ratios, $\alpha_f = N_f/M$ and $\alpha_p = N_p/M$, remain fixed. We interpret the extra terms in Eq. (S182) as small perturbations to the auxiliary fields,

$$\begin{aligned} \delta \eta_J &= \hat{u}_0 W_{0J} + \Delta y_0 \delta z_{\text{NL},J}(\vec{x}_0), & \delta \psi_j &= \Delta y_0 X_{0j}, \\ \delta \xi_a &= \Delta \beta_0 X_{a0} - \hat{w}_0 \delta z_{\text{NL},0}(\vec{x}_a), & \delta \zeta_j &= -\hat{w}_0 W_{j0}, \end{aligned} \tag{S184}$$

allowing us to expand each unknown quantity about its solution in the absence of the 0-indexed variables which correspond to the solutions for M data points, N_f input features, and N_p fit parameters,

$$\begin{aligned} \hat{w}_J &\approx \hat{w}_{J \setminus 0} + \sum_K \nu_{JK}^{\hat{w}} \delta \eta_K + \sum_k \phi_{Jk}^{\hat{w}} \delta \psi_k + \sum_b \chi_{Jb}^{\hat{w}} \delta \xi_b + \sum_k \omega_{Jk}^{\hat{w}} \delta \zeta_k \\ \hat{u}_j &\approx \hat{u}_{j \setminus 0} + \sum_K \nu_{jK}^{\hat{u}} \delta \eta_K + \sum_k \phi_{jk}^{\hat{u}} \delta \psi_k + \sum_b \chi_{jb}^{\hat{u}} \delta \xi_b + \sum_k \omega_{jk}^{\hat{u}} \delta \zeta_k \\ \Delta y_a &\approx \Delta y_{a \setminus 0} + \sum_K \nu_{aK}^{\Delta y} \delta \eta_K + \sum_k \phi_{ak}^{\Delta y} \delta \psi_k + \sum_b \chi_{ab}^{\Delta y} \delta \xi_b + \sum_k \omega_{ak}^{\Delta y} \delta \zeta_k \\ \Delta \beta_j &\approx \Delta \beta_{j \setminus 0} + \sum_K \nu_{jK}^{\Delta \beta} \delta \eta_K + \sum_k \phi_{jk}^{\Delta \beta} \delta \psi_k + \sum_b \chi_{jb}^{\Delta \beta} \delta \xi_b + \sum_k \omega_{jk}^{\Delta \beta} \delta \zeta_k. \end{aligned} \tag{S185}$$

We define each of the susceptibility matrices as a derivative of a variable with respect to an auxiliary fields,

$$\begin{aligned}
\nu_{JK}^{\hat{w}} &= \frac{\partial \hat{w}_J}{\partial \eta_K}, & \phi_{Jk}^{\hat{w}} &= \frac{\partial \hat{w}_J}{\partial \psi_k}, & \chi_{Jb}^{\hat{w}} &= \frac{\partial \hat{w}_J}{\partial \xi_b}, & \omega_{Jk}^{\hat{w}} &= \frac{\partial \hat{w}_J}{\partial \zeta_k}, \\
\nu_{jK}^{\hat{u}} &= \frac{\partial \hat{u}_j}{\partial \eta_K}, & \phi_{jk}^{\hat{u}} &= \frac{\partial \hat{u}_j}{\partial \psi_k}, & \chi_{jb}^{\hat{u}} &= \frac{\partial \hat{u}_j}{\partial \xi_b}, & \omega_{jk}^{\hat{u}} &= \frac{\partial \hat{u}_j}{\partial \zeta_k}, \\
\nu_{aK}^{\Delta y} &= \frac{\partial \Delta y_a}{\partial \eta_K}, & \phi_{ak}^{\Delta y} &= \frac{\partial \Delta y_a}{\partial \psi_k}, & \chi_{ab}^{\Delta y} &= \frac{\partial \Delta y_a}{\partial \xi_b}, & \omega_{ak}^{\Delta y} &= \frac{\partial \Delta y_a}{\partial \zeta_k}, \\
\nu_{jK}^{\Delta \beta} &= \frac{\partial \Delta \beta_j}{\partial \eta_K}, & \phi_{jk}^{\Delta \beta} &= \frac{\partial \Delta \beta_j}{\partial \psi_k}, & \chi_{jb}^{\Delta \beta} &= \frac{\partial \Delta \beta_j}{\partial \xi_b}, & \omega_{jk}^{\Delta \beta} &= \frac{\partial \Delta \beta_j}{\partial \zeta_k},
\end{aligned} \tag{S186}$$

with corresponding representations as second derivative of the loss function. Next, we substituting the expansions in Eq. (S185) into the 0-indexed equations in Eq. (S183). We then aim to approximate each of the resulting sums in these expanded equations.

2. Approximations of Large Sums: Unperturbed Quantities

We approximate each of the sums containing one of the unperturbed quantities, $\hat{w}_{J \setminus 0}$, $\hat{u}_{j \setminus 0}$, $\Delta y_{a \setminus 0}$, or $\Delta \beta_{j \setminus 0}$, using the central limit theorem in the same manner described in Sec. S1E2. The unperturbed quantities in each of these sums are statistically independent of all elements of both X and W with a 0-valued index. Using this fact, we find

$$\begin{aligned}
\sum_k \hat{u}_{k \setminus 0} W_{k0} + \sum_b \Delta y_{b \setminus 0} \delta z_{\text{NL},0}(\vec{x}_b) &\approx \sigma_{\hat{w}} z_{\hat{w}}, & \sigma_{\hat{w}}^2 &= \sigma_W^2 \frac{\alpha_f}{\alpha_p} \langle \hat{u}^2 \rangle + \sigma_{\delta z}^2 \alpha_p^{-1} \langle \Delta y^2 \rangle \\
\sum_b \Delta y_{b \setminus 0} X_{b0} &\approx \sigma_{\hat{u}} z_{\hat{u}}, & \sigma_{\hat{u}}^2 &= \sigma_X^2 \alpha_f^{-1} \langle \Delta y^2 \rangle \\
\sum_k \Delta \beta_{k \setminus 0} X_{0k} - \sum_K \hat{w}_{K \setminus 0} \delta z_{\text{NL},K}(\vec{x}_0) &\approx \sigma_{\Delta y} z_{\Delta y}, & \sigma_{\Delta y}^2 &= \sigma_X^2 \langle \Delta \beta^2 \rangle + \sigma_{\delta z}^2 \langle \hat{w}^2 \rangle \\
\sum_K \hat{w}_{K \setminus 0} W_{0K} &\approx \sigma_{\Delta \beta} z_{\Delta \beta}, & \sigma_{\Delta \beta}^2 &= \sigma_W^2 \langle \hat{w}^2 \rangle
\end{aligned} \tag{S187}$$

where $z_{\hat{w}}$, $z_{\hat{u}}$, $z_{\Delta y}$, and $z_{\Delta \beta}$ are all random variables with zero mean and unit variance and can easily be shown to be statistically independent from one another. We also define the mean squared averages

$$\langle \hat{w}^2 \rangle = \frac{1}{N_p} \sum_K \hat{w}_{K \setminus 0}^2, \quad \langle \hat{u}^2 \rangle = \frac{1}{N_f} \sum_k \hat{u}_{k \setminus 0}^2, \quad \langle \Delta y^2 \rangle = \frac{1}{M} \sum_b \Delta y_{b \setminus 0}^2, \quad \langle \Delta \beta^2 \rangle = \frac{1}{N_f} \sum_k \Delta \beta_{k \setminus 0}^2. \tag{S188}$$

3. Approximations of Large Sums: Square Susceptibilities

Next, we approximate each of the sums containing a square susceptibility matrix. Using the fact that all of the susceptibility matrices are statistically independent of all elements of both X and W with a 0-valued index, we follow the procedure in Sec. S1E3 to find

$$\begin{aligned}
\sum_{jk} \omega_{jk}^{\hat{u}} W_{j0} W_{k0} &\approx \sigma_W^2 \frac{\alpha_f}{\alpha_p} \omega, & \omega &= \frac{1}{N_f} \sum_k \omega_{kk}^{\hat{u}} \\
\sum_{ab} \chi_{ab}^{\Delta y} X_{a0} X_{b0} &\approx \sigma_X^2 \alpha_f^{-1} \chi, & \chi &= \frac{1}{M} \sum_b \chi_{bb}^{\Delta y} \\
\sum_{jk} \phi_{jk}^{\Delta \beta} X_{0j} X_{0k} &\approx \sigma_X^2 \phi, & \phi &= \frac{1}{N_f} \sum_k \phi_{kk}^{\Delta \beta} \\
\sum_{JK} \nu_{JK}^{\hat{w}} W_{0J} W_{0K} &\approx \sigma_W^2 \nu, & \nu &= \frac{1}{N_p} \sum_K \nu_{KK}^{\hat{w}}
\end{aligned} \tag{S189}$$

along with two additional sums

$$\begin{aligned} \sum_{JK} \nu_{JK}^{\hat{w}} \delta z_{\text{NL},J}(\vec{\mathbf{x}}_0) \delta z_{\text{NL},K}(\vec{\mathbf{x}}_0) &\approx \sigma_{\delta z}^2 \nu \\ \sum_{ab} \chi_{ab}^{\Delta y} \delta z_{\text{NL},0}(\vec{\mathbf{x}}_a) \delta z_{\text{NL},0}(\vec{\mathbf{x}}_b) &\approx \sigma_{\delta z}^2 \alpha_p^{-1} \chi. \end{aligned} \quad (\text{S190})$$

4. Approximations of Large Sums: Rectangular Susceptibilities

Analogously to those in Sec. S1E4, it is straightforward to show that each of the sums containing a rectangular susceptibility matrix approximates to zero in the thermodynamic limit.

5. Self-consistency Equations

Next, we substitute the expansions in Eq. (S185) into Eq. (S183) and apply the large sum approximations from the previous sections, resulting in a set of self-consistent equations for \hat{w}_0 , \hat{u}_0 , Δy_0 , and $\Delta\beta_0$,

$$\begin{aligned} \lambda \hat{w}_0 &\approx \sqrt{M} \alpha_p^{-\frac{1}{2}} \mu_z \langle y \rangle + \sigma_{\hat{w}} z_{\hat{w}} - \hat{w}_0 \left(\sigma_W^2 \frac{\alpha_f}{\alpha_p} \omega + \sigma_{\delta z}^2 \alpha_p^{-1} \chi \right) + \eta_0 \\ \hat{u}_0 &\approx \sigma_{\hat{u}} z_{\hat{u}} + \Delta\beta_0 \sigma_X^2 \alpha_f^{-1} \chi + \psi_0 \\ \Delta y_0 &\approx -\sqrt{N_p} \mu_z \langle \hat{w} \rangle + \sigma_{\Delta y} z_{\Delta y} + \Delta y_0 (\sigma_X^2 \phi - \sigma_{\delta z}^2 \nu) + \delta y_{\text{NL}}^*(\vec{\mathbf{x}}_0) + \varepsilon_0 + \xi_0 \\ \Delta\beta_0 &\approx \beta_0 - \sigma_{\Delta\beta} z_{\Delta\beta} - \hat{u}_0 \sigma_W^2 \nu + \zeta_0. \end{aligned} \quad (\text{S191})$$

We have also made use of the fact that the terms including X_{00} or W_{00} are infinitesimally small in the thermodynamic limit with zero mean and variances of $\mathcal{O}(1/N_f)$ and $\mathcal{O}(1/N_p)$, respectively. Solving these equations for the 0-indexed variables, we find

$$\begin{aligned} \hat{w}_0 &= \frac{\sqrt{M} \alpha_p^{-\frac{1}{2}} \mu_z \langle y \rangle + \sigma_{\hat{w}} z_{\hat{w}} + \eta_0}{\lambda + \sigma_W^2 \frac{\alpha_f}{\alpha_p} \omega + \sigma_{\delta z}^2 \alpha_p^{-1} \chi} \\ \hat{u}_0 &= \frac{\sigma_{\hat{u}} z_{\hat{u}} + \psi_0 + \sigma_X^2 \alpha_f^{-1} \chi (\beta_0 - \sigma_{\Delta\beta} z_{\Delta\beta} + \zeta_0)}{1 + \sigma_W^2 \sigma_X^2 \alpha_f^{-1} \chi \nu} \\ \Delta y_0 &= \frac{-\sqrt{N_p} \mu_z \langle \hat{w} \rangle + \sigma_{\Delta y} z_{\Delta y} + \delta y_{\text{NL}}^*(\vec{\mathbf{x}}_0) + \varepsilon_0 + \xi_0}{1 - \sigma_X^2 \phi + \sigma_{\delta z}^2 \nu} \\ \Delta\beta_0 &= \frac{\beta_0 - \sigma_{\Delta\beta} z_{\Delta\beta} + \zeta_0 - \sigma_W^2 \nu^2 (\sigma_{\hat{u}} z_{\hat{u}} + \psi_0)}{1 + \sigma_W^2 \sigma_X^2 \alpha_f^{-1} \chi \nu}. \end{aligned} \quad (\text{S192})$$

We derive a set of self-consistent equations for the scalar susceptibilities by taking appropriate derivatives of these variables with respect to the auxiliary fields,

$$\begin{aligned} \nu &= \frac{1}{N_p} \sum_K \nu_{KK}^{\hat{w}} \approx \mathbb{E}[\nu_{00}^{\hat{w}}] = \mathbb{E}\left[\frac{\partial \hat{w}_0}{\partial \eta_0}\right] = \frac{1}{\lambda + \sigma_W^2 \frac{\alpha_f}{\alpha_p} \omega + \sigma_{\delta z}^2 \alpha_p^{-1} \chi} \\ \omega &= \frac{1}{N_f} \sum_k \omega_{kk}^{\hat{u}} \approx \mathbb{E}[\omega_{00}^{\hat{u}}] = \mathbb{E}\left[\frac{\partial \hat{u}_0}{\partial \zeta_0}\right] = \frac{\sigma_X^2 \alpha_f^{-1} \chi}{1 + \sigma_W^2 \sigma_X^2 \alpha_f^{-1} \chi \nu} \\ \chi &= \frac{1}{M} \sum_b \chi_{bb}^{\Delta y} \approx \mathbb{E}[\chi_{00}^{\Delta y}] = \mathbb{E}\left[\frac{\partial \Delta y_0}{\partial \xi_0}\right] = \frac{1}{1 - \sigma_X^2 \phi + \sigma_{\delta z}^2 \nu} \\ \phi &= \frac{1}{N_f} \sum_k \phi_{kk}^{\Delta\beta} \approx \mathbb{E}[\phi_{00}^{\Delta\beta}] = \mathbb{E}\left[\frac{\partial \Delta\beta_0}{\partial \psi_0}\right] = -\frac{\sigma_W^2 \nu}{1 + \sigma_W^2 \sigma_X^2 \alpha_f^{-1} \chi \nu}. \end{aligned} \quad (\text{S193})$$

As for the random linear features model, we also introduce a fifth scalar susceptibility,

$$\kappa = \frac{1}{N_f} \sum_k \phi_{kk}^{\hat{u}} = \frac{1}{N_f} \sum_k \omega_{kk}^{\Delta\beta} \approx \mathbb{E}\left[\frac{\partial \hat{u}_0}{\partial \psi_0}\right] = \mathbb{E}\left[\frac{\partial \Delta\beta_0}{\partial \zeta_0}\right] = \frac{1}{1 + \sigma_W^2 \sigma_X^2 \alpha_f^{-1} \chi \nu}. \quad (\text{S194})$$

Using this formula for κ , we re-express the four other susceptibilities as

$$\begin{aligned}\omega &= \sigma_X^2 \alpha_f^{-1} \chi \kappa \\ \phi &= -\sigma_W^2 \nu \kappa \\ \nu &= \frac{1}{\lambda + \sigma_W^2 \sigma_X^2 \alpha_p^{-1} \chi (\kappa + \Delta\varphi)} \\ \chi &= \frac{1}{1 + \sigma_W^2 \sigma_X^2 \nu (\kappa + \Delta\varphi)}.\end{aligned}\tag{S195}$$

From here, we observe that these susceptibilities reduce to those for the random linear features model when $\Delta\varphi = 0$.

Next, we find self-consistent equations for the mean fit parameter and residual label error

$$\begin{aligned}\langle \hat{w} \rangle &= \frac{1}{N_p} \sum_K \hat{w}_K \approx \mathbb{E}[\hat{w}_0] = \nu \sqrt{M} \alpha_p^{-\frac{1}{2}} \mu_z \langle \Delta y \rangle \\ \langle \Delta y \rangle &= \frac{1}{M} \sum_b \Delta y_b \approx \mathbb{E}[\Delta y_0] = -\chi \sqrt{N_p} \mu_z \langle \hat{w} \rangle,\end{aligned}\tag{S196}$$

where we have set the auxiliary fields to zero. Solving these equations, it is clear that both averages are zero,

$$\langle \hat{w} \rangle = 0, \quad \langle \Delta y \rangle = 0.\tag{S197}$$

Finally, we square and average each of Eq. (S192) to find self-consistent equations for the four ensemble-averaged squared quantities (again setting the auxiliary fields to zero),

$$\begin{aligned}\langle \hat{w}^2 \rangle &= \frac{1}{N_p} \sum_K \hat{w}_{K \setminus 0}^2 \approx \mathbb{E}[\hat{w}_0^2] = \nu^2 \left(\sigma_W^2 \frac{\alpha_f}{\alpha_p} \langle \hat{u}^2 \rangle + \sigma_{\delta z}^2 \alpha_p^{-1} \langle \Delta y^2 \rangle \right) \\ \langle \hat{u}^2 \rangle &= \frac{1}{N_f} \sum_k \hat{u}_{k \setminus 0}^2 \approx \mathbb{E}[\hat{u}_0^2] = \kappa^2 \sigma_X^2 \alpha_f^{-1} \langle \Delta y^2 \rangle + \omega^2 (\sigma_\beta^2 + \sigma_W^2 \langle \hat{w}^2 \rangle) \\ \langle \Delta y^2 \rangle &= \frac{1}{M} \sum_b \Delta y_{b \setminus 0}^2 \approx \mathbb{E}[\Delta y_0^2] = \chi^2 (\sigma_X^2 \langle \Delta \beta^2 \rangle + \sigma_{\delta z}^2 \langle \hat{w}^2 \rangle + \sigma_{\delta y^*}^2 + \sigma_\epsilon^2) \\ \langle \Delta \beta^2 \rangle &= \frac{1}{N_f} \sum_k \Delta \beta_{k \setminus 0}^2 \approx \mathbb{E}[\Delta \beta_0^2] = \kappa^2 (\sigma_\beta^2 + \sigma_W^2 \langle \hat{w}^2 \rangle) + \phi^2 \sigma_X^2 \alpha_f^{-1} \langle \Delta y^2 \rangle.\end{aligned}\tag{S198}$$

Again we observe that these equations reduce to those for the random linear features model when $\sigma_{\delta z}^2 = 0$ (or equivalently, $\Delta\varphi = 0$).

6. Solution with Finite Regularization ($\lambda \sim \mathcal{O}(1)$)

Following the same procedure as Sec. S1 E 6 for the random linear features model, we start by solving the equations for χ and ν in Eq. (S195) for κ and setting them equal,

$$\kappa = \frac{1 - \chi - \sigma_W^2 \sigma_X^2 \Delta\varphi \nu}{\sigma_W^2 \sigma_X^2 \chi \nu} = \frac{\alpha_p (1 - \lambda \nu) - \sigma_W^2 \sigma_X^2 \Delta\varphi \nu}{\sigma_W^2 \sigma_X^2 \chi \nu},\tag{S199}$$

giving us a relation between ν and χ ,

$$\nu = \frac{\chi + \alpha_p - 1}{\lambda \alpha_p}.\tag{S200}$$

Substituting κ from Eq. (S194) into χ from Eq. (S195), inserting the expression for ν we just found, and multiplying out the denominators, we find a quartic equation for χ ,

$$\begin{aligned}0 &= \Delta\varphi \chi^4 + [2\Delta\varphi(\alpha_p - 1) + \alpha_p \bar{\lambda}] \chi^3 + [\Delta\varphi(\alpha_p - 1)^2 + ((1 + \Delta\varphi)\alpha_f + \alpha_p - 2)\alpha_p \bar{\lambda}] \chi^2 \\ &\quad + [((1 + \Delta\varphi)\alpha_f - 1)(\alpha_p - 1) + \alpha_f \alpha_p \bar{\lambda}] \alpha_p \bar{\lambda} \chi - \alpha_f \alpha_p^2 \bar{\lambda}^2,\end{aligned}\tag{S201}$$

where we have defined the dimensionless regularization parameter

$$\bar{\lambda} = \frac{\lambda}{\sigma_W^2 \sigma_X^2}. \quad (\text{S202})$$

Solving the quartic equation and solving for the remaining susceptibilities, we find exact solutions in the thermodynamic limit by solving Eq. (S198),

$$\begin{pmatrix} \langle \hat{w}^2 \rangle \\ \langle \hat{u}^2 \rangle \\ \langle \Delta y^2 \rangle \\ \langle \Delta \beta^2 \rangle \end{pmatrix} = \begin{pmatrix} 1 & -\sigma_W^2 \frac{\alpha_f}{\alpha_p} \nu^2 & -\sigma_{\delta z}^2 \alpha_p^{-1} \nu^2 & 0 \\ -\sigma_W^2 \omega^2 & 1 & -\sigma_X^2 \alpha_f^{-1} \kappa^2 & 0 \\ -\sigma_{\delta z}^2 \chi^2 & 0 & 1 & -\sigma_X^2 \chi^2 \\ -\sigma_W^2 \kappa^2 & 0 & -\sigma_X^2 \alpha_f^{-1} \phi^2 & 1 \end{pmatrix}^{-1} \begin{pmatrix} 0 \\ \sigma_\beta^2 \omega^2 \\ (\sigma_\varepsilon^2 + \sigma_{\delta y^*}^2) \chi^2 \\ \sigma_\beta^2 \kappa^2 \end{pmatrix}. \quad (\text{S203})$$

7. Solutions in Ridge-less Limit ($\lambda \rightarrow 0$)

In the ridge-less limit ($\lambda \rightarrow 0$), we make the ansatz that χ is $\mathcal{O}(1)$ in small $\bar{\lambda}$,

$$\chi \approx \chi_0 + \bar{\lambda} \chi_1. \quad (\text{S204})$$

Using this approximation, Eq. (S201) gives us the following equation at $\mathcal{O}(1)$:

$$\begin{aligned} 0 &= \Delta\varphi \chi_0^4 + 2\Delta\varphi(\alpha_p - 1)\chi_0^3 + \Delta\varphi(\alpha_p - 1)^2 \chi_0^2 \\ &= \Delta\varphi(\chi_0 + \alpha_p - 1)^2 \chi_0^2. \end{aligned} \quad (\text{S205})$$

This equation has two solutions for χ_0 ,

$$\chi_0^{(1)} = 1 - \alpha_p, \quad \chi_0^{(2)} = 0, \quad (\text{S206})$$

labeled by superscript (1) and (2). At $\mathcal{O}(\bar{\lambda})$, the resulting equation is

$$\begin{aligned} 0 &= 4\Delta\varphi \chi_0^3 \chi_1 + 6\Delta\varphi(\alpha_p - 1)\chi_0^2 \chi_1 + \alpha_p \chi_0^3 + 2\Delta\varphi(\alpha_p - 1)^2 \chi_0 \chi_1 \\ &\quad + ((1 + \Delta\varphi)\alpha_f + \alpha_p - 2)\alpha_p \chi_0^2 + ((1 + \Delta\varphi)\alpha_f - 1)(\alpha_p - 1)\alpha_p \chi_0 \\ &= [2\Delta\varphi(2\chi_0 + \alpha_p - 1)\chi_1 + \alpha_p \chi_0 + (1 + \Delta\varphi)\alpha_f - \alpha_p](\chi_0 + \alpha_p - 1)\chi_0. \end{aligned} \quad (\text{S207})$$

We find this equation to be uninformative after inserting either of the solutions for χ_0 . However, the $\mathcal{O}(\bar{\lambda}^2)$ equation does have unique solutions,

$$\begin{aligned} 0 &= \Delta\varphi(4\chi_0^3 \chi_2 + 6\chi_0^2 \chi_1^2) + 2\Delta\varphi(\alpha_p - 1)(3\chi_0^2 \chi_2 + 3\chi_0 \chi_1^2) + 3\alpha_p \chi_0^2 \chi_1 + \Delta\varphi(\alpha_p - 1)^2(2\chi_0 \chi_2 + \chi_1^2) \\ &\quad + 2((1 + \Delta\varphi)\alpha_f + \alpha_p - 2)\alpha_p \chi_0 \chi_1 + ((1 + \Delta\varphi)\alpha_f - 1)(\alpha_p - 1)\alpha_p \chi_1 + \alpha_f \alpha_p^2 \chi_0 - \alpha_f \alpha_p^2. \end{aligned} \quad (\text{S208})$$

Inserting $\chi_0^{(1)}$, this equation becomes

$$0 = \Delta\varphi(1 - \alpha_p)^2 \chi_1^2 - [\alpha_p - (1 + \Delta\varphi)\alpha_f](1 - \alpha_p)\alpha_p \chi_1 - \alpha_f \alpha_p^3 \quad (\text{S209})$$

with a pair of solutions,

$$\chi_1^{(1)} = \frac{1}{2\Delta\varphi \frac{(1 - \alpha_p)}{\alpha_p}} \left[\alpha_p - (1 + \Delta\varphi)\alpha_f \pm \sqrt{[\alpha_p - (1 + \Delta\varphi)\alpha_f]^2 + 4\Delta\varphi \alpha_f \alpha_p} \right]. \quad (\text{S210})$$

Similarly, inserting the second solution $\chi_0^{(2)}$, we find

$$0 = \Delta\varphi(\alpha_p - 1)^2 \chi_1^2 - [1 - (1 + \Delta\varphi)\alpha_f](\alpha_p - 1)\alpha_p \chi_1 - \alpha_f \alpha_p^2 \quad (\text{S211})$$

with a second pair of solutions,

$$\chi_1^{(2)} = \frac{1}{2\Delta\varphi \frac{(\alpha_p - 1)}{\alpha_p}} \left[1 - (1 + \Delta\varphi)\alpha_f \pm \sqrt{[1 - (1 + \Delta\varphi)\alpha_f]^2 + 4\Delta\varphi \alpha_f} \right]. \quad (\text{S212})$$

We note that the two solutions for χ_1 are qualitatively similar to the exact solution for χ in the model of linear regression, Eq. (S72). The implication is that the nonlinear nature of the activation function implicitly serves as a type of regularization via the quantity $\Delta\varphi$ which evaluates to zero in the linear limit.

Next, we solve for the solutions to ν . First, we make the ansatz

$$\nu \approx \frac{1}{\lambda} \nu_{-1} + \nu_0. \quad (\text{S213})$$

Using Eq. (S200) and inserting the first solution for χ , we find

$$\nu_{-1}^{(1)} = 0 \quad (\text{S214})$$

with the next order term

$$\nu_0^{(1)} = \frac{1}{\sigma_W^2 \sigma_X^2} \frac{1}{2\Delta\varphi(1-\alpha_p)} \left[\alpha_p - (1 + \Delta\varphi)\alpha_f \pm \sqrt{[\alpha_p - (1 + \Delta\varphi)\alpha_f]^2 + 4\Delta\varphi\alpha_f\alpha_p} \right]. \quad (\text{S215})$$

Similarly, the second solution for χ gives us

$$\nu_{-1}^{(2)} = \frac{1}{\sigma_W^2 \sigma_X^2} \frac{(\alpha_p - 1)}{\alpha_p}. \quad (\text{S216})$$

None of the remaining scalar susceptibilities have simple forms. Therefore, we use their representation in terms of ν and χ . Similarly, the solutions for $\langle \hat{w}^2 \rangle$, $\langle \Delta y^2 \rangle$, $\langle \hat{u}^2 \rangle$, and $\langle \Delta \beta^2 \rangle$ do not simplify significantly, but their limiting scaling behavior in terms of λ can still be determined. Using the fact that each of these quantities must be positive, it is straightforward to see that only two of the four solutions apply, depending on whether $\alpha_p > 1$ or $\alpha_p < 1$.

$$\begin{aligned} \chi &= \begin{cases} 1 - \alpha_p & \text{if } N_p < M \\ \frac{\lambda}{2\Delta\varphi\sigma_X^2\sigma_W^2} \frac{\alpha_p}{(\alpha_p-1)} \left[1 - \left(1 + \frac{\Delta\varphi}{\langle \varphi' \rangle^2} \right) \alpha_f + \sqrt{\left[1 - \left(1 + \frac{\Delta\varphi}{\langle \varphi' \rangle^2} \right) \alpha_f \right]^2 + 4\Delta\varphi\alpha_f} \right] & \text{if } N_p > M \end{cases} \\ \nu &= \begin{cases} \frac{1}{2\Delta\varphi\sigma_X^2\sigma_W^2} \frac{1}{(1-\alpha_p)} \left[\alpha_p - \left(1 + \frac{\Delta\varphi}{\langle \varphi' \rangle^2} \right) \alpha_f + \sqrt{\left[\alpha_p - \left(1 + \frac{\Delta\varphi}{\langle \varphi' \rangle^2} \right) \alpha_f \right]^2 + 4\frac{\Delta\varphi}{\langle \varphi' \rangle^2} \alpha_f \alpha_p} \right] & \text{if } N_p < M \\ \frac{1}{\lambda} \frac{(\alpha_p-1)}{\alpha_p} & \text{if } N_p > M \end{cases} \end{aligned} \quad (\text{S217})$$

In addition, $\langle \Delta y^2 \rangle$ is $\mathcal{O}(1)$ in small λ when $\alpha_p < 1$ and $\mathcal{O}(\lambda^2)$ when $\alpha_p > 1$. Following the two linear models, the training error is expressed as

$$\langle \mathcal{E}_{\text{train}} \rangle = \langle \Delta y^2 \rangle. \quad (\text{S218})$$

8. Test Error

To calculate the test error, we first approximate the ensemble average of the total test error as the average residual error of an arbitrary data point (y, \vec{x}) , as in Eq. (S94) for linear regression. The test error then becomes

$$\begin{aligned} \langle \mathcal{E}_{\text{test}} \rangle &= \mathbb{E} \left[\frac{1}{M'} \sum_b (\Delta y'_b)^2 \right] \\ &= \mathbb{E} [\Delta y^2] \\ &= \mathbb{E} \left[\left(\vec{x} \cdot \Delta \vec{\beta} - \sqrt{N_p} \mu_z \langle \hat{w} \rangle - \delta \vec{z}_{\text{NL}}(\vec{x}) \cdot \hat{\mathbf{w}} + \delta y_{\text{NL}}^*(\vec{x}) + \varepsilon \right)^2 \right] \\ &= \mathbb{E} \left[\left(\vec{x} \cdot \Delta \vec{\beta} \right)^2 \right] + \mathbb{E} \left[(\delta \vec{z}_{\text{NL}}(\vec{x}) \cdot \hat{\mathbf{w}})^2 \right] + \mathbb{E} \left[(\delta y_{\text{NL}}^*(\vec{x}))^2 \right] + \mathbb{E} \left[(\varepsilon)^2 \right] \\ &= \sigma_X^2 \mathbb{E} \left[\frac{1}{N_f} \sum_k \Delta \beta_k^2 \right] + \sigma_{\delta z}^2 \mathbb{E} \left[\frac{1}{N_p} \sum_K \hat{w}_K^2 \right] + \sigma_{\delta y^*}^2 + \sigma_\varepsilon^2 \\ &\approx \sigma_X^2 \langle \Delta \beta^2 \rangle + \sigma_{\delta z}^2 \langle \hat{w}^2 \rangle + \sigma_{\delta y^*}^2 + \sigma_\varepsilon^2. \end{aligned} \quad (\text{S219})$$

We note that this expression for the test error differs significantly from that for the two linear models due to the additional term $\sigma_{\delta z}^2 \langle \hat{w}^2 \rangle$, which captures error due to the nonlinear component of the hidden features.

9. Bias-Variance Decomposition

Following the derivations for the two linear models, the bias in the random nonlinear features model is given by

$$\begin{aligned}
\langle \text{Bias}^2[\hat{y}(\vec{x})] \rangle &= \mathbb{E} \left[\left(\vec{x} \cdot \Delta \vec{\beta}_1 - \sqrt{N_p} \mu_z \langle \hat{w}_1 \rangle - \delta \vec{z}_{\text{NL}}(\vec{x}) \cdot \hat{\mathbf{w}}_1 - \delta y_{\text{NL}}^*(\vec{x}) \right) \left(\vec{x} \cdot \Delta \vec{\beta}_2 - \sqrt{N_p} \mu_z \langle \hat{w}_2 \rangle - \delta \vec{z}_{\text{NL}}(\vec{x}) \cdot \hat{\mathbf{w}}_2 - \delta y_{\text{NL}}^*(\vec{x}) \right) \right] \\
&= \mathbb{E} \left[\left(\vec{x} \cdot \Delta \vec{\beta}_1 \right) \left(\vec{x} \cdot \Delta \vec{\beta}_2 \right) \right] + \mathbb{E}[(\delta \vec{z}_{\text{NL}}(\vec{x}) \cdot \hat{\mathbf{w}}_1)(\delta \vec{z}_{\text{NL}}(\vec{x}) \cdot \hat{\mathbf{w}}_2)] + \mathbb{E}[(\delta y_{\text{NL}}^*(\vec{x}))^2] \\
&= \sigma_X^2 \mathbb{E} \left[\frac{1}{N_f} \sum_k \Delta \beta_{1,k} \Delta \beta_{2,k} \right] + \sigma_{\delta z}^2 \mathbb{E} \left[\frac{1}{N_p} \sum_K \hat{w}_{1,K} \hat{w}_{2,K} \right] + \sigma_{\delta y^*}^2 \\
&\approx \sigma_X^2 \langle \Delta \beta_1 \Delta \beta_2 \rangle + \sigma_{\delta z}^2 \langle \hat{w}_1 \hat{w}_2 \rangle + \sigma_{\delta y^*}^2,
\end{aligned} \tag{S220}$$

along with the variance,

$$\begin{aligned}
\langle \text{Var}[\hat{y}(\vec{x})] \rangle &= \langle \mathcal{E}_{\text{test}} \rangle - \langle \text{Bias}^2[\hat{y}(\vec{x})] \rangle - \text{Noise} \\
&= \sigma_X^2 (\langle \Delta \beta^2 \rangle - \langle \Delta \beta_1 \Delta \beta_2 \rangle) + \sigma_{\delta z}^2 (\langle \hat{w}^2 \rangle - \langle \hat{w}_1 \hat{w}_2 \rangle).
\end{aligned} \tag{S221}$$

As a reminder, the subscripts 1 and 2 refer to parameters resulting from fitting training sets \mathcal{D}_1 and \mathcal{D}_2 drawn independently from the same data distribution (see previous models). These two expressions are similar to those in the two linear models, but also include properties of the fit parameters.

Next, we need to calculate the covariance of the residual parameter errors $\langle \Delta \beta_1 \Delta \beta_2 \rangle$, as well as the covariance of the fit parameters $\langle \hat{w}_1 \hat{w}_2 \rangle$. Following the derivation for the linear model in Sec. **S1 F 9**, we apply the self-consistent equations for the 0-indexed quantities, Eq. **(S192)**, to the two data sets, giving us

$$\begin{aligned}
\hat{w}_{1,0} &= \nu \sigma_{\hat{w}} z_{\hat{w}_1} \\
\hat{u}_{1,0} &= \kappa \sigma_{\hat{u}} z_{\hat{u}_1} + \omega(\beta_0 - \sigma_{\Delta \beta} z_{\Delta \beta_1}) \\
\Delta y_{1,0} &= \chi(\sigma_{\Delta y} z_{\Delta y_1} + \delta y_{\text{NL}}^*(\vec{x}_{1,0}) + \varepsilon_{1,0}) \\
\Delta \beta_{1,0} &= \kappa(\beta_0 - \sigma_{\Delta \beta} z_{\Delta \beta_1}) + \phi \sigma_{\hat{u}} z_{\hat{u}_1},
\end{aligned} \tag{S222}$$

and

$$\begin{aligned}
\hat{w}_{2,0} &= \nu \sigma_{\hat{w}} z_{\hat{w}_2} \\
\hat{u}_{2,0} &= \kappa \sigma_{\hat{u}} z_{\hat{u}_2} + \omega(\beta_0 - \sigma_{\Delta \beta} z_{\Delta \beta_2}) \\
\Delta y_{2,0} &= \chi(\sigma_{\Delta y} z_{\Delta y_2} + \delta y_{\text{NL}}^*(\vec{x}_{2,0}) + \varepsilon_{2,0}) \\
\Delta \beta_{2,0} &= \kappa(\beta_0 - \sigma_{\Delta \beta} z_{\Delta \beta_2}) + \phi \sigma_{\hat{u}} z_{\hat{u}_2}.
\end{aligned} \tag{S223}$$

Multiplying these equations and making the self-averaging approximation, we find

$$\begin{aligned}
\langle \hat{w}_1 \hat{w}_2 \rangle &= \frac{1}{N_p} \sum_K \hat{w}_{1,K} \hat{w}_{2,K} \approx \mathbb{E}[\hat{w}_{1,0} \hat{w}_{2,0}] = \nu^2 \mathbb{E}[\sigma_{\hat{w}}^2 z_{\hat{w}_1} z_{\hat{w}_2}] \\
\langle \hat{u}_1 \hat{u}_2 \rangle &= \frac{1}{N_f} \sum_k \hat{u}_{1,k} \hat{u}_{2,k} \approx \mathbb{E}[\hat{u}_{1,0} \hat{u}_{2,0}] = \kappa^2 \mathbb{E}[\sigma_{\hat{u}}^2 z_{\hat{u}_1} z_{\hat{u}_2}] + \omega^2 (\sigma_{\beta}^2 + \mathbb{E}[\sigma_{\Delta \beta}^2 z_{\Delta \beta_1} z_{\Delta \beta_2}]) \\
\langle \Delta y_1 \Delta y_2 \rangle &= \frac{1}{M} \sum_b \Delta y_{1,b} \Delta y_{2,b} \approx \mathbb{E}[\Delta y_{1,0} \Delta y_{2,0}] = \chi^2 \mathbb{E}[\sigma_{\Delta y}^2 z_{\Delta y_1} z_{\Delta y_2}] \\
\langle \Delta \beta_1 \Delta \beta_2 \rangle &= \frac{1}{N_f} \sum_k \Delta \beta_{1,k} \Delta \beta_{2,k} \approx \mathbb{E}[\Delta \beta_{1,0} \Delta \beta_{2,0}] = \kappa^2 (\sigma_{\beta}^2 + \mathbb{E}[\sigma_{\Delta \beta}^2 z_{\Delta \beta_1} z_{\Delta \beta_2}]) + \phi^2 \mathbb{E}[\sigma_{\hat{u}}^2 z_{\hat{u}_1} z_{\hat{u}_2}].
\end{aligned} \tag{S224}$$

Next, we calculate each of the four resulting expectation values of products of random variables. The average of

the product $z_{\hat{w}_1} z_{\hat{w}_2}$ is

$$\begin{aligned}
\mathbb{E}[\sigma_{\hat{w}}^2 z_{\hat{w}_1} z_{\hat{w}_2}] &= \mathbb{E} \left[\left(\sum_j \hat{u}_{1,j \setminus 0} W_{j0} + \sum_a \Delta y_{1,a \setminus 0} \delta z_{\text{NL},0}(\vec{\mathbf{x}}_{1,a}) \right) \left(\sum_k \hat{u}_{2,k \setminus 0} W_{k0} + \sum_b \Delta y_{2,b \setminus 0} \delta z_{\text{NL},0}(\vec{\mathbf{x}}_{2,b}) \right) \right] \\
&= \sum_{jk} \mathbb{E}[\hat{u}_{1,j \setminus 0} \hat{u}_{2,k \setminus 0}] \mathbb{E}[W_{j0} W_{k0}] + \sum_{ab} \mathbb{E}[\Delta y_{1,a \setminus 0} \Delta y_{2,b \setminus 0}] \mathbb{E}[\delta z_{\text{NL},0}(\vec{\mathbf{x}}_{1,a})] \mathbb{E}[\delta z_{\text{NL},0}(\vec{\mathbf{x}}_{2,b})] \\
&= \frac{\sigma_W^2}{N_p} \sum_k \mathbb{E}[\hat{u}_{1,j \setminus 0} \hat{u}_{2,j \setminus 0}] \\
&\approx \sigma_W^2 \frac{\alpha_f}{\alpha_p} \langle \hat{u}_1 \hat{u}_2 \rangle.
\end{aligned} \tag{S225}$$

while the average of the product $z_{\Delta\beta_1} z_{\Delta\beta_2}$ results in

$$\begin{aligned}
\mathbb{E}[\sigma_{\Delta\beta}^2 z_{\Delta\beta_1} z_{\Delta\beta_2}] &= \mathbb{E} \left[\sum_{JK} \hat{w}_{1,J \setminus 0} \hat{w}_{2,K \setminus 0} W_{0J} W_{0K} \right] \\
&= \sum_{JK} \mathbb{E}[\hat{w}_{1,J \setminus 0} \hat{w}_{2,K \setminus 0}] \mathbb{E}[W_{0J} W_{0K}] \\
&= \frac{\sigma_W^2}{N_p} \sum_K \mathbb{E}[\hat{w}_{1,K \setminus 0} \hat{w}_{2,K \setminus 0}] \\
&\approx \sigma_W^2 \langle \hat{w}_1 \hat{w}_2 \rangle,
\end{aligned} \tag{S226}$$

We find that the other two products average to zero due to the independence of X_1 and X_2 , giving us

$$\begin{aligned}
\mathbb{E}[\sigma_{\hat{u}}^2 z_{\hat{u}_1} z_{\hat{u}_2}] &= \mathbb{E} \left[\sum_{ab} \Delta y_{1,a \setminus 0} \Delta y_{2,b \setminus 0} X_{1,a0} X_{2,b0} \right] \\
&= \sum_{ab} \mathbb{E}[\Delta y_{1,a \setminus 0} \Delta y_{2,b \setminus 0}] \mathbb{E}[X_{1,a0}] \mathbb{E}[X_{2,b0}] \\
&= 0
\end{aligned} \tag{S227}$$

and

$$\begin{aligned}
\mathbb{E}[\sigma_{\Delta y}^2 z_{\Delta y_1} z_{\Delta y_2}] &= \mathbb{E} \left[\left(\sum_j \Delta \beta_{1,j \setminus 0} X_{1,0j} - \sum_J \hat{w}_{1,J \setminus 0} \delta z_{\text{NL},J}(\vec{\mathbf{x}}_{1,0}) \right) \left(\sum_k \Delta \beta_{2,k \setminus 0} X_{2,0k} - \sum_K \hat{w}_{2,K \setminus 0} \delta z_{\text{NL},K}(\vec{\mathbf{x}}_{2,0}) \right) \right] \\
&= \sum_{jk} \mathbb{E}[\Delta \beta_{1,j \setminus 0} \Delta \beta_{2,k \setminus 0}] \mathbb{E}[X_{1,0j}] \mathbb{E}[X_{2,0k}] + \sum_{JK} \mathbb{E}[\hat{w}_{1,J \setminus 0} \hat{w}_{2,K \setminus 0}] \mathbb{E}[\delta z_{\text{NL},J}(\vec{\mathbf{x}}_{1,0})] \mathbb{E}[\delta z_{\text{NL},K}(\vec{\mathbf{x}}_{2,0})] \\
&= 0.
\end{aligned} \tag{S228}$$

Substituting these results into Eq. (S224), we find the self-consistent equations

$$\begin{aligned}
\langle \hat{w}_1 \hat{w}_2 \rangle &= \nu^2 \sigma_W^2 \frac{\alpha_f}{\alpha_p} \langle \hat{u}_1 \hat{u}_2 \rangle \\
\langle \hat{u}_1 \hat{u}_2 \rangle &= \omega^2 (\sigma_\beta^2 + \sigma_W^2 \langle \hat{w}_1 \hat{w}_2 \rangle) \\
\langle \Delta y_1 \Delta y_2 \rangle &= 0 \\
\langle \Delta \beta_1 \Delta \beta_2 \rangle &= \kappa^2 (\sigma_\beta^2 + \sigma_W^2 \langle \hat{w}_1 \hat{w}_2 \rangle).
\end{aligned} \tag{S229}$$

Solving these equations exactly in the thermodynamic limit, we find the expressions

$$\begin{aligned}\langle \hat{w}_1 \hat{w}_2 \rangle &= \frac{\sigma_\beta^2}{\sigma_W^2} \frac{\sigma_W^4 \frac{\alpha_f}{\alpha_p} \omega^2 \nu^2}{\left(1 - \sigma_W^4 \frac{\alpha_f}{\alpha_p} \omega^2 \nu^2\right)} \\ \langle \hat{u}_1 \hat{u}_2 \rangle &= \sigma_\beta^2 \frac{\omega^2}{\left(1 - \sigma_W^4 \frac{\alpha_f}{\alpha_p} \omega^2 \nu^2\right)} \\ \langle \Delta \beta_1 \Delta \beta_2 \rangle &= \sigma_\beta^2 \frac{\kappa^2}{\left(1 - \sigma_W^4 \frac{\alpha_f}{\alpha_p} \omega^2 \nu^2\right)}.\end{aligned}\tag{S230}$$

S2. PARAMETER ERROR AND PARAMETER BIAS-VARIANCE DECOMPOSITION

In the main text, we note that the label predictions can be decomposed as follows:

$$\hat{y}(\vec{x}) = \vec{x} \cdot \hat{\beta} + \frac{\mu_Z}{\sqrt{N_p}} \sum_J \hat{w}_J + \delta \vec{z}_{\text{NL}}(\vec{x}) \cdot \hat{\mathbf{w}}.\tag{S231}$$

where the vector $\hat{\beta} = W \hat{\mathbf{w}}$ can be interpreted as the vector of ground truth parameters estimated by the model. We also note that this quantity can be defined as

$$\hat{\beta} \equiv \Sigma_{\vec{x}}^{-1} \text{Cov}_{\vec{x}}[\vec{x}, \hat{y}(\vec{x})].\tag{S232}$$

To prove this, we simply evaluate the above formula to find

$$\begin{aligned}\hat{\beta} &= \Sigma_{\vec{x}}^{-1} \text{Cov}_{\vec{x}}[\vec{x}, \hat{y}(\vec{x})] \\ &= \Sigma_{\vec{x}}^{-1} \text{Cov}_{\vec{x}}[\vec{x}, \vec{x} \cdot \hat{\beta} + \frac{\mu_Z}{\sqrt{N_p}} \sum_J \hat{w}_J + \delta \vec{z}_{\text{NL}}(\vec{x}) \cdot \hat{\mathbf{w}}] \\ &= \Sigma_{\vec{x}}^{-1} \text{Cov}_{\vec{x}}[\vec{x}, \vec{x}^T] \hat{\beta} \\ &= \hat{\beta}.\end{aligned}\tag{S233}$$

Here, we would like to show that the accuracy of these parameters in estimating the ground truth parameters plays an important role in the test error. To show this, we define the residual parameter error of each ground truth parameter as $\Delta \vec{\beta} = \vec{\beta} - \hat{\beta}$, and the total parameter error as

$$\mathcal{E}_{\text{param}} = \frac{1}{N_f} \|\vec{\beta}\|^2.\tag{S234}$$

If we take the ensemble average of this quantity, we find that

$$\langle \mathcal{E}_{\text{param}} \rangle = \langle \Delta \beta^2 \rangle,\tag{S235}$$

from which we see that the test error for a general model with nonlinear labels and hidden features can be expressed as

$$\langle \mathcal{E}_{\text{test}} \rangle = \sigma_X^2 \langle \mathcal{E}_{\text{param}} \rangle + \sigma_{\delta z}^2 \langle \hat{w}^2 \rangle + \sigma_{\delta y^*}^2 + \sigma_\varepsilon^2,\tag{S236}$$

demonstrating the link between the parameter error and the test error.

Furthermore, we can define a bias-variance decomposition for each of the squared residual parameter errors,

$$\text{E}_{\mathcal{D}}[\Delta \beta_j^2] = \text{Bias}[\hat{\beta}_j] + \text{Var}[\hat{\beta}_j],\tag{S237}$$

with the parameter bias and parameter variance, respectively, defined as

$$\text{Bias}[\hat{\beta}_j] = \text{E}_{\mathcal{D}}[\hat{\beta}_j] - \beta_j, \quad \text{Var}[\hat{\beta}_j] = \text{E}_{\mathcal{D}}[\hat{\beta}_j^2] - \text{E}_{\mathcal{D}}[\hat{\beta}_j]^2.\tag{S238}$$

In the ensemble average, each of these quantities is the same, giving us an ensemble-averaged parameter bias-variance decomposition,

$$\langle \mathcal{E}_{\text{param}} \rangle = \langle \text{Bias}^2[\hat{\beta}] \rangle + \langle \text{Var}[\hat{\beta}] \rangle. \quad (\text{S239})$$

To see how these quantities relate to the traditional bias and variance for the label predictions, we next find expressions for the ensemble-averaged parameter bias and variance.

To calculate the parameter bias, we use the same trick that we used to calculate the model bias, reinterpreting the squared average over \mathcal{D} as two separate averages over uncorrelated training sets, \mathcal{D}_1 and \mathcal{D}_2 , drawn from the same distribution. We find the following simple expression for the ensemble-averaged squared parameter bias:

$$\begin{aligned} \langle \text{Bias}^2[\hat{\beta}] \rangle &= \mathbb{E}_{\vec{\beta}} \left[\frac{1}{N_f} \sum_k \left(\mathbb{E}_{\mathcal{D}}[\hat{\beta}_k] - \beta_k \right)^2 \right] \\ &= \mathbb{E}_{\vec{\beta}, \mathcal{D}_1, \mathcal{D}_2} \left[\frac{1}{N_f} \sum_k \left(\hat{\beta}_{1,k} - \beta_k \right) \left(\hat{\beta}_{2,k} - \beta_k \right) \right] \\ &= \mathbb{E}_{\vec{\beta}, \mathcal{D}_1, \mathcal{D}_2} \left[\frac{1}{N_f} \sum_k \Delta\beta_{1,k} \Delta\beta_{2,k} \right] \\ &= \langle \Delta\beta_1 \Delta\beta_2 \rangle. \end{aligned} \quad (\text{S240})$$

Using this expression, along with that for the parameter error, we derive the following expression for the parameter variance:

$$\begin{aligned} \langle \text{Var}[\hat{\beta}] \rangle &= \langle \mathcal{E}_{\text{param}} \rangle - \langle \text{Bias}^2[\hat{\beta}] \rangle \\ &= \langle \Delta\beta^2 \rangle - \langle \Delta\beta_1 \Delta\beta_2 \rangle. \end{aligned} \quad (\text{S241})$$

From these expressions, we find the following simple relations between the model bias and variance and parameter bias and variance:

$$\begin{aligned} \langle \text{Bias}^2[\hat{y}] \rangle &= \sigma_X^2 \langle \text{Bias}^2[\hat{\beta}] \rangle + \sigma_{\delta z}^2 \langle \hat{w}_1 \hat{w}_2 \rangle + \sigma_{\delta y^*}^2 \\ \langle \text{Var}[\hat{y}] \rangle &= \sigma_X^2 \langle \text{Var}[\hat{\beta}] \rangle + \sigma_{\delta z}^2 \langle \hat{w}^2 \rangle. \end{aligned} \quad (\text{S242})$$

We plot the analytic results for the parameter error, parameter bias, and parameter variance for each model in Sec. S7.

S3. MATRIX FORMS OF SUSCEPTIBILITIES

In this section, we derive matrix forms for the susceptibility matrices that appear in the cavity derivations for the three models.

A. Linear Regression

For our model of linear regression, we start by writing the equations

$$\begin{aligned} \lambda \hat{w}_j &= \sum_b \Delta y_b X_{bj} + \eta_j \\ \Delta y_a &= \sum_k \Delta \beta_k X_{ak} + \delta y_{\text{NL}}^*(\vec{x}_a) + \varepsilon_a + \xi_a \\ \Delta \beta_j &= \beta_j - \hat{w}_j \end{aligned} \quad (\text{S243})$$

in matrix form, giving us

$$\begin{pmatrix} \lambda I_{N_f} & -X^T & 0 \\ 0 & I_M & -X \\ I_{N_f} & 0 & I_{N_f} \end{pmatrix} \begin{pmatrix} \hat{\mathbf{w}} \\ \Delta \vec{y} \\ \Delta \vec{\beta} \end{pmatrix} = \begin{pmatrix} \vec{\eta} \\ \delta \vec{y}_{\text{NL}}^* + \vec{\varepsilon} + \vec{\xi} \\ \vec{\beta} \end{pmatrix}. \quad (\text{S244})$$

Next, we define the Hessian matrix as the Laplacian of the loss [Eq. (S6)],

$$H = \nabla_{\hat{\mathbf{w}}}^2 L = \lambda I_{N_f} + X^T X, \quad (\text{S245})$$

and solve the matrix equation above to find

$$\begin{pmatrix} \hat{\mathbf{w}} \\ \Delta \vec{\mathbf{y}} \\ \Delta \vec{\beta} \end{pmatrix} = \begin{pmatrix} H^{-1} & H^{-1} X^T & H^{-1} X^T X \\ -X H^{-1} & I_M - X H^{-1} X^T & (I_M - X H^{-1} X^T) X \\ -H^{-1} & -H^{-1} X^T & I_{N_f} - H^{-1} X^T X \end{pmatrix} \begin{pmatrix} \vec{\eta} \\ \delta \vec{\mathbf{y}}_{\text{NL}}^* + \vec{\varepsilon} + \vec{\xi} \\ \vec{\beta} \end{pmatrix}. \quad (\text{S246})$$

Defining the gradient with respect to both sets of auxiliary variables as

$$\nabla_{\Xi} = (\nabla_{\vec{\eta}} \quad \nabla_{\vec{\xi}}), \quad (\text{S247})$$

we take the gradient of Eq. (S246) to find matrix forms for all the susceptibilities

$$\begin{pmatrix} \nu^{\hat{w}} & \chi^{\hat{w}} \\ \nu^{\Delta y} & \chi^{\Delta y} \\ \nu^{\Delta \beta} & \chi^{\Delta \beta} \end{pmatrix} = \nabla_{\Xi} \begin{pmatrix} \hat{\mathbf{w}} \\ \Delta \vec{\mathbf{y}} \\ \Delta \vec{\beta} \end{pmatrix} = \begin{pmatrix} H^{-1} & H^{-1} X^T \\ -X H^{-1} & I_M - X H^{-1} X^T \\ -H^{-1} & -H^{-1} X^T \end{pmatrix}. \quad (\text{S248})$$

Finally, we expand the inverse Hessian in small λ and keep terms up to $\mathcal{O}(\lambda^0)$,

$$H^{-1} = [\lambda I_{N_f} + X^T X]^{-1} \approx \frac{1}{\lambda} (I_{N_f} - X^+ X) + (X^T X)^+. \quad (\text{S249})$$

Substituting this into the solution for the susceptibilities, we find

$$\begin{pmatrix} \nu^{\hat{w}} & \chi^{\hat{w}} \\ \nu^{\Delta y} & \chi^{\Delta y} \\ \nu^{\Delta \beta} & \chi^{\Delta \beta} \end{pmatrix} \approx \begin{pmatrix} H^{-1} & X^+ \\ -X^{T+} & I_M - X X^+ \\ -H^{-1} & -X^+ \end{pmatrix}. \quad (\text{S250})$$

B. Random Linear Features Model

For the random linear features model, we perform the same procedure, writing the system of equations

$$\begin{aligned} \lambda \hat{w}_J &= \sum_k \hat{u}_k W_{kJ} + \eta_J \\ \hat{u}_j &= \sum_b \Delta y_b X_{bj} + \psi_j \\ \Delta y_a &= \sum_k \Delta \beta_k X_{ak} + \delta y_{\text{NL}}^*(\vec{\mathbf{x}}_a) + \varepsilon_a + \xi_a \\ \Delta \beta_j &= \beta_j - \sum_K \hat{w}_K W_{jK} + \zeta_j \end{aligned} \quad (\text{S251})$$

in matrix form,

$$\begin{pmatrix} \lambda I_{N_p} & -W^T & 0 & 0 \\ 0 & I_{N_f} & -X^T & 0 \\ 0 & 0 & I_M & -X \\ W & 0 & 0 & I_{N_f} \end{pmatrix} \begin{pmatrix} \hat{\mathbf{w}} \\ \hat{\mathbf{u}} \\ \Delta \vec{\mathbf{y}} \\ \Delta \vec{\beta} \end{pmatrix} = \begin{pmatrix} \vec{\eta} \\ \vec{\psi} \\ \delta \vec{\mathbf{y}}_{\text{NL}}^* + \vec{\varepsilon} + \vec{\xi} \\ \vec{\beta} + \vec{\zeta} \end{pmatrix}. \quad (\text{S252})$$

Noting that in this model $Z = XW$, we define the Hessian H , along with an additional matrix P ,

$$\begin{aligned} H &\equiv \nabla_{\hat{\mathbf{w}}}^2 L = \lambda I_{N_p} + Z^T Z \\ P &\equiv I_M - Z H^{-1} Z^T. \end{aligned} \quad (\text{S253})$$

Solving Eq. (S251), we find

$$\begin{pmatrix} \hat{\mathbf{w}} \\ \hat{\mathbf{u}} \\ \Delta \vec{\mathbf{y}} \\ \Delta \vec{\beta} \end{pmatrix} = \begin{pmatrix} H^{-1} & H^{-1}W^T & H^{-1}Z^T & H^{-1}Z^TX \\ -X^TZH^{-1} & I_{N_f} - X^TZH^{-1}W^T & X^TP & X^TPX \\ -ZH^{-1} & -ZH^{-1}W^T & P & PX \\ -WH^{-1} & -WH^{-1}W^T & -WH^{-1}Z^T & I_{N_f} - WH^{-1}Z^TX \end{pmatrix} \begin{pmatrix} \vec{\eta} \\ \vec{\psi} \\ \delta \vec{\mathbf{y}}_{\text{NL}}^* + \vec{\epsilon} + \vec{\xi} \\ \vec{\beta} + \vec{\zeta} \end{pmatrix}. \quad (\text{S254})$$

Next, we define the gradient as

$$\nabla_{\Xi} = (\nabla_{\vec{\eta}} \quad \nabla_{\vec{\psi}} \quad \nabla_{\vec{\xi}} \quad \nabla_{\vec{\zeta}}) \quad (\text{S255})$$

and apply it to the solutions to find

$$\begin{pmatrix} \nu^{\hat{w}} & \phi^{\hat{w}} & \chi^{\hat{w}} & \omega^{\hat{w}} \\ \nu^{\hat{u}} & \phi^{\hat{u}} & \chi^{\hat{u}} & \omega^{\hat{u}} \\ \nu^{\Delta y} & \phi^{\Delta y} & \chi^{\Delta y} & \omega^{\Delta y} \\ \nu^{\Delta \beta} & \phi^{\Delta \beta} & \chi^{\Delta \beta} & \omega^{\Delta \beta} \end{pmatrix} = \nabla_{\Xi} \begin{pmatrix} \hat{\mathbf{w}} \\ \hat{\mathbf{u}} \\ \Delta \vec{\mathbf{y}} \\ \Delta \vec{\beta} \end{pmatrix} = \begin{pmatrix} H^{-1} & H^{-1}W^T & H^{-1}Z^T & H^{-1}Z^TX \\ -X^TZH^{-1} & I_{N_f} - X^TZH^{-1}W^T & X^TP & X^TPX \\ -ZH^{-1} & -ZH^{-1}W^T & P & PX \\ -WH^{-1} & -WH^{-1}W^T & -WH^{-1}Z^T & I_{N_f} - WH^{-1}Z^TX \end{pmatrix}. \quad (\text{S256})$$

Expanding the inverse Hessian and P in small λ ,

$$H^{-1} = [\lambda I_{N_p} + Z^TZ]^{-1} \approx \frac{1}{\lambda} (I_{N_p} - Z^+Z) + (Z^TZ)^+P = I_M - ZZ^+ \quad (\text{S257})$$

expand the susceptibilities to find

$$\begin{pmatrix} \nu^{\hat{w}} & \phi^{\hat{w}} & \chi^{\hat{w}} & \omega^{\hat{w}} \\ \nu^{\hat{u}} & \phi^{\hat{u}} & \chi^{\hat{u}} & \omega^{\hat{u}} \\ \nu^{\Delta y} & \phi^{\Delta y} & \chi^{\Delta y} & \omega^{\Delta y} \\ \nu^{\Delta \beta} & \phi^{\Delta \beta} & \chi^{\Delta \beta} & \omega^{\Delta \beta} \end{pmatrix} \approx \begin{pmatrix} H^{-1} & H^{-1}W^T & Z^+ & Z^+X \\ -X^TZ^+ & I_{N_f} - X^TZ^+W^T & X^TP & X^TPX \\ -Z^+ & -Z^+W^T & P & PX \\ -WH^{-1} & -WH^{-1}W^T & -WZ^+ & I_{N_f} - WZ^+X \end{pmatrix}. \quad (\text{S258})$$

C. Random Nonlinear Features Model

Finally, we repeat the procedure for the random nonlinear features models. First, we rewrite the system of equations

$$\begin{aligned} \lambda \hat{w}_J &= \sqrt{M} \alpha_p^{-\frac{1}{2}} \mu_z \langle \Delta y \rangle + \sum_k \hat{u}_k W_{kJ} + \sum_b \Delta y_b \delta z_{\text{NL},J}(\vec{\mathbf{x}}_b) + \eta_J \\ \hat{u}_j &= \sum_b \Delta y_b X_{bj} + \psi_j \\ \Delta y_a &= -\sqrt{N_p} \mu_z \langle \hat{w} \rangle + \sum_k \Delta \beta_k X_{ak} - \sum_K \hat{w}_K \delta z_{\text{NL},K}(\vec{\mathbf{x}}_a) + \delta y_{\text{NL}}^*(\vec{\mathbf{x}}_a) + \varepsilon_a + \xi_a \\ \Delta \beta_j &= \beta_j - \sum_K \hat{w}_K W_{jK} + \zeta_j \end{aligned} \quad (\text{S259})$$

in matrix form as

$$\begin{pmatrix} \lambda I_{N_p} & -W^T & -(Z - XW)^T & 0 \\ 0 & I_{N_f} & -X^T & 0 \\ Z - XW & 0 & I_M & -X \\ W & 0 & 0 & I_{N_f} \end{pmatrix} \begin{pmatrix} \hat{\mathbf{w}} \\ \hat{\mathbf{u}} \\ \Delta \vec{\mathbf{y}} \\ \Delta \vec{\beta} \end{pmatrix} = \begin{pmatrix} \vec{\eta} \\ \vec{\psi} \\ \delta \vec{\mathbf{y}}_{\text{NL}}^* + \vec{\epsilon} + \vec{\xi} \\ \vec{\beta} + \vec{\zeta} \end{pmatrix}, \quad (\text{S260})$$

where we have replaced the terms proportional to μ_Z and the nonlinear component with $Z - XW$. We define the Hessian H and the matrix P the same as in the linear case,

$$\begin{aligned} H &\equiv \nabla_{\hat{\mathbf{w}}}^2 L = \lambda I_{N_p} + Z^TZ \\ P &\equiv I_M - ZH^{-1}Z^T, \end{aligned} \quad (\text{S261})$$

allowing us to write the solutions as

$$\begin{pmatrix} \hat{\mathbf{w}} \\ \hat{\mathbf{u}} \\ \Delta \vec{\mathbf{y}} \\ \Delta \vec{\beta} \end{pmatrix} = \begin{pmatrix} H^{-1} & H^{-1}W^T & H^{-1}Z^T & H^{-1}Z^TX \\ -X^TZH^{-1} & I_{N_f} - X^TZH^{-1}W^T & X^TP & X^TPX \\ -ZH^{-1} & -ZH^{-1}W^T & P & PX \\ -WH^{-1} & -WH^{-1}W^T & -WH^{-1}Z^T & I_{N_f} - WH^{-1}Z^TX \end{pmatrix} \begin{pmatrix} \vec{\eta} \\ \vec{\psi} \\ \delta \vec{\mathbf{y}}_{\text{NL}}^* + \vec{\epsilon} + \vec{\xi} \\ \vec{\beta} + \vec{\zeta} \end{pmatrix}. \quad (\text{S262})$$

Since these solutions are identical to those in the linear case (but for general Z), we know that the resulting susceptibility matrices will take the same form as Eq. (S258).

S4. SPECTRAL DENSITIES OF KERNEL MATRICES

Here, we derive the spectral densities for the kernel matrix Z^TZ for each model. To do this, we use the technique laid out in Ref. 55. For any symmetric matrix A of size $N \times N$, the spectral density can be written in the form

$$\rho(x) = \frac{1}{\pi} \lim_{\varepsilon \rightarrow 0^+} \text{Im} \frac{1}{N} \text{Tr} G(x - i\varepsilon) \quad (\text{S263})$$

where

$$G(z) = [zI_N - A]^{-1}. \quad (\text{S264})$$

is the Green's function.

In our case, we are interested in the case $A = Z^TZ$. From the cavity calculations, we observe that the susceptibility matrix

$$\nu^{\hat{w}}(\lambda) = [\lambda I_{N_p} + Z^TZ]^{-1} \quad (\text{S265})$$

is related to the Green's function via the relation $G(z) = -\nu^{\hat{w}}(-z)$. Allowing us to express the spectral density in terms of ν ,

$$\rho(x) = -\frac{1}{\pi} \lim_{\varepsilon \rightarrow 0^+} \text{Im} \nu(-x + i\varepsilon). \quad (\text{S266})$$

Therefore, all we will need to do is evaluate Eq. S266 using the appropriate function $\nu(\lambda)$ for each model.

Sometimes, there will be some fraction of eigenvalues at zero. While, the weight of this contribution can be directly calculated via Eq. S266, it will often be easier to instead examine the susceptibility matrix $\chi^{\Delta y}$ in the limit $\lambda \rightarrow 0$, which becomes

$$\chi^{\Delta y} = I_M - Z[\lambda I_{N_p} + Z^TZ]^{-1}Z^T \approx I_M - ZZ^+. \quad (\text{S267})$$

The matrix ZZ^+ is a projector so its trace is the rank of Z^TZ . The trace of $\chi^{\Delta y}$ is then

$$\begin{aligned} \chi &= \frac{1}{M} \text{Tr} \chi^{\Delta y} \\ &= \frac{1}{M} \text{Tr}(I - ZZ^+) \\ &= 1 - \frac{1}{M} \text{rank}(Z^TZ) \end{aligned} \quad (\text{S268})$$

The fraction of nonzero eigenvalues is then

$$\frac{1}{N_p} \text{rank}(Z^TZ) = \frac{1 - \chi}{\alpha_p} \quad (\text{S269})$$

and the number of eigenvalues at zero is

$$f_{\text{zero}} = 1 - \frac{1}{N_p} \text{rank}(Z^TZ) = \frac{\chi + \alpha_p - 1}{\alpha_p}. \quad (\text{S270})$$

A. Linear Regression

For linear regression, the kernel is a Wishart matrix of the form $A = X^T X$, where the elements of the matrix X are independent and identically distributed according to a normal distribution with zero mean, the expected eigenvalue spectrum is the Marchenko-Pastur distribution [50].

To show this, we start the self-consistency equations for the susceptibilities for this model,

$$\chi = \frac{1}{1 + \bar{\nu}}, \quad \bar{\nu} = \frac{1}{\bar{\lambda} + \alpha_f^{-1} \chi}, \quad (\text{S271})$$

where we have non-dimensionalized ν and λ by defining

$$\bar{\nu} = \sigma_X^2 \nu, \quad \bar{\lambda} = \frac{\lambda}{\sigma_X^2}. \quad (\text{S272})$$

Plugging χ into $\bar{\nu}$ and rearranging, we find a quadratic equation for $\bar{\nu}$,

$$\bar{\lambda} \bar{\nu}^2 + \left[(\alpha_f^{-1} - 1) + \bar{\lambda} \right] \bar{\nu} - 1 = 0. \quad (\text{S273})$$

Solving this equation, we find

$$\bar{\nu}(\bar{\lambda}) = \frac{-\left(\alpha_f^{-1} - 1\right) - \bar{\lambda} \pm \sqrt{\left[\left(\alpha_f^{-1} - 1\right) + \bar{\lambda}\right]^2 + 4\bar{\lambda}}}{2\bar{\lambda}}, \quad (\text{S274})$$

or

$$\nu(\lambda) = \frac{\sigma_X^2 \left(1 - \alpha_f^{-1}\right) - \lambda \pm \sqrt{D(\lambda)}}{2\sigma_X^2 \lambda}, \quad (\text{S275})$$

where we have defined the discriminant

$$D(\lambda) = \left[\sigma_X^2 \left(\alpha_f^{-1} - 1 \right) + \lambda \right]^2 + 4\sigma_X^2 \lambda. \quad (\text{S276})$$

Next, we substitute the above solution for ν into Eq. (S266) and simplify to find to find

$$\rho(x) = \frac{1}{2\sigma_X^2} \left[\sigma_X^2 \left(1 - \alpha_f^{-1} \right) \pm \text{Re} \sqrt{D(-x)} \right] \frac{1}{\pi} \lim_{\epsilon \rightarrow 0^+} \frac{\epsilon}{(x^2 + \epsilon^2)} \pm \frac{\text{Im} \sqrt{D(-x)}}{2\pi\sigma_X^2 x}. \quad (\text{S277})$$

We see that the first term is contains the definition of a delta function evaluated at zero,

$$\delta(x) = \frac{1}{\pi} \lim_{\epsilon \rightarrow 0^+} \frac{\epsilon}{(x^2 + \epsilon^2)}. \quad (\text{S278})$$

This allows us to evaluate the the coefficient of this delta function at zero so that the first term in the spectrum becomes

$$\begin{aligned} \frac{1}{2\sigma_X^2} \left[\sigma_X^2 \left(1 - \alpha_f^{-1} \right) \pm \text{Re} \sqrt{D(0)} \right] \delta(x) &= \frac{1}{2} \left[\left(1 - \alpha_f^{-1} \right) \pm \left| 1 - \alpha_f^{-1} \right| \right] \delta(x) \\ &= \max \left(0, 1 - \alpha_f^{-1} \right) \delta(x). \end{aligned} \quad (\text{S279})$$

On the second line we have chosen the signs of the solutions (\pm) so that the spectral density at zero is always non-negative.

To simplify the second term in Eq. (S266), we need to find the interval over which $D(-x) < 0$. Solving $D(-x) = 0$,

$$D(-x) = x^2 - 2x\sigma_X^2 \left(\alpha_f^{-1} + 1 \right) x + \sigma_X^4 \left(\alpha_f^{-1} - 1 \right)^2 = 0, \quad (\text{S280})$$

we find the limits of the interval to be

$$\begin{aligned}
x_{\pm} &= \frac{2\sigma_X^2(\alpha_f^{-1} + 1) \pm \sqrt{4\sigma_X^4(\alpha_f^{-1} + 1)^2 - 4\sigma_X^4(\alpha_f^{-1} - 1)^2}}{2} \\
&= \sigma_X^2(\alpha_f^{-1} + 1) \pm 2\sigma_X^2\sqrt{\alpha_f^{-1}} \\
&= \sigma_X^2\left(1 \pm \sqrt{\alpha_f^{-1}}\right)^2.
\end{aligned} \tag{S281}$$

The second term in the spectrum then becomes

$$\pm \frac{\text{Im} \sqrt{-(x_+ - x)(x - x_-)}}{2\pi\sigma_X^2 x} = \frac{\sqrt{(x_+ - x)(x - x_-)}}{2\pi\sigma_X^2 x}, \tag{S282}$$

where we have again chosen the plus sign so that the spectrum always non-negative.

The complete spectrum is then written as

$$\rho(x) = \max\left(0, 1 - \alpha_f^{-1}\right)\delta(x) + \begin{cases} \frac{1}{2\pi\sigma_X^2 x} \sqrt{(x_{\max} - x)(x - x_{\min})} & \text{if } x \in [x_{\min}, x_{\max}] \\ 0 & \text{otherwise} \end{cases} \tag{S283}$$

with

$$\begin{aligned}
x_{\min} &= \sigma_X^2\left(1 - \sqrt{\alpha_f^{-1}}\right)^2 \\
x_{\max} &= \sigma_X^2\left(1 + \sqrt{\alpha_f^{-1}}\right)^2.
\end{aligned} \tag{S284}$$

As expected, this is the Marchenko-Pastur distribution.

B. Random Linear Features Model

The kernel for the random linear features model takes the form $Z = W^T X^T X W$, where the elements of both X and W are independent and distributed according to separate normal distributions with zero mean. The matrix is known as a Wishart product matrix and its spectrum has been worked out in detail in Ref. 51. To reproduce this analytic result, we start with three of the susceptibilities from the cavity derivation,

$$\chi = \frac{1}{1 + \bar{\nu}\kappa}, \quad \bar{\nu} = \frac{1}{\bar{\lambda} + \alpha_p^{-1}\chi\kappa}, \quad \kappa = \frac{1}{1 + \alpha_f^{-1}\chi\bar{\nu}}, \tag{S285}$$

where we have non-dimensionalized ν and λ by defining

$$\bar{\nu} = \sigma_W^2 \sigma_X^2 \nu, \quad \bar{\lambda} = \frac{\lambda}{\sigma_W^2 \sigma_X^2}. \tag{S286}$$

Solving each of the equations for χ and $\bar{\nu}$ for κ and then setting them equal we find

$$\kappa = \frac{1 - \chi}{\chi\bar{\nu}} = \frac{\alpha_p(1 - \bar{\lambda}\bar{\nu})}{\chi\bar{\nu}}. \tag{S287}$$

From here, we find the following relation between χ and $\bar{\nu}$:

$$\chi = \alpha_p \bar{\lambda} \bar{\nu} - \alpha_p + 1 \tag{S288}$$

Next, we substitute κ into original equation for $\bar{\nu}$, solve for χ , and then substitute this result into Eq. (S288). If we then eliminate any denominators, we find a cubic equation for $\bar{\nu}$,

$$(\alpha_p \bar{\lambda} \bar{\nu})^3 + [1 - \alpha_p + \alpha_f - \alpha_p] (\alpha_p \bar{\lambda} \bar{\nu})^2 + [(1 - \alpha_p)(\alpha_f - \alpha_p) + \alpha_f \alpha_p \bar{\lambda}] (\alpha_p \bar{\lambda} \bar{\nu}) - \alpha_f \alpha_p^2 \bar{\lambda} = 0. \tag{S289}$$

Solving this cubic equation analytically is very involved, so we refer to the solution in Ref. 51. Instead, we will solve this equation numerically for negative imaginary roots of $\nu(\lambda)$ with $\lambda = -x$, according to Eq. (S266). However, we also need to find the interval over which the eigenvalue spectrum is positive. To do this, we rewrite the equation in general form for $\alpha_p \bar{\lambda} \bar{\nu}$,

$$(\alpha_p \bar{\lambda} \bar{\nu})^3 + a_2 (\alpha_p \bar{\lambda} \bar{\nu})^2 + a_1 (\alpha_p \bar{\lambda} \bar{\nu}) + a_0 = 0, \quad (\text{S290})$$

where the coefficients are

$$\begin{aligned} a_0 &= -\alpha_f \alpha_p^2 \bar{\lambda} \\ a_1 &= (1 - \alpha_p)(\alpha_f - \alpha_p) + \alpha_f \alpha_p \bar{\lambda} \\ a_2 &= 1 - \alpha_p + \alpha_f - \alpha_p. \end{aligned} \quad (\text{S291})$$

The discriminant for a cubic equation is expressed in terms of these coefficients as

$$D(\lambda) = R^2 - Q^3 \quad (\text{S292})$$

with

$$\begin{aligned} Q &= \frac{1}{9}(a_2^2 - 3a_1) \\ R &= \frac{1}{54}(9a_2 a_1 - 27a_0 - 2a_2^3). \end{aligned} \quad (\text{S293})$$

To find the limiting eigenvalues, we then solve the equation $D(\lambda) = 0$ (with $\lambda = -x$) numerically for the largest and smallest non-negative real roots.

To find the weight of the delta function component at zero, we use the solution for ν that we found previously, giving us

$$\begin{aligned} f_{\text{zero}} &= \frac{\chi + \alpha_p - 1}{\alpha_p} \\ &= \begin{cases} 1 - \frac{\alpha_f}{\alpha_p} & \text{if } N_f < N_p, M \\ 0 & \text{if } N_p < N_f, M \\ 1 - \alpha_p^{-1} & \text{if } M < N_f, N_p \end{cases} \\ &= \max\left(0, 1 - \frac{\alpha_f}{\alpha_p}, 1 - \alpha_p^{-1}\right). \end{aligned} \quad (\text{S294})$$

C. Random Nonlinear Features Model

Finally, we derive the eigenvalue for the kernel of the random nonlinear features model. Previously this result was derived in Ref. 52. To reproduce this analytic result, we again start with three of the susceptibilities from the cavity derivation,

$$\bar{\nu} = \frac{1}{\bar{\lambda} + \alpha_p^{-1} \chi (\kappa + \Delta\varphi)}, \quad \chi = \frac{1}{1 + \bar{\nu} (\kappa + \Delta\varphi)}, \quad \kappa = \frac{1}{1 + \alpha_f^{-1} \chi \bar{\nu}}. \quad (\text{S295})$$

where we have non-dimensionalized ν and λ by defining

$$\bar{\nu} = \sigma_W^2 \sigma_X^2 \nu, \quad \bar{\lambda} = \frac{\lambda}{\sigma_W^2 \sigma_X^2}. \quad (\text{S296})$$

Solving each of the equations for χ and $\bar{\nu}$ for κ and then setting them equal we find

$$\kappa = \frac{1 - \chi - \Delta\varphi \bar{\nu}}{\chi \bar{\nu}} = \frac{\alpha_p (1 - \bar{\lambda} \bar{\nu}) - \Delta\varphi \bar{\nu}}{\chi \bar{\nu}}, \quad (\text{S297})$$

From here, we find the following relation between χ and $\bar{\nu}$:

$$\chi = \alpha_p \bar{\lambda} \bar{\nu} - \alpha_p + 1 \quad (\text{S298})$$

Next, we substitute κ into original equation for $\bar{\nu}$, solve for χ , and then substitute this result into Eq. (S298). If we then eliminate any denominators, we find a quartic equation for $\bar{\nu}$,

$$\begin{aligned} 0 = & \Delta\varphi(\alpha_p\bar{\lambda}\bar{\nu})^4 + [2\Delta\varphi(1-\alpha_p) + \alpha_p\bar{\lambda}] (\alpha_p\bar{\lambda}\bar{\nu})^3 \\ & + [\Delta\varphi(1-\alpha_p)^2 + \alpha_p(\alpha_f(1+\Delta\varphi) - \alpha_p + 1 - \alpha_p)\bar{\lambda}] (\alpha_p\bar{\lambda}\bar{\nu})^2 \\ & + \alpha_p[(\alpha_f(1+\Delta\varphi) - \alpha_p)(1-\alpha_p) + \alpha_f\alpha_p\bar{\lambda}] \bar{\lambda}(\alpha_p\bar{\lambda}\bar{\nu}) - \alpha_f\alpha_p^3\bar{\lambda}^2. \end{aligned} \quad (\text{S299})$$

Again solving this quartic equation analytically is very involved, so instead, we will solve this equation numerically for negative imaginary roots of $\nu(\lambda)$ with $\lambda = -x$, according to Eq. (S266). However, to find the interval over which the spectrum is positive, we rewrite the equation in general form for $\alpha_p\bar{\lambda}\bar{\nu}$,

$$0 = a_4(\alpha_p\bar{\lambda}\bar{\nu})^4 + a_3(\alpha_p\bar{\lambda}\bar{\nu})^3 + a_2(\alpha_p\bar{\lambda}\bar{\nu})^2 + a_1(\alpha_p\bar{\lambda}\bar{\nu}) + a_0. \quad (\text{S300})$$

where the coefficients are

$$\begin{aligned} a_0 &= -\alpha_f\alpha_p^3\bar{\lambda}^2 \\ a_1 &= \alpha_p[(\alpha_f(1+\Delta\varphi) - \alpha_p)(1-\alpha_p) + \alpha_f\alpha_p\bar{\lambda}] \bar{\lambda} \\ a_2 &= \Delta\varphi(1-\alpha_p)^2 + \alpha_p(\alpha_f(1+\Delta\varphi) - \alpha_p + 1 - \alpha_p)\bar{\lambda} \\ a_3 &= 2\Delta\varphi(1-\alpha_p) + \alpha_p\bar{\lambda} \\ a_4 &= \Delta\varphi \end{aligned} \quad (\text{S301})$$

The discriminant for a quartic equation is expressed in terms of these coefficients as

$$D(z) = R^2 - 4Q^3 \quad (\text{S302})$$

with

$$\begin{aligned} R &= 2a_2^3 - 9a_1a_2a_3 + 27a_0a_3^2 + 27a_1^2a_4 - 72a_0a_2a_4 \\ Q &= a_2^2 - 3a_1a_3 + 12a_0a_4. \end{aligned} \quad (\text{S303})$$

To find the limiting eigenvalues, we then solve the equation $D(\lambda) = 0$ (with $\lambda = -x$) numerically for the largest and smallest non-negative real roots.

To find the weight of the delta function component at zero, we use the solution for ν that we found previously, giving us Size of delta function

$$\begin{aligned} f_{\text{zero}} &= \frac{\chi + \alpha_p - 1}{\alpha_p} \\ &= \max(0, 1 - \alpha_p^{-1}) \end{aligned} \quad (\text{S304})$$

S5. ACCURACY OF MINIMUM PRINCIPAL COMPONENT

In this section, we derive expressions for the predicted labels \hat{y} as a function of projections of the data points along the minimum principal component $\hat{\mathbf{h}}_{\min} \cdot \bar{\mathbf{z}}(\bar{\mathbf{x}})$ used to assess model accuracy in Figs. 5 and 6. We seek two different predictions of the labels as a function of $\hat{\mathbf{h}}_{\min} \cdot \bar{\mathbf{z}}(\bar{\mathbf{x}})$: the labels \hat{y}_{train} that result from a finite training set and the labels \hat{y}_{test} that result from fitting to an average test set, or equivalently, the full data distribution (the limit of a training set of size $M \rightarrow \infty$).

Given a training set consisting of M data points $\mathcal{D} = \{(y_b, \bar{\mathbf{x}}_b)\}_{b=1}^M$ with corresponding hidden features $\bar{\mathbf{z}}_a = \bar{\mathbf{z}}(\bar{\mathbf{x}}_a)$, we start by decomposing the kernel matrix into n principal components $\hat{\mathbf{h}}_i$ with non-zero eigenvalues σ_i^2 ,

$$Z^T Z = \sum_{i=1}^n \sigma_i^2 \hat{\mathbf{h}}_i \hat{\mathbf{h}}_i^T. \quad (\text{S305})$$

We define the principal components so that they form an orthonormal basis of (hidden) features,

$$\hat{\mathbf{h}}_i \cdot \hat{\mathbf{h}}_j = \delta_{ij}. \quad (\text{S306})$$

We define the minimum component $\hat{\mathbf{h}}_{\min}$ as the principal component with the smallest non-zero eigenvalue σ_{\min}^2 . Next, we define the empirical variance of $\hat{\mathbf{h}}_i \cdot \bar{\mathbf{z}}_a$ (holding $\hat{\mathbf{h}}_i$ fixed) within the training set and derive its relationship to the eigenvalue σ_i^2 ,

$$\begin{aligned} \text{Var}_{\bar{\mathbf{x}} \in \mathcal{D}} [\hat{\mathbf{h}}_i \cdot \bar{\mathbf{z}}(\bar{\mathbf{x}}) | \hat{\mathbf{h}}_i] &= \frac{1}{M} \sum_{a=1}^M (\hat{\mathbf{h}}_i \cdot \bar{\mathbf{z}}_a)^2 \\ &= \frac{1}{M} \hat{\mathbf{h}}_i^T Z^T Z \hat{\mathbf{h}}_i \\ &= \frac{\sigma_i^2}{M}. \end{aligned} \quad (\text{S307})$$

Similarly, we define the empirical covariance of $\hat{\mathbf{h}}_i \cdot \bar{\mathbf{z}}_a$ and the labels y_a (again, holding $\hat{\mathbf{h}}_i$ fixed),

$$\begin{aligned} \text{Cov}_{\bar{\mathbf{x}} \in \mathcal{D}} [\hat{\mathbf{h}}_i \cdot \bar{\mathbf{z}}(\bar{\mathbf{x}}), y(\bar{\mathbf{x}}) | \hat{\mathbf{h}}_i] &= \frac{1}{M} \sum_{a=1}^M (\hat{\mathbf{h}}_i \cdot \bar{\mathbf{z}}_a) y_a \\ &= \frac{1}{M} \hat{\mathbf{h}}_i^T Z^T \bar{\mathbf{y}}. \end{aligned} \quad (\text{S308})$$

Using the expression for the predicted labels in Eq. (3) and the exact solution for the fit parameters in the ridge-less limit in Eq. (11), we express the predicted label for an arbitrary test data point $\bar{\mathbf{z}}'$ in terms of the empirical variance and covariance as

$$\begin{aligned} \hat{y} &\approx \bar{\mathbf{z}}' \cdot (Z^T Z)^+ Z^T \bar{\mathbf{y}} \\ &= \bar{\mathbf{z}}' \cdot \sum_{i=1}^n \frac{1}{\sigma_i^2} \hat{\mathbf{h}}_i \hat{\mathbf{h}}_i^T Z^T \bar{\mathbf{y}} \\ &= \sum_{i=1}^n \frac{\text{Cov}_{\bar{\mathbf{x}} \in \mathcal{D}} [\hat{\mathbf{h}}_i \cdot \bar{\mathbf{z}}(\bar{\mathbf{x}}), y(\bar{\mathbf{x}}) | \hat{\mathbf{h}}_i]}{\text{Var}_{\bar{\mathbf{x}} \in \mathcal{D}} [\hat{\mathbf{h}}_i \cdot \bar{\mathbf{z}}(\bar{\mathbf{x}}) | \hat{\mathbf{h}}_i]} (\hat{\mathbf{h}}_i \cdot \bar{\mathbf{z}}'). \end{aligned} \quad (\text{S309})$$

Dropping all terms except for the one containing the minimum component, we find the expression for the predicted labels as a function of $\hat{\mathbf{h}}_{\min} \cdot \bar{\mathbf{z}}'$ resulting from fitting the training data,

$$\hat{y}_{\text{train}}(\hat{\mathbf{h}}_{\min} \cdot \bar{\mathbf{z}}') = \frac{\text{Cov}_{\bar{\mathbf{x}} \in \mathcal{D}} [\hat{\mathbf{h}}_{\min} \cdot \bar{\mathbf{z}}(\bar{\mathbf{x}}), y(\bar{\mathbf{x}}) | \hat{\mathbf{h}}_{\min}]}{\text{Var}_{\bar{\mathbf{x}} \in \mathcal{D}} [\hat{\mathbf{h}}_{\min} \cdot \bar{\mathbf{z}}(\bar{\mathbf{x}}) | \hat{\mathbf{h}}_{\min}]} (\hat{\mathbf{h}}_{\min} \cdot \bar{\mathbf{z}}'). \quad (\text{S310})$$

To find this relationship for an average test set, we extend the empirical variance and covariance to consider an infinitely large data set, or equivalently, average over all possible data points $(y, \bar{\mathbf{x}})$ with hidden features $\bar{\mathbf{z}}(\bar{\mathbf{x}})$. However, we still hold $\hat{\mathbf{h}}_{\min}$ fixed since it is a result of the training set. The resulting relationship is

$$\hat{y}_{\text{test}}(\hat{\mathbf{h}}_{\min} \cdot \bar{\mathbf{z}}') = \frac{\text{Cov}_{\bar{\mathbf{x}}} [\hat{\mathbf{h}}_{\min} \cdot \bar{\mathbf{z}}(\bar{\mathbf{x}}), y(\bar{\mathbf{x}}) | \hat{\mathbf{h}}_{\min}]}{\text{Var}_{\bar{\mathbf{x}}} [\hat{\mathbf{h}}_{\min} \cdot \bar{\mathbf{z}}(\bar{\mathbf{x}}) | \hat{\mathbf{h}}_{\min}]} (\hat{\mathbf{h}}_{\min} \cdot \bar{\mathbf{z}}'). \quad (\text{S311})$$

According to Eq. (S307), we calculate the spread of the training data points along the minimum principal component,

$$\sigma_{\text{train}}^2 = \text{Var}_{\bar{\mathbf{x}} \in \mathcal{D}} [\hat{\mathbf{h}}_{\min} \cdot \bar{\mathbf{z}}(\bar{\mathbf{x}}) | \hat{\mathbf{h}}_{\min}] = \frac{\sigma_{\min}^2}{M}. \quad (\text{S312})$$

We find that it is related to the minimum eigenvalue of the kernel matrix.

We also derive the true variance of data points along $\hat{\mathbf{h}}_{\min}$ for an average test set,

$$\sigma_{\text{test}}^2 = \text{Var}_{\bar{\mathbf{x}}} [\hat{\mathbf{h}}_{\min} \cdot \bar{\mathbf{z}}(\bar{\mathbf{x}}) | \hat{\mathbf{h}}_{\min}]. \quad (\text{S313})$$

In the next few sections, we derive this variance, along with the covariance with respect an average test set, or the full data distribution, for each model, along with expressions for \hat{y}_{test} .

A. Linear Regression

In linear regression without basis functions, the input features and hidden features are identical such that $Z = X$. The covariance then becomes

$$\begin{aligned}\text{Cov}_{\vec{x}}\left[\hat{\mathbf{h}}_{\min} \cdot \vec{z}(\vec{x}), y(\vec{x}) | \hat{\mathbf{h}}_{\min}\right] &= \text{Cov}_{\vec{x}}\left[\hat{\mathbf{h}}_{\min} \cdot \vec{x}, \vec{x} \cdot \vec{\beta} + \delta y_{\text{NL}}^*(\vec{x}) + \varepsilon | \hat{\mathbf{h}}_{\min}\right] \\ &= \hat{\mathbf{h}}_{\min}^T \text{Cov}_{\vec{x}}[\vec{x}, \vec{x}^T] \vec{\beta} \\ &= \frac{\sigma_X^2}{N_f} \hat{\mathbf{h}}_{\min}^T \vec{\beta},\end{aligned}\tag{S314}$$

where we have used the fact that

$$\text{Cov}_{\vec{x}}[\vec{x}, \vec{x}^T] = \frac{\sigma_X^2}{N_f} I_{N_f}.\tag{S315}$$

We also calculate the variance,

$$\begin{aligned}\text{Var}_{\vec{x}}\left[\hat{\mathbf{h}}_{\min} \cdot \vec{z}(\vec{x}) | \hat{\mathbf{h}}_{\min}\right] &= \text{Var}_{\vec{x}}\left[\hat{\mathbf{h}}_{\min} \cdot \vec{x} | \hat{\mathbf{h}}_{\min}\right] \\ &= \text{Cov}_{\vec{x}}\left[\hat{\mathbf{h}}_{\min} \cdot \vec{x}, \hat{\mathbf{h}}_{\min} \cdot \vec{x} | \hat{\mathbf{h}}_{\min}\right] \\ &= \hat{\mathbf{h}}_{\min}^T \text{Cov}_{\vec{x}}[\vec{x}, \vec{x}^T] \hat{\mathbf{h}}_{\min} \\ &= \frac{\sigma_X^2}{N_f} \hat{\mathbf{h}}_{\min} \cdot \hat{\mathbf{h}}_{\min} \\ &= \frac{\sigma_X^2}{N_f}.\end{aligned}\tag{S316}$$

Using these results, the predicted labels for an average test set as a function of $\hat{\mathbf{h}}_{\min} \cdot \vec{z}'$ are then

$$\hat{y}_{\text{test}}(\hat{\mathbf{h}}_{\min} \cdot \vec{z}') = \hat{\mathbf{h}}_{\min}^T \vec{\beta} (\hat{\mathbf{h}}_{\min} \cdot \vec{z}'),\tag{S317}$$

while the expected spread is

$$\sigma_{\text{test}}^2 = \frac{\sigma_X^2}{N_f}.\tag{S318}$$

B. Random Linear Features Model

In the random linear features model, the covariance is

$$\begin{aligned}\text{Cov}_{\vec{x}}\left[\hat{\mathbf{h}}_{\min} \cdot \vec{z}(\vec{x}), y(\vec{x}) | \hat{\mathbf{h}}_{\min}\right] &= \text{Cov}_{\vec{x}}\left[\hat{\mathbf{h}}_{\min} \cdot W^T \vec{x}, \vec{x} \cdot \vec{\beta} + \delta y_{\text{NL}}^*(\vec{x}) + \varepsilon | \hat{\mathbf{h}}_{\min}\right] \\ &= \hat{\mathbf{h}}_{\min}^T W^T \text{Cov}_{\vec{x}}[\vec{x}, \vec{x}^T] \vec{\beta} \\ &= \frac{\sigma_X^2}{N_f} \hat{\mathbf{h}}_{\min}^T W^T \vec{\beta}\end{aligned}\tag{S319}$$

and the variance is

$$\begin{aligned}\text{Var}_{\vec{x}}\left[\hat{\mathbf{h}}_{\min} \cdot \vec{z}(\vec{x}) | \hat{\mathbf{h}}_{\min}\right] &= \text{Var}_{\vec{x}}\left[\hat{\mathbf{h}}_{\min} \cdot W^T \vec{x} | \hat{\mathbf{h}}_{\min}\right] \\ &= \text{Cov}_{\vec{x}}\left[\hat{\mathbf{h}}_{\min} \cdot W^T \vec{x}, \hat{\mathbf{h}}_{\min} \cdot W^T \vec{x} | \hat{\mathbf{h}}_{\min}\right] \\ &= \hat{\mathbf{h}}_{\min}^T W^T \text{Cov}_{\vec{x}}[\vec{x}, \vec{x}^T] W \hat{\mathbf{h}}_{\min} \\ &= \frac{\sigma_X^2}{N_f} \hat{\mathbf{h}}_{\min}^T W^T W \hat{\mathbf{h}}_{\min}.\end{aligned}\tag{S320}$$

The predicted labels are then

$$\hat{y}_{\text{test}}(\hat{\mathbf{h}}_{\min} \cdot \vec{\mathbf{z}}') = \frac{\hat{\mathbf{h}}_{\min} W^T \vec{\beta}}{\hat{\mathbf{h}}_{\min}^T W^T W \hat{\mathbf{h}}_{\min}} (\hat{\mathbf{h}}_{\min} \cdot \vec{\mathbf{z}}'), \quad (\text{S321})$$

and the expected spread is

$$\sigma_{\text{test}}^2 = \frac{\sigma_X^2}{N_f} \hat{\mathbf{h}}_{\min}^T W^T \vec{\beta}. \quad (\text{S322})$$

C. Random Nonlinear Features Model

In the random nonlinear features model, the covariance is

$$\begin{aligned} \text{Cov}_{\vec{\mathbf{x}}}[\hat{\mathbf{h}}_{\min} \cdot \vec{\mathbf{z}}(\vec{\mathbf{x}}), y(\vec{\mathbf{x}}|\hat{\mathbf{h}}_{\min})] &= \text{Cov}_{\vec{\mathbf{x}}}[\hat{\mathbf{h}}_{\min} \cdot W^T \vec{\mathbf{x}} + \hat{\mathbf{h}}_{\min} \cdot \delta \vec{\mathbf{z}}_{\text{NL}}(\vec{\mathbf{x}}), \vec{\mathbf{x}} \cdot \vec{\beta} + \delta y_{\text{NL}}^*(\vec{\mathbf{x}}) + \varepsilon | \hat{\mathbf{h}}_{\min}] \\ &= \hat{\mathbf{h}}_{\min}^T W^T \text{Cov}_{\vec{\mathbf{x}}}[\vec{\mathbf{x}}, \vec{\mathbf{x}}^T] \vec{\beta} \\ &\approx \frac{\sigma_X^2}{N_f} \hat{\mathbf{h}}_{\min}^T W^T \vec{\beta}, \end{aligned} \quad (\text{S323})$$

and the variance is

$$\begin{aligned} \text{Var}_{\vec{\mathbf{x}}}[\hat{\mathbf{h}}_{\min} \cdot \vec{\mathbf{z}}(\vec{\mathbf{x}}) | \hat{\mathbf{h}}_{\min}] &= \text{Var}_{\vec{\mathbf{x}}}[\hat{\mathbf{h}}_{\min} \cdot W^T \vec{\mathbf{x}} + \hat{\mathbf{h}}_{\min} \cdot \delta \vec{\mathbf{z}}_{\text{NL}}(\vec{\mathbf{x}}) | \hat{\mathbf{h}}_{\min}] \\ &= \text{Cov}_{\vec{\mathbf{x}}}[\hat{\mathbf{h}}_{\min} \cdot W^T \vec{\mathbf{x}} + \hat{\mathbf{h}}_{\min} \cdot \delta \vec{\mathbf{z}}_{\text{NL}}(\vec{\mathbf{x}}), \hat{\mathbf{h}}_{\min} \cdot W^T \vec{\mathbf{x}} + \hat{\mathbf{h}}_{\min} \cdot \delta \vec{\mathbf{z}}_{\text{NL}}(\vec{\mathbf{x}}) | \hat{\mathbf{h}}_{\min}] \\ &= \hat{\mathbf{h}}_{\min}^T (W^T \text{Cov}_{\vec{\mathbf{x}}}[\vec{\mathbf{x}}, \vec{\mathbf{x}}^T] W + \text{Cov}_{\vec{\mathbf{x}}}[\delta \vec{\mathbf{z}}_{\text{NL}}(\vec{\mathbf{x}}), \delta \vec{\mathbf{z}}_{\text{NL}}^T(\vec{\mathbf{x}})]) \hat{\mathbf{h}}_{\min} \\ &= \frac{\sigma_X^2}{N_f} \hat{\mathbf{h}}_{\min}^T W^T W \hat{\mathbf{h}}_{\min} + \Delta \varphi \frac{\sigma_W^2 \sigma_X^2}{N_p} \hat{\mathbf{h}}_{\min}^T \hat{\mathbf{h}}_{\min} \\ &= \frac{\sigma_X^2}{N_f} \hat{\mathbf{h}}_{\min}^T W^T W \hat{\mathbf{h}}_{\min} + \Delta \varphi \frac{\sigma_W^2 \sigma_X^2}{N_p}. \end{aligned} \quad (\text{S324})$$

The predicted labels are then

$$\hat{y}_{\text{test}}(\hat{\mathbf{h}}_{\min} \cdot \vec{\mathbf{z}}') = \frac{\hat{\mathbf{h}}_{\min}^T W^T \vec{\beta}}{(\hat{\mathbf{h}}_{\min}^T W^T W \hat{\mathbf{h}}_{\min} + \Delta \varphi \sigma_W^2 \frac{\alpha_f}{\alpha_p})} (\hat{\mathbf{h}}_{\min} \cdot \vec{\mathbf{z}}'). \quad (\text{S325})$$

The expected spread is

$$\sigma_{\text{test}}^2 = \frac{\sigma_X^2}{N_f} \hat{\mathbf{h}}_{\min}^T W^T W \hat{\mathbf{h}}_{\min} + \Delta \varphi \frac{\sigma_W^2 \sigma_X^2}{N_p}. \quad (\text{S326})$$

S6. NUMERICAL SIMULATION DETAILS

In this section, we explain our procedures for generating numerical results.

A. General Details

In all plots of training error, test error, bias, and variance, each point (or pixel for $2d$ plots) is averaged over 1000 independent simulations, unless located exactly at a phase transition, in which case, each point is averaged over 150000 simulations. Small error bars are shown each plot, representing the error on the mean. In all simulations, we use training and test sets of size $M = M' = 512$, a signal-to-noise ratio of $(\sigma_{\beta}^2 \sigma_X^2 + \sigma_{\delta y^*}^2) / \sigma_{\varepsilon}^2 = 10$, and a regularization

parameter of $\lambda = 10^{-6}$. We also use a linear teacher model $y^*(\vec{x}) = \vec{x} \cdot \vec{\beta}$ ($\sigma_{\delta y^*}^2 = 0$) in most cases. In Fig. 6, we use a nonlinear teacher model of the form

$$y^*(\vec{x}) = \frac{\sigma_\beta^2 \sigma_X^2}{\langle f' \rangle} f\left(\frac{\vec{x} \cdot \vec{\beta}}{\sigma_X^2 \sigma_\beta^2}\right) \quad (\text{S327})$$

with $f(h) = \tanh(h)$. In this case, we find that $\langle f' \rangle = 0.6057$ and $\langle f^2 \rangle = 0.3943$, resulting in $\sigma_{\delta y^*}^2 / \sigma_\beta^2 \sigma_X^2 = \Delta f = 0.0747$.

To find the solution for a particular regression problem, we solve a different (but equivalent) system of equations depending on whether $N_p < M$ or $N_p > M$, allowing us to reduce the size of the linear system we need to solve. If $N_p < M$, we solve the system of N_p equations

$$[\lambda I_{N_p} + Z^T Z] \hat{\mathbf{w}} = Z^T \vec{y} \quad (\text{S328})$$

for the N_p unknown fit parameter $\hat{\mathbf{w}}$ where I_{N_p} is the $N_p \times N_p$ identity matrix. This equation is identical to that in Eq. (10) in the main text.

Alternatively, If $N_p > M$ we solve a system of M equations,

$$[\lambda I_M + Z Z^T] \hat{\mathbf{a}} = \vec{y}, \quad (\text{S329})$$

for the M unknowns $\hat{\mathbf{a}}$ where I_M is the $M \times M$ identity matrix. We then convert to fit parameters via the formula

$$\hat{\mathbf{w}} = Z^T \hat{\mathbf{a}}. \quad (\text{S330})$$

B. Bias-Variance Decompositions

To efficiently calculate the ensemble-averaged bias and variance, we take inspiration from Eq. (S99). During each simulation, we independently generate two training data sets \mathcal{D}_1 and \mathcal{D}_2 and perform regression separately on both, resulting in two sets of fit parameter $\hat{\mathbf{w}}_1$ and $\hat{\mathbf{w}}_2$, respectively. Using the results from the first training set, we calculate the training error, test error, parameter error and mean-squared parameter size. For each training set, we then calculate the residual label errors, $\Delta \vec{y}_1$ and $\Delta \vec{y}_2$, and the residual parameter error, $\Delta \vec{\beta}_1$ and $\Delta \vec{\beta}_2$, for both data sets. Finally, we record three different overlaps between quantities resulting from the two different data sets: the model error overlap $\Delta \vec{y}_1 \cdot \Delta \vec{y}_2$, the parameter error overlap $\Delta \vec{\beta}_1 \cdot \Delta \vec{\beta}_2$, and the fit parameter overlap $\hat{\mathbf{w}}_1 \cdot \hat{\mathbf{w}}_2$. When averaged over many simulations, these quantities approximate the ensemble averages, $\langle \Delta y_1 \Delta y_2 \rangle$, $\langle \Delta \beta_1 \Delta \beta_2 \rangle$, and $\langle \hat{w}_1 \hat{w}_2 \rangle$, respectively, used to calculate the model and parameter bias and variance.

C. Eigenvalue Decompositions of Kernel Matrices

For each of the numerical eigenvalue distributions for the kernel matrices presented in the main text, we choose $M = 4096$. We then average over the distributions for 10 independently sampled matrices when $\alpha_p = 1$ or $\alpha_p = 8$ and over 80 matrices when $\alpha_p = 1/8$. In this way, we ensure that the same number of non-zero eigenvalues is present in the part of the histograms corresponding to the bulk of the distributions (the distribution excluding the delta function at zero). For $M < N_p$ we calculate the eigenvalues of $Z^T Z$, while for $M > N_p$ we instead calculate the eigenvalues of $Z Z^T$ since this matrix is smaller and contains the same non-zero eigenvalues. In the later case, we then manually append an additional $N_p - M$ zero-valued eigenvalues to the distribution.

D. Spread Along Minimum Principal Components

For each the scatter plots in Figs. 5 and 6, we consider training and test sets of size $M = M' = 200$, with all other parameters specified in Sec. S6A. We then calculate the principal component corresponding to the minimum eigenvalue numerically and use this to plot the relationship learned by the model for the training set, as detailed in Sec. S5. For the test set, we show the relationship for an average test set rather than the specific test shown, again using the formulas detailed in Sec. S5. We note that these formulas still require the minimum principal component calculated for the training set.

In Fig. 5, the spread of the the training set compared to a test set as a function of α_p is calculated using 100 simulations for each point. For each simulation, we record the ratio $\sigma_{\text{train}}/\sigma_{\text{test}}$ (see Sec. S5) and then average this quantity across simulations for each α_p .

S7. COMPLETE NUMERICAL RESULTS

In this section, we provide complete comparisons between the analytic and numerical results when lacking from the main text.

For linear regression, comparisons to numerical results for the training error, test error, bias, and variance are depicted in Fig. 2 in the main text. In Fig. S1, we provide comparisons to numerical results for the parameter error, parameter bias, and parameter variance, given respectively by

$$\begin{aligned}\langle \mathcal{E}_{\text{param}} \rangle &= \langle \Delta \beta^2 \rangle \\ \langle \text{Bias}^2[\hat{\beta}] \rangle &= \langle \Delta \beta_1 \Delta \beta_2 \rangle \\ \langle \text{Var}[\hat{\beta}] \rangle &= \langle \Delta \beta^2 \rangle - \langle \Delta \beta_1 \Delta \beta_2 \rangle\end{aligned}\tag{S331}$$

see Sec. S2), along with the mean-squared fit parameter size $\langle \hat{w}^2 \rangle$. Error bars for each point indicate the error on the mean.

For the random linear features model, Fig. S2 provides comparisons to numerical results for the training error, test error, bias, and variance, and Fig. S3 compares results for the parameter error, parameter bias, parameter variance and mean-squared parameter size. In Figs. S4 and S5, we report analogous results for the random nonlinear features model.

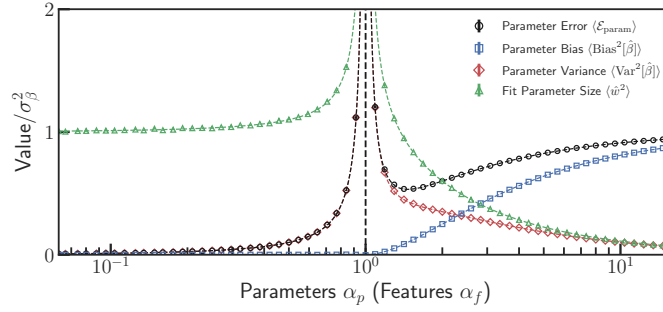


FIG. S1. **Comparison of analytic and numerical results for linear regression: Parameter bias-variance decomposition and fit parameter size.** Solutions are plotted as a function of $\alpha_p = N_p/M$ (or equivalently, $\alpha_f = N_f/M$ for this model). Analytic solutions are indicated as dashed lines with numerical results shown as points. Depicted are the parameter error (black circles), parameter bias (blue squares), parameter variance (red squares), and fit parameter size (green triangles). A black dashed vertical line marks the interpolation threshold $\alpha_p = 1$.

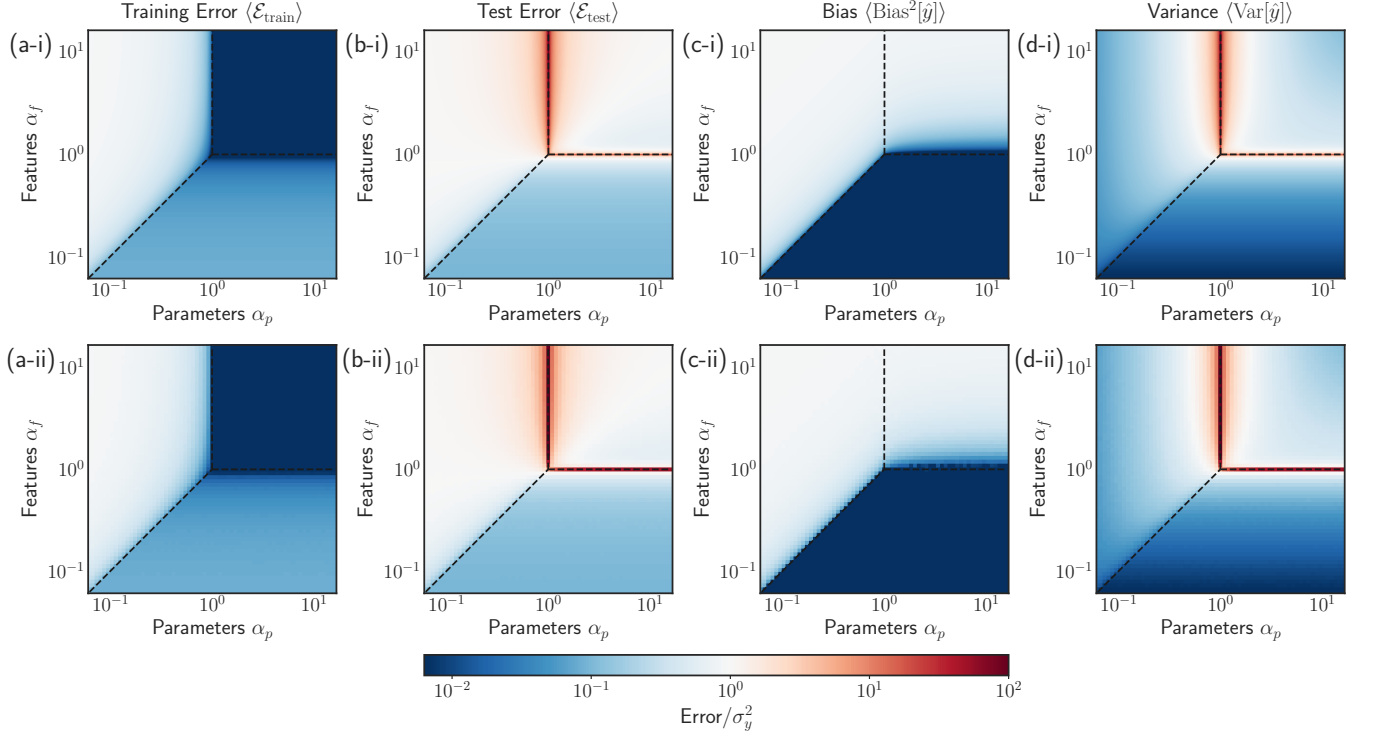


FIG. S2. **Comparison of analytic and numerical results for the random linear features model: Training error and bias-variance decomposition.** (Top Row) Analytic solutions and (Bottom Row) numerical results are shown as a function of $\alpha_p = N_p/M$ and $\alpha_f = N_f/M$. Plotted are the ensemble-averaged (a) training error, (b) test error, (c) squared bias, and (d) variance. In each panel, black dashed lines show boundaries between different regimes of solutions depending on which is smallest of the quantities M , N_f , or N_p . The vertical and horizontal lines bound the interpolation, or over-parameterized, regime, located at $\alpha_p > 1$ and $\alpha_f > 1$, while the diagonal line marks the boundary between the biased and unbiased regime for a linear teacher models. All solutions have been scaled by the variance of the training set labels $\sigma_y^2 = \sigma_\beta^2 \sigma_X^2 + \sigma_\epsilon^2$.

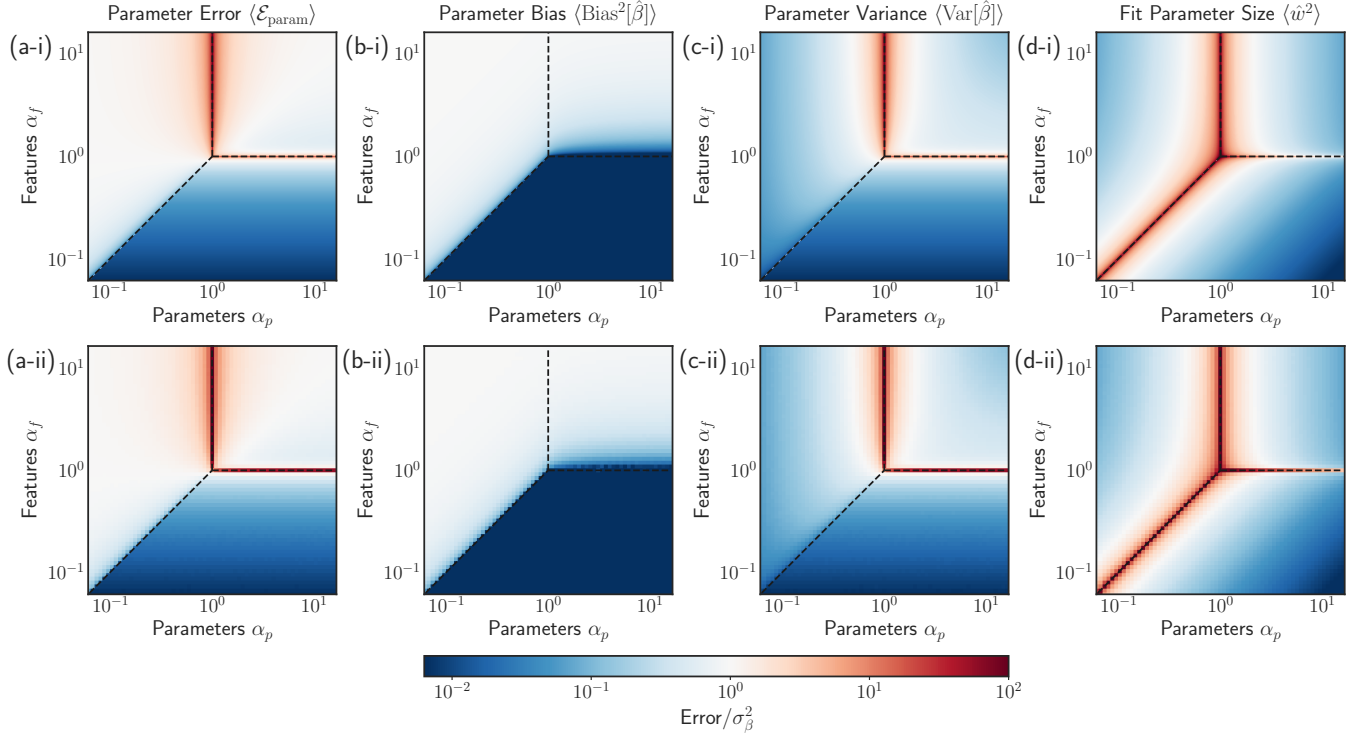


FIG. S3. **Comparison of analytic and numerical results for the random linear features model: Parameter bias-variance decomposition and fit parameter size.** (Top Row) Analytic solutions and (Bottom Row) numerical results are shown as a function of $\alpha_p = N_p/M$ and $\alpha_f = N_f/M$. Plotted are the ensemble-averaged (a) parameter error, (b) squared parameter bias, (c) parameter variance, and (d) fit parameter size. In each panel, black dashed lines show boundaries between different regimes of solutions depending on which is smallest of the quantities M , N_f , or N_p . The vertical and horizontal lines bound the interpolation, or over-parameterized, regime, located at $\alpha_p > 1$ and $\alpha_f > 1$, while the diagonal line marks the boundary between the biased and unbiased regimes for a linear teacher model.

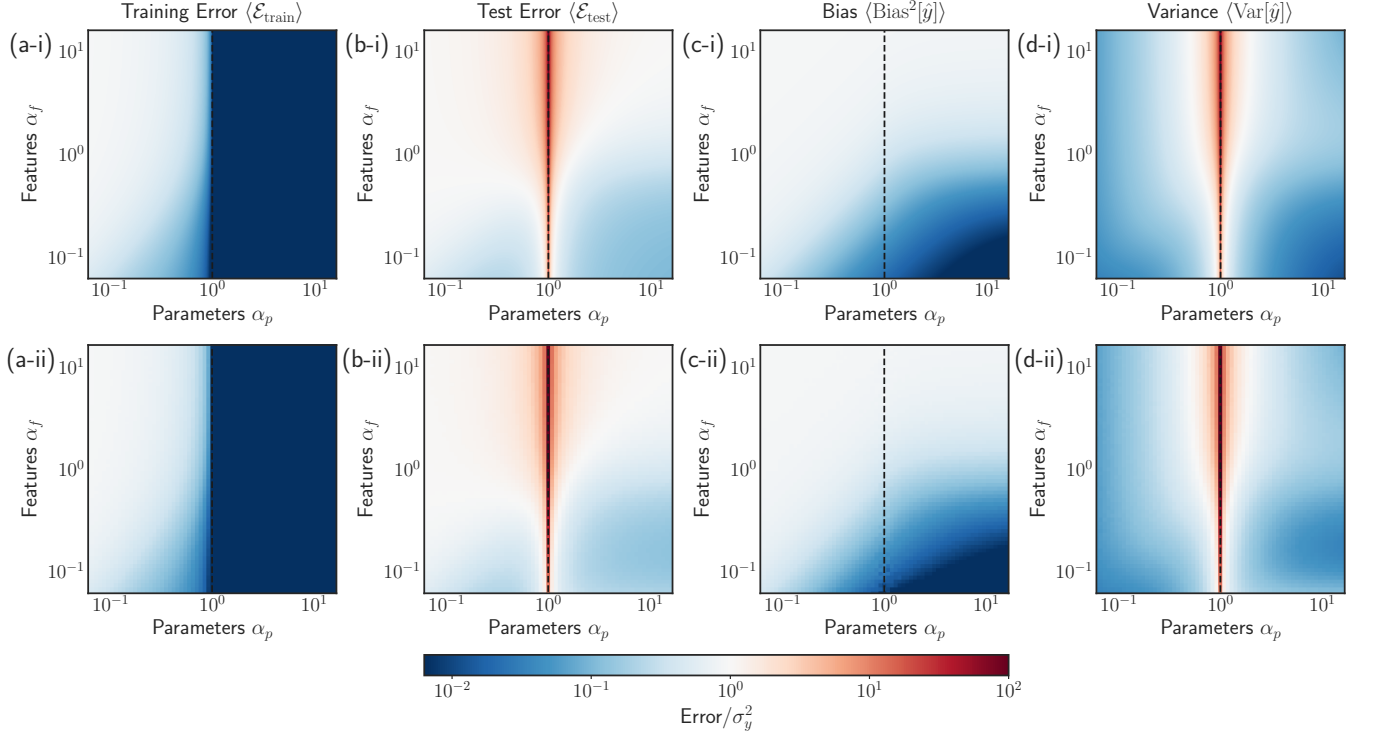


FIG. S4. **Comparison of analytic and numerical results for the random nonlinear features model: Training error and bias-variance decomposition.** (Top Row) Analytic solutions and (Bottom Row) numerical results are shown as a function of $\alpha_p = N_p/M$ and $\alpha_f = N_f/M$. Plotted are the ensemble-averaged (a) training error, (b) test error, (c) squared bias, and (d) variance. In each panel, a black dashed line marks the boundary between the under- and over-parameterized regimes at $\alpha_p = 1$. All solutions have been scaled by the variance of the training set labels $\sigma_y^2 = \sigma_\beta^2 \sigma_X^2 + \sigma_\varepsilon^2$.

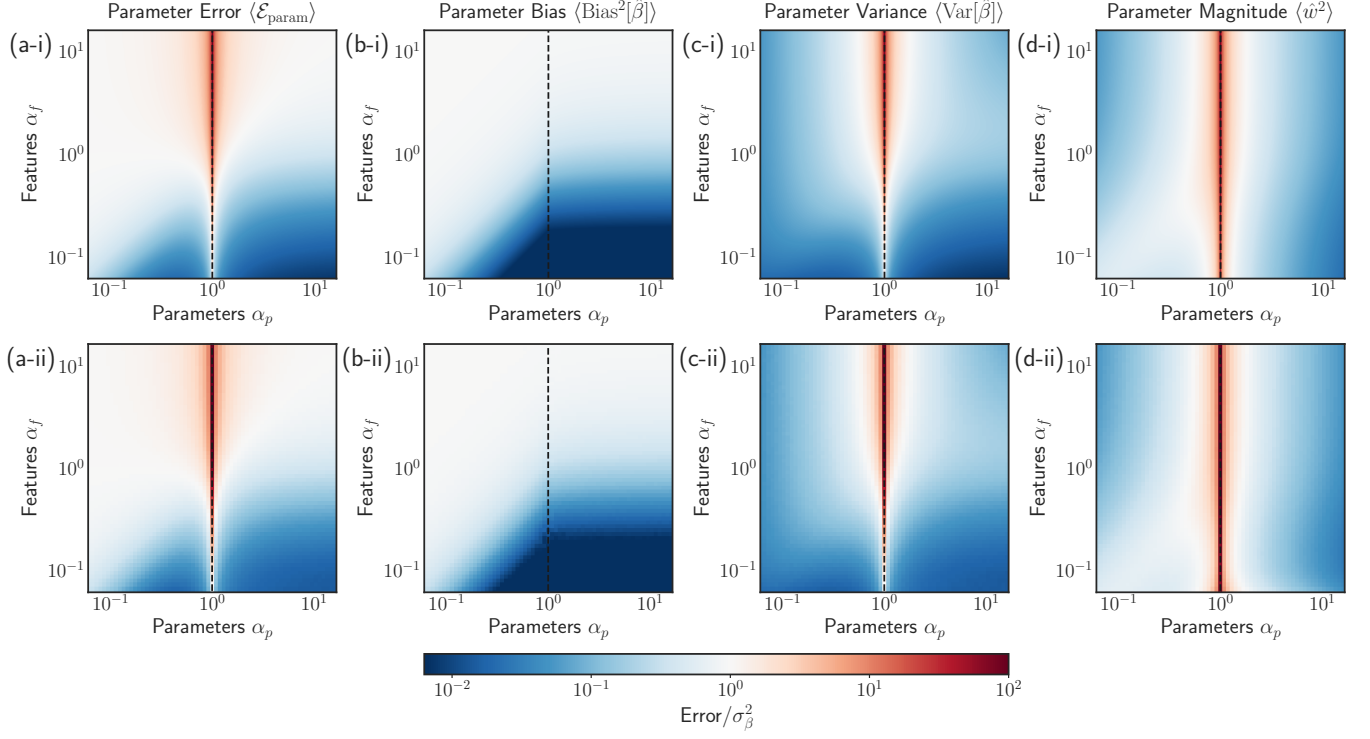


FIG. S5. **Comparison of analytic and numerical results for the random linear features model: Parameter bias-variance decomposition and fit parameter size.** (Top Row) Analytic solutions and (Bottom Row) numerical results are shown as a function of $\alpha_p = N_p/M$ and $\alpha_f = N_f/M$. Plotted are the ensemble-averaged (a) parameter error, (b) squared parameter bias, (c) parameter variance, and (d) fit parameter size. In each panel, a black dashed line marks the boundary between the under- and over-parameterized regimes at $\alpha_p = 1$.